Multi-scale interactions between riparian vegetation and hydrogeomorphic processes (the lower Allier River)

Borbála Hortobágyi

Université Clermont Auvergne, Clermont-Ferrand
UFR Lettres Culture et Sciences Humaines
GEOLAB (UMR 6042 CNRS/UCA/UL)

Multi-scale interactions between riparian vegetation and hydrogeomorphic processes (the lower Allier River)

Interactions multi-échelles entre la végétation riveraine et les processus hydrogéomorphologiques (bas-Allier)

Borbála HORTOBÁGYI

Thèse pour l'obtention du Doctorat de géographie

présentée et soutenue publiquement le 16 mars 2018

Membres du jury

Walter BERTOLDI, Docteur, Université de Trento
Dov CORENBLIT, Maître de conférences, Université Clermont Auvergne
Simon DUFOUR, Maître de conférences, Université Rennes 2
Emmanuèle GAUTIER, Professeur, Université Paris 1
Jean-Luc PEIRY, Professeur, Université Clermont Auvergne
Hervé PIÉGAY, Directeur de recherche CNRS, École Normale Supérieure de Lyon
Michal TAL, Maître de conférences, Aix-Marseille Université

Université Clermont Auvergne, Clermont-Ferrand
UFR Lettres Culture et Sciences Humaines
GEOLAB (UMR 6042 CNRS/UCA/UL)

Multi-scale interactions between riparian vegetation and hydrogeomorphic processes (the lower Allier River)

Borbála HORTOBÁGYI

Thèse pour l'obtention du Doctorat de géographie

présentée et soutenue publiquement le 16 mars 2018

Membres du jury

Walter BERTOLDI, Docteur, Université de Trento
Dov CORENBLIT, Maître de conférences, Université Clermont Auvergne
Simon DUFOUR, Maître de conférences, Université Rennes 2
Emmanuèle GAUTIER, Professeur, Université Paris 1
Jean-Luc PEIRY, Professeur, Université Clermont Auvergne
Hervé PIÉGAY, Directeur de recherche CNRS, École Normale Supérieure de Lyon
Michal TAL, Maître de conférences, Aix-Marseille Université

Abstract / Keywords

Abstract – In ecosystems, such as rivers, salt marshes, mangroves, coastal dunes which are exposed to frequent and regular hydrogeomorphic fluxes (i.e. physical disturbances), feedbacks between geomorphology (water, sediment and landforms) and plants (e.g. *Populus nigra* L.*, Salix alba* L.*, Salix purpurea* L. in rivers) can occur. Vegetation establishment is controlled by hydrogeomorphic processes which in turn are modulated by vegetation. Such feedbacks control riparian ecosystem dynamics. In this thesis, we addressed two main questions in an effort to better understand feedbacks between riparian vegetation and hydrogeomorphic processes: (i) How does riparian vegetation respond to hydrogeomorphic constraints? (ii) How, and to what extent, do established engineer plants affect fluvial geomorphology? We studied these questions through a nested multi-scale approach from landscape pattern to plant trait scales on the dynamic wandering Allier River (France). We tested the applicability of the method of photogrammetry to quantify the response and the effect of riparian vegetation and biogeomorphic feedbacks at different spatio-temporal scales (i.e. corridor, alluvial bar and individual). At the corridor scale, we searched for the topographic signature of riparian vegetation in the landscape, using photogrammetric and LiDAR data. At the intermediate alluvial bar scale, we investigated the aptitude of three dominant pioneer riparian Salicaceae species (*P. nigra*, *S. purpurea* and *S. alba*) to establish and to act as ecosystem engineers by trapping fine sediment. At the finest, plant trait scale, we quantified the relation between response trait attributes of young *P. nigra* plants and their exposure to three different levels of mechanical stress (a highly exposed bar-head, a less exposed bar-tail, a chute channel). We identified some difficulties or failures to properly apply photogrammetry in biogeomorphic feedback studies. However, photogrammetry appeared as a useful tool to quantify a set of relevant parameters to respond to fundamental research questions concerning biogeomorphic feedbacks at the three nested spatial scales. At the broadest, the topographic signature of vegetation was not easy to capture because of the complex shifting mosaic of landforms of the Allier River. However, by focusing on more connected, restricted areas (i.e. alluvial bars), the signature of vegetation could be captured. It

seems to increase with increasing vegetation height corresponding to the evolutionary phases of the fluvial biogeomorphic succession (FBS) model. At the intermediate, alluvial bar scale, biogeomorphic feedbacks could be well identified. The capacity of riparian plants to establish and act as ecosystem engineers depended both on species and their physiognomy, their age and their location on alluvial bars. At the finest, individual plant scale, we captured the contrasting morphological and biomechanical response of *P. nigra* to variable mechanical stress exposure from a trait perspective. In all hierarchical levels, scale-related biogeomorphic feedbacks were detected and described in a conceptual model. The three scales were considered as cycles composed of four different phases, which can have a variable temporality. The broadest spatio-temporal scale represents the evolution over several decades of the landscape mosaic resulting from the balance between constructive (vegetation establishment, growth and succession) and destructive (floods) forces. The intermediate spatio-temporal scale can be described as the internal biogeomorphic succession of vegetation patches, corresponding to the transition between the geomorphic, pioneer, biogeomorphic and ecological phase of the FBS. Finally, the finest spatio-temporal scale represents the life cycle of engineer plants, during which engineer plants are adapting to hydrogeomorphic processes that lead them to reach their window of opportunity and afterwards to cross their engineering threshold. Scales are linked by top-down and bottom-up interactions. Our findings highlight the importance of considering the role of biogeomorphic processes occurring at fine scale on those occurring at broad scale and *vice versa*.

Keywords – fluvial biogeomorphology, multi-scale, feedback, ecosystem engineer, Allier River.

Résumé / Mots-clés

Résumé – Dans les écosystèmes, tels que les rivières, les marais salés, les mangroves, les dunes côtières, qui sont exposés à des flux hydrogéomorphologiques fréquents et réguliers (c'est-à-dire à des perturbations physiques), des rétroactions se mettent en place entre la géomorphologie (eau, sédiments et formes fluviales) et les plantes (par exemple *Populus nigra* L., *Salix alba* L., *Salix purpurea* L. dans les rivières). L'établissement de la végétation est contrôlé par des processus hydrogéomorphologiques qui, en retour, sont modulés par la végétation. De telles rétroactions contrôlent la dynamique des écosystèmes riverains. Dans cette thèse, nous avons abordé deux questions principales afin de mieux comprendre les rétroactions entre la végétation riveraine et les processus hydrogéomorphologiques : (i) comment la végétation riveraine répond-elle aux contraintes hydrogéomorphologiques ? (ii) comment et dans quelle mesure les plantes ingénieures, une fois établies, affectent-elles la géomorphologie fluviale ? Nous avons étudié ces questions sur la rivière Allier (France) à travers une approche emboîtée multi-échelles allant de l'échelle du patron paysager au trait de plante. Nous avons testé l'applicabilité de la méthode de photogrammétrie pour quantifier la réponse et l'effet de la végétation riveraine et des rétroactions biogéomorphologiques à différentes échelles spatio-temporelles (corridor, banc alluvial et individu). À l'échelle du corridor, nous avons recherché la signature topographique de la végétation riveraine dans le paysage, en utilisant des données photogrammétriques et LiDAR. À l'échelle intermédiaire du banc alluvial, nous avons étudié l'aptitude des trois espèces pionnières dominantes riveraines de Salicaceae (*P. nigra*, *S. purpurea*, *S. alba*) à s'établir et à agir comme ingénieurs d'écosystème en piégeant les sédiments fins. À l'échelle la plus fine du trait de plante, nous avons quantifié la relation existante entre les attributs de trait de réponse des jeunes plantes de *P. nigra* et leur exposition à trois niveaux différents de stress mécanique (tête de banc fortement exposée, queue de banc moins exposée, chute alluviale). Nous avons identifié les difficultés et les erreurs à ne pas commettre pour appliquer correctement la photogrammétrie dans les études des rétroactions biogéomorphologiques. En tout état de cause, la photogrammétrie s'est avérée être un

outil performant pour quantifier un ensemble de paramètres pertinents pour répondre à des questions de recherche fondamentale aux trois échelles spatiales considérées. À l'échelle la plus large, la signature topographique de la végétation est particulièrement difficile à identifier en raison de la dynamique complexe des formes fluviales de la rivière Allier. Cependant, en concentrant les observations sur des zones de taille réduite et fortement connectées (bancs alluviaux bordant le chenal), la signature de la végétation a pu être identifiée par cette méthode. Elle semble augmenter avec la croissance de la hauteur végétale (progression temporelle de la succession biogéomorphologique), ce qui est en accord avec le modèle de succession biogéomorphologique fluviale (SBF). À l'échelle intermédiaire du banc alluvial, les rétroactions biogéomorphologiques pouvaient être bien identifiées. La capacité des plantes riveraines à s'établir et à agir comme ingénieurs d'écosystème dépend à la fois des espèces et de leur physionomie, de leur âge et de leur position respective sur les bancs alluviaux. À l'échelle la plus fine de l'individu, nous avons capturé la réponse morphologique et biomécanique contrastée de *P. nigra* à l'exposition aux différents niveaux de contrainte mécanique d'un point de vue de trait. Dans tous les niveaux hiérarchiques, des rétroactions biogéomorphologiques liées aux échelles ont été détectées et synthétisées dans un modèle conceptuel. Aux trois échelles, nous avons considéré qu'elles prennent la forme de cycles composés de quatre phases distinctes et qui peuvent avoir une temporalité variable. L'échelle spatio-temporelle la plus large représente l'évolution de la mosaïque paysagère sur plusieurs décennies résultant de l'équilibre entre les forces constructives (établissement de la végétation, croissance et succession) et destructrices (crues morphogènes). L'échelle spatio-temporelle intermédiaire est la succession biogéomorphologique des taches de végétation, qui correspond à la transition entre les phases géomorphologique, pionnière, biogéomorphologique et écologique de la SBF. Enfin, l'échelle spatio-temporelle la plus fine représente le cycle de vie des plantes ingénieures, au cours duquel ces dernières s'adaptent aux processus hydrogéomorphologiques qui les conduisent à saisir leur fenêtre d'opportunité et à franchir ensuite leur seuil d'ingénierie. Les échelles sont liées par des interactions *top-down* et *bottom-up*. Nos résultats soulignent l'importance de considérer le rôle des processus biogéomorphologiques se produisant à une échelle fine sur ceux se produisant à une échelle large et *vice versa*.

Mots-clés – biogéomorphologie fluviale, multi-échelles, rétroaction, ingénieur d'écosystème, rivière Allier.

"…
Oh természet, oh dicső természet!
Mely nyelv merne versenyezni véled?
Mily nagy vagy te! mentül inkább hallgatsz,
Annál többet, annál szebbet mondasz. –
Késő éjjel értem a tanyára
Fris gyümölcsből készült vacsorára.
Társaimmal hosszan beszélgettünk.
Lobogott a rőzseláng mellettünk.
Többek között szóltam én hozzájok:
„Szegény Tisza, miért is bántjátok?
Annyi roszat kiabáltok róla,
S ő a föld legjámborabb folyója."
Pár nap mulva fél szendergésemböl
Félrevert harang zugása vert föl.
Jön az árviz! jön az árviz! hangzék,
S tengert láttam, ahogy kitekinték.
Mint az őrült, ki letépte láncát,
Vágtatott a Tisza a rónán át,
Zúgva, bőgve törte át a gátot,
El akarta nyelni a világot!"

Petőfi Sándor: A Tisza

"…
O Nature, glorious Nature, who would dare
with reckless tongue to match your wondrous fare?
How great you are! And the more still you grow,
the lovelier are the things you have to show!
Late, very late, I came back to the farm
and supped upon fresh fruit that made me warm,
and talked with comrades far into the night,
while brushwood flames beside us flickered bright.
Then, among other topics, I exclaimed:
„Why is the Tisza here so harshly blamed?
You wrong it greatly and belie its worth:
surely, it's the mildest river on the earth! "
Startled, a few days later in those dells
I heard the frantic pealing of the bells:
„The flood, the flood is coming!" they resound.
And gazing out, I saw a sea around.
There, like a maniac just freed from chains,
the Tisza rushed in rage across the plains;
roaring and howling through the dyke it swirled,
greedy to swallow up the whole wide world."

Sándor Petőfi: The Tisza (Kirkconnell Watson)

Summary

Remerciements

Je souhaiterai adresser mes remerciements aux personnes qui m'ont apporté leur aide et qui ont contribué à l'élaboration de cette thèse. Sans leur aide et leur soutien dans le travail et dans la vie de tous les jours, je n'aurais pas réussi à réaliser cette thèse.

Je tiens en particulier à remercier sincèrement mes directeurs de thèse, Jean-Luc Peiry et Dov Corenblit, qui m'ont guidée, conseillée et encouragée tout au long de la réalisation de ce doctorat. Je souhaite également remercier les membres du jury d'avoir accepté de porter un regard critique sur ce travail : Walter Bertoldi, Simon Dufour, Emmanuèle Gautier, Hervé Piégay et Michal Tal. Je remercie aussi Johannes Steiger, qui a suivi mon travail depuis le master, pour ses corrections rigoureuses, son calme rassurant et son écoute. Un grand merci à Franck Vautier et à Erwan Roussel, pour leur savoir-faire et leurs nombreuses aides sur des questions en géomatique mais aussi pour les conversations enrichissantes et toujours encourageantes.

Ma gratitude va également à l'ensemble des membres de Géolab, pour leur accueil, leur aide et leur sympathie. Un merci particulier à Olivier Voldoire qui s'est toujours rendu disponible pour répondre à mes questions concernant les missions de terrain et pour son aide sur l'installation de la station hydrologique. Aussi à Alexandre Garreau, qui m'a accompagnée sur le terrain quand j'en avais vraiment besoin. J'ai une pensée forte pour tous mes collègues et amis qui ont consacré du temps pour m'aider sur le terrain : Pierre-André Dejaifve (RNVA), Guillaume Leroux (LPO), Franck, Ana, Virginia, Paul, Gaspard, Arthur, Audrey, Denis, Benoit. Mention spéciale à Pierre-André (pour sa gentillesse, son soutien et les discussions enrichissantes), à Virginia (pour nos discussions scientifiques et personnelles, son aide sur R, la soirée scrapbooking…) et à Denis (pour notre travail commun, son endurance pour continuer à déterrer des peupliers seul quand je n'y arrivais plus à cause du mal de dos, sa bonne humeur, ses encouragements, ses idées de recettes et son aide pour leur réalisation). La vie quotidienne agréable au laboratoire avec les déjeuners accompagnés de la lecture de l'horoscope de La Montagne *était importante pour moi et m'a fortement aidée pour arriver au bout de cette thèse. Merci Chantal,*

Irène, Aude, Ana, Estelle et Yannick pour ces moments conviviaux qui m'ont permis de recharger les batteries, merci Audrey d'avoir fondé le club des gourmets et de nous avoir cuisiné des petits plats de nombreuses fois et bien évidemment merci à mes collègues doctorants (Paul-Edgar, Alfredo, Adrien et Loïc) pour la bonne ambiance qui régnait dans notre bureau. Merci aussi à Marie-Françoise André pour son écoute et ses conseils. La liste des personnes sympathiques que j'ai côtoyées à la MSH et qui m'ont aidée et soutenue au moins avec quelques mots gentils serait aussi longue (Paul, Aline, Zulimar, Marion, Bertrand…). Un énorme merci à Claude pour la mise en page de la thèse.

J'adresse enfin mes plus sincères remerciements à mes amis et à ma famille, qui m'ont soutenue et encouragée tout au long de ces années, de près ou de loin. Merci à Sandra, Ana, Coline, Valentina, Audrey, Erwan, Franck, Camille, Alexis, Coco, Jana, Karoline, Élodie, Thomas, Julcsi et à ma famille de m'avoir « supportée » quand mon moral était à zéro. Merci pour toutes les formes de vos encouragements et pour les moments que nous avons pu passer ensemble (discussions autour d'un verre, repas, sorties VTT, rugby, voyages, conférences, workshops…). Il m'est impossible de détailler ici toutes les aides dont vous m'avez fait bénéficier tant elles sont nombreuses.

Köszönöm!

Chapter I. Introduction

"Space and time lie at the heart of geomorphology."
Pauline R. Couper

1. General Introduction

In ecosystems such as rivers, salt marshes, mangroves, coastal dunes which are frequently exposed to frequent and regular hydrogeomorphic fluxes (i.e. physical disturbances), feedbacks between geomorphology (water, sediment and landforms) and plants (e.g. *Populus nigra* L.*, Salix alba* L.*, Salix purpurea* L. in rivers from the Nothern hemisphere) can occur (Corenblit et al., 2015a). Under certain conditions, the interaction between the physical disturbance regime and plant characteristics can represent the main driver of the ecosystem structure (i.e. habitat properties and species assemblage) and function. Such dynamic ecosystems, where engineer plants respond to and affect hydrogeomorphic processes, have been defined as *'biogeomorphic ecosystems'* (BE) (Balke et al., 2014; Corenblit et al., 2015b). Within BEs, the synergetic construction of fluvial landforms and vegetation succession have been described within the ecosystem engineer framework as a *'biogeomorphic succession'* (Corenblit et al., 2007). The fluvial biogeomorphic succession (FBS) model comprises four phases of biogeomorphic ecosystem development: (i) *geomorphologic phase* (creation of bare alluvial bars, either newly or through the destruction of present vegetation; exclusive control of hydrogeomorphic processes on fluvial landform dynamics and diaspore dispersal (Wolman and Miller, 1960; Hughes, 1997)) (ii) *pioneer phase* (recruitment of vegetation on bare alluvial surfaces; strong unidirectional control of the hydrogeomorphic environment on seedlings survival and growth (Mahoney and Rood, 1998; Johnson, 2000; Guilloy-Froget et al., 2002; Francis et al., 2005; Stella and Battles, 2010)) (iii) *biogeomorphic phase* (establishment of vegetation; strong feedbacks between water flow, sediment dynamics and pioneer

riparian plants (Edwards et al., 1999; Bendix and Hupp, 2000; Gurnell, 2014)) (iv) *ecological phase* (maturation and stabilization of the riparian ecosystem; domination of biotic interactions such as competition (Pautou et al., 1997; Piégay et al., 2003)).

In rivers, which represent the biogeomorphic model studied in this thesis, hydrogeomorphic processes filter plant species thus controlling species composition at the community scale (Richter and Richter, 2000). Only few pioneer riparian woody plant species such as *Populus* spp. and *Salix* spp. in the northern hemisphere have the capacity to recruit and establish on alluvial bars in highly disturbed riparian environment (Gurnell, 2014). Beside their responses to the hydrogeomorphic constraints those engineer plants also affect hydrogeomorphic processes and landforms. Such dynamics lead to biogeomorphic feedbacks. The occurrence and the intensity of biogeomorphic feedbacks are strongly dependent on the flood regime, sediment transport and texture, topography but also on plants density, physiognomy, morphology, biomechanics, and species assemblage. Plants are not 'static' objects, they have the capacity to sense their environment and to adjust on the long, mid and instantaneous terms respectively their genotype, phenotype and morphological configuration depending on the geomorphic environment. Plant's adaptations or responses allow them to enhance resistance, resilience within ecosystems, where they are exposed to hydrogeomorphic disturbances.

The response to and the effect of vegetation on hydrogeomorphology can be overviewed from multiple spatio-temporal scales. Numerous biological parameters adjust to the geomorphic environment; from the scale of individual plants (e.g. morphological and biomechanical traits), through the patch scale (e.g. taxonomic composition, mean trait values and physiognomy of a population or community), and to the scale of the entire riparian community mosaic (e.g. floristic assemblages and related mean trait value and physiognomy of the communities). Geomorphic changes caused by vegetation effects on hydrogeomorphic processes also occur at different spatio-temporal scales, e.g. the formation of sediment tails (i.e. obstacle marks, (Rodrigues et al., 2007)) downstream isolated trees during single flood events; the formation of pioneer fluvial islands at the cohort and community scales over several years; and the formation of a dynamic steady state fluvial landscape mosaic over several decades (Corenblit et al., 2016b; Garófano-Gómez et al., 2017). For a better understanding and quantification of feedbacks between fluvial geomorphology and riparian vegetation, the quantification of relevant geomorphic and biological parameters is necessary at different nested spatio-temporal scales (Salo, 1990; O'Neill et al., 1991; de Boer, 1992; Bendix, 1994; Phillips, 1995).

The corridor scale is concerned with feedbacks occurring between parameters describing the mosaic of vegetation communities corresponding to different habitat

conditions and stages of succession and the mosaic of geomorphic units (e.g. main and secondary channels, fluvial islands, benches, active tract, and floodplain levels). The bar scale is concerned with feedbacks between parameters describing the physiognomy and taxonomic consitution of a cohort or community and the morphology and texture of related meso-scale fluvial landforms such as vegetated strips (Gurnell et al., 2012), pioneer islands (Gurnell et al., 2001) and wooded benches (Erskine et al., 2009). The micro-site scale is concerned with feedbacks between individual plant morphological and biomechanical reponse attributes and more or less coalescent obstacle marks (sediment tails) generated by these plants. Traits are defined as morphological, biomechanical, physiological and phenological plant properties which can be measured at the level of individuals. An "attribute" is the value or the modality taken by a trait (*sensu* Violle et al. (2007)). Within a biogeomorphic perspective we can distinguish response, effect and feedback traits. "Response trait" represents attribute changes in response to the environmental conditions (e.g. water flow, sediment erosion, transportation, deposition), while "effect traits" are those that influence environmental conditions (e.g. flow characteristics, geomorphic landforms), community or ecosystem properties. "Feedback traits" develop in response to environmental modifications induced by the plant itself (Corenblit et al., 2015b). A cross-scale analysis which combines geomorphic and biological parameters at the three different scales requires: (i) the development of an appropriate conceptual framework and (ii) appropriate field, spatial and statistical methods and tools for testing it (Tormos et al., 2011; Dufour et al., 2012).

A biogeomorphic conceptual framework is proposed here to study feedbacks between geomorphology and riparian vegetation at different spatial scales, i.e. corridor, bar and micro-site (Figure 1). These three spatial scales are considered to be relevant because at each of these scales, the congruency between geomorphic and biological processes lead to a characteristic biogeomorphic feedback that relates to (i) the initial hydrogeomorphic effect on vegetation; (ii) the vegetation's effect on geomorphology; (iii) the feedback (vegetation's response to the modification it induced itself onto geomorphology) (Figure 1).

As mentioned before, plants are adapting their morphology and biomechanics depending on the geomorphic environment. These morphological changes will influence their capacity to establish on alluvial bars and their aptitude to enhance fluvial landform construction such as wooded pionner fluvial islands and benches. Interactions between plants and hydrogeomorphic processes occurring at individual scale might have an effect on those occurring at larger scale on a longer time period within the fluvial corridor. To understand such bottom-up and top-down biogeomorphic processes, it is crucial to

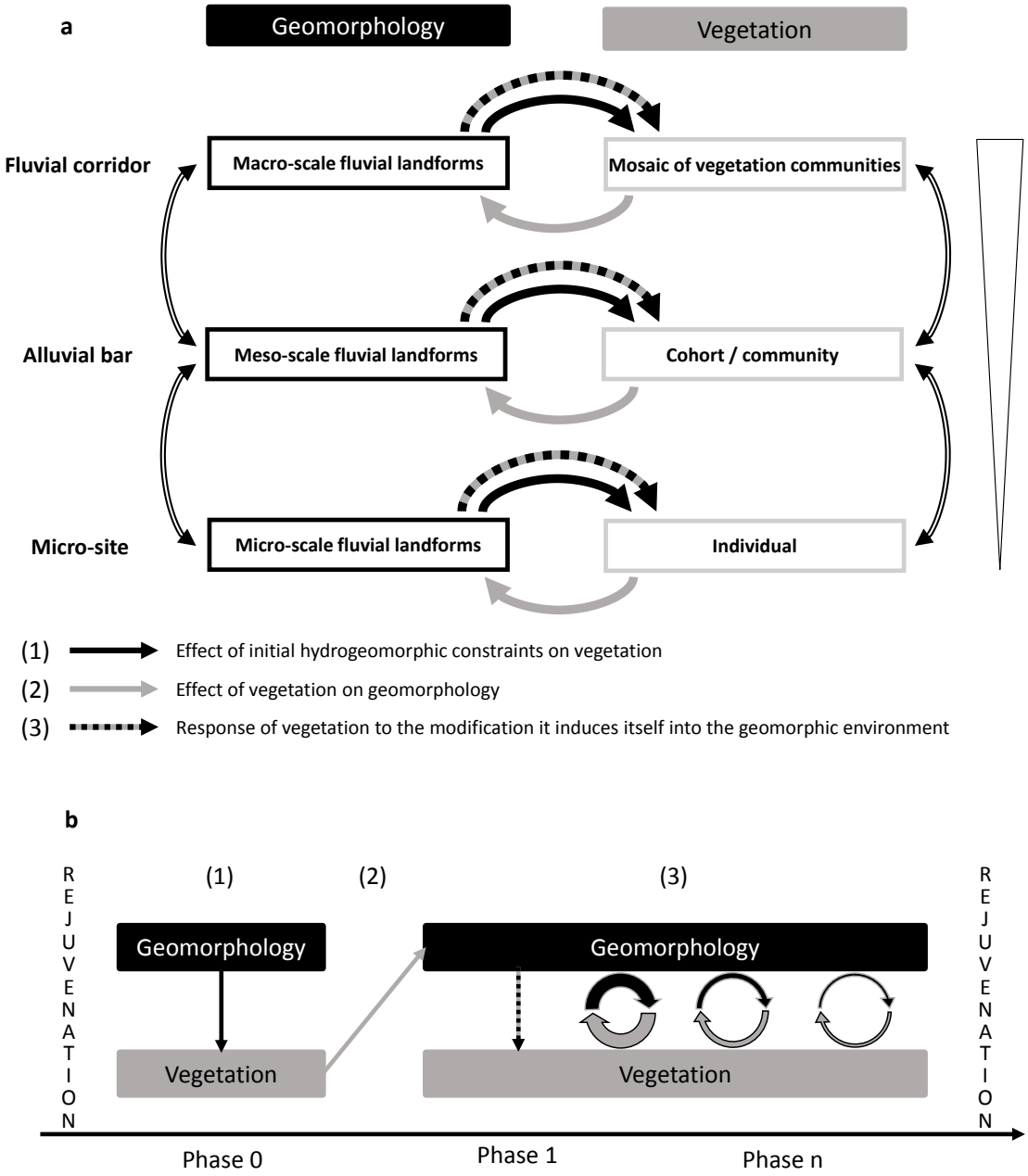

Figure 1. a) Biogeomorphic conceptual framework with three nested spatial scales: feedbacks between geomorphology and vegetation occur between the related components at the corridor, bar and micro-site scales. b) From an initial stage (bare sediment after rejuvenation) where (1) freshly deposited sediment allows vegetation recruitment. (2) Once established, vegetation modifies geomorphology, for example by enhancing sediment trapping. (3) Finally, vegetation responds to the modification it induced itself into the geomorphic environment and feedback loops between geomorphology and vegetation occur. Initially, feedbacks are strong but slowly decrease during the progression of the biogeomorphic succession until the next rejuvenation resets the system to its initial phase.

get a quantification of key processes occurring from individual scale, i.e. morphological and biomecanical plant response to hydrogeomorphic constraints to their effects at the scales of alluvial bars and fluvial corridor.

The proposed conceptual model can be applied to high to intermediate energy rivers (island braided, wandering and free meandering with respective specific stream powers ranging from 300 to 30 to W m^{-2}) where vegetation has the capacity to act as a physical ecosystem engineer but can still be removed during flood events (Gurnell et al., 2012).

The methods of lasergrammetry and photogrammetry will be texted in this thesis for studying feedbacks bertween riparain woody vegetation and geomorphology. These methods are currently providing high accuracy information on the height of the earth's surface, including vegetation. These data allow to classify vegetation by its height, and identify the different phases of the biogeomorphological succession. These fast developing methods are opening new opportunities in biogeomorphic studies to work at different spatio-temporal scales. For example, aerial photogrammetry can be applied for broad scale analysis and also opens opportunity to exploit historical aerial images, while terrestrial photogrammetry can be used for studies at individual scale.

In this thesis, key components of the biogeomorphic conceptual framework with the three nested spatial scales presented will be tested. Chapter one represents the state of the art and the conceptual framework of the thesis. In the second methodological chapter, the applicability of the photogrammetry to quantify the effect and the response of riparian vegetation and biogeomorphic feedbacks from corridor to trait scale (three spatial scales) will be presented (Figure 2). This chapter highlights the importance of methodological development in fluvial biogeomorphology for research applied at multiple spatio-temporal scales, such as the development of photogrammetry. The third chapter is a case study at corridor scale exploring the topographic signature of riparian vegetation, using photogrammetric and LiDAR data. The fourth chapter, will give the most complete analysis of vegetation effect and response and will cover the topic of feedbacks in certain degree at the intermediate scale of alluvial bar. An analysis of response traits will be presented in the fifth chapter including the topic of feedbacks in certain degree.

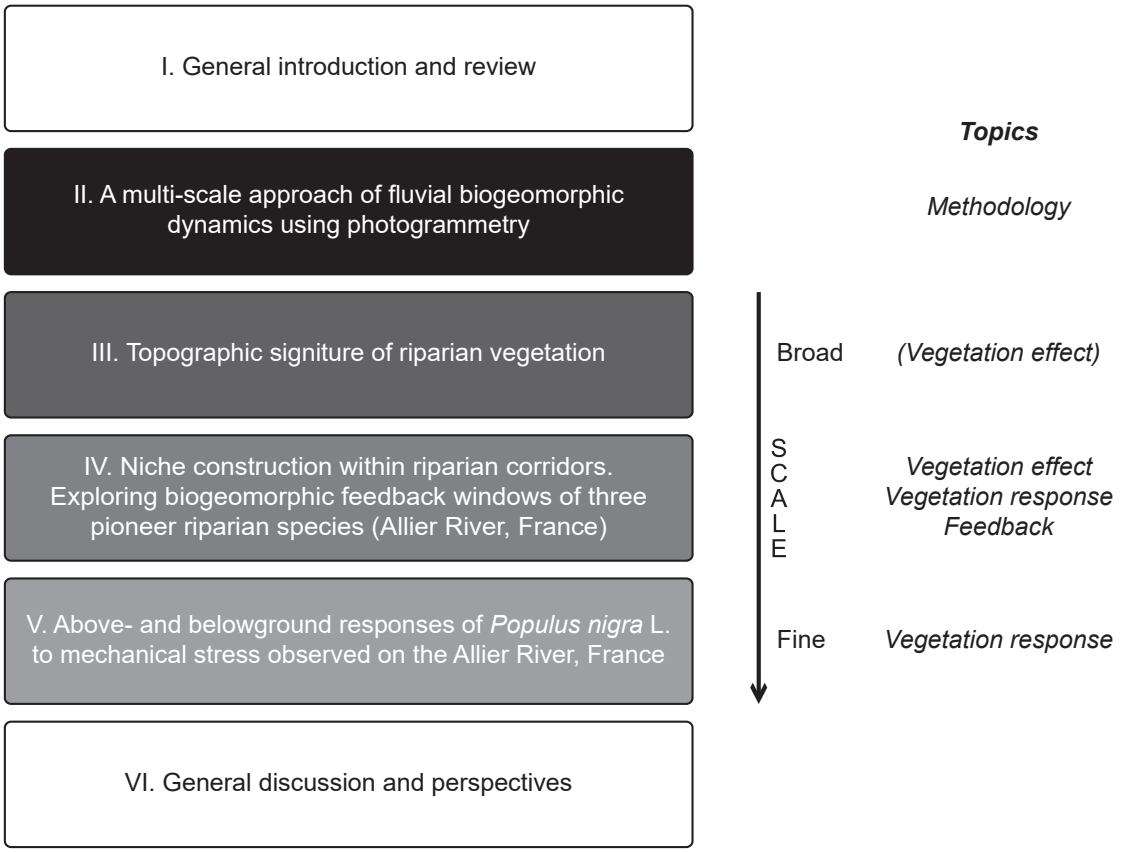

Figure 2. Overall presentation of thesis chapter and their key topics.

2. Review

2.1. Scale

There is a relation between the size of landforms and their temporal persistence (Schumm and Lichty, 1965; Frissell et al., 1986). Processes which are occurring at short time and fine spatial scale have an influence on long time and broad spatial scale processes (Lane and Richards, 1997). However, linking together the processes occurring at the different spatio-temporal scales is emphasized to be a challenge, such as for example the relative importance of fine scale processes on boarder scale processes. The discipline of biogeomorphology in particular is concerned with such challenge (Phillips, 1995; Eichel, 2017a; Stallins and Corenblit, 2017). As described earlier, there are many reciprocal interactions (i.e. feedbacks) between abiotic and biotic component of the landscape at different spatial scales from micro to global scale (Bouma et al., 2013; Gurnell, 2014; Corenblit et al., 2015a). Important conceptual efforts were initiated to link fine scale abiotic-biotic feedbacks to broad scale landscape evolution, however, the

mechanisms of scale linkage is not yet sufficiently understood (Stallins, 2006; Gurnell, 2014). This question is crucial to be solved for a better understanding and modeling of resistance and resilience capacity of biogeomorphic ecosystems (e.g. rivers), modulated by biogeomorphic feedbacks at multiple spatio-temporal scales.

In the first part of this scale section, a general overview with definitions will be given about scale in geomorphology and ecology. In the second part of this section, the review will be focused on river and biogeomorphic systems. Selected examples are given for rivers, first considered as an abiotic system. Then, selected relevant frameworks integrating hydrological, geomorphic and ecological components are presented. Specific examples were also selected here for their special focus on vegetation integration into scale concepts.

2.1.1. The notion of scale in geomorphology and ecology

Scale is the spatial and temporal dimension of an object (Turner et al., 1989). According to Habersack (2000) "the term scale refers to a characteristic time or length, and the process of scaling means to change the scale in space or time". Scale issue is a common topic in geomorphology (de Boer, 1992; Church, 1996), landscape ecology (Urban et al., 1987; O'Neill et al., 1989; Turner et al., 1989), river science (Ward, 1998; Latterell et al., 2006; Thorp et al., 2006), as well as in biogeomorphology (Phillips, 1995; Bouma et al., 2013; Eichel, 2017a), since the interest of these disciplines covers board range of time and spatial scales. It is essential to study complex systems through multi-scale approaches to understand the spatial pattern and the variety of physical and ecological processes operating (Urban et al., 1987; Wu, 1999). Analysing the system at only one scale may lead to misinterpretation or misunderstanding of its structure and function (Allen and Starr, 1982; Parsons and Thoms, 2007). The most important is to apprehend how the system description alters across multiple scales (Levin, 1992).

De Boer (1992), in his review on hierarchy, defined the geomorphic system as a result of the interaction of processes operating at multiple levels, and which levels can be dominant or secondary. A geomorphic system is a nested, hierarchical structure: 'every geomorphic system consists of, and physically contains, a hierarch of ever smaller, lower-level systems, but is at the same time part of, and physically contained by, a hierarchy of ever larger, higher level systems'. The idea of hierarchical systems (i.e. interacting components are the components of a larger system) was suggested by (Allen and Starr, 1982; O'Neill, 1986) in ecology, presenting a useful theoretical basis for explaining scale problem (Wu and Loucks, 1995).

Other important theory offering a way to deal with spatial heterogeneity was the 'pattern-process hypothesis' proposed by Watt (1947) which, by combining with the hierarchy theory, led to the concept of patch dynamic (Wu and Loucks, 1995; Wu and Levin, 1997). In the hierarchical patch dynamic concept, the fundamental structural and functional unit is the patch, which can have multiple size, shape, successional stage, content, duration, structural complexity, and boundary characteristics at given scales (Wu and Loucks, 1995; Wu, 1999). The hierarchical patch mosaic is generated, maintained, modified and destroyed mostly by disturbances which operate over different spatio-temporal scales. In this nested hierarchical organisation, there are top down constraints imposed by higher level patches on lower level ones and bottom up constraints imposed by lower level patches on the higher ones (Wu and Loucks, 1995). Since the transferability between scales is decreasing with the number of intervening levels, the most suitable is to take into consideration only three adjacent levels: the focal patch level and the ones immediately above and below it (O'Neill et al., 1989; Wu and Loucks, 1995; Wu, 1999). The focal level relates to the characteristic scale of the phenomenon of interest, the higher level provides the boundary conditions, while lower level the initiating conditions. In ecological systems both nonequilibrium and stochastic processes are present, however they are relative and scale-dependent. More stochastic processes are expected to occur at finer scale (Wu, 1999). Frequently, patch processes of nonequilibrium operating in lower level create metastability at higher level (Wu and Loucks, 1995).

Ecosystems are considered as complex systems, because they are characterized by large number of components, nonlinear interactions, time delays and feedbacks, and spatial heterogeneity. From a perspective of scaling they are difficult to handle principally because of the complex interactions among components (Wu, 1999). One of the first challenge to understand complex systems is to identify the relative importance of the parameters influencing a process at given scales, since the relative importance of a parameter might vary between different scales. A second challenging point might be the translation across scales. Some approaches exist, such as bottom-up (e.g. reductionism, extrapolation) and top-down, depending if we want to predict phenomena at broader or at finer scales. However, translations within heterogeneous landscape appears to be limited (Turner et al., 1989). Slaymaker (2006) also emphasized the difficulty of scale linkage. The author pointed out five methods of identifying scaling relations in drainage basin sediment budgets, such as (i) fractal approach; (ii) theory hierarchy approach; (iii) non-linear dynamic systems approach; (iv) panarchy approach and (v) hybrid approach. The difficulty of scale linkage and translation may also be related to the phenomenon of emergence. Emergent properties within a system are higher level properties which cannot be predicted from lower level properties, for example by a reductionist approach (de Boer, 1992; Church,

1996; Harrison, 2001). In any open system with the presence of irreversible processes, emergent properties exist, such as within a geomorphological landscape (Harrison, 2001).

Beside the spatiality, the notion of scale also englobes the aspect of temporality. The interdependent space and time scale effect on geomorphic processes was recognized by Schumm and Lichty (1965) and called the principles of spatial and temporal causality (Phillips, 1995). Authors described the different type of variables operating at three time levels (high: 'cyclic time', middle: 'graded time' and low level: 'steady time'), where large scale factors are linked to long temporal scale and small scale factor to short time period (Schumm and Lichty, 1965). At different scales, there is a difference in the temporal response of the system to changes. There are two possible responses: the reaction time (i.e. a period of time between the disturbance and the beginning of morphological changes) and the relaxation time (i.e. the period of time between the morphological changes and the equilibrium) (de Boer, 1992). Reaction may occur immediately after disturbance (e.g. river bank's response to flood after critical shear stress/shear strength thresholds exceeding), or may be delayed (e.g. if exceeding the threshold relies on soil wetting or pore water pressure). The relaxation time can also be variable. For example the relaxation time of sand dunes after a wind storm is expected to be rapid, contrary to channel incision (Phillips and van Dyke, 2016). The return period of disturbance events are in general shorter than the reaction and relaxation times of a natural geomorphic system. Thus, a geomorphic system can be regarded as the accumulative results of previous disturbances (Wu et al., 2012). At large spatial scale a system should be studied over a long time period because larger spatial units have longer reaction and relaxation time, while small scale systems can be analysed over shorter timespans (de Boer, 1992; Harrison, 2001). In geomorphic systems, processes of low magnitude are operating on a fine scale and have a high frequency, and produce a smoother and more regular morphology. While processes of high magnitude are operating on a broad scale and have a low frequency in geomorphic systems, and produce a rather irregular morphology (de Boer, 1992). The problem of scale linkage also concerns time scale. Phillips (1995) called attention of biogeomorphologist to the possible differences which might exist between the time scale of vegetation changes and the one of geomorphic changes and thus the problem of linking processes operating at different time scales. The author proposed four approaches to respond to the problem and applied on a coastal plain.

2.1.2. Scale in fluvial systems and in biogeomorphology

Within riparian ecosystems, the natural disturbance regime (i.e. flood frequency, magnitude and timing) has a strong structuring role on geomorphic and ecological

patterns and processes. Riparian biodiversity is controlled by the interactions between hydrogeomorphic processes and geomorphic features (Ward, 1998; Stanley et al., 2010). Fine scale process studies are crucial for understanding riparian ecosystems dynamics, but they have to be replaced in their broader and long-term contexts (Dollar et al., 2007). The recognition of the importance of scale, hierarchy, spatio-temporal heterogeneity, complexity, variability and stochasticity within river systems (Ward, 1998; Benda et al., 2004; Dollar et al., 2007; Parsons and Thoms, 2007; Winemiller et al., 2010) leaded to at least a partial rejection of the one-dimensional, equilibrium ecohydrological frameworks, such as for example the River Continuum Concept (Vannote et al., 1980). The hierarchy theory was rapidly adopted to study riverine landscape (Frissell et al., 1986) and recognized as a useful concept to improve river conservation and management strategies (Parsons and Thoms, 2007). In the riparian context, numerous geomorphological classifications were based on a hierarchical system (Schumm and Lichty, 1965; Frissell et al., 1986; Montgomery and Buffington, 1998; Thoms et al., 2004). Frissell et al (1986) described the fluvial system as a nested hierarchical system composed of six hierarchical levels (watershed, stream, segment, reach, "pool-riffle" and microhabitat) where structures and processes occurring at small scale levels are constrained by the structures and processes occurring at larger scales (Figure 3). This framework incorporates riparian vegetation at reach scale as an element for classification.

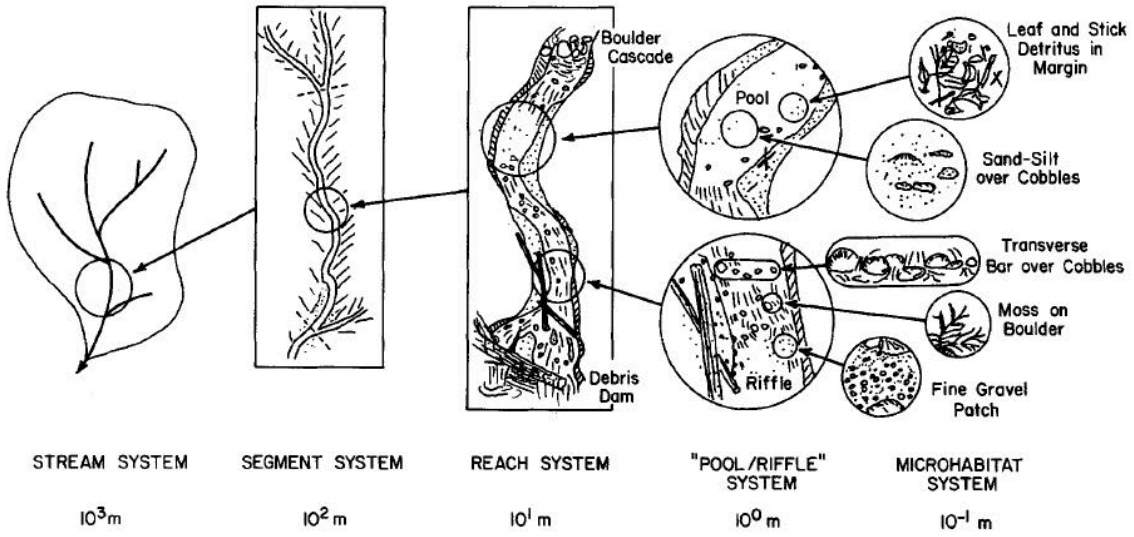

Figure 3. Hierarchical organization of a stream system and its habitat subsystems (Frissell et al., 1986).

Based on the multi-scalar framework of Frissell et al. (1986): segment (10^2 to 10^3 channel widths, W), reach (10^1 to 10^2 W), and morphological-unit (10^{-1} to 10^1 W), Pasternack and Wyrick (2017) quantified the spatial organization of topographic changes in river by using

near-census data. Near-census is a spatially explicit, process-based approach which uses for its basic building block the 1-m scale. The study was undertaken on a regulated river with the objective of advancing knowledge in river management. The authors demonstrated that the geomorphic impact of the dam on the regulated Yuba River (California, USA) is scale dependent. Thus studying processes at the wrong scale(s) might lead to misinterpretation. In the same vein, Thorp et al. (2006) proposed the framework called Riverine Ecosystem Synthesis (RES) with the aim to better understand ecological patterns within rivers across spacio-temporal scales. The RES integrated previous concepts, such as for example the hierarchical patch dynamics model of Wu and Loucks (1995) which is a terrestrial landscape model and the eco-geomorphological framework of Thoms and Parsons (2002).

In an interdisciplinary context, important efforts were made to link biological and physical components within river systems (Parsons et al., 2003). Newson and Newson (2000) linked channel habitat types to spatial geomorphological scales while Parsons and Thoms (2007) applied the hierarchy theory to describe the link between river morphology parameters and the hierarchical pattern of deposited wood distribution. Thoms and Parsons (2002) combined hierarchical frameworks from three disciplines (hydrology, geomorphology and ecology). The aim of this work was to improve river management strategies by underpinning that hydrological modifications of different scales are resulting in multiples biological and physical responses in river systems (Figure 4).

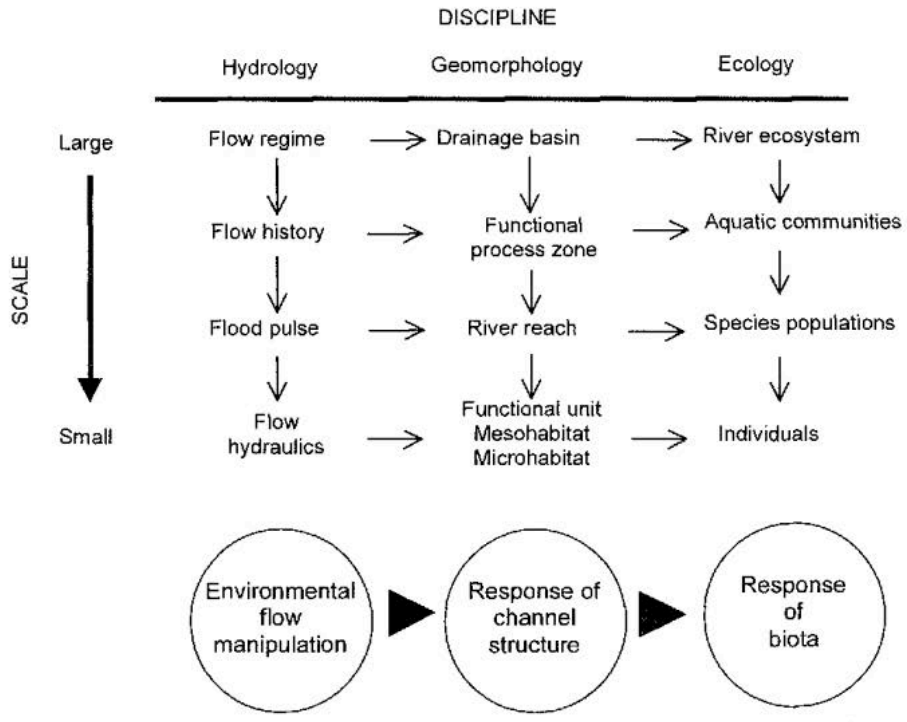

Figure 4. Multiscale relationships between hydrology, fluvial geomorphology and ecology (Thoms and Parsons, 2002).

Dollar et al. (2007) also proposed individual hierarchical frameworks composed of different levels of organizational for the domains of hydrology, geomorphology and ecology (Figure 5). The authors provided a multi-level flow chain model describing interactions between components and which allows to determine the outcomes of specific changes. This model has four main components: (i) the abiotic/biotic agent of change or driver; (ii) the template or substrate upon which the driver acts; (iii) controllers of the agent of change or driver and (iv) an entity or process that responds to the agent of change or driver. For example, the model could describe interactions between vegetation, flowing water and sediment type. However, it is crucial to specify the scale of process interaction, because from one scale to another a driver may become a responder and vice versa.

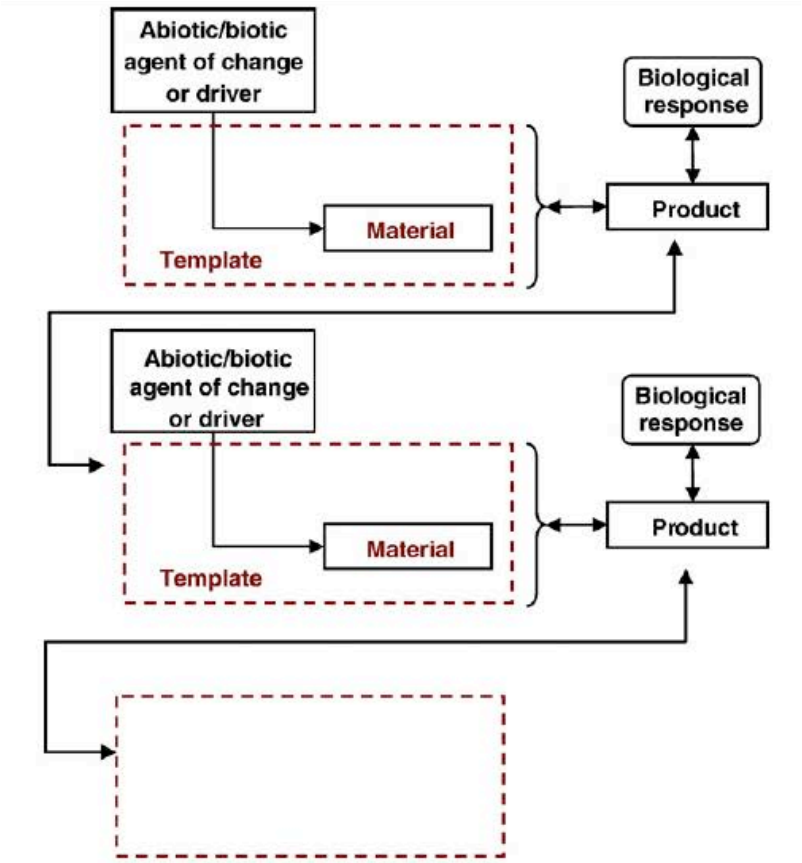

Figure 5. A flow-chain model for describing process interactions between subsystems and between different levels or scales within organizational hierarchies (Dollar et al., 2007).

Most recently, the REFORM framework was created to offer aid in river management and to gain a better process-based understanding of hydrogeomorphological processes (Gurnell et al., 2016). This is a multi-scalar, hierarchical framework rooted in previous frameworks. This hydrogeomorphic hierarchical framework which incorporates also

vegetation responses and effects is composed of 8 spatial scales (region, catchment, landscape unit, segment, reach, geomorphic unit, hydraulic unit and river element) and their indicative spatial extent and temporal scale of persistence/adjustment. At the finest scale (element scale) individual plants are considered (Table 1), which might be crucial to include for example following river management interventions when detailed data is necessary for monitoring.

Table 1. Spatial units included within the REFORM framework (Gurnell et al., 2016).

Spatial unit (alternative equivalent terms)	Indicative space and time scales	Description	Delineation criteria
Region (ecoregion, biogeographical region)	$>10^4$ km^2 $>10^4$ years	Relatively large area that contains characteristic assemblages of natural communities and species that are the product of the broad influence of climate, relief, tectonic processes, etc	Differences in main climatic variables and distribution of main vegetation types
Catchment (drainage basin, watershed)	$10^2 - 10^5$ km^2 $10^3 - 10^4$ years	Area of land drained by a river and its tributaries	Topographic divide (watershed)
Landscape unit (physiographic unit)	$10^2 - 10^3$ km^2 $10^2 - 10^3$ years	Portion of a catchment with similar landscape morphological characteristics (topography/landform assemblage)	Topographic form (elevation, relief–dissection, often reflecting rock type(s) and showing characteristic land cover assemblages)
Segment (sector)	$10^1 - 10^2$ km $10^1 - 10^2$ years	Section of river subject to similar valley-scale influences and energy conditions	Major changes of valley gradient Major tributary confluences (significantly increasing upstream catchment area, river discharge) Valley confinement (confined, partly-confined, unconfined) In mountainous areas, very large lateral sediment inputs
Reach	$10^{-1} - 10^1$ km (20+ channel widths) $10^1 - 10^2$ years	Section of river along which boundary conditions are sufficiently uniform that the river maintains a near consistent internal set of process-form interactions	Channel morphology (particularly planform) Floodplain features (minor changes in downstream slope, sediment calibre, may be relevant) Artificial discontinuities that affect longitudinal continuity (e.g. dams, major weirs/check dams that disrupt water and sediment transfer)
Geomorphic unit (morphological unit, mesohabitat, sub-reach)	$10^0 - 10^2$ m (0.1 – 20 channel widths) $10^0 - 10^1$ years	Area containing a landform created by erosion or deposition of sediment, sometimes in association with vegetation. Geomorphic units can be located within the channel (bed and mid-channel features), along the channel edges (marginal and bank features) or on the floodplain	Major morphological units of the channel or floodplain distinguished by distinct form, sediment structure/calibre, water depth/velocity structure and sometimes large wood or plant stands (e.g., aquatic/riparian, age class)
Hydraulic unit	$10^{-1} - 10^1$ m (5–20 D_{50}) $10^{-1} - 10^1$ years	Spatially distinct patch of relatively homogeneous surface flow and substrate character. A single geomorphic unit can include from one to several hydraulic units	Patches with a consistent flow depth/velocity/bed shear stress for any given flow stage and characterized by a narrow range in sediment particle size
River element	$10^{-2} - 10^1$ m ($10^0 - 10^1$ D_{50}) $10^{-2} - 10^0$ years	Element of river environments including an individual and patches of sediment particles, plants, wood	Significant isolated elements creating specific habitat types

Hough-Snee et al. (2015) showed that riparian plant community composition is intimately linked to environmental filters operating at multiple spatial scales, such as landscape, watershed and reach scales. Out of these three scales, the landscape scale filters showed up as the most responsible for shaping vegetation assemblage. The River Scaling Concept

(RSC) is a framework which can be applied to study processes and patterns of running water and considering abiotic and biotic components including the time dimension. It is based on a procedure of two steps. The first one is the downscaling phase, when abiotic conditions have to be studied from catchment-wide scale to point scale through sectional and local scales. The second step is the upscaling, when information of fine scale is interpreted at larger scales (Habersack, 2000). Cammeraat (2002) showed through two examples that linear upscaling cannot be used to understand the hydrogeomorphic response of catchments because thresholds and non-linear processes are involved at several scales. By comparing two contrasting areas, a semi-arid system in southern Spain and a humid temperate system in Luxembourg, the author identified the processes occurring at given scales and their connections between scales, leading to emergent properties.

A more recent and an alternative framework for the hierarchy theory to describe the behaviour of multiscale ecological system is the concept of panarchy (Holling, 2001). In the concept of panarchy, the hierarchical nested structure is composed of connected adaptive cycles. Smaller cycles (representing faster processes) experiment and test, while larger ones (representing slower processes) stabilise and conserve accumulated memory. The cycles are connected by two different linking mechanisms, by 'revolt' and 'remember'. This framework was recently successfully applied in biogeomorphic studies; for exmaple Stallins and Corenblit (2017) modelled resilience properties of barrier dunes at different spatio-temporal scales, while Eichel (2017a) applied it on lateral moraine slopes.

To our knowledge, there are very few studies where plant traits (*sensu* Violle et al., 2007) were linked to larger scale and to geomorphic changes. Simon and Collison (2002) studied the link between riparian vegetation effect on streambank stability. The authors encouraged further research on the link between plant species and more specifically their mechanical trait attributes and streambank stability. In a flume experiment, Bouma et al (2013) demonstrated that plant trait effect can be scale dependent and while plant engineering effect on sediment/topography leads to positive feedbacks at one spatial scale, it might lead to negative feedbacks on other scale. The occurrence of scale dependent feedbacks was also revealed within fluvial systems by showing the constructing and protecting role of engineer plants at local (in-site) scale and their erosive effect at off-site determining biogeomorphic organization at broad scale (Gurnell et al., 2005; Murray et al., 2008; Francis et al., 2009; Corenblit et al., 2015b). Recently, a trait based classification was provided by O'Hare et al. (2016) identifying groups of traits which are likely to affect sediment accrual or stabilization.

The existence of linkages between processes acting at fine scale (e.g. development of specific effect and response traits, ecosystem engineering of individual plants) and broad

scale (e.g. micro to patch scale landform construction and long term biogeomorphic feedbacks at the landscape scale) was also suggested in the domain of biogeomorphology (Parsons and Thoms, 2007; Corenblit et al., 2011, 2015a; Gurnell, 2014). As described earlier, Phillips (1995) underpinned the time scale differences between vegetation dynamics and geomorphic changes and proposed four theoretical approaches which can help to identify the temporal scale to consider for geomorphic and vegetation processes mutually and individually. A flume experiment on salt marsh species demonstrated how species-specific vegetation traits can influence broader scale geomorphic processes on salt marshes (Bouma et al., 2013). On lateral moraines the panarchy concept was applied to represent the functioning and the structure of a biogeomorphic ecosystem (Eichel, 2017b, 2017a). The author links biogeomorphic feedbacks from the ecosystem engineering scale (cm^2 - m^2; seconds to years), in particular the life cycle of *Dryas octopetala* L, to landscape scale (ha - km^2, decades to centuries).

2.2. The hydrogeomorphic control on riparian vegetation dynamic at multiple spatio-temporal scales

2.2.1. The effect of hydrogeomorphic disturbances on riparian vegetation

Disturbances are destructive events and environmental fluctuations occurring at different spatial and temporal scales that affect riparian vegetation community and its physical environment. Hydrogeomorphic disturbances within fluvial biogeomorphic ecosystems are characterized by their spatial extent, frequency, return interval, duration, predictability, magnitude intensity, severity and synergism (Pickett and White, 1985). Glasby and Underwood (1996) (in Lake (2008)) in the definition of perturbation incorporated both the disturbance and its consequence, the biotic response. Hydrogeomorphic disturbances related to water and sediment flows during floods and stress related mainly to droughts during low water stage have a major ecological influence on riparian environments (Steiger et al., 2005). These factors enhance environmental heterogeneity and biological, diversity (Ward, 1998; Lake, 2008). Hydrogeomorphic processes associated with the disturbance regime within river corridors are submersion, erosion, transport and accumulation of sediment. These processes control vegetation dynamics by the creation of bare soil for colonisation and destruction of vegetated areas. They also influence access to water and nutrient and the exposure to mechanical constraints. They thus control recruitment and establishment conditions (Hupp and Osterkamp, 1996; Poff et al., 1997). Hydrogeomorphic

processes influence riparian vegetation at different spatio-temporal scales from the broad, landscape scale to the fine, plant trait scales.

At landscape scale, habitat diversity in the riparian zone is related to the hydrogeomorphic disturbance regime with regular and repeated regeneration of plant succession associated with hydrogeomorphological fluxes (Petts, 1990). These disturbances are generating contrasted geomorphological patterns (fluvial style) and a highly dynamic landscape of habitat mosaic along river dimensions (Gregory et al., 1991; Ward, 1998; Osterkamp and Hupp, 2010). Classically, a four dimensional framework is employed to study riverine landscape unit functioning: longitudinal, transverse, vertical and temporal (Amoros et al., 1987; Ward, 1989; Camporeale et al., 2013). The respective influence of each type of process seems to be related mainly to the degree of exposure to hydrological disturbances (such as duration and frequency of submersion), i.e. hydrologomorphic connectivity. The intensity of the hydrological disturbance changes over a transverse gradient (decreasing from the channel to non-submersible terraces) and its main control factors are relative altitude and distance from the main channel. This transverse gradient of hydrogeomorphic connectivity can be considered as the main structuring factor of river dynamics within the fluvial corridor, and jointly from an ecological point of view the dynamics of plant communities succession (Pautou et al., 1997; Bendix and Hupp, 2000; Corenblit et al., 2007; Bornette et al., 2008). The riparian ecosystem develops in a contrasting way along the gradient. Close to the main channel (low altitude), exposed vegetation is generally the youngest or most recently rejuvenated, dominated by pioneer herbaceous or woody shrubs (e.g. poplars or willows). Moving away from the channel (increasing altitude), the average age of the vegetation increases (Gregory et al., 1991). The degree of exposure to floods along the transverse gradient is therefore a major factor influencing changes in vegetation composition in the river corridor, from the early phases to the mature phases (Pautou et al., 1997; Bendix, 1999; Bendix and Hupp, 2000). In fluvial context, ecological succession is considered as a stochastic process because of its low predictability linked to river flow stochastic behaviour (Corenblit et al., 2007). Ecological succession is driven by flood disturbances which can interrupt and reset succession, resulting to a dynamic and complex distribution of vegetation patches (Camporeale et al., 2013), which is termed the shifting habitat mosaic (Stanford et al., 2005).

Vegetation is exposed to prolonged submersions, mechanical destruction by flow and sediment burial. Hydroperiod (or annual flooding period) has a crucial role in diaspore dispersion, seed germination, seedling establishment and survival of vegetation due to anaerobic conditions associated with floods (Wharton et al., 1982). Water flow may also partially or completely destroy vegetation by uprooting (Brookes et al., 2000) or by

brakeage of the aerial parts (Bendix, 1999). Damaged vegetation can die or regenerate through vegetative processes (Brookes et al., 2000). The adaptability of plants to hydrogeomorphic constraints is species dependent. Salicaceae species are particularly well adapted to the fluvial environment thanks to their morphological (height, diameter, and number of stems), biomechanical (flexibility, resistance to breakage) and life history traits (Karrenberg et al., 2002). The total destruction of established vegetation leads to the regeneration of the succession, while the partial destruction induces regressions or accelerations in the process of maturation of species assemblages over time (Corenblit, 2006). The morphological and biomechanical characteristics of plants change in space and time (e.g. evolution from herbaceous stages to mixed structures and trees), their degree of resistance is thus also variable.

In the early stage of the biogeomorphic life cycle (the model which fusions the biological life cycle of plants and the biogeomorphic succession model (Corenblit et al., 2014)), successful colonisation by riparian plants depends on the relation between the hydrogeomorphic disturbance regime, initial habitat conditions, seed dispersal and seedling recruitment dynamics (Mahoney and Rood, 1998; Perona et al., 2012; Balke et al., 2014). The most favourable sites for recruitment are characterised by fine, moist sediment exposed to light, thus also exposed to flow pulses and annual floods (Cooper et al., 1999; Johnson, 2000). A conceptual vegetation recruitment model was proposed (*'recruitment box model'*) by Mahoney and Rood (1998) based on four key parameters of recruitment: (i) flow variability; (ii) period of seed dispersion; (iii) rate of stream stage decline; and (iv) elevation above the low stream stage. The modle showed that seedling recruitment is a stochastic processes very sensitive to hydrogeomorphic variability.

Studies treating the effect of hydrogeomorphic disturbances are mainly focusing on the link with vegetation succession at broad scale. For example, the freely meandering Allier river generates a diverse mosaic landscape with a regular regeneration of the vegetation depending on the hydro periods (Geerling et al., 2006; Garófano-Gómez et al., 2017). The modification of fluvial dynamics may cause durable geomorphological changes leading to modifications of the structure and the development riparian vegetation, as seen in Southern Italy (Aucelli et al., 2011). Recent studies have also demonstrated in gravel-bed rivers the regulating role of hydrogeomorphic connectivity on riparian vegetation recruitment. Whereas the expansion of already established vegetation is controlled by local climate conditions, especially the air temperature during the growing season (Räpple et al., 2017). At finer scale, during a key stage of vegetation colonisation (i.e. recruitment), hydrogeomorphic processes have a crucial role as described earlier by Mahoney and Rood (1998). Beside the conceptual model of Mahoney and Rood (1998),

field studies are also confirmed the determining role of fluvial processes on sexual and asexual reproduction (Johnson, 2000; Francis, 2006) and the influence of flow regulation on recruitment (Stella et al., 2004).

2.2.2. The response of vegetation to hydrogeomorphic disturbances

We can distinguish different plant response related to hydrogeomorphic perturbation based on the timing: resistance (immediate response during disturbance; e.g. canopy reconfiguration in the fluid, branch sacrifice) or resilience (delayed response between perturbations). Resilience has two forms: ecological and engineering. Holling (1973) defined the ecological resilience as the capacity of a system to maintain its structural and functional integrity in case of disturbance. The quality of the system to return to a state of equilibrium after a disturbance is described by the engineering resilience (Pimm, 1984; Carpenter et al., 2001; Gunderson et al., 2010).

Some vegetation species have developed specific response traits which allow them to adapt to fluvial environments and increase their resistce and resilience (Karrenberg et al., 2002; Lytle and Poff, 2004). Different kind of response traits exists, such as morphological, biomechanical, physiological and phenological. Response traits are influencing the survival and growth pattern of a plant during its life cycle; thus they might influence the ability of the plant to affect geomorphology and to induce biogeomorphic feedbacks from fine to broad spatial and temporal scale. Karrenberg et al. (2002) summarized the life history characteristics of Salicaceae which allow them to adapt to the regularly disturbed environment. For example, Salicaceae populations have a long seed dispersal period during the adequate period of the year that cops with the hydrological regime with an effective way of dispersion by running water and wind (Karrenberg et al., 2002). However recruitment is modulated at fine scale by multiple factors, such as for example the soil texture, stratigraphy and moisture (Shafroth et al., 2000). The vegetative reproduction is an adaptive response within a highly disturbed environment when reproduction by seeds is difficult (Barsoum et al., 2004). Such phenological response traits were filtered by the disturbance regime over a long time period (Corenblit et al., 2015a). Response traits express the adaptation of riparian vegetation to hydrogeomorphic constraints (Merritt, 2013). Once the recruitment is successful, it is mainly the morphological (growth rate, biomass, architecture; e.g. small and streamlined leaves and canopy) and biomechanical (stem flexibility; e.g. brittle stems with breaking points) response traits which contribute to the resistance and the resilience of the plant to hydrogeomorphic constraints (Corenblit et al., 2014, 2015a). Response traits can be recognized at different

spatial and temporal scales. At patch scale, Corenblit et al. (2016a) described differences in plant physiognomy within the up- and downstream part of *Populus nigra* L. cohorts on the Garonne River. The most exposed upstream part of the patch was composed of a higher number of stems which remained smaller than the one located on the protected part of the patch. Response traits are also varying in time. The morphology of *P. nigra* is evolving during the biogeomorphic succession from a rather flexible multi-stemmed architecture to a single semi-rigid one (Corenblit et al., 2014). At individual level, plants are adapting their above- and belowground morphology depending on the level of exposure to environmental factors, in particular the one related to hydrogeomorphic disturbances (Puijalon et al., 2011). Bywater-Reyes et al. (2015) demonstrated by a field experiment when testing the vulnerability of seedlings to uprooting, that plant traits related to seedling size (e.g. frontal area and root length) are correlated with uprooting vulnerability. Chapter V, based by an *in situ* experiment, will focus on such capacity of plants to adapt their morphology and biomecanics to hydrogeomorphic constraints.

2.3. *Riparian vegetation effect on hydrogeomorphology, the engineering role of riparian vegetation*

2.3.1. Ecosystem engineering

Living organisms (plants, animals and microorganisms) can affect geomorphological process by biostabilisation, bioconstruction, bioturbation and bioerosion at variable spatio-temporal scales (Butler, 1995; Naylor et al., 2002; Corenblit et al., 2007, 2011) and thus influence landscape evolution topography (Dietrich and Perron, 2006). Riparian vegetation has an influencing effect from local morphodynamics (micro site) to overall river morphology (Millar, 2000; Murray and Paola, 2003; Tal et al., 2004; Gurnell and Petts, 2006). It modifies flow properties and alluvial sediment cohesion, thus control erosion, transport and deposition process. With its aboveground part, vegetation increases substrate stability, thus prevents or delays erosion (Thorne, 1990; Abernethy and Rutherfurd, 1998; Camporeale et al., 2013). For example rivers banks with close to 20% by volume of roots can be up to 20 000 times more stable than those without vegetation (Smith, 1976). The fact that the trees improve the cohesion of the substrate is linked to two parameters. Roots, by mechanically fixing the sediments, increase the substrate cohesion and on the other hand they improve the drainage of the substrate making it more compact and therefore less subject to gravity movement (Tabacchi et

al., 2000; Corenblit, 2006). The aerial part of the vegetation also has an important role in stabilizing the substrate by modifying the flow field (Hickin, 1984; Bennett et al., 2008), thus promoting deposition and increasing the critical rate of sediment movement (Samani and Kouwen, 2002; Corenblit et al., 2009). Vegetation has a stabilizing role on the substrate, but at the same time, in the case of an overhanging position on the cohesive banks, it is subject to gravitational movements by adding surcharge. Thus, trees can also become channel instability factors (Abernethy and Rutherfurd, 1998; Camporeale et al., 2013). Bioconstruction is the accumulation of sediment and organic matter during floods induced by the presence of vegetation or wood debris (Corenblit et al., 2008). Surfaces covered by riparian vegetation have an increased roughness, thus during the flood period, flow properties are generally significantly modified (Hupp and Osterkamp, 1996; Tabacchi et al., 1998). Indeed, the vegetation functions as a dissipatif structure and reduces the height and the erosive power of the water layer, decreasing the shear stress and increasing fine sediment deposition (Gurnell and Petts, 2002). In general, where vegetation occurs in a dense matt, a higher sediment rates has been observed (Nanson and Beach, 1977), however, sedimentation rates also depends on other factors, such as distance from the main channel, duration of flood and the diameter of the plant (Steiger et al., 2001b, 2001a). If vegetation is capable to modify its hydrogeomorphic environment and generate feedbacks, it might also depend on which species are present. Combining the role of hydrogeomorphic factors and the species in fluvial landform construction and possible feedback generation on alluvial bars is leading us to the question of the effect of biogeomorphic functional diversity. Chapter IV will specifically tackle this topic.

Numerous researches have demonstrated the landform constructing effect of vegetation within fluvial context (Gurnell et al., 2005; Corenblit et al., 2007; Bertoldi et al., 2011). Organisms, which are modifying their physical environment and thus (directly or indirectly) are modulating the resource access to other species are called ecosystem engineers (Jones et al., 1994). It was suggested that some riparian plant species can act as ecosystem engineers and control riparian ecosystem structure and function by significantly modifying hydrogeomorphic processes, landforms and fluvial habitats (Edwards et al., 1999; Gurnell and Petts, 2002; Corenblit et al., 2007, 2011, 2014; Gurnell, 2014).

The effect of riparian vegetation on hydrogeomorphic processes can be studied at different spatio-temporal scales. Vegetation trapping sediment can induce topographic raise over a short period (few years), bank stabilisation and channel narrowing (Kondolf and Curry, 1986; Friedman et al., 1996; Johnson, 2000). The migration rate of the River Missouri, USA, along the unforested banks can be multiplied by three compared to the forested ones (Burckhardt and Todd, 1998). On the Tagliamento river, Bertoldi et al.

(2011) demonstrated the role of riparian vegetation in channel morphology. Bywater-Reyes et al. (2017) quantified the influence of woody riparian vegetation on channel topography at two nested spatial scales, at reach and patch scale. Authors demonstrated a strong link between vegetation density and topography at both spatial scales, however the correlation was weaker at boarder scale. The strongest multi-scale feedbacks appeared to be within the intermediate vegetation height range, when the alteration of hydrogeomorphic processes is the highest.

2.3.2. Effect traits

In studies about the ecosystem engineering role of plants, the role of species traits was highlighted (Bouma et al., 2013; Corenblit et al., 2015a). Plant traits which were identified to originate a significant effect in geomorphology, are named effect traits. Corenblit et al. (2015a) classified effect traits in three major groups: (i) traits which influence sediment retention and cohesion; (ii) traits which result fluid stress divergence and (iii) traits which induce physicochemical modifications and biogenic accumulation. A better knowledge about the effect trait is crucial, because ecosystem engineer plant species, potentially characterised by different traits, have an influence at broader scales within fluvial biogeomorphic ecosystems (habitat and landform mosaic dynamics and fluvial style). Such bottom-up effects were describe as self-organisation processes (Francis et al., 2009). Some examples have already be given at the section above about the stabilizing and bioconstructing role of vegetation. More specifically, plant morphological effect traits controling sediment dynamics were also investigated in fluvial context (Euler et al., 2014) and within salt marshes (Bouma et al., 2013), highlighting the role of traits such as for example the inclination, the permeability, the density and the flexibility of shoots. The study of Bouma et al. (2013) and others (Kui et al., 2014; Manners et al., 2015; Diehl et al., 2017b) underpinned the morphological differences between species leading to variable influence on landform dynamics. Experimental approaches also demonstrated the variable effect of plant traits (e.g. diameter, frontal area) on flow hydraulic alteration and thus on sediment transport (Nepf et al., 2013). Diehl et al. (2017a) classified 34 species into ecological and into morphological guilds. Guilds are “assemblages of plant species that are functionally similar” (Diehl et al., 2017a). Authors demonstrated, that there is a strong linkage between ecological response guilds and morphological effect guilds (which induce modification in topography). This result suggests a similitude between plants having similar response traits and their morphology, thus plants responding in a similar way to hydrogeomorphic constraints, are also modifying topography in a similar way. *Tamarix* and *Populus* species can be found in the same ecological and morphological

guilds during their earlier life history stages. On the other hand, some studies showed that proliferation of *Tamarix* in river floodplains for the disadvantage of native *Populus* can induce major geomorphic changes, as observed on the lower Green River (USA) (Birken and Cooper, 2006). At finer scale, experiments also demonstrated the higher capacity of *Tamarix* to enhance topographic changes (Kui et al., 2014; Manners et al., 2015). These researches highlights the importance of species-specific multi-scale studies. This is the context in which the Chapter IV lies. In that chapter, we will study the different response of three riparian species to hydrogeomorphic constraints which reflects a variable spatial distribution on alluvial bars and a variable physiognomy. In that chapter, we also demonstrate species-specific landform construction.

2.4. *Feedbacks between riparian vegetation and hydrogeomorphic processes at multiple spatio-temporal scales*

Vegetation is constrained by hydrogeomorphic processes, however the level of vulnerability to hydrogeomorphic processes is decreasing during its establishment. Consequently, by modulating landform properties, vegetation can actively control its vulnerability to hydrogeomorphic processes and thus its survival and growth (Gurnell and Petts, 2002). On a bar surface, Gurnell and Petts (2002) illustrated the relationship between aggradation and vegetation recruitment and growth by a conceptual model (Figure 6).

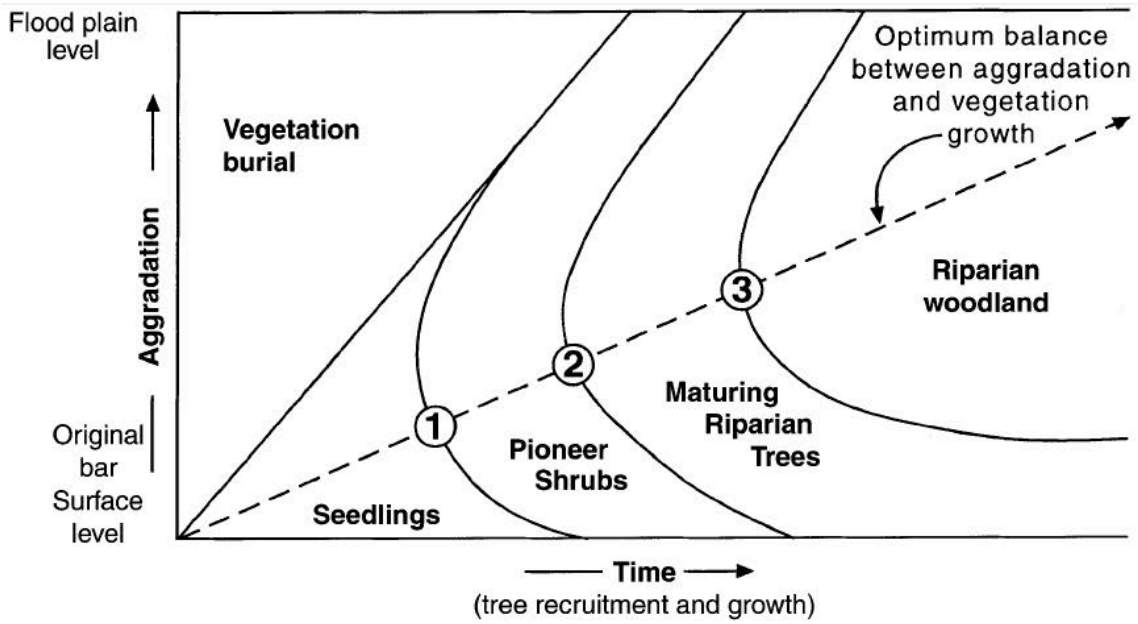

Figure 6. Schematic representation of the relationship between tree recruitment and growth and the rate of aggradation of a bar surface (Gurnell and Petts, 2002).

In biogeomorphic ecosystems, established vegetation can induce positive feedbacks between landform construction and vegetation growth. Corenblit et al. (2014) related to the FBS model the "*biological life cycle*" of *Populus nigra* L. to develop the concept of biogeomorphic life cycle. More specifically, this concept links *P. nigra* life stages from the dispersal of plant diaspore to the sexual maturity and the co-occurring hydrogeomorphic processes and landforms which control *P. nigra* population's dynamic. On the other hand, established *P. nigra* plants influence hydrogeomorphic processes leading to positive feedbacks between plant growth and fluvial landform construction. An example of a positive feedback is when the plant in response to a physical process (e.g. sediment accumulation) regulates its growth in a maner that increases its performence (Francis et al., 2009). In this case, regulated vegetation growth can be considered as feedback traits (Corenblit et al., 2015a). It was suggested, that positive feedbacks at patch scale can lead to the development of a functional biogeomorphic unit when pioneer riparian plants are growing together, in order to increase their anchorage and their growth performance. Individuals at the exposed, upstream part of the patch are offering a shelter resulting in a (i) higher patch resistance, (ii) higher chances to reach sexual maturity and (iii) to regenerate in freshly deposited sediment at downstream part of the patch leading to increased resilience (Corenblit et al., 2016a). Such functional biogeomorphic units were observed on the Tagliamento River, where deposited downed trees and sprouting driftwood enhance sediment accumulation, facilitate vegetation recruitment by a sheltering effect and originate island formation, thus increase biogeomorphic resilience (Gurnell et al., 2005). It was also shown, that vegetation patches contribute to their resilience by trapping fine sediment which forms obstacle marks and, at the same time, seeds transported by hydrochory (Corenblit et al., 2016b). From a functional trait based approach view, functional traits as "any trait which impacts fitness indirectly *via* its effects on growth, reproduction and survival" (Violle et al., 2007). Species which develop similar effect traits or response traits related to ecosystem processes, can be assigned into functional types (Lavorel and Garnier, 2002). Based on the theory of functional typology, O'Hare et al. (2016) generated a typology using an existing plant trait dataset as a basis. Authors distinguished two species categories based on their trait characteristics; (i) species which are rather induce sediment accumulattion and (ii) species which are able to stabilize sediment.

To place biogeomorphic feedbacks in a broad temporal scale, it was suggested that the biogeomorphic life cycle of pioneer engineer species should be viewed from an evolutionary perspective (Corenblit et al., 2014). Niche construction is the process, when organisms modify significantly their environment in a way that it alters the selection pressure resulting in an evolutionary response (Odling-Smee et al., 2003). *P. nigra* plants,

by trapping fine sediment, nutrient and organic matter, are modifying their environment and increasing their fitness, which might be considered as a positive niche construction (Corenblit et al., 2014).

Chapter II. A multi-scale approach of fluvial biogeomorphic dynamics using photogrammetry

Hortobágyi, B., Corenblit, D., Vautier, F., Steiger, J., Roussel, E., Burkart, A., Peiry, J.-L., 2017c. A multi-scale approach of fluvial biogeomorphic dynamics using photogrammetry. J. Environ. Manage. 202, 348–362. doi:10.1016/j.jenvman.2016.08.069

Abstract – Over the last twenty years, significant technical advances turned photogrammetry into a relevant tool for the integrated analysis of biogeomorphic cross-scale interactions within vegetated fluvial corridors, which will largely contribute to the development and improvement of self-sustainable river restoration efforts. Here, we propose a cost-effective, easily reproducible approach based on stereophotogrammetry and Structure from Motion (SfM) technique to study feedbacks between fluvial geomorphology and riparian vegetation at different nested spatio-temporal scales. We combined different photogrammetric methods and thus were able to investigate biogeomorphic feedbacks at all three spatial scales (i.e., corridor, alluvial bar and micro-site) and at three different temporal scales, i.e., present, recent past and long term evolution on a diversified riparian landscape mosaic. We evaluate the performance and the limits of photogrammetric methods by targeting a set of fundamental parameters necessary to study biogeomorphic feedbacks at each of the three nested spatial scales and, when possible, propose appropriate solutions. The RMSE varies between 0.01 and 2 m depending on spatial scale and photogrammetric methods. Despite some remaining difficulties to properly apply them with current technologies under all circumstances in fluvial biogeomorphic studies, e.g., the detection of vegetation density or landform topography under a dense vegetation canopy, we suggest that photogrammetry is a promising instrument for the quantification of biogeomorphic feedbacks at nested spatial scales within river systems and for developing appropriate river management tools and strategies.

Keywords – Fluvial biogeomorphologic feedbacks; stereophotogrammetry; structure from motion; multi-scale analysis; fluvial landforms; riparian vegetation.

1. Introduction

Within rivers, interactions between water, sediment and vegetation play an important role in fluvial and riparian landscape dynamics at large scales (fluvial corridor) (Hughes, 1997; Steiger et al., 2005). Interactions between these elements are generating feedbacks between fluvial landforms and vegetation dynamics (Corenblit et al., 2007). Hydrogeomorphic processes (water flow, sediment erosion, transport and deposition) affect vegetation dynamics negatively by reducing biomass, or positively by providing recruitment sites, nutrients and organic matter (Scott et al., 1997; Edwards et al., 1999; Francis et al., 2009; Stella et al., 2011; O'Hare et al., 2012). In turn, vegetation modulates water flow, sediment dynamics and landform topography (Gurnell et al., 2005; Corenblit et al., 2007; Bertoldi et al., 2011).

The fluvial biogeomorphic succession (FBS) model proposed by Corenblit et al. (2007) explicitly described the synergetic construction of fluvial landforms and vegetation succession as a transition between four phases (i.e., geomorphic, pioneer, biogeomorphic, ecological) of biogeomorphic organization. This model pointed to the necessity to better identify and quantify the geomorphic and biological parameters that strongly interact and generate biogeomorphic feedbacks within biogeomorphic ecosystems (Corenblit et al., 2015a). Biogeomorphic feedbacks relate to (i) the initial effect of hydrogeomorphic constraints on vegetation; (ii) the effect of vegetation on geomorphology; and (iii) the response of vegetation to the modification it induces itself onto geomorphology (Table 2). The analysis and comprehension of these feedbacks at a large scale also requires the quantification of relevant interrelated geomorphic and biological parameters at lower nested spatio-temporal scales (Salo, 1990; O'Neill et al., 1991; de Boer, 1992; Bendix, 1994; Phillips, 1995). Such a cross-scale analysis must be based on appropriate methods and tools adapted to quantify with high accuracy geomorphic as well as biological parameters.

Remote sensing supported by manned aircrafts, photography and later satellite data, has been used since the late 19th century to investigate landscapes (Jensen, 1986). Stereophotogrammetry (traditional photogrammetry) allows to generate three-dimensional information from overlapping stereo-pairs (Lane et al., 1993; Boureau, 2008; White et al., 2013). The method was widely applied in geoscience to extract accurate topographic data (Birdseye, 1940; Eardley, 1942; Lane, 2000; Chandler et al., 2002). Thanks to recent advances in photogrammetry, the development of Structure from Motion (SfM) technique provides a fast, low-cost and user-friendly technique to obtain three-dimensional data (Westoby et al., 2012; Micheletti et al.,

2015). In addition, within the last decades, classical remote sensing platforms were accompanied by the development of unmanned aerial vehicles (UAV) that range from huge autonomous planes to very small and cheap 'toys' (Anderson and Gaston, 2013). Recently, UAVs opened up new opportunities for the remote sensing of small regions. Because small UAVs are inexpensive, user friendly and can be quickly deployed in the field, a high monitoring frequency can be achieved permitting the monitoring of landscapes and landform changes on fine spatial scales (Rango et al., 2009; Hervouet et al., 2011; Dandois and Ellis, 2013; Dufour et al., 2013). SfM and stereophotogrammetry are operating on the same principles which is to use images acquired from multiple viewpoints in order to construct dense three-dimensional point clouds of a surface (Westoby et al., 2012; Fonstad et al., 2013). However, a major difference exists between the two photogrammetric methods. SfM uses image matching algorithms which are able to recognize conjugate features even in randomly acquired images despite the presence of significant variability of changes in image scale and in view point (Fonstad et al., 2013; Jensen and Mathews, 2016). In contrast, in traditional photogrammetry the user has to determine the camera positions and orientation and strips of images with approximately 60% of overlap acquired in parallel flight lines and observable control points in the images with known coordinates are required (James and Robson, 2012; Westoby et al., 2012; Fonstad et al., 2013; Micheletti et al., 2015). On one hand, a big advantage of the SfM method is the greater ease of use where expert supervision is unnecessary (black-box tool). On the other hand this results in much lower data quality control and makes it difficult or impossible to identify the origin of errors (Micheletti et al., 2015). Stereophotogrammetry is more time-consuming and requires a more expensive equipment and specialized user expertise, but has already proved its applicability for present and past fluvial biogeomorphic succession monitoring (Vautier et al., 2016). For a more detailed comparison between stereophotogrammetry and SfM technique, the reader is referred to Fonstad et al. (2013).

Within the riparian context, remote sensing imagery data such as orthophotos deliver information about the land cover, e.g., vegetation and river planform changes (Geerling et al., 2006; Petit, 2006; Corenblit et al., 2010; Carbonneau and Piégay, 2012). In complement, the three-dimensional information generated using photogrammetry allows for the description of vegetation height (Gong et al., 2000; Mitchell et al., 2007; Gillan et al., 2014; Jensen and Mathews, 2016) and fluvial landform topography (Lane, 2000; Carbonneau et al., 2003; Westaway et al., 2003; Woodget et al., 2015). Other recent tools such as LiDAR, were widely applied successfully to study riparian vegetation monitoring and topography (Mason

et al., 2003; Farid et al., 2006; Straatsma and Middelkoop, 2007; Antonarakis et al., 2008; Geerling et al., 2009; Arroyo et al., 2010; Bertoldi et al., 2011; Michez et al., 2013). The combination of photogrammetric DSMs at different acquisition dates with a recent LiDAR DTM offers detailed information about the evolution of vegetation height as well as about landform topography under vegetation cover if the topography remains stable during the period of interest (St-Onge et al., 2008; Véga and St-Onge, 2008). However LiDAR technology remains costly and does not allow retrospective studies in the case of highly dynamic and changing environments such as river corridors because of their very recent development, whereas many large archives of stereo aerial photographs exist (Marston et al., 1995; Miller et al., 1995; Rhemtulla et al., 2002; Fox and Cziferszky, 2008; Stepper et al., 2015) which allow to use stereophotogrammetry to study present and past fluvial biogeomorphic dynamics (Vautier et al., 2016).

The aim of this article is to (i) propose a standardized, cost-effective and easily reproducible approach based on photogrammetry to study feedbacks between fluvial geomorphology and riparian vegetation at different nested spatio-temporal scales; and (ii) evaluate the performance of photogrammetric methods on a diversified riparian landscape mosaic by targeting a set of fundamental parameters necessary to study those feedbacks. We will focus on landform topography and vegetation morphology which are two interrelated components of the fluvial biogeomorphic succession at three relevant nested spatial scales of the analysis of fluvial biogeomorphic ecosystems: (i) fluvial corridor (called hereafter: corridor); (ii) alluvial bar (called hereafter: bar); and (iii) micro-site. The application of photogrammetry for studying the biogeomorphic feedbacks at the three spatial scales will be discussed in relation with the fundamental questions listed in Table 2 and in relation with necessary parameters to quantify these feedbacks.

Table 2. The application of photogrammetrical methods at three nested spatial scales. For each of the three scales, we identified our main objectives and fundamental research questions related to fluvial biogeomorphic feedbacks discussed in this paper. The codes identify each research question and are used below in the results and discussion sections.

Spatial scale and main objectives	Code	Research questions
Corridor → to better understand how riparian vegetation succession adjusts to the current hydrogeomorphic disturbance regime (magnitude, flood frequency, duration and timing) and how in turn the vegetation affects macro-scale landform dynamics and the associated river style	C1	Following morphogenetic floods, how do the localization (x, y, z) and the disturbance regime affect the overall structure of the vegetation mosaic? How do morphogenetic floods affect the overall structure of the vegetation mosaic?
	C2	How does the vegetation mosaic structure affect the mosaic of geomorphic landform units and the associated river style?
	C3	How does the vegetation mosaic and therefore the vegetation succession respond to its proper changes it causes in macro-scale geomorphology?
Bar → to define feedbacks between cohort/ community physiognomy and the construction of meso-scale landforms such as pioneer islands and benches	B1	How do hydrogeomorphic constraints, locations for resource access (distance and elevation from main channel or secondary channel) and bar types affect vegetation patch physiognomy and plant growth rates?
	B2	How does vegetation patch physiognomy (e.g., surface cover, density, mean height, biovolume) affect meso-scale geomorphology (e.g., length, width and relative elevation to water level)?
	B3	How do vegetation patches respond to their proper changes they cause in meso-scale geomorphology?
Micro-site → to define feedbacks between plant traits and the micro-site (local) topography	M1	How do hydrogeomorphic constraints affect plant traits (e.g., height, width, frontal area, biovolume)?
	M2	How do plant traits affect micro-site geomorphology (e.g., length, width and sediment depth)?
	M3	How do individual plants respond in return to their proper changes they cause in micro-scale geomorphology?

2. Material and methods

2.1. *Study site*

The study reach is located in the lower Allier river, France, in the National Natural Reserve of the *Val d'Allier* (Figure 7). Here the gravel bed river is in a transitional, dynamic wandering state tending *versus* meandering and is characterized by lateral erosion in the outer bends of meanders and point bar formation in the inner bends with moderate

anthropogenic impacts (Petit, 2006; Dejaifve and Esquirol, 2011). Because of the very active lateral channel erosion and large gravel bar formation, landforms and vegetation succession have a high turnover which results into a spatially and temporally diverse landscape mosaic with a heterogeneous spatial distribution of vegetation patches of different sizes and ages (Geerling et al., 2006). The four phases of the biogeomorphic succession (see Corenblit et al. (2007) for a detailed description) are represented within the fluvial corridor and provide a good opportunity for testing the usefulness and the limits of photogrammetry to study feedbacks between geomorphology and vegetation that trigger fluvial biogeomorphic succession. The study reach also provides coherent landform units at the three spatial scales considered here, i.e., corridor, bar and micro-site scales. At the corridor scale, analyses were performed within the 10 km river reach (Figure 7a). A representative partially wooded point bar with a length of 780 m and a width of 270 m was selected within the 10 km long reach (Figure 7b). Two young poplar individuals of less than five years and their sediment tails (Figure 7c) were investigated on this point bar at the micro-site scale.

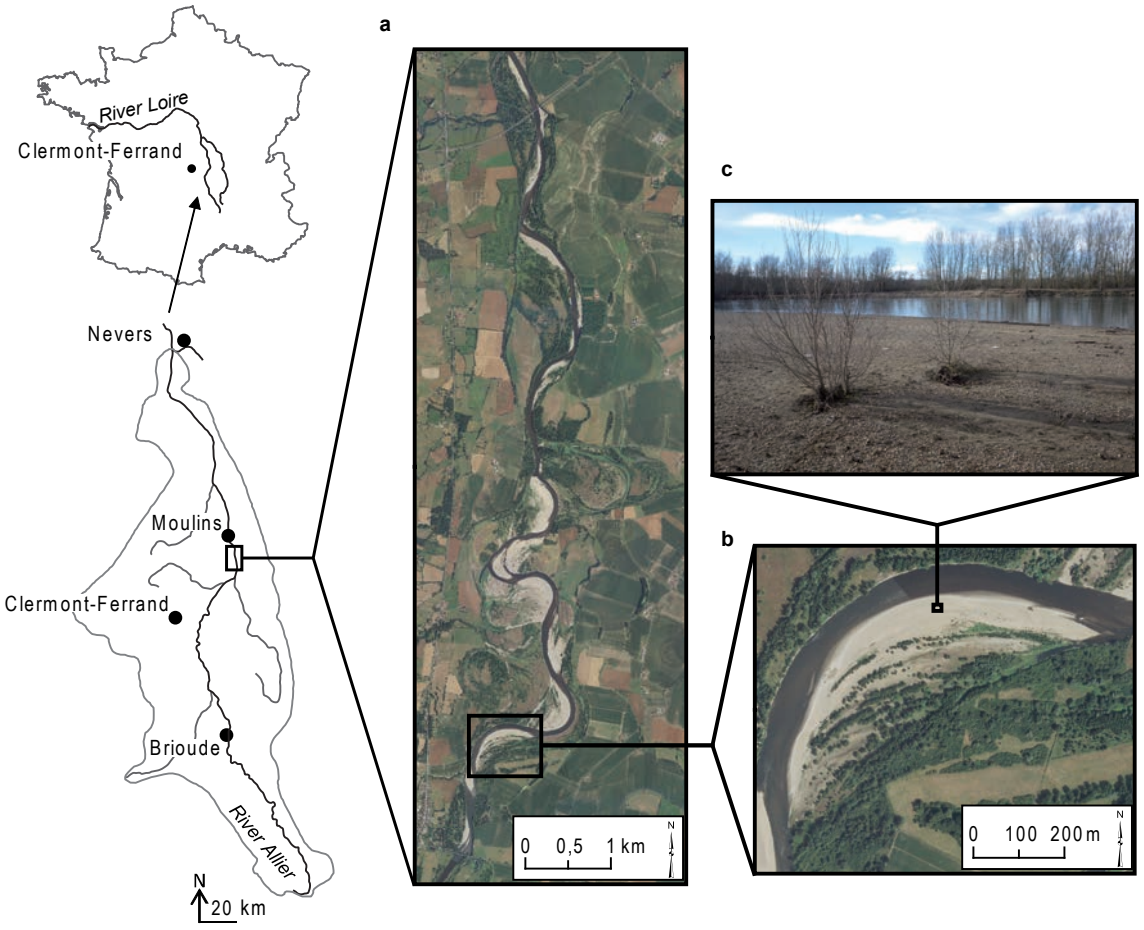

Figure 7. Location of the study site on the Allier river (France); a) corridor scale, b) bar scale, c) micro-site scale with two young multi-stemmed poplars and downstream sediment tails.

2.2. Acquisition of remote sensing data

2.2.1. Corridor scale

A series of photographs was taken at the corridor scale in August 2014 by airplane (Cessna172) at a flight altitude of 500 m to cover an area of 2300 ha. The airplane was equipped by a Canon EOS 6D camera, which enabled us to produce photographs with a resolution of 10 cm/pixel (Figure 8a).

At the corridor scale, we used two other data sources of traditional aerial photographs: (i) stereo-pairs of digital photographs with a 0.30 m resolution, taken on 5th of August 2009 and obtained from the archives of the Geographic Information Center of Auvergne Region (CRAIG - *Centre Régional Auvergnat de l'Information Géographique*) and (ii) soft

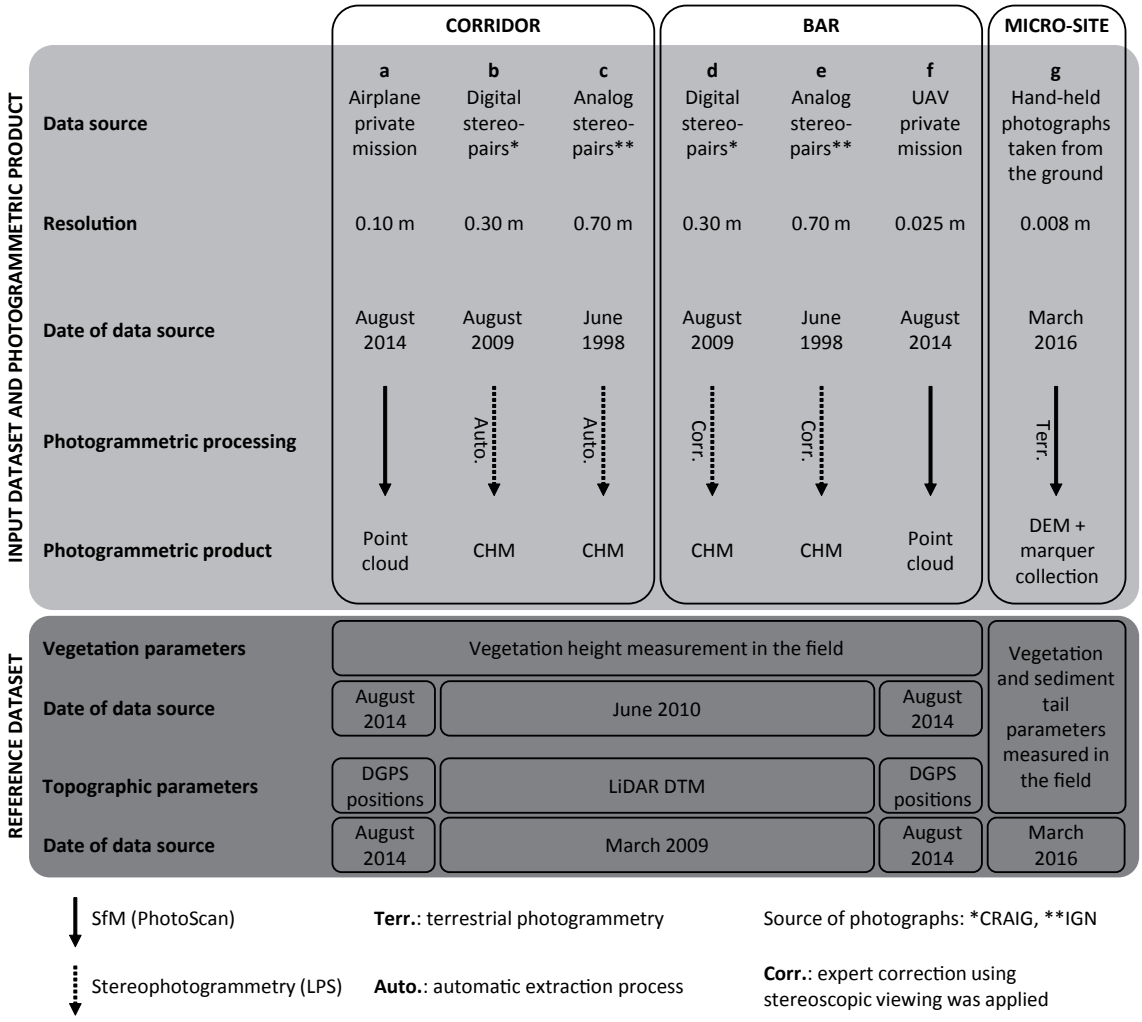

Figure 8. Overall workflow of photogrammetric processes from input dataset to photogrammetric product and reference dataset used for verification of vegetation and topographic parameters.

copies of stereo-pairs of analog photographs with a 0.70 m resolution, taken on 20th of June 1998 and obtained from the archives of the French National Geographic and Forestry Institute (IGN - *Institut National de l'Information Géographique et Forestière*) (Figure 8b,c).

2.2.2. Bar scale

At the bar scale, the same set of traditional aerial photographs (digital and analog) as the one at the corridor scale was used (Figure 8d,e). In addition, a series of photographs was taken in August 2014 at the scale of a point bar with a UAV Falcon-8 (Asctec GmbH, Krailing, Germany). A Sony NEX-5n (16 megapixel) camera with a wide angle 16 mm lens was used for the UAV flight at an altitude of 80 m. This enabled us to produce a series of high quality photographs with a resolution of 25 mm/pixel (Figure 8f).

2.2.3. Micro-site

At the micro-site scale, a PENTAX WG-3 (16 megapixels) camera was used to take photographs of two leafless multi-stemmed young poplars and their sediment tails on 9th of March 2016. The choice to use leafless plants for generating 3D morphological models was taken to test the performance of terrestrial photogrammetry in the worst phenological conditions, and thus to identify the limits of the use of terrestrial photogrammetry in such restrictive conditions. Photographs were taken during a period without wind all around the two poplar trees at eye height (1.8 m) as well as from a higher elevation of about 4 m using a telescopic rod (Figure 8g).

2.3. Photogrammetric model processing

We used two types of images: (i) classical digital and analog aerial stereo-pairs of photographs of national archives taken with metric cameras for which manufacturer's calibration reports are provided and that generate distortion free images; and (ii) digital images taken both from air (small airplane or UAV) and from the ground with consumer-grade (non-metric, high level of distortion) cameras (close-range images). Stereophotogrammetrical analyses were based on classical aerial photographs and close-range images with SfM technique. We will use hereafter the terms 'terrestrial

photogrammetry' for the SfM technique with images taken from the ground with hand-held camera or a camera mounted on telescopic rod, and 'aerial photogrammetry' or just 'photogrammetry' when the dataset consisted of aerial photographs.

2.3.1. Corridor scale

Photogrammetric processing at the corridor scale with airplane photographs was carried out using an SfM software, called Agisoft PhotoScan (Figure 8a). We generated a 3D point cloud following the upcoming steps: featured detection and matching, 3D sparse cloud reconstruction, georeferencing, production of 3D dense point cloud (Nouwakpo et al., 2016). For georeferencing we used targets of 35 x 35 cm placed on the ground surface and localized with a DGPS (Megellan Promark 500) before the flight. Finally the geroreferenced point cloud was exported to LAS format and imported in ArcGIS software.

Using classical aerial photographs (2009 - digital, 1998 - analog), the photogrammetric processing at the corridor scale was performed with LPS 2012 software (ERDAS IMAGINE) (Figure 8b,c) and the LPS Automatic Terrain Extraction (ATE) algorithm (image matching algorithm). We first produced DSMs (all elevations including land and vegetation) and then DTMs (only ground surface points) by means of filtering procedures which allow to exclude all elevation points (vegetation) and to keep only bare-earth points. A canopy height model (CHM) was produced in ArcGIS to describe the vertical nature of the cover by subtraction of the DTM from the DSM. For more details related to stereophotogrammetric procedures with classical aerial photographs, the reader should refer to Vautier et al. (2016). Since no manual correction of the DTMs and the DSMs was applied, we call this procedure hereafter 'automatic procedure'.

2.3.2. Bar scale

Within the study reach at the corridor scale, a point bar was chosen to carry out model processing at the bar scale using traditional aerial photographs at two dates (1998, 2009). The workflow is similar to the one applied for model processing at the corridor scale using the automatic procedure, but a post-processing step was added (Figure 8d,e) which consisted of manual corrections of the mass point clouds derived from the automatic extraction by using the Terrain Editor module of LPS. This module allows the visualization of mass points with polarized glasses by superimposing them on the stereo-pairs from which they are derived. This expert correction using stereoscopic viewing

consists in modification of the position of points in Z coordinates, removal of aberrant points (outliers) and additions of points in areas where the point density was insufficient to accurately model subtle variations in topography and canopy. This additional step highly improves models' quality (Vautier et al., 2016).

The photographs taken with a UAV are covering the same point bar as the traditional aerial photographs. We used an identic SfM workflow as that described for the corridor scale with the airplane photographs (Figure 8f). For the georeferencing we used 18 targets placed on the field and localized by a DGPS (Megellan Promark 500). The geroreferenced point cloud was exported to LAS format and imported in ArcGIS software.

2.3.3. Micro-site scale

The 3D dense point cloud processing at the micro-site scale was based on photographs taken with a hand-held photo camera following the same SfM workflow as for the airplane and the UAV photographs (Figure 8g). For the georeferencing we used 20 x 20 cm targets disposed on the ground surface all around the two trees localized with a DGPS (Megellan Promark 500). However, the georeferenced dense point cloud was not exported to LAS format. Instead, we generated in PhotoScan a polygonal mesh model based on the dense cloud data before exporting the DEM in a raster GeoTIFF format for import to ArcGIS. The DEM was used to compute three topographic parameters (ground height, maximum length and width) in ArcGIS related to the sediment tails in order to assess their morphology. However, with the presented SfM workflow we were not able to generate a suitable quality point cloud of the morphology of leafless multi-stemmed young trees. Therefore, we developed an alternative method in Agisoft PhotoScan based on an expert approach which does not require a 3D dense point cloud generation to measure vegetation traits. We retained the first three steps of the original workflow (featured detection and matching, 3D sparse cloud reconstruction, georeferencing) and then we placed additional numerical markers on the photographs, for example at the ground level and the highest points of the trees. In order to achieve a better accuracy, the same points (e.g., top height) were indicated with a marker on four images at least. The additional numerical markers are the same type of markers we use in general for the georeferencing procedure. Since the spare point cloud was georeferenced, the software generated the X, Y, and Z coordinates of the additional markers. Thus, we obtain a marker collection allowing to calculate distances between markers, i.e., in our example the height of the tree. Following these steps, six vegetation parameters (maximum height; width and depth of the crown, i.e., the maximum width measured

in the upstream-downstream axis; the number of stems and their diameters at 20 and 120 cm above the ground) were computed in order to assess plant morphological traits.

2.4. Reference dataset collection and validation

2.4.1. Corridor and bar scale

We used two reference datasets for the validation of the six photogrammetric models produced at the corridor and bar scales. Each of the two datasets contains measurements of vegetation height and topographic parameters. The first dataset (vegetation height measurements in the field and DGPS positions) served to validate the two models obtained by the SfM technique (Figure 8a,f), the second one (vegetation height measurements in the field and LiDAR DTM) to validate the four models obtained by the method of stereophotogrammetry (Figure 8b,c,d and e). The measurements were restricted to the point bar which was chosen for the study at the bar scale because all the spectrum of possible physiognomic configurations (isolated trees, shrubs, herbs, vegetation patches of different size and density, bare soil) at the corridor scale was present on this site.

Isolated trees and larger vegetation patches of various heights may differently influence the quality and the precision of 3D vegetation height models (Vautier et al., 2016). In order to obtain reliable field data to verify the accuracy of the models obtained by the SfM technique, three different methods of vegetation height and ground control measurements were applied in August 2014. (i) We selected isolated or nearly isolated trees and shrubs and measured the highest point of each individual plant. A 5 m measuring rod and a laser telemeter were used to measure the height of individuals of different types of vegetation (trees, shrubs, and herbs) with contrasting heights ranging from 0.1 m to 23 m. We performed measurements from three different angles with the laser telemeter. (ii) We measured the three highest points of the dense vegetation patch within circular plots with a radius of 5 m to obtain dominant vegetation height. We repeated the measurements twice for all circular plots from two different angles. (iii) To test the accuracy of the surface topography of the 3D point cloud, 228 ground points were measured with a centimeter precision DGPS in the field in addition to control points used for georeferencing the models.

In the second step, LAS data obtained by SfM technique was imported to ArcGIS software. By using the LAS Dataset toolset, vegetation height measurements were

carried out directly on the point cloud. For the topography data, points with the same X, Y coordinates than the DGPS points were extracted from the 3D point cloud. In a third step, in order to calculate the accuracy of this method, we compared the results obtained from the point clouds with our field data collected on the study site.

In order to quantify the accuracy of stereophotogrammetric vegetation height models generated by automatic and manual procedures, 117 tree height measurements were undertaken in the field in June 2010 using a SUUNTO forestry hypsometer. Field measurements and the vegetation height models were than confronted using linear regression models. All DTMs derived by the method of stereophotogrammerty were compared to available 2009 LiDAR data to verify their accuracy (more details are provided in Vautier et al. (2016)). For the model of 1998, only mature trees were used (which are supposed not to have changed in height) and geomorphologically stable areas were chosen for topography validation.

2.4.2. Micro-site scale

In the field, we measured with a rod, a caliper and a ruler the following vegetation parameters on the two poplars: maximum height; width and depth of the crown, i.e., the maximum width measured in the upstream-downstream axis; the number of stems and their diameters at 20 and 120 cm above the ground. We also measured topographic parameters in the field, such as maximum length and width of sediment tails and ground height. We extracted sediment tail parameters of DEM in ArcGIS, with the Profile Graph tool of 3D Analyst toolbar. Finally, we confronted field data with measurements on the photogrammetric product.

3. Results

Accuracies of 3D models obtained for vegetation parameters (mainly height) and for topography by using different photogrammetric methods at the three different scales are variable (Table 3). The RMSE (in m) is calculated from the differences between field measurements and measurements on the 3D models.

Table 3. Accuracy of different photogrammetric methods at the three spatial scales (RMSE is calculated from the differences between reference data and measurements on the 3D models). *These parameters were also quantified by Vautier et al. (2016).

Scale	Method	Image type	Parameters or type of dataset used for validation process		N	RMSE (m)
Corridor	**a** SfM - aerial	Digital (airplane)	Vegetation	Vegetation height	10 (plot)	0.94
					59 (individual)	1.36
			Geomorphology	DGPS positions	228	0.48
	b Stereoph. - auto.	Digital stereo pairs	Vegetation	Vegetation height	117	2.05
			Geomorphology	LiDAR DTM 2009*	56671	0.98
Bar	**d** Stereoph. - corr.	Digital stereo pairs	Vegetation	Vegetation height*	117	1.14
			Geomorphology	LiDAR DTM 2009*	379429	0.42
	e Stereoph. - corr.	Analog stereo pairs	Vegetation	Vegetation height*	9	1.66
			Geomorphology	LiDAR DTM 2009*	439997	0.58
	f SfM - aerial	Digital (UAV)	Vegetation	Vegetation height	7 (plot)	0.56
					71 (individual)	0.45
			Geomorphology	DGPS positions	228	0.33
Micro-site	**g** SfM - terrestrial	Digital (hand-held)	Vegetation	Max. height	2	0.04
				Max. width	2	0.16
				Max. depth	2	0.18
				Number of stem	2	0.00
				Stem ø; 20 cm above ground	6	0.01
				Stem ø; 120 cm above ground	2	0.01
			Geomorphology	DGPS positions	10	0.01
				Max. length of obstacle marks	2	0.47
				Max. width of obstacle marks	2	0.10

3.1. Corridor scale

Both in the respect of vegetation height and topography, the model based on airplane photographs at the corridor scale shows a lower accuracy than the model derived from UAV photographs. The linear regression model we employed between canopy height measured in the field and on the point cloud shows a significant underestimation. This underestimation is mainly related to small vegetation (<2.5 m), which most of the time does not appear within the point cloud or for which heights are impossible to determine because of outliers (noise). The greatest over- and underestimations of the vegetation are respectively 1.2 m and -3.4 m. The vegetation height measured on the point cloud is highly correlated to vegetation height field measurements (R^2=0.98; p<0.0001) (Figure 9a). The RMSE calculated from the topographic difference between the point cloud and the DGPS measurements is 0.48 m (Table 3), the average is 0.17 m ± 0.45 m (sd) (Figure 10a).

The canopy height model derived from the stereophotogrammetric automatic procedure at the corridor scale using digital photographs is strongly correlated to vegetation height field measurements (R^2=0.94; p<0.0001) (Figure 9b). Nevertheless, the vegetation height tends to be underestimated by an average of 1.24 m, the greatest over- and underestimations are respectively 2.89 m and -5.46 m. The most important errors are related to higher size classes (>15 m). The RMSE calculated from the topographic difference between the DTM derived by automatic procedure and LiDAR DTM is 0.98 m (Table 3), the average is -0.27 m ± 0.94 m (sd) (Figure 10b).

The canopy height model derived from analog photographs using the automatic method shows a low quality (R^2=0.66; p<0.0001) (Figure 9c). Since vegetation height is a key parameter in fluvial biogeomorphology, we consider that stereophotogrammetry without applying manual correction is not an adequate method for analog

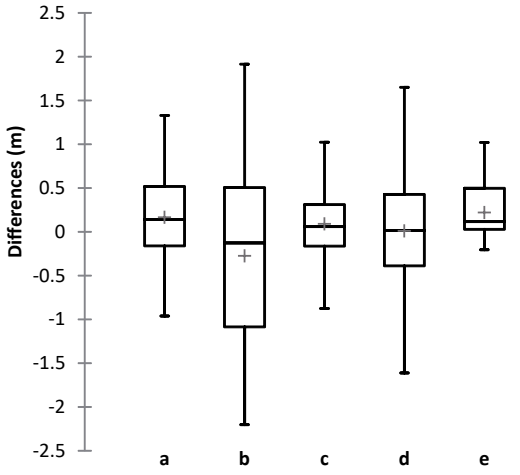

Figure 10. Box plots showing topographic measurement differences between photogrammetric methods and the reference measurements (The mean value is indicated by the grey cross). a) SfM, airplane images; b) Stereophotogrammetry, automatic procedure, digital images; c) Stereophotogrammetry, manual corrections, digital images; d) Stereophotogrammetry, manual corrections, analog images; e) SfM, UAV images.

stereo-pair aerial photographs. This method is therefore excluded from the procedure of topographic accuracy quantification and from Table 3.

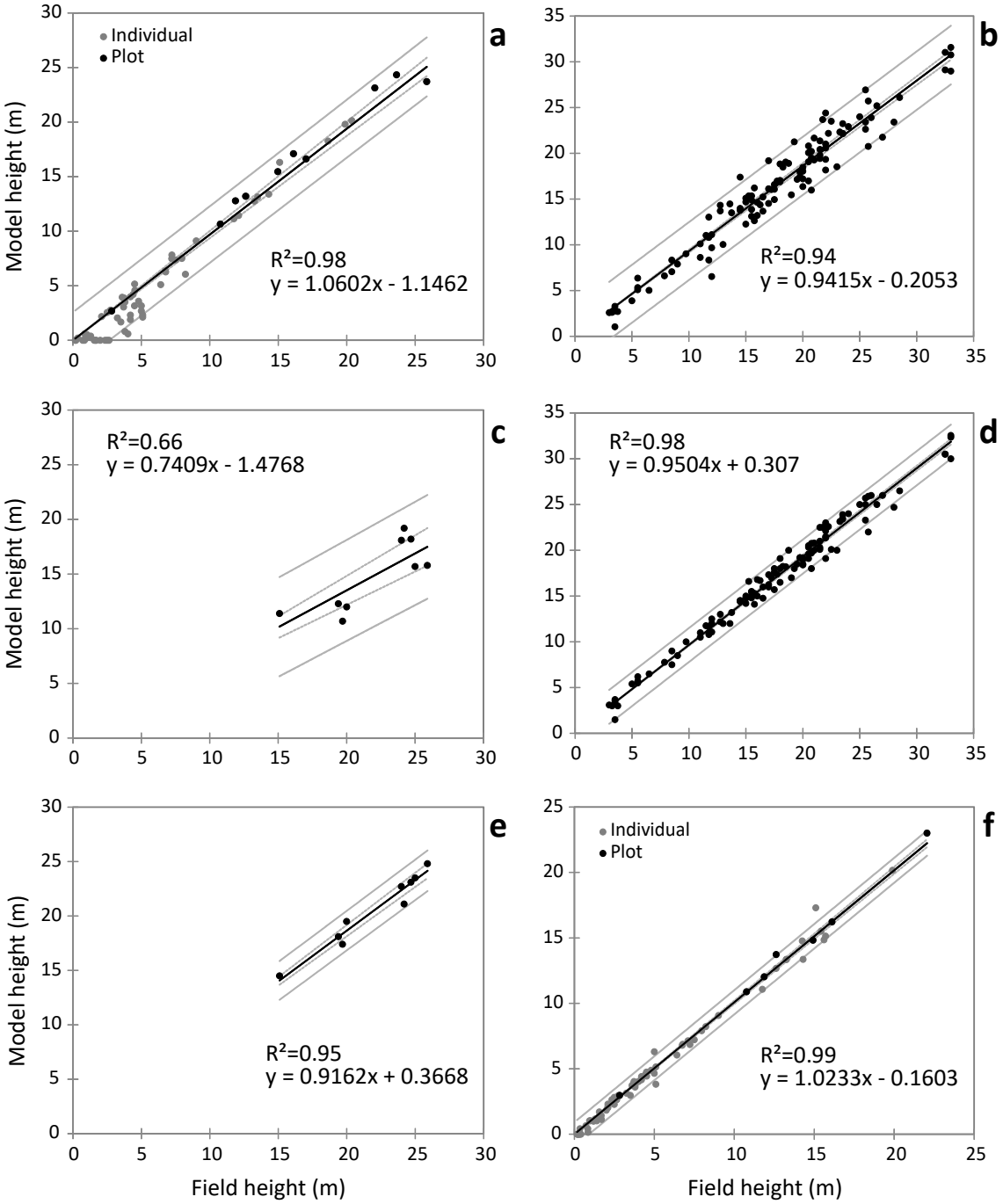

Figure 9. Linear regressions showing the relation between vegetation height measurement on photogrammetric products and reference measurements (α=0.05, p<0.0001). a) SfM, airplane images; b) Stereophotogrammetry, automatic procedure, digital images; c) Stereophotogrammetry, automatic procedure, analog images; d) Stereophotogrammetry, manual corrections, digital images; e) Stereophotogrammetry, manual corrections, analog images; f) SfM, UAV images.

3.2. Bar scale

The vegetation height model at the bar scale based on digital stereo-pairs derived by applying the method of stereophotogrammetry with manual correction is better correlated to vegetation height field measurements (R^2=0.98; p<0.0001) than to heights derived from automatic modelling (Figure 9d). After manual corrections the accuracy improved, but the vegetation height is still underestimated by an average of 0.57 m (Table 3). Greatest over- and underestimations are respectively 1.35 m and -3.75 m. Greater underestimation than -2 m occurs only for trees higher than 20 m. The RMSE calculated from the topographic difference between DTM derived by manual procedure and LiDAR DTM is 0.42 m (Table 3), the average is 0.09 m ± 0.41 m (sd) (Figure 10c).

The manual correction strongly improves the quality of the canopy height model derived from analog stereo-pairs (R^2=0.95; p<0.0001) (Figure 9e). Even though, the average underestimation of vegetation height (1.48 m) remains greater than for the canopy height model derived from digital stereo-pairs. The RMSE calculated from the topographic difference between DTM derived by manual procedure and LiDAR DTM is 0.58 m (Table 3), the average is 0.01 m ± 0.58 m (sd) (Figure 10d).

We obtain the highest accuracy in respect to vegetation height and topography within aerial photogrammetric methods when using SfM technique combined with UAV photographs. The difference between vegetation height measured in the field and on the point cloud shows that 83.3 % of the 3D model's error is situated between -0.5 and 0.5 m, and the two measurements are highly correlated (R^2=0.99; p<0.0001) (Figure 9f). Results show a significant overestimation for higher (>13 m) vegetation classes. The greatest overestimation is 2.2 m and the greatest underestimation is -1.3 m. The RMSE calculated from the topographic difference between the point cloud and the DGPS measurements is 0.33 m (Table 3), the average is 0.22 m ± 0.25 m (sd) (Figure 10e).

3.3. Micro-site scale

Terrestrial photogrammetry at the micro-site scale shows good results, the RMSE remains below 0.2 m for all vegetation parameters (Table 3). The highest errors are related to the tree crown parameters (depth, width and height). The parameters we obtain by terrestrial photogrammetry from sediment tails' measurements have a lower accuracy

than the measured vegetation parameters. RMSE is respectively 0.47 m and 0.10 m for the length and width of the two sediment tails (Table 3).

4. Discussion

At all three spatial scales (i.e., corridor, bar, micro-site) first the accuracy of photogrammetric methods and second the adequacy of photogrammetric methods to study feedbacks between fluvial geomorphology and riparian vegetation at the three spatio-temporal scales are discussed and summarized in Table 3.

4.1. Corridor scale

The present study showed that digital stereo-pair aerial photographs are promising for monitoring fluvial landforms and riparian vegetation characteristics at large spatial scales (fluvial corridor) when the method of stereophotogrammetry combined with the automatic procedure is applied (Figure 8b and Figure 11). This method can give a good overview of the spatial pattern of the four different phases of the fluvial biogeomorphic succession at a given date. However the automatic extraction process tends to smooth the representation of vegetation cover (Korpela, 2004; Véga, 2006; Magnusson et al., 2007) and underestimate canopy height. Several authors have already observed these inaccuracies in vegetation height measurements when using photogrammetry (Brown and Arbogast, 1999; Miller et al., 2000; St-Onge et al., 2004; Gillan et al., 2014). Our results show that stronger underestimation of vegetation height occurs more probably for higher vegetation.

Vegetation is considered to be difficult to model with photogrammetry because multiple factors influence measurement quality, e.g., geometry of the crown, radiometric properties, structure of the stand, and density of the canopy. Those parameters are highly variable depending on species type, phenology and the variability of air temperature and precipitations in between years. In addition, automatic extraction might lead to anomalous representation of areas with shadows and abrupt edges. The most significant errors are related to isolated trees, trees with a sparse foliage or a texture which is difficult to differentiate from the ground surface, forest margins, high river banks, vegetation

patches with very heterogeneous vegetation heights (Vautier et al., 2016). These effects have more influence on analog photograph based models, especially in low-textured areas with important shadow coverage. Therefore, the accuracy we reach by means of automatic extraction specifically based on analog photographs (Figure 8c) is low and we consider it as insufficient for fluvial biogeomorphic analyses.

Besides vegetation morphology, other extrinsic factors influence vegetation height models' quality such as variations in luminosity during data acquisition, insufficient contrast of the images or wind which results instable vegetation and 3D point clouds noisy or inaccurate. The question of model validation is also an important issue. Two options prevail. Nowadays LiDAR technique offers the most accurate vegetation height models which can be used for photogrammetric vegetation height model validation if they are acquired synchronously with the photogrammetric dataset. The other option we applied here was to compare photogrammetric vegetation height models to data directly collected in the field. This classical way to measure vegetation height is widely used in forestry. However, even if we multiplied measurements for each tree, uncertainties in precision remain, especially for tall trees (>15 m). The observer needs to be far enough from the tree (depending on the size of the tree), to have a good visibility of the tree top and at the same time has to be able to see the trunk which is often surrounded by understory vegetation. Thus, this uncertainty of field measurements might play a role in error calculations of the model.

In this paper we were mainly focusing on one vegetation parameter, the height, but other parameters could also be extracted using photogrammetry, such as vegetation patch morphometry (patch width, length) or fragmentation. An interesting perspective would be to combine photogrammetric data with spectral information which allows to provide information about the species composition of the riparian vegetation (Dunford et al., 2009; Dufour et al., 2012; Dandois and Ellis, 2013).

At the corridor scale, we consider stereophotogrammetry based on digital stereo-pairs of aerial photographs as a well-adapted tool for quantifying feedbacks between the mosaic of geomorphic units (i.e., macro-scale topography) and the mosaic of vegetation communities, except based on analog ones. Stereophotogrammerty is relevant to measure all the necessary parameters to answer all the questions (C1 to C3; Table 2 and Table 4) proposed at the corridor scale, except those concerning the pioneer phase of the biogeomorphic succession. Only seedlings constitute the vegetation of this phase and therefore plants cannot be detected because of the resolution of the photographs and the associated error of the CHM (RMSE = 2.05 m).

Photogrammetry, especially SfM is now widely used because of its simplicity. Our aim was to quantify the accuracy of SfM in a fluvial biogeomorphic context at large spatial scales with the simplest workflow (data acquisition and processing) which can be easily reproduced in river research studies and used for river management. Our results show that the method presents many advantages for studying biogeomorphic dynamics within riparian corridors and that it permits to quantify its limitations as well. SfM technique at the corridor scale globally provided good results, and had higher accuracies measuring vegetation (RMSE = 0.94 m for plot and 1.36 m for individual) and topography (RMSE = 0.48 m) than the automatically generated stereophotogrammetric models. However, some errors occurred, i.e., occasionally vegetation could not be detected and outliers occurred. These errors are most likely related to a deviation from the initial flight plan which resulted in a lack of overlap between images, whereas other areas were overflown twice or three times practically on the same path. Bemis et al. (2014) emphasized that the surface we want to reconstruct has to be covered by at least two (preferably more) images which are taken from different positions. Our results showed that if a surface is covered by several images which result from several very close overflights, the accuracy of the reconstructed 3D surface is lower than that for surfaces covered only twice but with a greater angular change between images. Even though the accuracy is increasing with greater angular change between images, the differences should not exceed 25^{o} (Moreels and Perona, 2007). Thus we could certainly reach a better accuracy if the flight plan is not only well defined, but also well respected. The SfM technique at corridor scale should be tested again with a respected flight plan to quantify its exact limits. Image blur is also decreasing the accuracy of 3D surface reconstruction by the presence of anomalous points located below or above the terrain surface (Jensen and Mathews, 2016). That was the case with airplane images. But as blurring affected homogeneously the image set quality, it does not explain the fact that vegetation was not detected in certain areas. Nevertheless, our results are encouraging because even when considering the detected problems, greater quality is achieved than with stereophotogrammetry and the 3D models are operational for biogeomorphic studies.

If a greater accuracy is needed, additional parameters should be taken into consideration during data acquisition and 3D data processing. Recent studies have analyzed the quality of SfM for DEM construction at various spatial scales when using consumer-grade cameras (Rosnell and Honkavaara, 2012; James and Robson, 2014; Javernick et al., 2014; Dietrich, 2016). These studies reported that digital models derived from images of non-metric cameras can show systematic errors such as vertical errors expressed as a ‘central doming’ (James and Robson, 2014). This systematic error is often associated with consumer-grade digital cameras and their inaccurately specified lens distortion

parameters obtained through self-calibration processes (Wackrow and Chandler, 2008, 2011). In traditional photogrammetry, these artefacts are minimized through the use of 'metric' cameras with well-defined camera models and negligible radial distortion (James and Robson, 2014). Since it became very common and widespread to use the SfM technique with consumer-grade cameras taken in UAS (unmanned aerial system) platforms, Wackrow and Chandler (2008, 2011) developed a methodology to minimize the systematic error surfaces using convergent image configuration. To overcome the problem of systematic error caused by the parallel camera geometry, James and Robson (2014) suggested additional capture and inclusion of oblique images in the image network. Similarly, Rupnik et al. (2015) confirmed that adopting an oblique camera position and increasing the overlap reduces the magnitude of noise and improves 3D precision and accuracy. In addition, collecting RAW imagery could reduce the difficulties related to exposure and could provide more color information over the darker areas of water and shadowed areas (Dietrich, 2016).

Results from this study show that SfM, just like the above-mentioned stereophotogrammetrty, is also an adapted tool for the quantification of feedbacks between the mosaic of geomorphic units and the mosaic of vegetation communities and that it is relevant to measure parameters to respond to all questions (C1 to C3; Table 2 and Table 4) that we asked at the corridor scale, but again, with the exception of the pioneer phase. Combining this 3D data with spectral information could possibly help to detect the pioneer phase. Our results suggest that if overlap problems are solved, a greater accuracy can be achieved than with stereophotogrammetry, thus allowing smaller-size vegetation such as herbs to be detected. In order to solve the problem of coverage gaps and low overlap, we recommend to increase the camera interval and to use closer flight lines. With UAVs, this problem can be avoided if an automated flight mode respecting the flight plan is used. The high RMSE value for individual trees arises from this overlap problem.

4.2. Bar scale

Manual correction using stereo-vision is time-consuming, thus it can only be applied at a restricted spatial scale such as an alluvial bar (Figure 11). However, expert correction provides a crucial advantage for improving the fundamental understanding and quantification of biogeomorphic feedbacks. It allows to benefit from a worldwide existing archival imagery database which is frequently unexploited and free of charge (Rhemtulla

et al., 2002; Fox and Cziferszky, 2008; Bizzi et al., 2016) and to extract three-dimensional information from the past and therefore monitor biogeomorphic feedbacks on alluvial bars on longer timescales. In addition, manual correction improved the accuracy of 3D-models (digital and analog photographs), consequently, vegetation growth rates can be calculated with a better precision and topographic variations can be detected more precisely. Despite this improvement, the vegetation height tends nevertheless to be underestimated, especially higher vegetation (>20 m). This tendency is even more present after manual correction. The manual correction is more efficient to correct vegetation underestimation for lower vegetation (<20 m) and to reduce overestimation in general. For a more detailed discussion on this dataset, see Vautier et al. (2016).

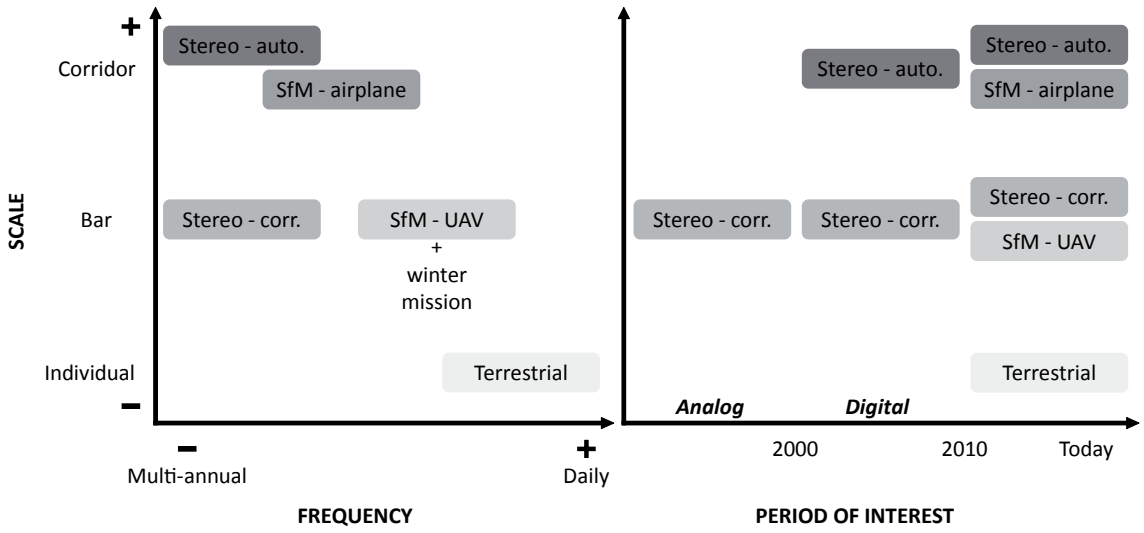

Figure 11. Photogrammetric methods represented by the recommended scale of use and their possible frequency of application.

At the bar scale we tested the applicability of the stereophotogrammetric method with manual edition based on digital and analog stereo-pairs of aerial photographs. This method is appropriate to quantify feedbacks between meso-scale fluvial landforms and vegetation cohorts or the establishment of communities and it is relevant to quantify the majority of the parameters necessary to answer questions B1 to B3 (i.e., at the bar scale; Table 2 and Table 4), except two parameters, which are known to be difficult to measure by photogrammetry, i.e., stem density and diameter, and topographic elevation under dense vegetation. If it is possible to estimate the number of trees within each vegetation patch, a minimum stem density can be deduced. But as Balenovi'c et al. (2015) pointed out, stereophotogrammetry usually leads to an underestimation of the number of trees. The topographic elevation was also shown as a challenging parameter to obtain by stereophotogrammetry when vegetation cover is dense (Lane, 2000; White

et al., 2013). We suggest that the topographic measurements based on classical digital or analog photographs is the most accurate during the geomorphic and the pioneer phases which are dominated by bare surfaces, and during the ecological phase, when the raised topography reaches a more homogenous state than the one related to the biogeomorphic phase. Conversely, pioneer strips, islands and benches highly connected to hydrogeomorphic perturbations tend to produce a strong topographic differentiation compared to non-vegetated surrounding areas. If there are no vegetation gaps within the pioneer strips to allow access to topographic information, DTMs might be misleading.

Furthermore, our results show that UAVs allow cost-effective high frequency (i.e., multi-annual) and high resolution monitoring of fluvial landforms and riparian vegetation dynamics at the scale of alluvial bars. Among the different aerial photogrammetric methods which we tested at the bar and corridor scales, the UAV provided the best accuracy for vegetation height (RMSE = 0.45 m at individual level) as well as for topography (RMSE = 0.33 m) (Table 3). The vegetation height accuracy we obtained is very close to the high accuracy obtained by Gillan et al. (2014) who used UAV for determining vegetation height of individual shrubs (RMSE = 0.42 m) in a semi-arid environment, conversely to results obtained by Gillan et al. (2014), Jensen and Mathews (2016) who tested the SfM technique for tree height canopy estimation in an oak-juniper woodland ecosystem and obtained RMSEs between 0.81 and 1.24 m. Our results obtained with UAV are very promising because riparian environments are composed of a mosaic of contrasting pioneer vegetation types and physiognomies including trees, shrubs and herbs of different ages. We observed that vegetation height underestimation is more frequent for tall trees than for shrubs that have a more compact morphology. This is confirmed by Korpela (2004, 2007) who also pointed out that treetop detection remains difficult in comparison to other plant cover types. We suggest that height estimation is particularly difficult for trees having a pronounced peak shape as it is the case for many poplar species (which composed the majority of our tree samples) and for isolated trees in comparison to tree heights within dense vegetation patches. Concerning topographic surfaces, the accuracy of our DTM (RMSE = 0.33 m) derived from UAV images is similar to the one found by Hugenholtz et al. (2013) using UAV images (RMSE = 0.29 m), which they consider equivalent to the RMSE of bare earth DTMS using LiDAR.

UAVs' easy logistics also permit to overfly and monitor bars immediately after flood events and to collect imagery data several times a year and thus to constitute complementary datasets, e.g., summer surveys for a better vegetation representation and winter surveys for a better ground visibility and therefore a more accurate representation of the topography (Dandois and Ellis, 2013). Such sub-annual and annual frequency

monitoring can be employed for the quantification of responses and effects of riparian vegetation to single floods. Until recently, aerial photographs, e.g., of the IGN national databases which are taken every 3-5 years, only permitted to analyze the cumulative responses and effects of riparian vegetation to past hydrological events (Figure 11). The limited spatial scale applicability of UAV's can be compensated by utilizing helicopters (Dietrich, 2016) or micro-light aircrafts (James and Robson, 2012) which both allow to cover larger surfaces than UAVs. However, the use of these two methods results in a decreased resolution of 3D models and also requires more organization time and more time-consuming logistics (e.g., positioning of targets on the ground surface). In scientific research, UAVs and small aircrafts are now widely used because image data can easily be processed by SfM which is a fast, automated, low-cost method and requires little expertise (Micheletti et al., 2015). With multi-image photogrammetry, the workflow is easier than in stereophotogrammetry and working time does not significantly increase if more photographs are used (contrary to stereophotogrammetry where georeferencing time depends on image numbers).

The applicability of SfM using UAV photographs at the bar scale was tested to evaluate the possibility to quantify feedbacks between vegetation cohorts or communities and meso-scale fluvial landforms such as pioneer islands, vegetated strips and wooded benches. Our results indicate that this method is relevant to quantify the majority of the parameters necessary to respond to our questions at the bar scale (B1 to B3; Table 2 and Table 4), except, once again, the stem density and the topographic elevation under vegetation. Fritz et al. (2013) used a UAV-based photogrammetric point cloud to detect tree stem density in open stands. They collected images during the leafless stage with a camera angle of 45^{o} and a double zigzag flight pattern, and succeeded to detect 71% of overall stems. The same method could be used at the bar scale to complete the missing parameters (i.e., stem density and diameter). However, in the youngest multi-stemmed pioneer riparian patches of less than 5 years even leafless point clouds might not be successful to detect stem density and diameter. Such woody pioneer islands, strips or benches are isolated meso-scale landforms compared to forestry plots located inside the forest. Thus, we suggest that a possible solution would be to collect the missing parameters not only by flying over these patches, but also by taking many additional images by flying around them during winter. Meso-scale monitoring by SfM should also offer the possibility to collect information at the micro-site scale (individual and sediment tail). The very dense point cloud supplied provides the opportunity to measure additional parameters (e.g., tree width, depth, frontal area exposed to flow).

4.3. Micro-site scale

At the micro-site scale, the reconstitution of vegetation morphology and architecture with a high accuracy is of a crucial importance for the disciplines of plant ecology and physiology, and more recently for biogeomorphology. Studies of tree architecture dealing with terrestrial LiDAR, image-based methods or other methods like a 3D digitizer are rather frequent (Watanabe et al., 2005; Tan et al., 2007; Côté et al., 2009; Livny et al., 2010; Crespel et al., 2013). In particular, terrestrial laser scanning (TLS) was widely used to generate accurate dense point clouds of trees and allows tree attribute measurements such as tree height, DBH and stem curves (Liang et al., 2012; Yu et al., 2013; Liang et al., 2014b; Olofsson et al., 2014). However, these methods still remain costly and they require heavy equipment to be transported in the field or expert knowledge in algorithm development. As an alternative, Forsman et al. (2016) used terrestrial photogrammetry to estimate tree stem attributes within 10-m radius field plots, supplying very promising results (i.e., stem diameter RMSE of 2.8-9.5 cm) but only applied for bigger stem diameter than in our study (maximum diameters = 0.07 and 0.06 m). However, their multi-camera rig containing five cameras is heavy and quite big. The methodologies and tools proposed here and tested on the river Allier seem to be better adapted to field measurements of vegetation morphology and related micro-topographic features with little material (camera, rod, targets, DGPS) to carry and set up and flexible enough to be repeated at high frequencies (Figure 11).

Our results suggest that terrestrial photogrammetry is not suitable to generate a point cloud reconstituting the architecture of leafless multi-stemmed woody vegetation. However, Liang et al. (2014a) successfully used terrestrial photogrammetry with the same software as we did (Agisoft PhotoScan) to measure the DBH of individual tree stems in a 30 x 30 m plot. This significant difference may relate to the size of the DBH of the trees which ranged from 10 cm to 51 cm within a mature forest stand. The authors also noticed that the method has a limited capability to model stem diameters less than 10 cm, which was our case (maximum diameters = 7 and 6 cm). Since our study aimed to test terrestrial photogrammetry and the generation of 3D point clouds in the most challenging leafless and multi-stemmed conditions, our results are not directly comparable to those of Liang et al. (2014a), but rather complementary. We estimate that future developments of new algorithms will improve the capacity of SfM to model plant morphology and architecture. For example, Liang et al. (2014a) used a point cloud classification based on spectral data which greatly improved tree mapping efficiency and DBH estimation. At this stage, it still has to be tested if the

application of this type of point cloud classification is helpful within the riparian environment during summer, i.e. growing season, to classify the point cloud into a group of points corresponding to the canopy and the one to the stem.

Regarding the vegetation parameters at the individual scale, the highest error is related to crown depth measurements (RMSE = 0.18 m; Table 3). In our study, this error might be related to the two selected individuals which are located very close to each other and are positioned nearly on the imaginary axis which is perpendicular to the direction of the flow. Thus, in the view that is used to measure vegetation depth, trees are positioned one behind the other. Therefore, it is difficult to determine which branches belong to which tree. Based on this observation, we suggest that the most suited sampling strategy for quantifying vegetation parameters at the individual scale is to take the images manually in a relatively close distance with a very large overlapping in order to easily localize identical points between two images. Another solution for analyzing the relation between one tree and its sediment tail would be to target only fully isolated trees when possible.

Conversely to the vegetation, the sediment tails are compact and thus are very well visible on the point cloud, as well as on the 3D model (Figure 12). At this micro-scale regarding topographic parameters, the highest error compared to manual field measurements concerned the sediment tail length (RMSE = 0.47 m; Table 3). However, this is not surprising because in the field sediment tails are usually difficult to delimitate objectively and the measurement of the associated parameter generally includes a part of subjectivity which depends on the observer. It might be easier to determine objectively sediment tail parameters by visualizing topographic profiles in ArcGIS and eventually applying automatic statistical selection procedures based on variations in slope curvature or even texture (Figure 12). For the sediment tail modelling, we found that best results are achieved if photographs are taken both from a telescopic rod and by hand with a complete (360^{o}) round around the tree and its sediment tail. The terrestrial photogrammetric method described here represents an effective, low-cost alternative to traditional manual topographic surveying and can offer even a finer description of topographic landforms.

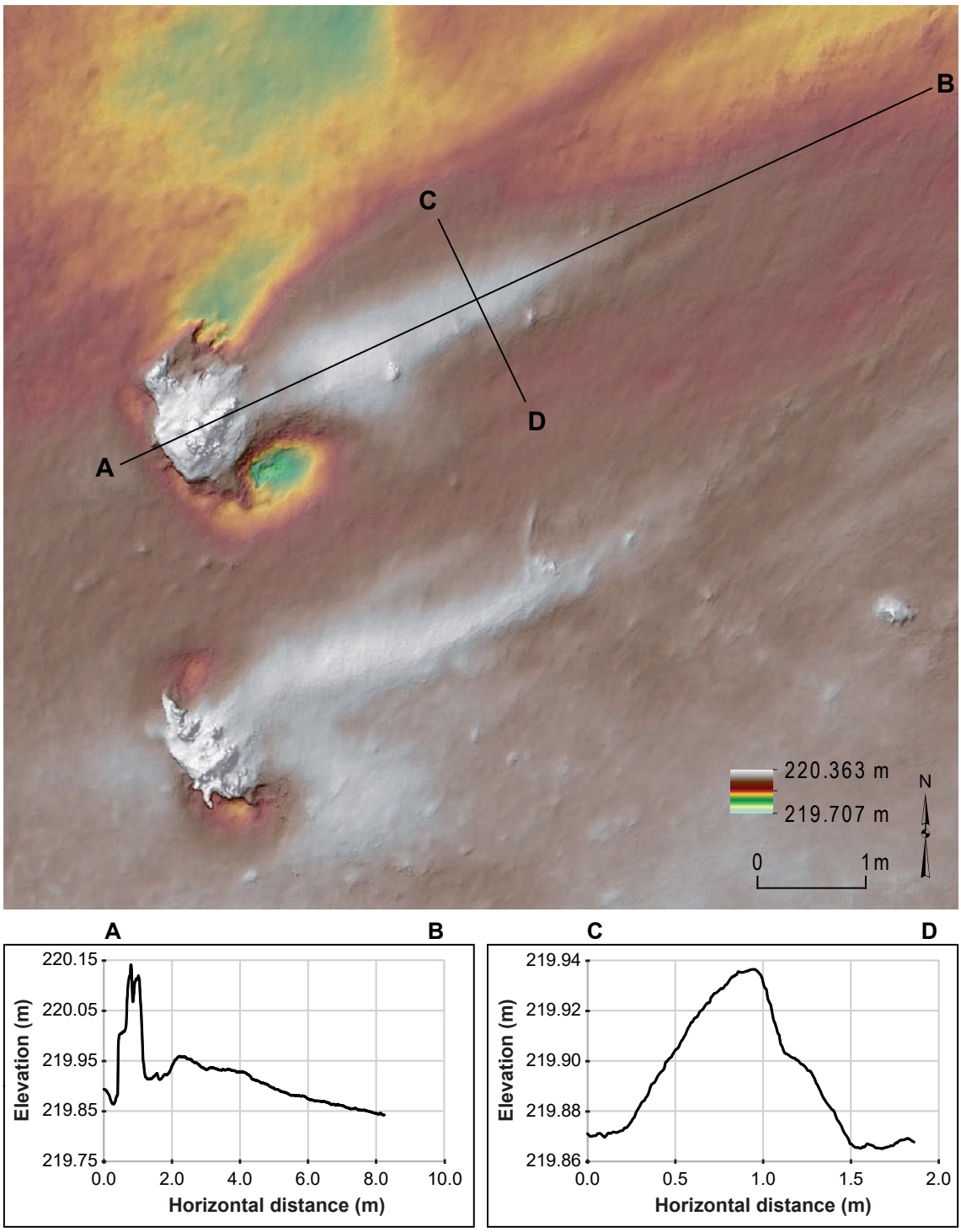

Figure 12. Digital elevation model of sediment tails of the two individuals and two topographic profiles. The first one is a longitudinal profile (A-B) through the poplar and the sediment tail corresponding to the axis upstream-downstream, the second one (C-D) is a cross section of the sediment tail.

At the micro-site scale, we consider that the method of terrestrial photogrammetry is relevant to measure with a sufficient accuracy the geomorphic and biological parameters useful to respond to all questions (M1 to M3; Table 2 and Table 4) related to the biogeomorphic feedback: (i) the direct effects of hydrogeomorphic constraints on plant traits can be monitored following floods; (ii) the effects of the morphological response traits on the local geomorphology can be monitored following each single flood event; and (iii) the morphological response of the plant to the biologically driven geomorphic changes can be monitored between floods. The 3D quantitative description of both topographic and biological parameters makes it possible to undertake correlation analyses between those interacting factors and further to detect changes in vegetation morphology related to local topographic changes under biotic control. Today, there is a fundamental question in ecology about how the different species or different plant morphologies are affecting the topographic variations in biogeomorphic ecosystems. Bouma et al. (2013) demonstrated by a flume experiment how the flow and thus the spatial pattern of salt marsh sediment deposition and erosion is influenced by species-specific vegetation traits. Similarly to this study, our method could be applied in river science to produce quantitative data for a better understanding feedbacks between plant traits and topographic evolution. In addition to the topographic and vegetation parameters we tested here, other parameters could easily be included, such as frontal area, by placing enough number of digital markers in PhotoScan, and then transform it into a polygon using a GIS software and calculate its surface, as well as the aerial biovolume by measuring vegetation width, depth and height, or the sediment tail's volume.

Table 4. Non exhaustive list of geomorphic and vegetation parameters needed to be measured to answer to our questions concerning biogeomorphic feedbacks and their feasibility (Y=yes, N=no, UC=under condition) to measure them by using photogrammetry.

Question	Geomorphic parameters	Feasible	Vegetation parameters	Feasible	Remarks
C1	Topography before vegetation establishment (after destructive flood)	Y	- Height	Y	- Better accuracy can be achieved with SfM
			- Patch richness	Y	
			- Patch shape	Y	
			- Patch size	Y	
			- Fragmentation index	Y	
			- Shannon index	Y	
C2	Relative part of main- and secondary channels, active tract and floodplain	Y	Same as C1	Same as C1	
C3	As C2	Y	- Geomorphic phase	Y	- The RMSE is higher than the height limit of the pioneer phase, thus it is not possible to include pioneer phase in biogeomorphic study at this scale
			- Pioneer phase (h<1 m)	N	
			- Biogeomorphic phase (h=1-7 m)	Y	
			- Ecological phase (h>7 m)	Y	
B1	- Location X, Y, Z	Y	- Surface cover	Y	- Stem density measurement only if scattered patch
			- Density	UC	- By UAV smaller vegetation can be detected than by stereophotogrammetry
			- Height	Y	- Use of existing archival imagery data by stereophotogrammetry (manual edition)
			- Biovolume	Y	
B2	- Length	Y	Same as B1	Same as B1	- Same remarks as B1
	- Width	Y			- Elevation under cover only if we have some visible ground point to interpolate or UAV flight during leafless period for better DTM
	- Elevation	UC			
B3	Same as B2	Same as B2	Same as B1	Same as B1	
M1	- Length	Y	- Height	Y	- Vegetation parameter measurements are time-consuming but accurate
	- Width	Y	- Width	Y	- Several other parameters can be measured, depending only on question of time
	- Height	Y	- Depth	Y	
	- Volume	Y	- Number of stems	Y	
			- Diameter of stem	Y	
			- Frontal area exposed to flow	Y	
			- Biovolume	Y	
M2	Same as M1	Same as M1	Same as M1	Same as M1	
M3	Same as M1	Same as M1	Same as M1	Same as M1	

4.4. Application of photogrammetry at large spatial scale for sustainable river management

For an appropriate river management, there is a need to identify and describe the different subsystems where the same management principles can be applied (Piégay, 1996). Once homogeneous subsystems are statistically delineated (e.g., functional sectors) using automatic classification methods (Alber and Piégay, 2011; Leviandier et al., 2012; Notebaert and Piégay, 2013), the here presented photogrammetric methods can be applied for a better quantification and understanding of feedbacks between riparian vegetation and geomorphology along the upstream downstream gradient. In this way, rivers can be studied in a very integrative way at large scale (entire river corridor) allowing to identify necessary actions for a sustainable river management within each functional sectors in which plants and geomorphology interact at the three nested scales.

In addition, both stereophotogrammetry with digital stereopairs and SfM with airplane images could be applied at broader spatial scales, although it implies to spend more time for 3D data processing. In the case of SfM technique the computing time would increase, in the case of stereophotogrammetry the model processing workflow would take longer.

We presented here the application of traditional stereophotogrammetry for biogeomorphic diachronic analysis but there is as well a strong potential in SfM technique to monitor past vegetation and topography dynamics (Gomez et al., 2015) at large scale. For river management and restoration, quantitative data related to vegetation and topographic dynamics are necessary to be produced with easily reproductive methods at large scale, such as the combination of SfM technique with existing national aerial photograph databases (Michez et al., 2013). But this field still requires error quantification on extracted topographical and vegetation data.

5. Concluding remarks and perspectives

Photogrammetry is a useful tool to quantify a set of relevant parameters to respond to fundamental research questions concerning biogeomorphic feedbacks at three different nested spatial scales, i.e., from the fluvial corridor to the micro-site. Nevertheless, we identified some difficulties or failures to properly apply photogrammetry in biogeomorphic feedback studies, such as the detection of vegetation density, landform

topography under dense vegetation and the pioneer phase at the corridor scale. Possible solutions to resolve problems related to the acquisition of accurate 3D point cloud data were proposed and discussed. Furthermore, archival images have shown to be very useful to study past and long term evolution of fluvial biogeomorphic processes because current technology offers more possibilities than technologies available when archival images were acquired.

Rivers and their fluvial corridors are complex open systems and can be viewed as a nested hierarchy of subsystems interconnected together (Amoros et al., 1987). Transitions between biogeomorphic processes occurring at small scales (e.g., responses of individual plant traits to hydrogeomorphic constraints) and their effects on the local geomorphology during one single flood event and those occurring at larger scales (e.g., adjustment of the landscape mosaic over few decades related to the biogeomorphic succession and effects of the mosaic structure on vegetation recruitment and establishment patterns) are still not well quantified and understood. Hierarchical biogeomorphic bottom-up and top-down cross-scale studies are still difficult to conceptualize and perform, but such efforts have now become necessary in biogeomorphology to fully understand river responses to anthropogenic impacts and environmental change. Photogrammetry is a promising instrument for the quantification of biogeomorphic feedbacks at nested spatial scales within river systems and for developing appropriate river management tools and strategies.

Chapter III. Topographic signature of riparian vegetation at corridor and bar scales

1. Introduction

Within dynamic river systems, the recruitment, expansion, composition, growth and succession of riparian vegetation is higly controlled by hydrogeomorphis parameters (topography, sediment texture, exposure to floods). The strong control of hydrogeomorphology on vegetation colonisation results in an heterogeneous spatial and temporal landscape mosaic (Naiman and Decamps, 1997; Richter and Richter, 2000; Ward et al., 2002). Vegetation succession is regularly interrupted or rejuvenated (i.e. partial or entire destruction of vegetation) durgin flood disturbances. In island braided river reaches rejuvenation is mainly related to large torrential floods that abruptly destroy fluvial islands and vegetation benches (Gurnell et al., 2001). In free meandering river systems, rejuvenation is mainly associated to progressive bank erosion and channel migration oruccuring also during ordinary foods (annual and quasi-annual floods) (Geerling et al., 2006). In the two cases, tall riparian trees can add surcharge on river banks when they are high and sandy, and induce gravitational movements engendering channel instability (Abernethy and Rutherfurd, 1998; Camporeale et al., 2013). At the same time young pionner riparian vegetation can induce sediment trapping and stabilisation on alluvial bars with their above- and belowground part, thus it is capable, within the upstrem-downstream limits of island-braided and meandering fluvial styles, to modify topography and channel evolution (Corenblit and Steiger, 2009; Manners et al., 2015). Geomorphic changes, in turn, affect matter and energy fluxes ditribution within the fluvial corridor and thus habitat properties and their exposure to hydrogeomorphic contraints. It was shown that, in the cases of island braided and meandering rivers, such reciprocal coupling between vegetation and geomorphic dynamics generally result in very specific spatio-temporal organisational sequences of fluvial landforms and releated

vegetation patches (Tal et al., 2004; Corenblit et al., 2007; Bertoldi et al., 2011). Such predictible synergetic inter-related construction of fluvial landforms and vegetation succession was described in the fluvial biogeomorphic succession (FBS) model (Corenblit et al., 2007) (for more detail about the engineering effect of riparian vegetation and the biogeomorphic succession model, see Chapter I), representing potentially a signature of life into the landscape (Corenblit et al., 2007; Bertoldi et al., 2011). Based on the consideration that topography-vegetation reciprocal interactions vary in intensity in space and in time (Corenblit et al., 2007, 2014), it was suggested that the topographic signature of vegetation in the landscape can be easily quantifiyed with the frequency histogram of topographic classes and related vegetation succession classes (defined by the heigth). However few studies provided continuous quantitative data on vegetation's geomorphic effect and resulting topographic signature in the landscape (Bertoldi et al., 2011; Bywater-Reyes et al., 2017). In partucular, such an analysis has never been undertaken in the context of wandering rivers which reprensent a very particular case.

In Chapter II, we showed the potentials and difficulties to use the method of photogrammetry in biogeomorphological studies. In this chaper, we exploit airborn LiDAR data and the method of photogrammetry to analyse the relation between riparian vegetation and river topography. We test here, whether or not we can statistically detect the topographic signature of vegetation within dynamic wandering rivers, such as the Allier. It was shown that the topographic signature of life is easy to identify in the case of island braided (Bertoldi et al., 2011) and meandering (Corenblit et al., 2016a) river reaches because vegetation-geomorphic feedbacks resultes in very well defined topographic units within the fluvial corridor (e.g. wooded fluvial islands, point bars and floodplain levees). We belive the wandering river style (i.e. a transition state between braided and meandering fluvial styles (Malavoi and Bravard, 2010)) represents a special case where a huge noise generated by strong fluctuations in vegetation and geomorphic dynamics and their interactions could lead to some difficulties to clearly identify a toporaphic signature of life. First, the analysis is carried out at corridor scale, then on selected areas of alluvial bars within the corridor based on a dataset of 2009. The exploration of this finer scale allow to concentrate only on the primary succession and capture the signature of the biogeomorphic succession. These scales are the broadest within this thesis from spatio-temporal point of view. The objectives of this chapter are:

(i) to explore the spatial distribution of riparian vegetation of different height regarding connectivity gradients (e.g. distance from and elevation above the main channel) and;

(ii) to capture if possible in a dynamic wandering contexte the topographic signature of riparian vegetation within the active tract.

2. Methods

In the present analysis, we combined different data types, such as LiDAR data and data extracted from digital true color aerial photographs to provide a reliable analysis on vegetation's topographic signature. The workflow coupling the different methods is summarized in Figure 13. We used LiDAR data (source: Cambridge University) to generate a digital elevation model (DTM) because it allows a better representation of topography under vegetation cover than DTM obtained by photogrammetry, especially because LiDAR data was captured in March 2009 when vegetation foliage is still low. The classification of LiDAR point cloud (i.e. separation of ground and aboveground points) was realized by the service provider and it was not possible to redo the classification. We considered that the classification of aboveground points was not always satisfactory, therefore vegetation height data was extracted by the method of photogrammetry based on aerial photographs of August 2009 (source: CRAIG).

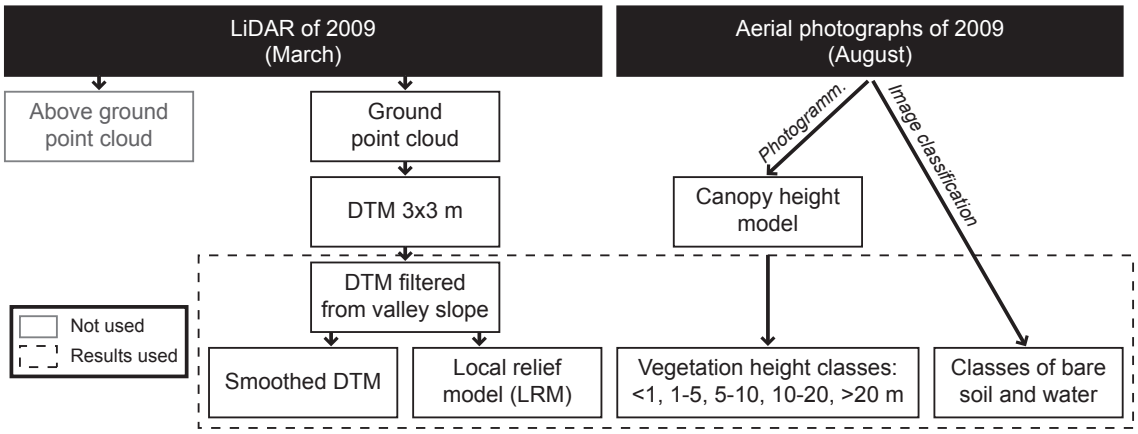

Figure 13. Methodologic workflow of LiDAR, photogrammetric and image classification data processing.

2.1. Extraction of elevation from LiDAR data

The LiDAR data was used to obtain a DTM. The ground point cloud was transformed to a DTM of 3 m resolution. In a first step, the valley slope was filtered from the DTM, then a local relief model (LRM) was extracted. The LRM is obtained with the subtraction of a smoothed elevation model (generated by a low-pass filter with a 15 m window) from the DTM.

2.2. Vegetation height extraction by photogrammetry

Classical digital aerial photographs of 2009 were processed by the method of stereophotogrammetry as described in Chapter II, section 2.3.2 to extract vegetation height. Vegetation height model was classified in five classes as found in literature (Bertoldi et al., 2011): <1 m, 1-5 m, 5-10 m, 10-20 m and >20 m. For the fine scale analysis on alluvial bars, the last two height classes (10-20 m and >20 m) were fusioned due to their low sample size.

2.3. Image classification for bare soil extraction

To determine the bare soil surface, the method of supervised classification was used based on aerial photographs using ERMapper software.

2.4. Extraction of GIS data information

Some additional information was extracted in ArcGIS, such as distance from the center of the main channel and the position on the upstream-downstream gradient of alluvial bars. For this last parameter, which was only calculated at bar sclae, values were related to a percentage where 0% corresponds to upstream and 100% to downstream part of alluvial bars.

2.5. Study reach

The study reach is located in the lower Allier River, and corresponds to the corridor scale described in Chapter II. The selected reach is 10 km long and is located between the town of Châtel-de-Neuvre and the national road n°79 within the "*Réserve Naturelle Nationale du Val d'Allier*". In order to perform a fine scale analysis, 11 alluvials bars were selected within the study reach. The most hydrologically connected areas were visually selected; they are represented by the mixture of bare soil and vegetation cover. We selected these restricted areas to maximize our chance to work on the primary succession, and that we capture the signature of the biogeomorphic succession (i.e. topographic signature of the vegetation related to hydrogeomorphic connection). We excluded secondary succession (i.e. dry disconnected areas and secondary channels) and the influence of grazing. This

choice was made, because the elimination of areas of secondary succession at corridor scale is considered to be uncertain without a diachronic analysis. Figure 14 shows an example of a context where possibily primary succession is represented by older trees surrounded by secondary succession represented by shrubs and development of vegetation at low elevation linked to a secondary channel.

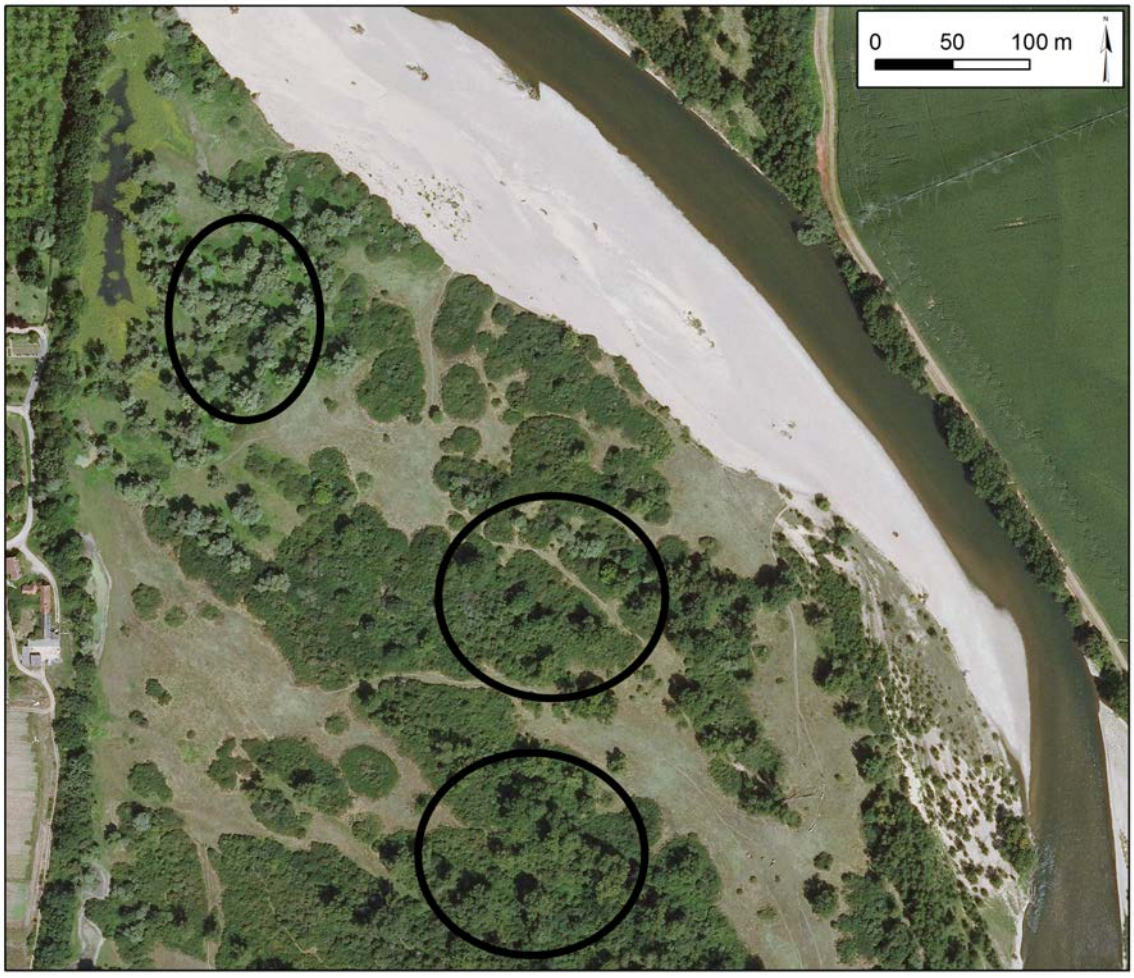

Figure 14. Some examples of possible presence of primary and secondary succession where their distinction might be uncertain.

The fine scale analysis allows a tight connection to the study focusing on the establishment and the biogeomorphic feedbacks of three riparian species on alluvial bars (Chapter IV) during their earlier stage, when the majority of vegetation is not visible on aerial photographs.

The area benefits from a certain protection status and has experienced moderate anthropogenic impacts (e.g. few bank protections or rip rap) (Petit, 2006; Dejaifve and Esquirol, 2011). The erosion rate between 2005 and 2013 calculated for each alluvial bar varies between 1.54 and 16.49 m²/m/year.

Figure 15. The study reach and the selected alluvial bars for fine scale analysis.

2.6. Statistical analysis

For data anlysis, descriptive statistics were used, such as boxplots and violinplots performed with the statistical computing software R (R Core Team, 2015). Boxplots visulases summary satistics (i.e. median, 25% quantile and 75% quantile) and outlying points. Then, analysis of variance (ANOVA) and the Tukey test are applied to determine the differences among group means.

3. Results

3.1. Corridor scale

3.1.1. Distance from the main channel

At corridor scale, bare soil class can be found significantly closer to the main channel compared to vegetation (Figure 16). Bare soil is concentrated close to the main channel, while vegetation is located at farther distance, and established at higher variability of distances as bare soil.

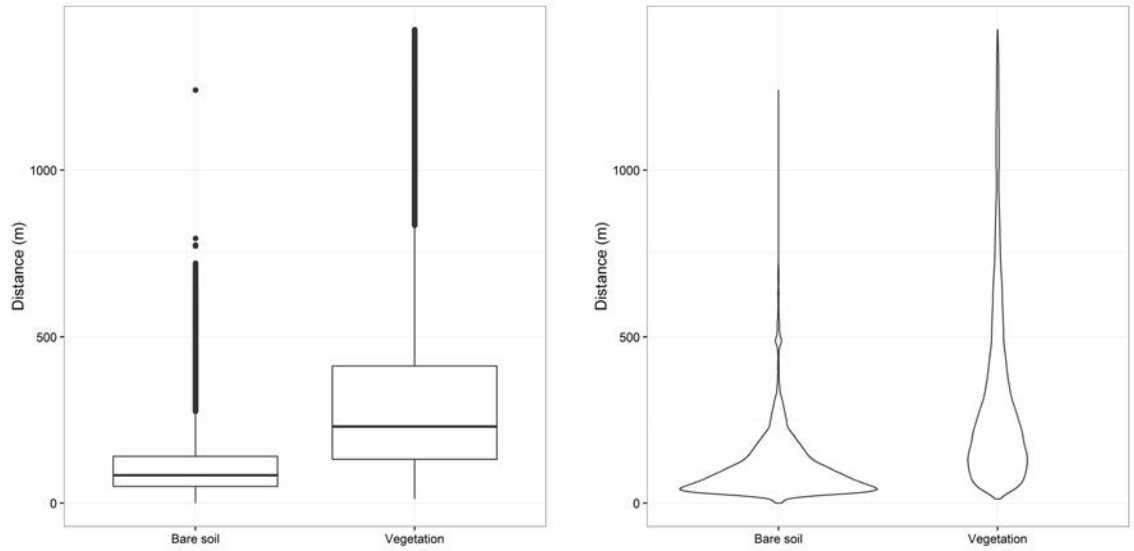

Figure 16. Boxplots (a) and violin plots (b) of differences between distance from the main channel of bare soil and vegetation at corridor scale.

The analysis of variance is significant (p value is <0.0001) between vegetation height classes and bare soil, and the Tukey test showed that classes of 1-5 m and 10-20 m are not different. Smaller vegetation is located in generally farther from the main channel than the higher ones.

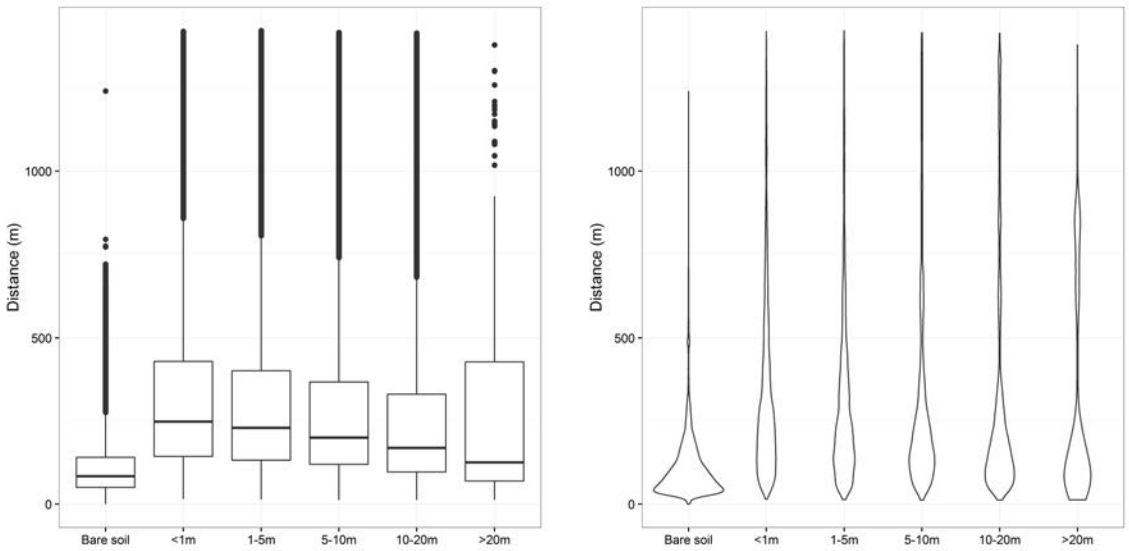

Figure 17. Boxplots (a) and violin plots (b) of differences between the distance from the main channel of bare soil and five vegetation height classes at corridor scale.

Table 5. Analysis of variance of the distance from the main channel between bare soil and vegetation height classes at corridor scale (Tukey test).

Category	LS means	Standard error	Groups					
Bare soil	111.220	0.753	A					
>20 m	275.771	6.208		B				
1-5 m	309.391	0.677			C			
10-20 m	311.676	1.162			C			
5-10 m	317.863	1.050				D		
<1 m	324.980	0.465						E

3.1.2. Topography

Bare soil can be found mainly at the lowest elevation, close to water level (Figure 18), and around 2.5-1 m above the channel. Above 1 m, the proportion of bare soil class is decresing strongly. Vegetation appears at -0.5 m below main channel level, including higher vegetation classes. Proportionally vegetation is the most abundant around 0.5-1 m. Above 1 m elevation there is shift, where the frequency of smaller vegetation classes becomes higher than higher ones.

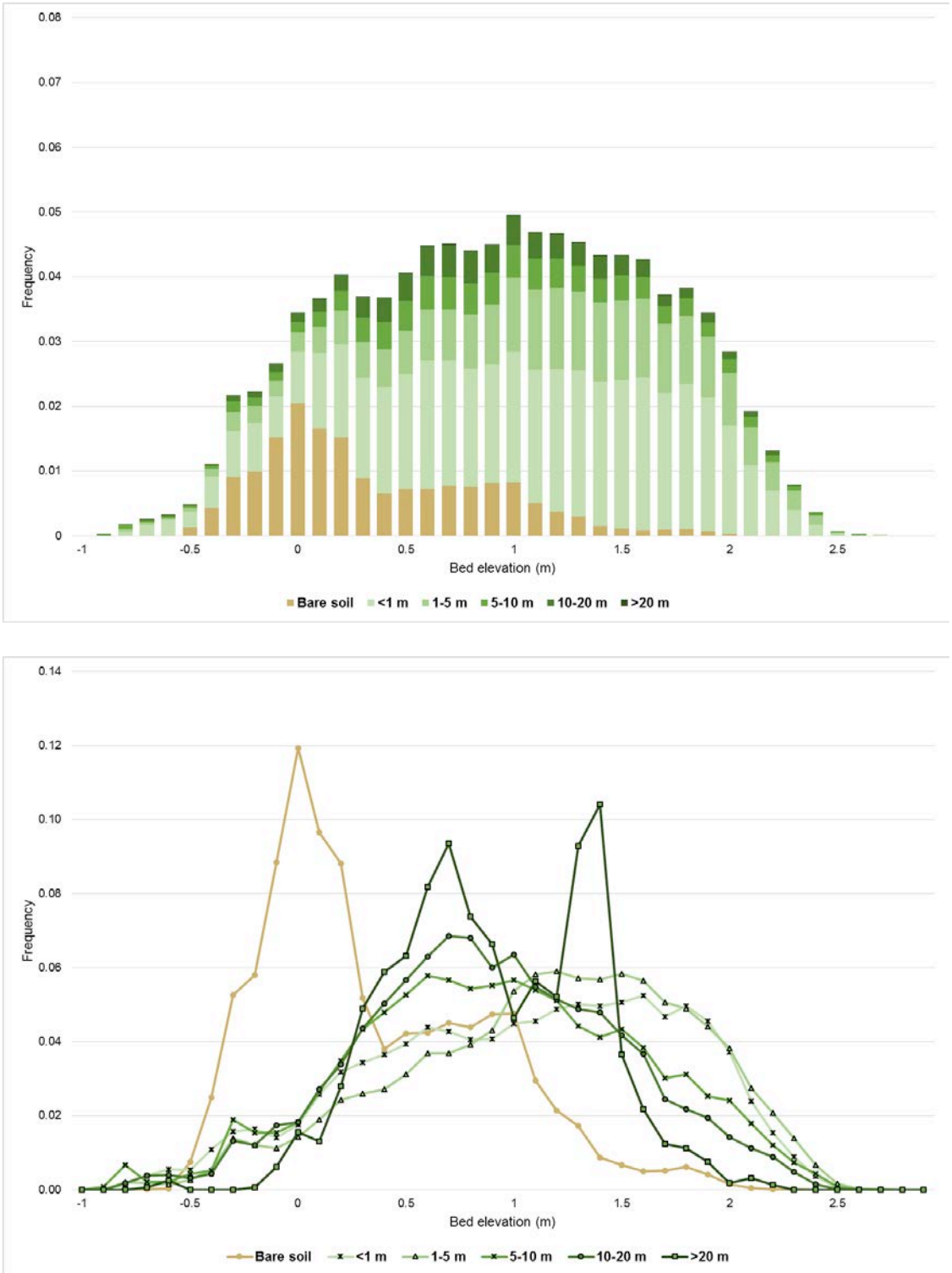

Figure 18. a) Frequency distribution of the bed elevation (mean elevation above water level) according to bare soil and vegetation height classes at corridor scale. Each bar is subdivided according to the proportion of pixels at that elevation. b) Separate elevation frequency distribution of pixels occupied by bare soil and vegetation height classes at corridor scale.

Vegetation can be found at significantly higher bed elevation than bare soil (Figure 19) as confirmed by variance analysis ($p<0.0001$). The violin plots (Figure 19b) allow a better representation of value distribution, especially in case of bare soil. Bare soil can be found mostly close to channel but an important part of this class is located between 0.5 and 1 m elevation from the channel, meanwhile the presence of vegetation is more and more important with increasing elevation.

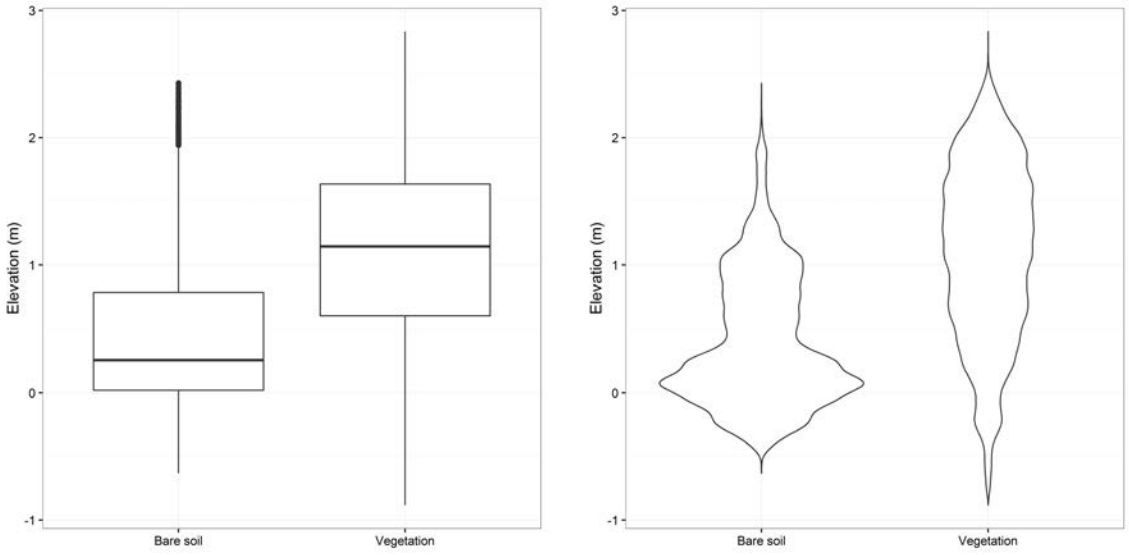

Figure 19. Boxplots (a) and violin plots (b) of differences between bed elevation of bare soil and vegetation classes at corridor scale.

The distribution of bed elevation between bare soil and the five vegetation height classes is represented on Figure 20. The variance analysis shows significant differences (p value is <0.0001) and a Tukey test shows the differences between the groups (Table 6). Bare soil is located at the lowest mean elevation. The highest vegetation classes are classified in the same group. The vegetation located in the highest class of bed elevation is also grouped with the tree height class of 5-10 m. The smallest vegetation classes are different from all other classes and located at the highest mean elevation. Vegetation higher than 20 m is associated to two height classes (5-10 m and 10-20 m).

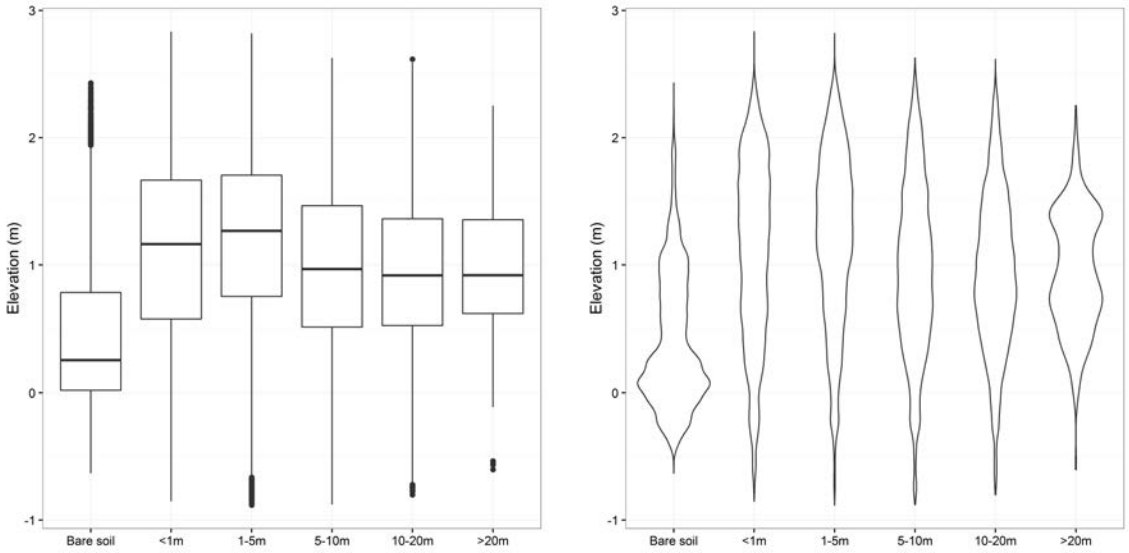

Figure 20. Boxplots (a) and violin plots (b) of differences between bed elevation of bare soil and five vegetation height classes at corridor scale.

Table 6. Analysis of variance of bed elevation differences between bare soil and vegetation height classes at corridor scale (Tukey test).

Category	LS means	Standard error	Groups				
Bare soil	0.404	0.002	A				
10-20 m	0.938	0.003		B			
>20 m	0.952	0.016		B	C		
5-10 m	0.978	0.003			C		
<1 m	1.098	0.001				D	
1-5 m	1.204	0.002					E

3.1.3. *Local relief model (LRM)*

The difference between the mean LRM value of bare soil and vegetation is also significant. Lower values are attributed to bare soil than to vegetation (Figure 21).

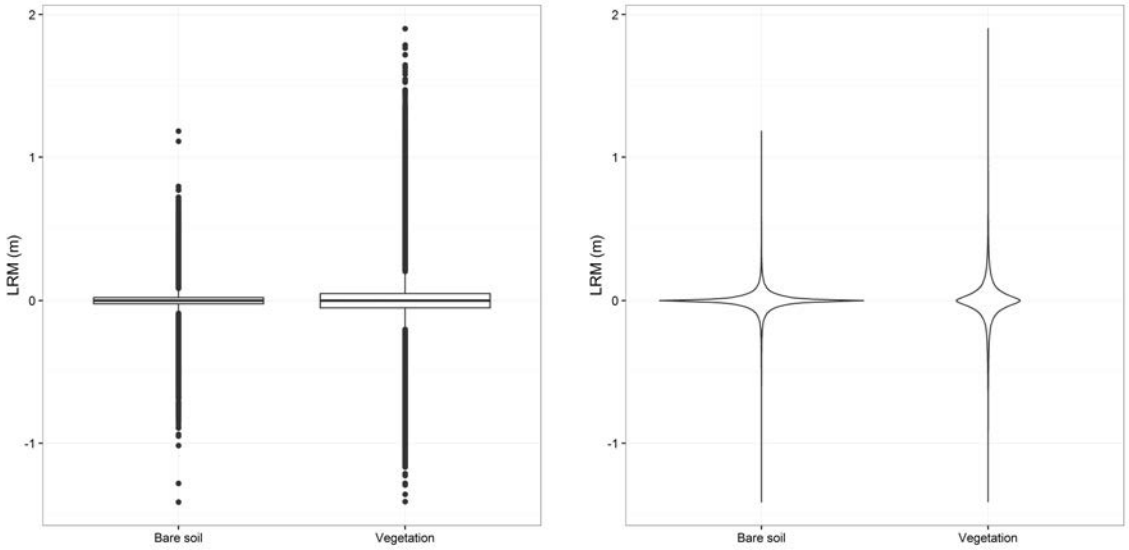

Figure 21. Boxplots (a) and violin plots (b) of differences between the LRM of bare soil and vegetation at corridor scale.

The variance analysis of LRM shows that there is a significant difference (<0.015) between bare soil and vegetation height classes. The height classe of 1-5 m is different from all other classes, and the 5 other classes are distributed in two groups. The classes of 5-10 m, 10-20 m and >20 m represent a group with a higher LRM value, and the classes of >20 m, <1 m and bare soil are characterised by a lower LRM value.

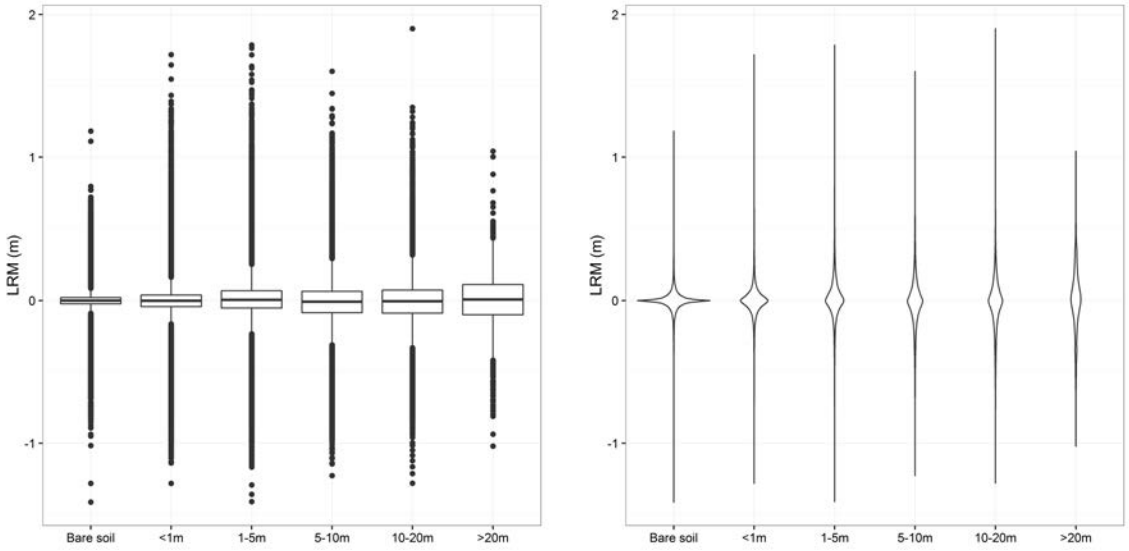

Figure 22. Boxplots (a) and violin plots (b) of differences between the LRM of bare soil and vegetation height classes at corridor scale.

Table 7. Analysis of variance of differences of LRM between bare soil and vegetation height classes at corridor scale (Tukey test).

Category	LS means	Standard error	Groups		
5-10 m	-0.016	0.001	A		
10-20 m	-0.014	0.001	A		
>20 m	-0.005	0.003	A	B	
<1 m	-0.004	0.000		B	
Bare soil	-0.004	0.000		B	
1-5 m	0.010	0.000			C

3.2. Alluvial bar scale

3.2.1. Distance from the main channel

Bare soil class can be found significantly closer to the main channel compared to vegetation (Figure 23 and Table 8). Bare soil is concentrated close to the main channel, then its proportion decreases with the distance. Meanwhile vegetation is located at variable distance.

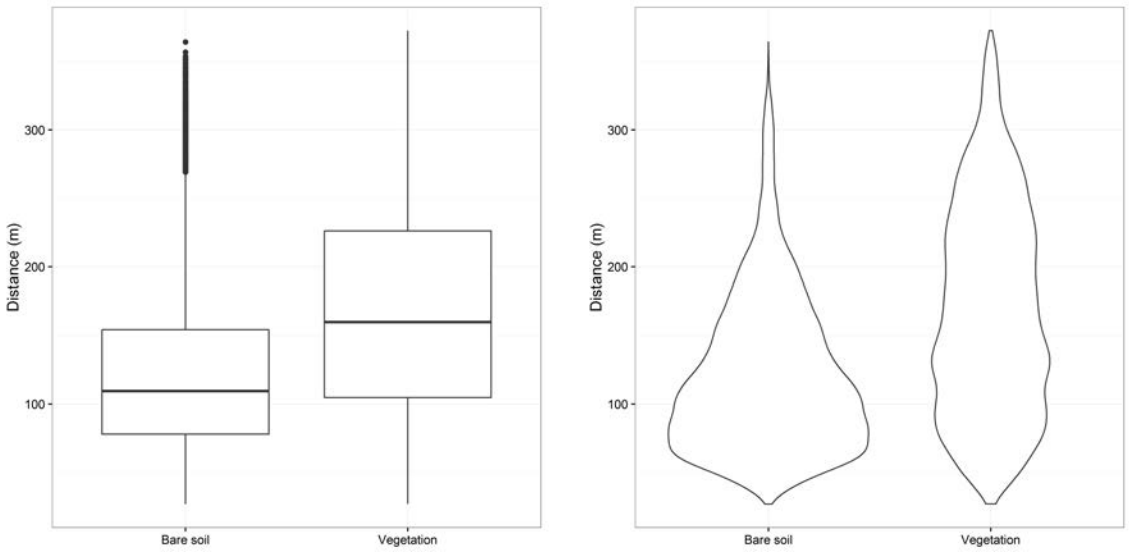

Figure 23. Boxplots (a) and violin plots (b) of differences between distance from the main channel of bare soil and vegetation at bar scale.

Table 8. Analysis of variance of the distance from the main channel between bare soil and vegetation classes (Tukey test).

Category	LS means	Standard error	Groups	
Bare soil	121.520	0.296	A	
Vegetation	167.909	0.349		B

The analysis of variance is significant (p value <0.0001) between vegetation classes and bare soil, and the Tukey test shows that the three lower vegetation height classes are differentiated from the others, meanwhile the highest class (>10 m) is in the same group as bare soil (Table 9). There is a tendency showing that higher vegetation is located closer to the main channel.

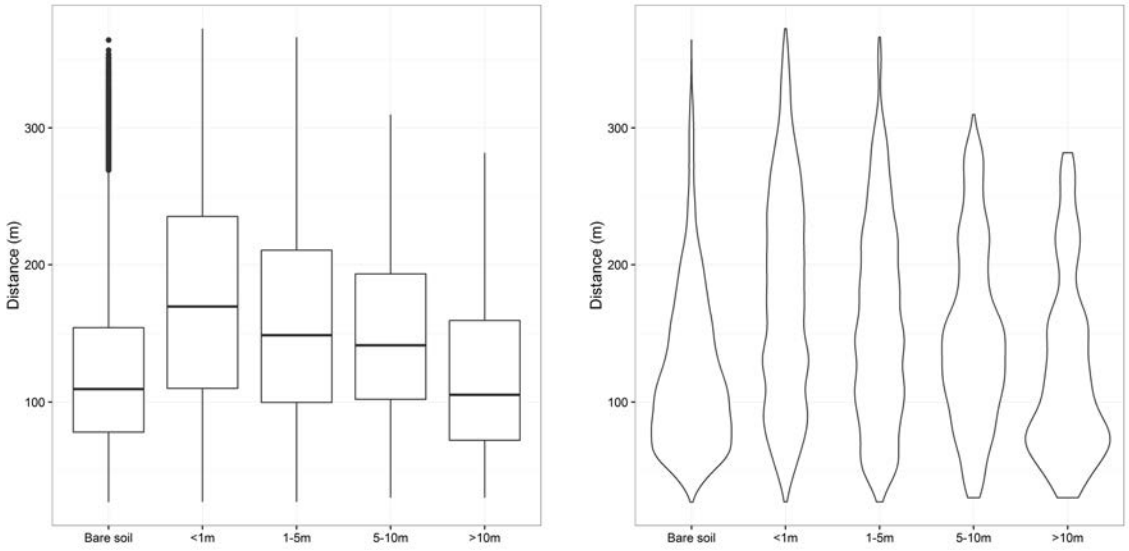

Figure 24. Boxplots (a) and violin plots (b) of differences between the distance from the main channel of bare soil and five vegetation height classes at bar scale.

Table 9. Analysis of variance of the distance from the main channel between bare soil and vegetation height classes at bar scale (Tukey test).

Category	LS means	Standard error	Groups			
Bare soil	121.520	0.294	A			
>10 m	122.384	2.098	A			
5-10 m	148.721	1.258		B		
1-5 m	156.631	0.790			C	
<1 m	174.828	0.413				D

3.2.2. Upstream-downstream gradient of alluvial bars

Bare soil and vegetation classes' distribution is also analysed regarding their position on the upstream-downstream gradient of energy of the alluvial bars. In average, vegetation is located rather upstream than bare soil (Figure 25), with a significant difference (Table 10).

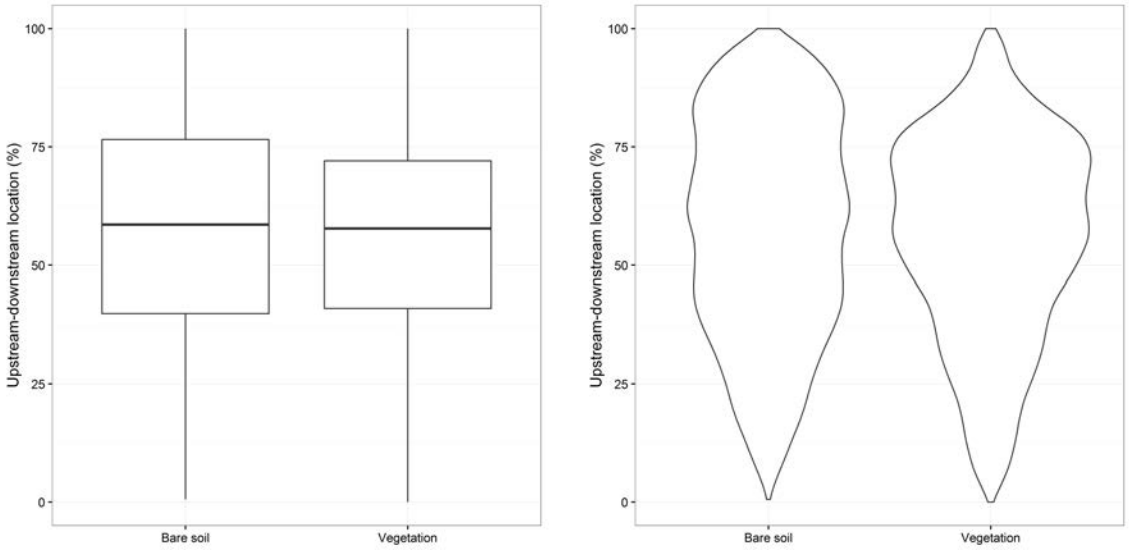

Figure 25. Boxplots (a) and violin plots (b) of differences between the upstream-downstream position (0% - upstream, 100% - downstream) of bare soil and vegetation at bar scale.

Table 10. Analysis of variance of the upstream-downstream position (0% - upstream, 100% - downstream) of bare soil and vegetation class (Tukey test).

Category	LS means	Standard error	Groups	
Vegetation	55.457	0.118	A	
Bare soil	57.352	0.100		B

When comparing bare soil and vegetation height classes, the highest vegetation class is located at the most upstream part of alluvial bars (Figure 26), and the smallest one at the most downstream part. All classes showed a significant difference (Table 11).

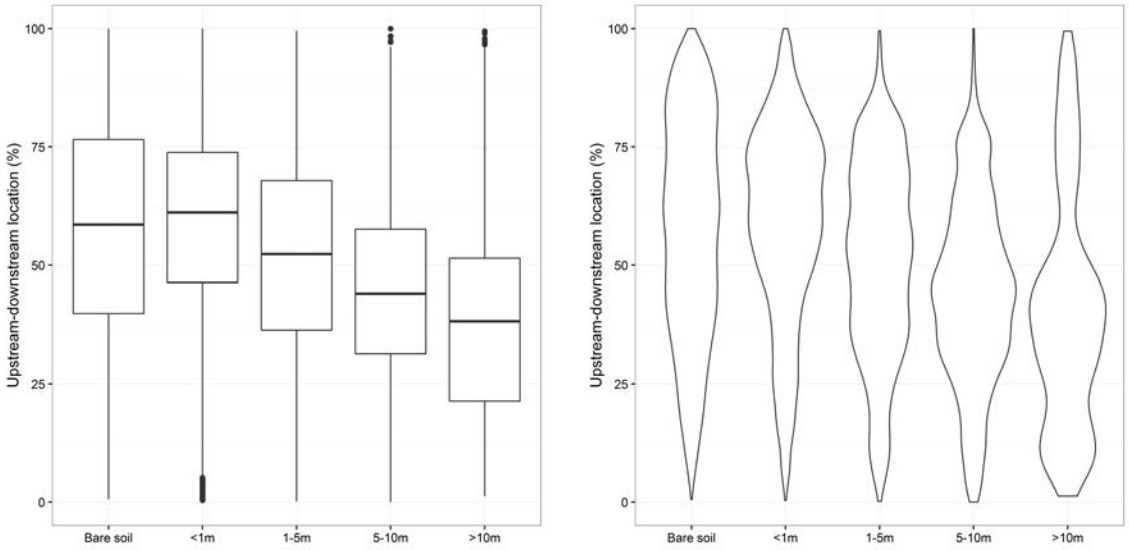

Figure 26. Boxplots (a) and violin plots (b) of differences between the upstream-downstream position (0% - upstream, 100% - downstream) of bare soil and five vegetation height classes at bar scale.

Table 11. Analysis of variance of the upstream-downstream position (0% - upstream, 100% - downstream) of bare soil and vegetation height classes at bar scale (Tukey test).

Category	LS means	Standard error	Groups				
>10 m	40.406	0.709	A				
5-10 m	44.219	0.425		B			
1-5 m	51.156	0.267			C		
Bare soil	57.352	0.099				D	
<1 m	58.429	0.140					E

3.2.3. Topography

Bare soil is mainly present close to the main channel but not exclusively (Figure 27). Bare soil class has also a higher frequency around 1 m above the water level. The dominant vegetation class is the smallest one (<1 m). Vegetation appears at -0.5 m below main channel level, but in majority smaller vegetation classes are present. Proportionally, vegetation is the most abundant around 0.5-1 m, with a peak of vegetation >10 m and <1 m. Around 1.5 m elevation, the frequency of vegetation classes becomes higher.

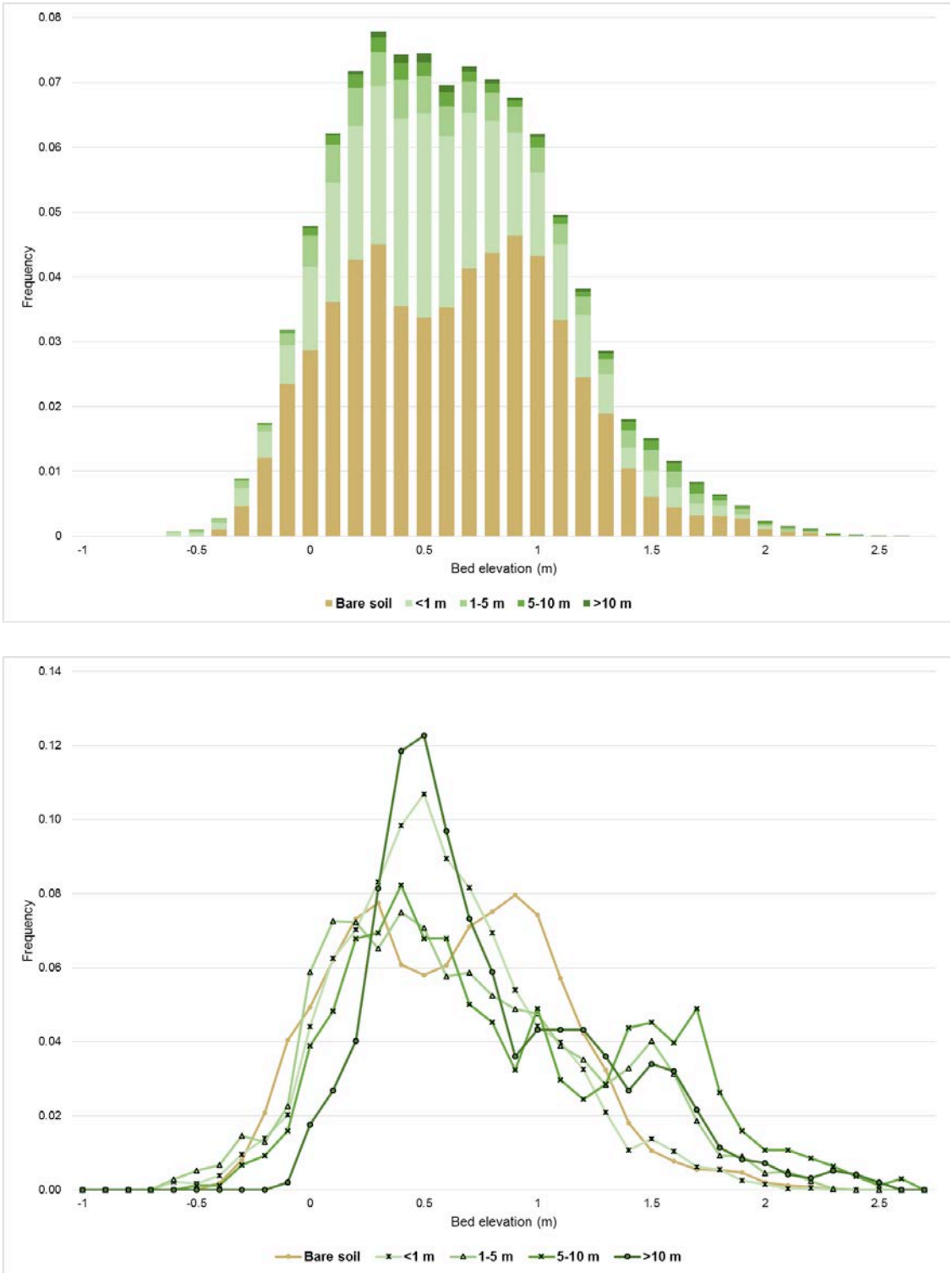

Figure 27. Frequency distribution of the bed elevation (elevation above water level) according to bare soil and four vegetation height classes on alluvial bars. Each bar is subdivided according to the proportion of pixels at that elevation. b) Separate elevation frequency distribution of pixels occupied by bare soil and vegetation height classes at bar scale.

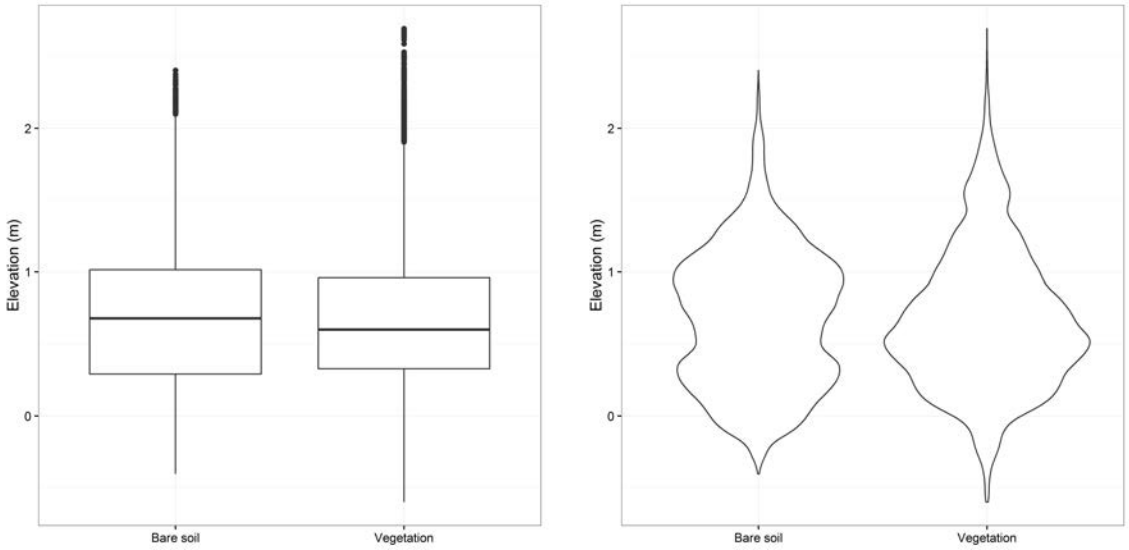

Figure 28. Boxplots (a) and violin plots (b) of differences between bed elevation of bare soil and vegetation classes at bar scale.

There is no significant difference between the bed elevation of bare soil and vegetation classes (Figure 28 and Table 12). Bare soil can be found mostly close to channel but an important part of this class is located around 1 m elevation from the channel. Vegetation is mostly established at around 0.5 m elevation above the main channel.

Table 12. Analysis of variance of bed elevation differences between bare soil and vegetation classes (Tukey test).

Category	LS means	Standard error	Groups
Vegetation	0.671	0.003	A
Bare soil	0.674	0.002	A

The distribution of bed elevation between bare soil and the four vegetation height classes is represented on Figure 29. The variance analysis was significant (p value is <0.0001) and a Tukey test shows where the differences are between the groups (Table 13). The lowest mean bed elevation corresponds to the lowest vegetation height class (<1 m), then it is the bare soil classe, the height class of 1-5 m and finally the highest vegetation classes (5-10 m and >10 m) which are not significantly different.

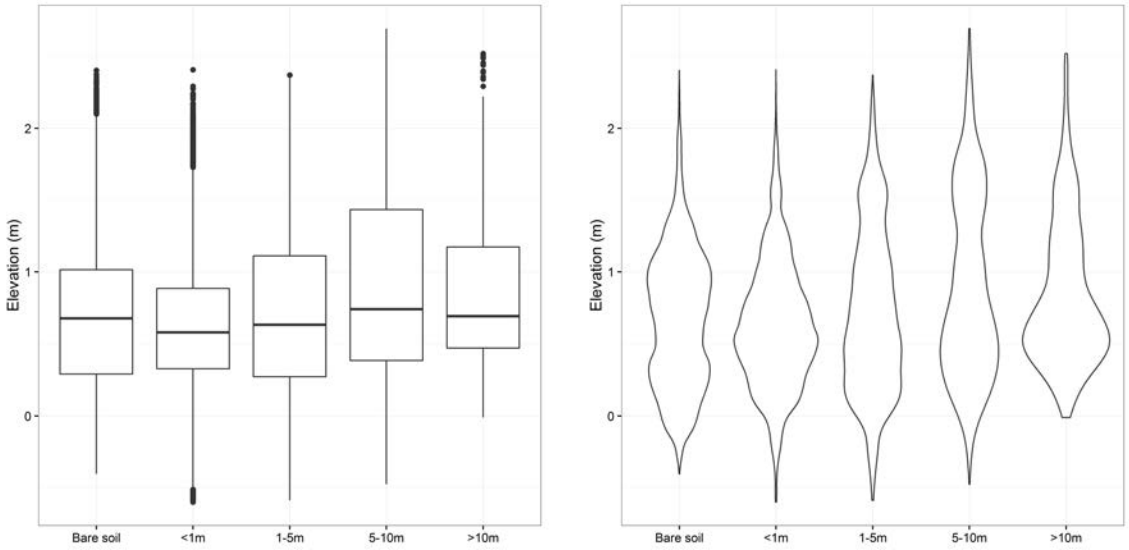

Figure 29. Boxplots (a) and violin plots (b) of differences between bed elevation of bare soil and five vegetation height classes at bar scale.

Table 13. Analysis of variance of bed elevation differences between bare soil and vegetation height classes at bar scale (Tukey test).

Category	LS means	Standard error	Groups			
<1 m	0.628	0.003	A			
Bare soil	0.674	0.002		B		
1-5 m	0.719	0.006			C	
>10 m	0.842	0.015				D
5-10 m	0.889	0.009				D

3.2.4. Local relief model (LRM)

The mean value of the local relief model is significantly lower for the bare soil class (p value is <0.0001) than under vegetation (Table 14 and Figure 30). The variability of LRM values under vegetation is higher.

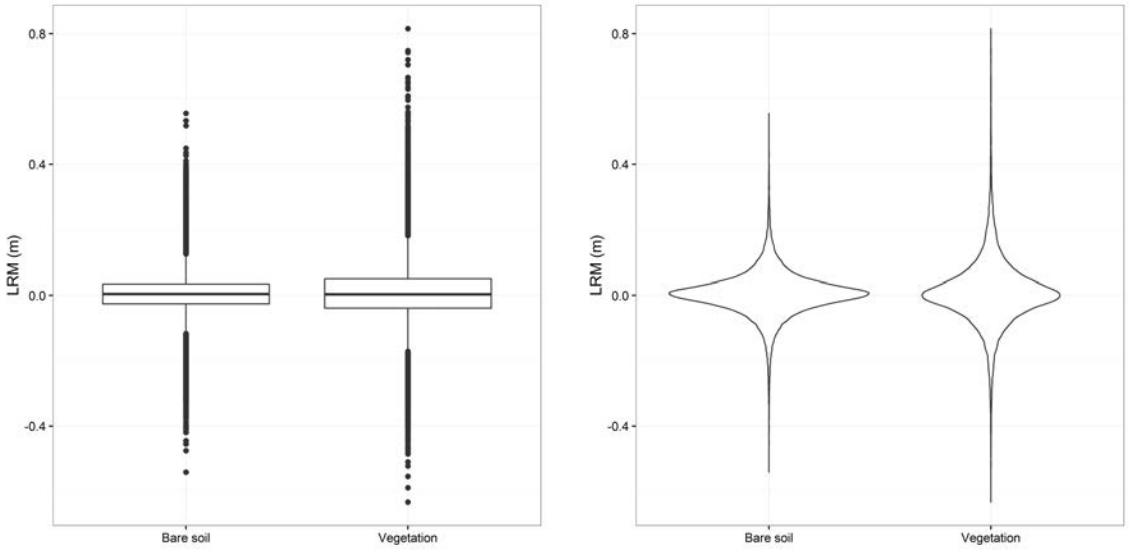

Figure 30. Boxplots (a) and violin plots (b) of differences between the LRM of bare soil and vegetation at bar scale.

Table 14. Analysis of variance of LRM between bare soil and vegetation classes at bar scale (Tukey test).

Category	LS means	Standard error	Groups	
Bare soil	0.004	0.000	A	
Vegetation	0.007	0.000		B

The average LRM value is increasing with vegetation height classes. Bare soil class has a higher value than the lowest vegetation height class. The difference is also significant when comparing all vegetation height classes (Figure 31 and Table 15). Groups are significantly different except in the case of the two highest vegetation classes.

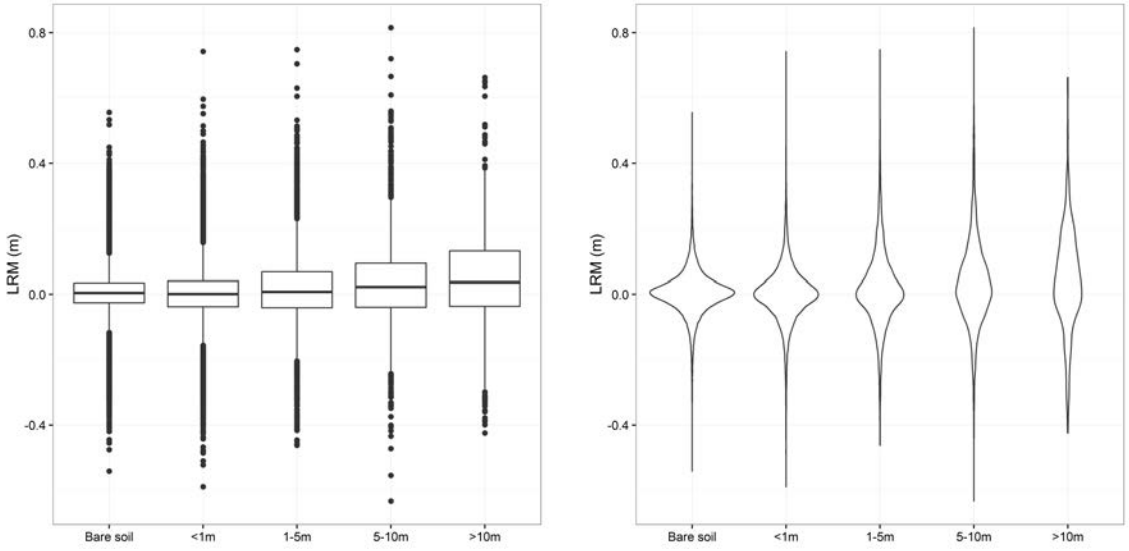

Figure 31. Boxplots (a) and violin plots (b) of differences between the LRM of bare soil and vegetation height classes at bar scale.

Table 15. Analysis of variance of differences of LRM between bare soil and vegetation height classes at bar scale (Tukey test).

Category	LS means	Standard error	Groups			
<1 m	0.001	0.001	A			
Bare soil	0.004	0.000		B		
1-5 m	0.016	0.001			C	
5-10 m	0.033	0.002				D
>10 m	0.041	0.003				D

4. Discussion

4.1. *Methods*

The simultaneous use of LiDAR and photogrammetric data proved to be a good combination. LiDAR data made possible to study topography under vegetaton cover, which is not possible in such a detail by photogrammetry. Photogrammetry allowed us to obtain a better quality canopy height model, that the original LiDAR one. The use aerial photographs also allowed the selection of the bare soil surfaces by image analysis (classification). However, certain disadvantages of these methods were also detected. During data analysis, we noticed an overestimation of topographic elevation under the vegetation class of 1-5 m (Figure 32). This problem might be linked to filtering quality of

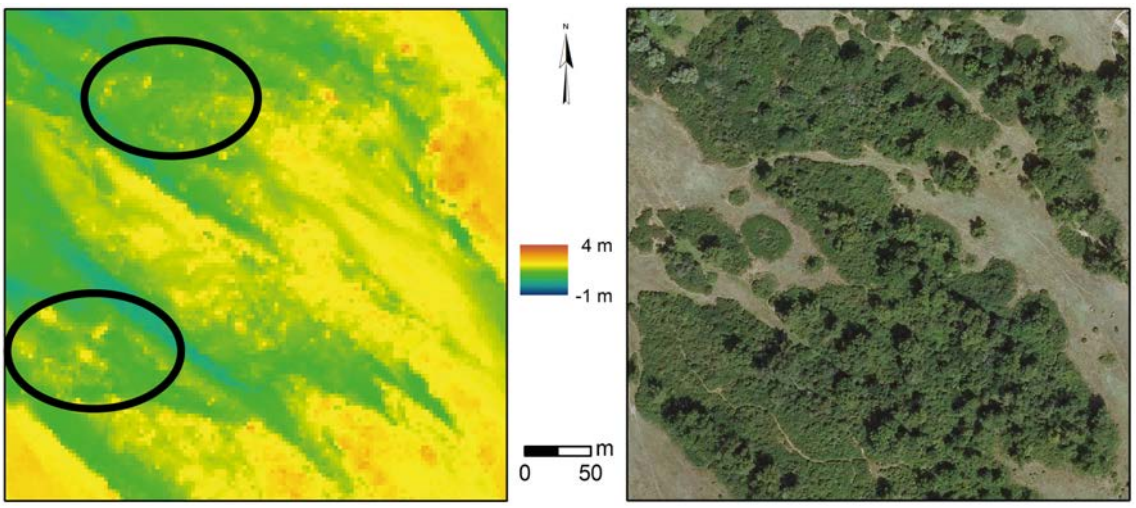

Figure 32. Example of the overestimation of topographic elevation under the vegetation class of 1-5 m. LiDAR DTM on the left side showing some "patchiness" of higher elevation sectors indicating filering imprecision. Aerial photograph of the same area on the right side with dense vegetation cover.

the ground point cloud. In this height class we can find dense shrubs and it is possible that the laser signal did not reach the ground or some points were classified as ground and not as vegetation. This problem is less present at bar scale where dense shrubby vegetation (e.g. *Prunus spinosa*) has a lower occurence.

Another methodological issue was revealed, which is related to the way we classify the vegetation by its height. Since a tree is higher in its centre than at its border, a tree or a vegetation patch can be categorized in multiple height classes (Figure 33). Thus the relation between vegetation patch height and topography might be distorted or smoothed. However, the data analysis was repeated on the alluvial bars based on manually digitalized data and results were very close to the one obtained based on photogrammetric data.

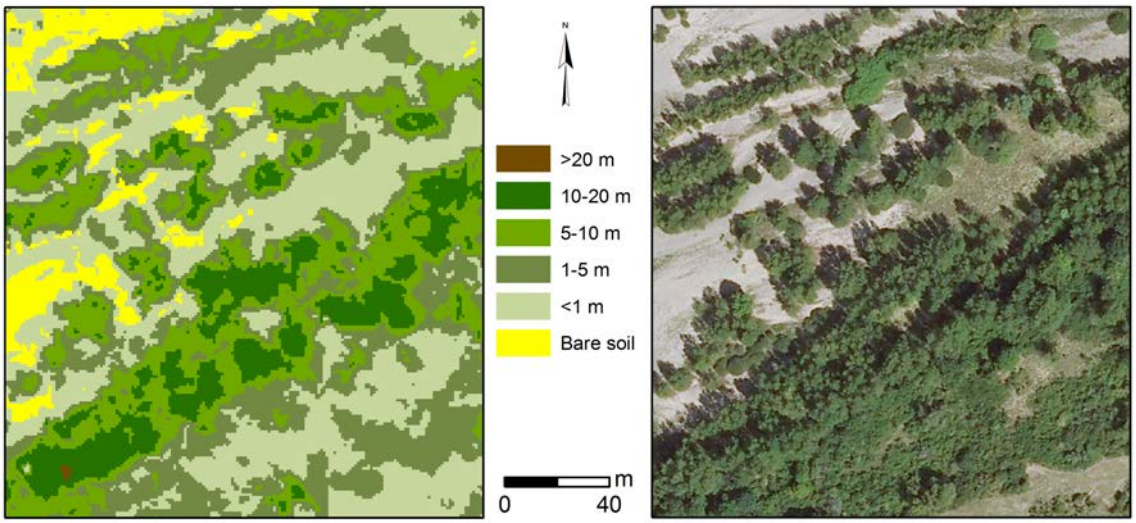

Figure 33. Example of the vegetation height classification resulting concentric classification within vegetation patches.

The local relief model (LRM) might be overestimated at certain zones at corridor scale. High river banks in erosion (usually covered by high vegetation) have high LRM values, however it is not possible to deduce a direct link between high LRM value and vegetation's engineering. This inaccuracy is not present at bar scale, since zones with abrupt elevation differences are not included.

4.2. Spatial extent of vegetation and its relation with topography

4.2.1. Corridor scale

Tendencies related to a topographic signature of vegetation in the landscape are not easily capturable at the corridor scale within a wandering context. The Allier River at corridor scale is a complex shifting landscape mosaic. The mosaic at lower elevation which are more connected to hydrogeomorphic processes and composed both of bare soil and vegetated areas (dominant species are the Salicaceaes according to Garófano-Gómez (2017)). There are also areas at higher elevation which are dryer with herbaceous and shrub species (dominant species are *Sedum* sp., moss, *Prunus* sp., *Crataegus* sp. and *Populus nigra* according to Garófano-Gómez (2017)), where hydrogeomorphic processes have a less important/dominant role in landscape shapening and where dry secondary succession takes place. As explained in the methodological section, results at the scale of the corridor reflect the signature of the biogeomorphic succession but also of secondary succession combined also to the influence of cow grazing. Thus, some caution must be taken for results interpretaion at corridor scale. The choice to not exclude these areas in a first step was made, because the elimination of surfaces with secondary succession and exposed to grazing was considered to be uncertain without a diachronic analysis and the results would have been in any case incertain.

We calculated the local relief model, because it shows surfaces which are higher (or lower) compared to their environment. Such surfaces can revel eventually sediment trapping by riparian vegetation. Boxplots and violin plots of LRM at corridor scale contain many outlyers which makes interpretation challenging. Mean values are very close with a maximum attributed to the class 1-5 m, which might be related, to the low filtering quality of the DTM. With increasing height, boxplots are becoming larger, indicating a higher variability of values, thus possibily an increasing topographic signature. This denotes that our results are possibily in line with the biogeomorphic succession model which shows that more mature vegetation stages induced over time a more important cumulative topographic accretion that the young stages. However, the wandering Allier river is caracterised by a shifting habitat mosaic (Geerling et al., 2006; Garófano-Gómez et al., 2017), which diminish the signature of the FBS model. The elements inducing some ‘noise’ in the FBS model are given below. These elements are context-specific of the Allier River.

Smaller vegetation classes were found farther from the main channel and at higher elevation. These results are not exacly in line with the theorical biogeomorphic succession

model applied to the humide temperate context where the forest represent the post-pionner and mature stages stages at raised surfaces on river benches and floodplains. In that model, the age of vegetation increases with increasing distance from the main channel (Corenblit et al., 2007). In our analysis, possibily small (herbaceous) vegetation is in majority a result of a secondary succession on earlier disconnected surface which result in the study reach of sudden channel shifts, huge sandy sediment accreations occuring during large floods and cretating extensive raised and dry surfaces where Salicaceae recuitement will be inhibited. Certain of these areas are also subject of cow grazing which maintain it open. In addition, the high mean elevation of 1-5 m class might possibly be related to the filtering default of the DTM. The fact that higher vegetation is located close to the main channel can be explained by the fact that high river banks are regulary eroded within the study reach. Those eroding banks are colonized by high (old) trees (Figure 34).

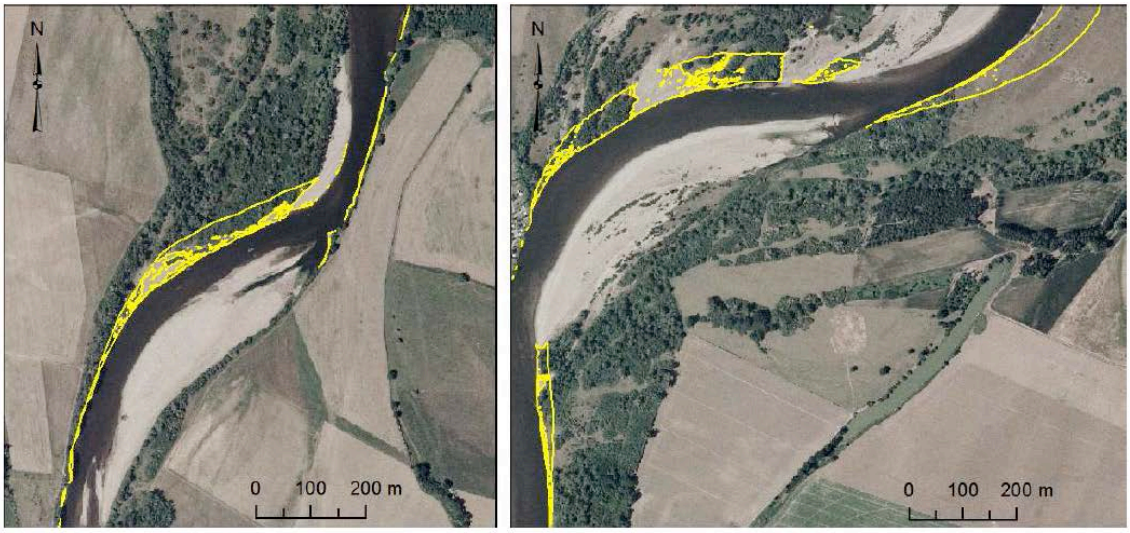

Figure 34. Example of areas with vegetation destruction (indicated by yellow) between 2002-2005 (aerial photographe of 2002, source: IGN) (Hortobágyi, 2012).

The presence of vegetation (including high vegetation classes) below the water level (Figure 18) is related to the establishment of riparain trees in secondary channels (often *Salix* spp.). Stella et al. (2011) described such dynamics, showing in the Sacramento River, USA, that secondary channels can function as refugees for cottonwood recruiment in disturbace-prone ecosystems. On the Allier River, the preferencial establishment elevation of higher vegetation classes was between 0.5-1 m elevation.

4.2.2. Bar scale

Beside the 'noise' originating from the complex shifting mosaic of the river Allier, at bar scale, the FBS model seems to be better supported by our results. The spatial organisation of landscape units (bare soil and vegetation height classes) does not strictly follow the canonical one descibed in the FBS model, nevertheless their topographic elevation and related signature are in accordance with. The spatial and elevational parameters, as well as the strength of the topographic signature of the vegetation is summerized on the Figure 35.

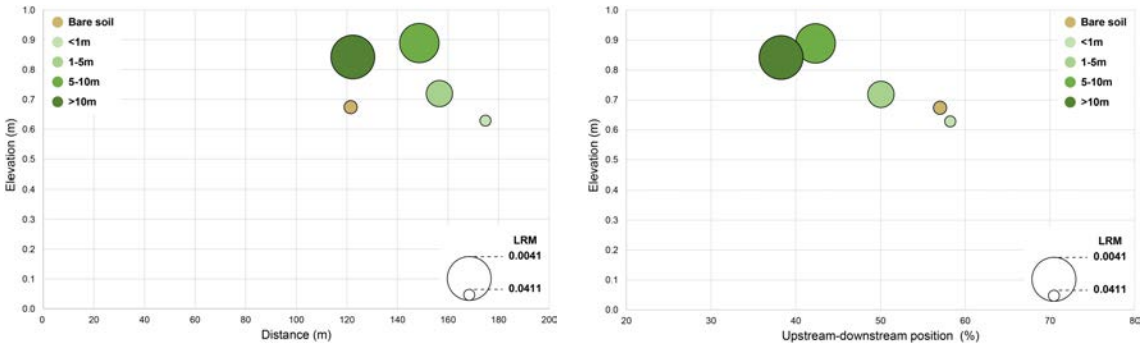

Figure 35. Vegetation height classes distributon along two connectivity gradiets (distance from main channel, upstream-downstream gradient of energy) and their elevation from main channel. The surface of the cercles is proportional to the mean value of local relief model (LRM).

Regarding the spatial organisation of landscape units, as the case at the corridor scale, at bar scale we also found bare soil closer the main channel and the distance from the main channel is decreasing with an increasing vegetation height. The biggest proportion of vegetation was found at three quarter of alluvial bars (Figure 25b), with higher vegetation located upstream and close to the main channel (Figure 26). This might be explained by active lateral and downstream migration of alluvial bars resulting from the erosion of older patches which established and grew in more downstream parts of the alluvial bar, closer to the main channel (Hortobágyi et al., 2017b). Suprisingly, the difference was not significant between the mean elevation of bare soil and vegetation class, however vegetation's presence was concentrated around the elevation of 0.5 m meanwhile the presence of bare soil was concentrated below 0.5 m and around 1 m elevation (Figure 28). As explained in the previsous section, within the context of the study reach, bare soil at higher elevation might be the sign of unsuccessful recruitment of riparain ligneous vegetation as a result of a raised dry surface too much disconnect from the water table in a sandy gravel bed material. Such surface are spatially extensive within the study reach

and they are regularly created durging large floods and channel lateral migration. That would explain to a certain extend the difficlty to find a clear topographic signature of vegetation as described in the FBS or the biogeomorohic life cycle models where highest surfaces should be systematically colonized by a post-pionner forest.

Concerning the relation between vegetation height classes, their elevation and their topographic signature, at bar scale, the FBS model seems to be in line with our results. Higher vegetation was located at higher elevation (Figure 29), creating higher amplitude impact on the relief (Figure 31). The vegetation height classes of 5-10 m and >10 m are not different in elevation, neither in their topographic signature. This may be related to the fact that the maximal sediment trapping effect is reached early during establishment (approx. first 5 years) when the height of the vegetation is around 5-10 m. Corenblit et al. (2016a) obtained similar results on the channelized Garonne River, France. Authors pointed out rapid and important physiognomic changes of *Populus nigra* individuals with increasing height. From 15 m height, the stem density within *P. nigra* patches is decreasing drastically and their diameter is increasing. Authors explained these changes with the decreasing exposure of vegetation patches to hydrogeomorphic contraints, thanks to the rapid landform accretion. The flow energy of the Allier River is possibly lower with a related lower mechanical stress compared to the channalized Garonne River where the concentrated flow carrying a huge quantity of fine sediments (Steiger and Gurnell, 2003) must have a high energy during large flood. In addition, the channel of the Allier River shows a high rate of lateral migration. Thus, physiognomic changes of plants might undergo earlier (i.e. from 5-10 m) on the Allier River than on the Garrone River (i.e. 15 m).

At bar scale, the frequency histogram is more compact and peaked compared to the corridor scale. The preferencial establishment elevation of higher vegetation classes is aroud 0.5 m elevation at bar scale and around 0.5-1 m elevation at corridor scale, which was confirmed by other studies. A second, much smaller peak appeared around 1.5 m (Figure 27). On the island braided Tagliamento River (Italy) in reaches with lower vegetation extent, this value was comprised between 0.5-1 m, and second (smaller) peak appeared around 1.3 m (Bertoldi et al., 2011) as we could see at bar scale (Figure 27). On the Santa Maria River (Arizona), which is a braided to wandering, labile channel, Bywater-Reyes (2017) also obtained the maximum vegetation frequency around 0.5 m. The authors showed, that the greatest elevation was associated to intermediate height classes (1-5 m and 5-10 m), while on the Allier River to the highest ones (5-10 m, >10 m). These differences can be linked to a combinaison of multiple elements. A possible explication might be the difference in species composition. On the Santa Maria River, *Tamarix* is present, which has a shrubby, multi-stemmed morphology offering a high ability in sediment trapping (Kui et al., 2014;

Manners et al., 2015). *Tamarix*, which we suppose to be integrated in height classes of 1-5 m and 5-10 m, might actively increase topographic elevation of these intermediate classes. It is also important to underpin, that proportionally to other height classes, at bar scale the presence of vegetation >10 m was low.

4.3. *Topographic signature of riparian vegetation, the question of spatio-temporal scale and upstream-downstream longitudinal gradient of energy*

The balance between the role of physiscal processes in landform dynamics and the vegetation-mediated landform construction is changing along the upstream-downstream gradient of energy (Figure 36). Gurnell et al. (2012) in a rewiev paper, described the increasing role of vegetation in fluvial landform construction from the upstream to the downstream stections along the gradient of enegry. The authors also emphasized that, as a result of the complex interactions between hydrogeomorphic processes and vegetation characteristics (morphological, biomechanical and life history traits), the engineering effect of vegetation can be expressed by different forms expressing at very specific saptiotemporal scales. Therefore, the topographic signature of the vegetation might be expressed at different spatio-temporal scales depending on the location along the gradient of energy. The temporal scale of landfom construction and destruction (turnover) can vary from a single flood event to thousands of years between the torrentiel and the anastomosing river style. Sediment tails of few cm to few meters may dominate in torrential and braided sections; pionner islands of 10 to 100 m in island braided sections; a combination of mature islands, benches and floodplain levees in wandering sections; pionner and mature floodplain levees in meandering and anastomosing sections. In such trasition, the variation of the reprodcution type of Salicaceae species along the gradient of energy may also have decisive role in the topographic siganture of life. Within higher energy systems (e.g. braided and island braided), the role of asexual reproduction have a greater importance with a resulting local patchy effects on geomorphology compared to lower energy systems (e.g. meandering), where sexual reproduction is the dominant and results in large dense cohorts effects. Within braided and island braided sections, the signature of life may be detectable in the topography at the individual (sediment trail) to small patch (pioneer island) scales after single flood events. For exemple, the topographic signature of vegetation was detected on the island braided Tagliamento River through vegetated islands, which are initiated by dead driftwook and can grow by

their coalescence and have a high turnover (Gurnell et al., 2001), riparian vegetation and island formation). On the wandering Tech River, levee-like strip landforms construction is induced by Salicaceae seedlings (Gurnell et al., 2012). Within meandering river sections, signature of life may be detectable in the topography at the scale of the corridor (floodplain construction) over decades and centuries. For exmaple, Corenblit et al. (2016a) showed on the Garonne River the fast colonisation of point bars by *Populus nigra* L. and their engineering effect resulting a high rate of vertical fine sediment accretion (9 cm $yr.^{-1}$ 5 cm $yr.^{-1}$), therefore the development of biogeomorphic units, i.e. vegetated poit bars. Our results shows that the signature of life in the topography within wandering river sections, such as the one of the Allie River, is more problematic because of its trasition state. The landscape mosaic variability and overlaping of the different spatio-temporal scales of landform construction and dectruction induce a huge noise that at least partially attenuates the signal of the biogeomorphic succession in the landscape.

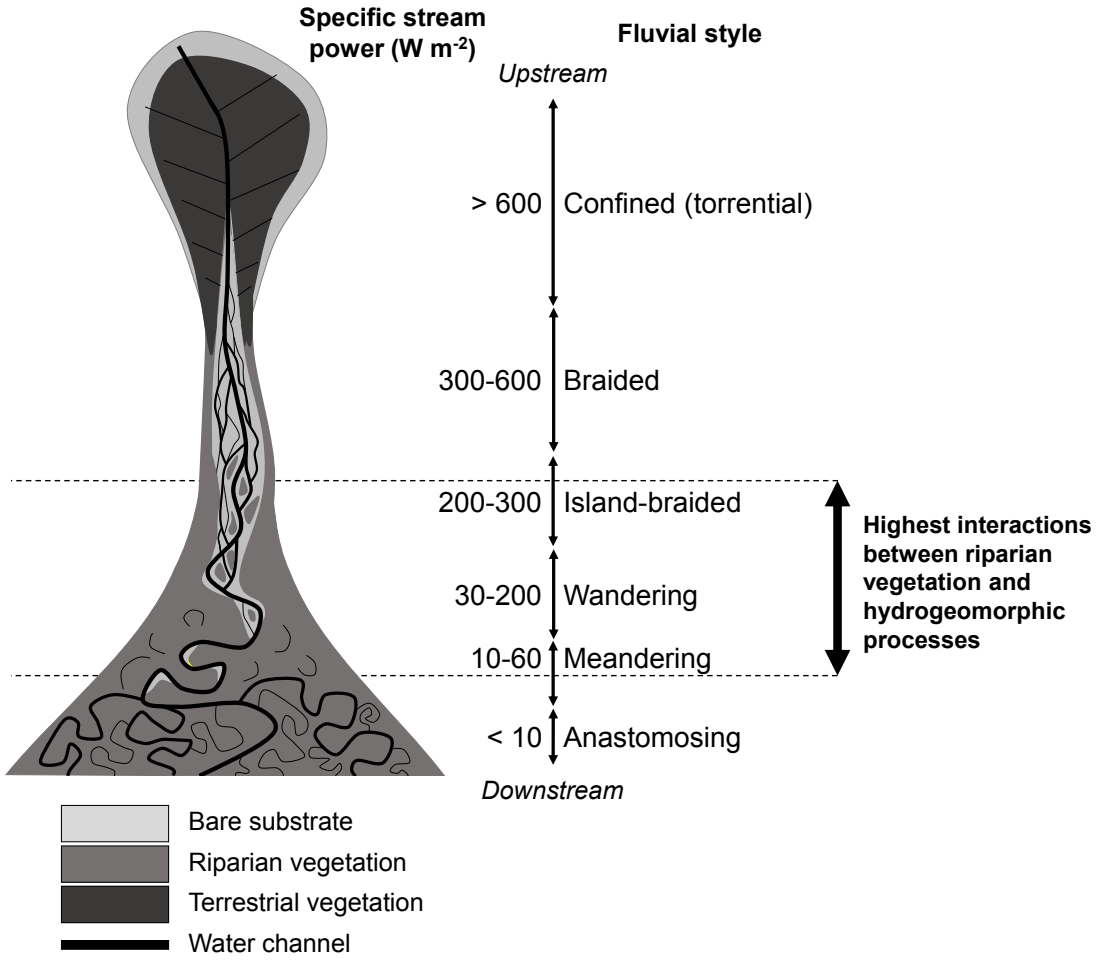

Figure 36. Domain of high interactions between riparian vegetation and hydrogeomorphic processes along the upstream-downstream longitudinal gradient of energy of a river (modified from Corenblit et al. (2017)).

5. Conclusion and perspectives

In this chapter we used the local relief model as a proxy of vegetation induced landform construction. Our analysis showed that the topographic signature of the vegetation is strongly scale dependent. At corridor scale, we showed topographic elevation difference between biotic and abiotic entities. The role of connectivity gradients is less significant as it is at finer scale, suggesting a very heterogeneous landscape mosaic. At the finer bar scale, in contrast, connectivity gradients shows a more important organisational role on riparian vegetation's distribution. Our results are partially in line with the fluvial biogeomorphic succession (FBS) model. On the Allier River the topographic signature seems to increase with increasing vegetation height (what we correspond to an evolution in the biogeomorphic succession), matching to the FBS model. However, the height distribution of riparian vegetation on the most connected part of alluvial bars along the longitudinal gradient is the opposite of the one discribed in the FBS model, which can certainly be explained by the active lateral migration of the channel. Our results thus suggest, that the relative position of vegetation patches, and their changing position on alluvial bars (related to channel migration) would be an interesting complementary parameter of the FBS model. However, based on our results, it is difficult to estimate the role of riparian woody vegetation on the evolutionary trajectory of the Allier River at corridor scale. We could see that at bar scale, woody vegetation enhance landform construction the most efficiently until the size range of 5-10 m. Then (i) thsese pathces might be disconnected from frequent floods, which could stimulate further sediment accumulation within patches, or (ii) because of the lateral migration of the channel, the patches composed of high (old) vegetation are located rather at the upstream part of the alluvial bars and exposed to erosive hydrogeomorphic process. Our results suggest, that the vegetation established on allvial bars, which is highly connected to hydrogeomorphic processes, has a topographic signature, but these biogeomorphic landforms have a high turnover with low resistance and high resilience. Therefore the presence of the oldest vegetation patches within the fluvial corridor might be the result of (i) a sudden channel shift, or (ii) asexual regeneration of *P. nigra*, or (iii) secondary succession close to abandoned channels. The Allier River, which is qualified with a high turnover indicates, that the balance is leaning to the side of physiscal processes' role in landform dynamics rather than on the vegetation-mediated landform construction. A diachronic study would be ueful to obtain the necessary information. In addition, it would help to idenfify primary and secondary succession, the areas of vegetation destruction and establishment and to link vegetation height to age. A 3D diachronic study would be the key to quantify the effect of vegetation on topographic changes in space and time, including the parameter of vegetation growth rate.

Chapter IV. Niche construction within riparian corridors: Exploring biogeomorphic feedback windows of three pioneer riparian species (Allier River, France)

Hortobágyi, B., Corenblit, D., Steiger, J., Peiry, J.-L., 2017b. Niche construction within riparian corridors. Part I: Exploring biogeomorphic feedback windows of three pioneer riparian species, Allier River, France. Geomorphology. doi:http://dx.doi.org/10.1016/j.geomorph.2017.08.048

Abstract – Within riparian corridors, biotic-abiotic feedback mechanisms occur between woody vegetation strongly influenced by hydrogeomorphic constraints (e.g., sediment transport and deposition, shear stress, hydrological variability), fluvial landforms, and morphodynamics, which in turn are modulated by the established vegetation. During field investigations in spring 2015, we studied 16 alluvial bars (e.g., point and lateral bars) within the dynamic riparian corridor of the Allier River (France) to assess the aptitude of three pioneer riparian Salicaceae species (*Populus nigra* L., *Salix purpurea* L., and *Salix alba* L.) to establish and act as ecosystem engineers by trapping sediment and constructing fluvial landforms. Our aim is to empirically identify the preferential *establishment area* (EA; i.e., the local areas where species become established) and the preferential *biogeomorphic feedback window* (BFW; i.e., where and to what extent the species and geomorphology interact) of these three species on alluvial bars within a 20-km-long river reach. Our results show that the EA and BFW of all three species vary significantly along the longitudinal profile, i.e., upstream-downstream exposure on the alluvial bars, as well as transversally, i.e., the main hydrological connectivity gradient from the river channel toward the floodplain. In the present-day context of the Allier River, *P. nigra* is the most abundant species, appearing to act as the main engineer species affecting landform dynamics at the bar scale; *S. purpurea* is established and acts as an ecosystem engineer at locations on alluvial bars that are most exposed to hydrosedimentary flow dynamics, while *S. alba* is established on the bar tail close to secondary channels and affects the geomorphology in mixed patches along with *P. nigra*. Our study highlights the role of functional trait diversity of riparian engineer species in controlling the extent of fluvial landform construction along geomorphic gradients within riparian corridors exposed to frequent hydrogeomorphic disturbances.

Keywords – establishment area; biogeomorphic feedback window; longitudinal and transverse gradients of alluvial bars; riparian Salicaceae species.

List of acronyms

BFW: biogeomorphic feedback window
EA: establishment area
NMDS: nonmetric multidimensional scaling
PN: *Populus nigra* L.
RSS: riparian Salicaseae species
SA: *Salix alba* L.
SD: standard deviation
SP: *Salix purpurea* L.
WoO: window of opportunity

1. Introduction

On alluvial bars of high-energy river reaches, interactions occur between pioneer riparian woody vegetation and hydrogeomorphic processes (Gurnell, 2014). Hydrogeomorphic conditions (sediment texture, exposure to shear stress, topographic level, and hydrological variability) exert a strong influence on vegetation dynamics, and in turn, the established vegetation can modulate the water flow as well as the sediment, landform geomorphology, and topography (Gurnell et al., 2005; Corenblit et al., 2007; Bertoldi et al., 2011). These reciprocal interactions lead to strong feedbacks between fluvial landforms and riparian vegetation during the early stages of vegetation succession.

A significant literature on biogeomorphic topics has emerged over the last 20 years in an attempt to develop conceptual models to explain feedbacks between fluvial geomorphology and riparian vegetation dynamics. In ecology, the concepts of *ecosystem engineer* (Jones et al., 1994) at the community level and *niche construction* (Odling-Smee et al., 2003) at the population level have been applied in the riparian context where certain engineer plant species appear to control riparian ecosystem structure and function by significantly modifying hydrogeomorphic processes, landforms and fluvial habitats (Edwards et al., 1999; Gurnell and Petts, 2006; Corenblit et al., 2007, 2011, 2014; Gurnell, 2014). Such dynamic ecosystems, which are subject to frequent physical disturbances (e.g., floods in rivers) and exhibiting ecological and potentially ecoevolutionary feedbacks between geomorphology and engineer plants, have been defined as *biogeomorphic ecosystems* (Balke et al., 2014; Corenblit et al., 2015a). Within biogeomorphic ecosystems, the synergetic construction of fluvial landforms, the vegetation succession, and the life cycle of riparian trees have been described (i) within the ecosystem engineer framework as a *biogeomorphic succession* (Corenblit et al., 2007) and (ii) within the niche construction framework as a *biogeomorphic life cycle* (Corenblit et al., 2014).

In the initial stages of the biogeomorphic succession and biogeomorphic life cycle, successful colonization by riparian Salicaceae species (RSS) depends on the relations between the hydrogeomorphic disturbance regime, initial habitat conditions, seed dispersal, and seedling recruitment dynamics (Mahoney and Rood, 1998; Perona et al., 2012; Balke et al., 2014). Mahoney and Rood (1998) initially proposed a vegetation recruitment model (*recruitment box model*) based on four key parameters of recruitment: (i) flow variability; (ii) period of seed dispersal; (iii) rate of stream stage decline; and (iv) elevation above the low stream stage. Balke et al. (2011, 2014) defined the concept of *Window of Opportunity* (WoO) in a biogeomorphic ecosystem as a 'sequence of a disturbance-free period of sufficient length for seedling anchorage following a dispersal event'. In the field, we identify the *establishment area* (EA) within a disturbance-driven biogeomorphic ecosystem as the geographic area where vegetation is actually established following a WoO. Once ecosystem engineer species exceed the establishment threshold, a critical engineering threshold must also be exceeded to allow biogeomorphic feedbacks to occur (Corenblit et al., 2007). The concept of a *biogeomorphic feedback window* (BFW), as proposed by Eichel et al. (2015) for high mountain environments, provides a suitable framework for identifying the occurrence of spatio-temporal feedbacks between geomorphic and vegetation dynamics. These authors (*op. cit*.) successfully used ordination (nonmetric multidimensional scaling) and *post hoc* correlation methods to analyse the relation between engineer plant species and geomorphic processes and identified the optimal conditions for the occurrence of biogeomorphic feedbacks between specific plant assemblages and hillslope processes leading to the development of solifluction lobes. In the case of fluvial environments, we define BFW as a specific spatio-temporal envelope of interactions taking place between hydrogeomorphic and RSS dynamics (e.g., *Populus nigra* L., *Salix purpurea* L., and *Salix alba* L.) that trigger strong biogeomorphic feedbacks.

In our study, we investigate the spatial extent of this BFW, i.e., the geographic areas within the riparian corridor where RSS can act as ecosystem engineers. The resistance and resilience of biogeomorphic ecosystems are intimately linked to the BFWs of engineer plants (Corenblit et al., 2015a). In the ecological literature, mainly two forms of resilience are distinguished: (i) ecological resilience *sensu* Holling (1973) corresponds to the ability of a system to retain essential processes when disturbed while maintaining its structural and functional integrity before changing to another domain of attraction, i.e., it can be measured as the magnitude of disturbance that the system can tolerate and still persist (Holling, 1973; Carpenter et al., 2001); and (ii) engineering resilience, which is a more traditional view, representing the ability of a system to resist physical disturbance; it can be measured as the rate at which the system returns to equilibrium following a disturbance

(Pimm, 1984; Carpenter et al., 2001; Gunderson et al., 2010). We use resilience here in the sense of ecological resilience and resistance in the sense of engineering resilience. The latter reflects the physical resistance of plants and fluvial landforms to mechanical constraints during hydrogeomorphological disturbances (floods). Vegetation can establish and resist hydrogeomorphic constraints to a certain point and thus generate feedbacks by modifying the hydrogeomorphic environment. As a result, vegetation will influence the resistance of landforms to hydrogeomorphic disturbances and enhance their recovery after destructive-dominated flood events, therefore also affecting the persistence of biogeomorphic landforms, i.e., ecological resilience.

By filtering morphological, biomechanical, phenological, and physiological traits, hydrogeomorphic processes control species composition on alluvial bars in the early stages of succession (Richter and Richter, 2000). Few woody riparian species develop traits adapted to the highly disturbed riparian environments where shear stress, erosion, sediment burial, and drought make it difficult for plants to establish (Gurnell, 2014). The RSS such as poplars and willows are recognized as the main species capable of (i) establishing on exposed alluvial bars and (ii) potentially affecting the geomorphology. Such species have developed particular traits in response to hydrogeomorphic disturbances, adapting their reproduction (sexual and asexual modalities), as well as their morphological and biomechanical properties to fluvial environments (Karrenberg et al., 2002; Lytle and Poff, 2004). A significant body of research has identified several riparian engineer species belonging to the Salicaceae (Gurnell, 2014), including, for example, *Populus nigra* L., which is widely distributed within the European continent (Gurnell and Petts, 2006).

However, to our knowledge, the distinction between RSS concerning their specific affinity to establish on alluvial bars and their effect on geomorphology has been given little consideration. The RSS exhibit large variations in their physiological, morphological, and biomechanical functional attributes and thus (i) they may colonize different areas with contrasted habitat conditions on alluvial bars (Johnson, 2000; Guilloy-Froget et al., 2002; Pasquale et al., 2013), and (ii) they potentially affect geomorphology differently because they are not distributed over the same range of exposure to hydrogeomorphic constraints and display different morphologies and biomechanical attributes at the interspecific level, but also at the intraspecific level in relation with environmental conditions (Hortobágyi et al., 2017a). Based on these considerations, we hypothesize that RSS act differently as ecosystem engineers within a given river reach and that their effects on geomorphology vary in intensity according to their location along (i) the upstream-downstream gradient of exposure on alluvial bars; (ii) the transverse gradient of connectivity from the main channel toward the floodplain; and (iii) to their physiognomic attributes such as stem height, diameter, and density.

We focus on the biogeomorphic succession or the biogeomorphic life cycle of RSS (Corenblit et al., 2007, 2014), from the end of the pioneer phase (1 year) to the end of the biogeomorphic phase (10 years) before entering into the ecological phase. At the beginning of the pioneer phase (after germination and during the beginning of the growth season, corresponding to the first 6 months), RSS seedlings may exert a surface protection and stabilizing effect when grouped in dense aggregates. However, these seedlings are not yet able to have a strong effect on hydrogeomorphic processes and fluvial landforms. If RSS seedlings resist drought during the summer (first 6 months) and then floods during the autumn-winter period (second 6 months), they start to be potentially capable of affecting hydrogeomorphic processes. The ecological phase can be determined by multiple criteria, e.g., taxonomic and topographic (Corenblit et al., 2009) or pedologic (Bätz et al., 2015). We determine here the onset of the ecological phase as the moment when *P. nigra* (the most abundant species in our study area) finishes constructing its optimal habitat and reaches sexual maturity (see part 2 this issue; Corenblit et al., (2017)). Under optimal conditions, this time lapse is 10 years on average (Isebrands and Richardson, 2014), but may be delayed or even impeded when the vegetation is exposed to very high-energy hydrogeomorphic conditions or in the case of channelized and regulated rivers. During the ecological phase, vegetation is rather disconnected from annual floods and sediment fluxes, and their interactions with hydrogeomorphic processes are weak (Corenblit et al., 2009). Conversely, the biogeomorphic phase is characterized by the possibility of strong interactions between vegetation and hydrogeomorphic processes. Under specific spatio-temporal conditions, a *biogeomorphic feedback window* (BFW) may open and lead to biogeomorphic feedbacks during this critical phase of riparian ecosystem organization. We focus here on the three most abundant ligneous RSS: *Populus nigra* L., *Salix purpurea* L., and *Salix alba* L., found on the alluvial bars of a dynamic reach of the Allier River, France. The hypothesis tested here is that the occurrence and location of the EA and BFW are likely to vary for these three species, depending on their distribution on the alluvial bars along the upstream-downstream (longitudinal) exposure gradient and main channel-floodplain (transverse) gradient of connectivity. In this empirical study, the main objectives are as follows:

1. to determine the EA of *P. nigra*, *S. purpurea*, and *S. alba* on alluvial bars along the upstream-downstream exposure gradient and the transverse gradient of connectivity from the main channel toward the floodplain;
2. to ascertain whether the three species act as ecosystem engineers, i.e., the existence of a biogeomorphic feedback window (BFW) for each species, which leads to significant biogeomorphic feedbacks; and
3. if point 2 proves to be the case, to determine the specific BFW of each species.

2. Methods

2.1. *Study reach*

The study reach is located in the lower Allier River (France), which is a dynamic wandering/meandering gravel bed river (Figure 37). A 20 km reach was chosen between the Sioule River confluence and Moulins. This reach is characterized by active lateral erosion on the outer bends of meanders, with point bar formation and migration on the inner bends within the *Réserve Naturelle Nationale du Val d'Allier*. The area benefits from a certain protection status and has experienced moderate anthropogenic impacts (e.g., few bank protections or rip rap) (Petit, 2006; Dejaifve and Esquirol, 2011). The erosion rate between 2005 and 2013 calculated for each alluvial bar varies between 1.54 and 16.49 m²/m/y (Figure 37).

2.2. *Life history of* Populus nigra, Salix purpurea *and* Salix alba

We focus on three pioneer woody riparian plant species belonging to the Salicaceae family, *Populus nigra*, *Salix purpurea*, and *Salix alba*, which are widely distributed in high-energy river reaches in Europe and which are dominant on the alluvial bars of the Allier River. All three species potentially act as ecosystem engineers but in different ways according to their specific physiognomic attributes, location on the alluvial bars, and abundance (Table 16). In terms of water access, *P. nigra, S. purpurea*, and *S. alba* are all mesohygrophilic species. However, *S. alba* requires a high and stable water table (Isebrands and Richardson, 2014; Houston Durrant et al., 2016). *Populus nigra* seedlings are considered to be more resistant to drought than *S. alba* (Splunder et al., 1996). A comparative study of *S. alba* and *S. purpurea* reveals better drought resistance of the latter species (Lavaine, 2013). This plant species produces less biomass, showing less reduction in structural root production (roots with a diameter up to 5 mm) and a high shoot-to-root ratio under conditions of stress. In the absence of induced drought stress, *S. purpurea* shows a very high aboveground biomass production (more marked than belowground) but a lower growth rate than *S. alba*. *Salix purpurea* is also a stress-tolerant species in relation to extreme heat, drought, and long periods of submersion (Isebrands and Richardson, 2014), and thus it is well adapted to become established on gravel bars. *Populus nigra* also colonizes exposed moist sandy alluvial surfaces, which provide the optimum seedbed following seasonal flooding (Isebrands and Richardson,

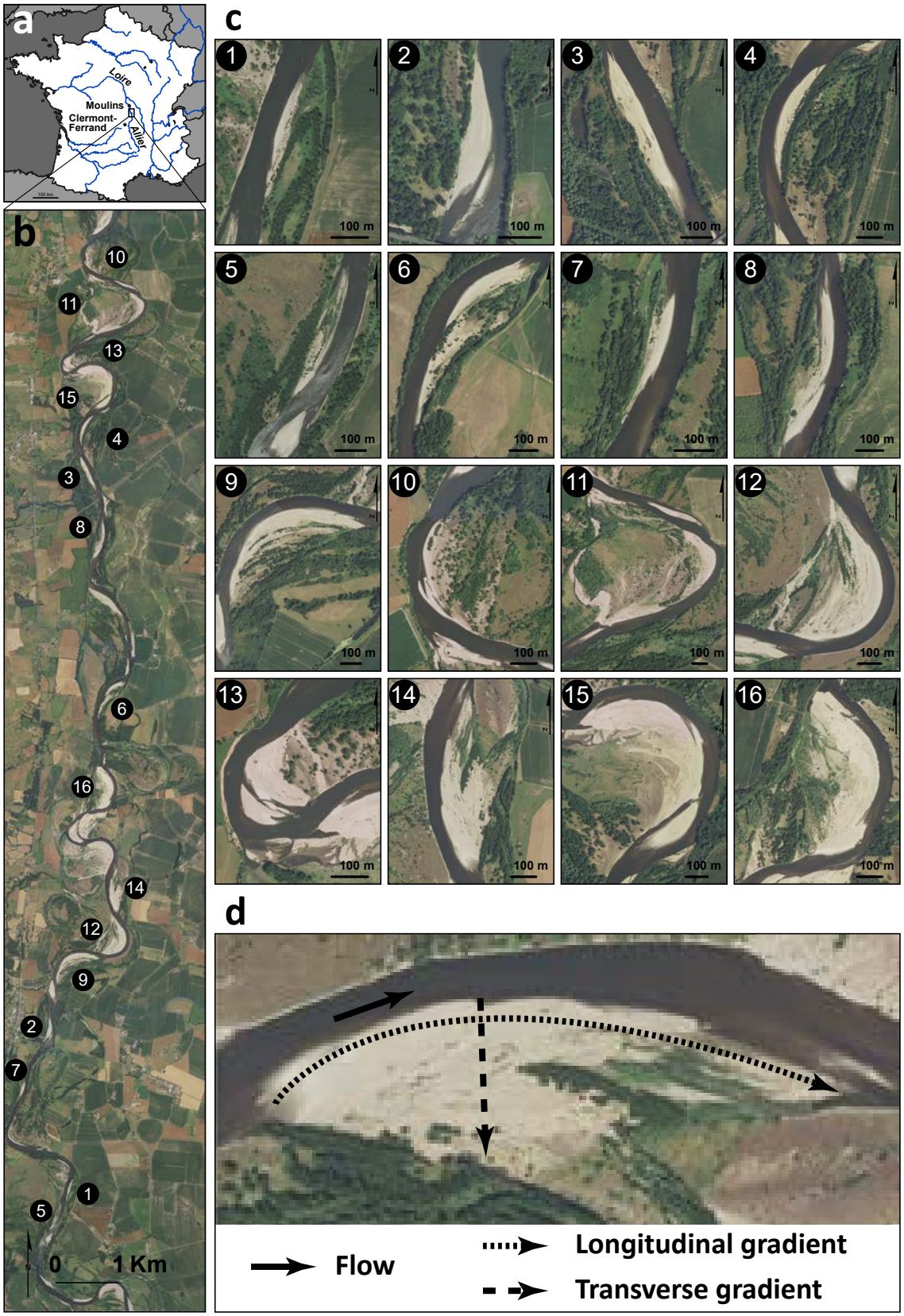

Figure 37. The study reach of the Allier River and the 16 alluvial bars ranked from 1 to 16 according to increasing lateral erosion rate (1.45, 1.61, 1.74, 1.78, 1.93, 2.01, 3.13, 4.37, 5.26, 5.57, 7.59, 7.61, 8.65, 10.10, 16.49 m²/m/y) calculated from aerial photographs taken in 2005 and 2013.

Table 16. Ecological summary of *Populus nigra* L., *Salix purpura* L. and *Salix alba* L. (Karrenberg et al., 2002; Rameau et al., 2008; Lavaine, 2013; Isebrands and Richardson, 2014)

Parameters	*Populus nigra* L.	Salix purpura L.	*Salix alba* L.
Morphotype	Tree, reaching heights of 40m and diameters over 2m at maturity	Shrub, medium-sized to tall shrub or small tree can grow up to 4m but usually 1–2m tall, branches of 0.6-1.5cm diameter	Tree, attaining heights of 30m and trunks up to 1m or more in diameter
Reproduction	Sexual and vegetative		
Seed dispersal	Large quantities (poplars can produce 30–50 million seeds in a single season) of tiny seeds attached to a cottony coma dispersed by wind (anemochory) or water (hydrochory)		
Seed longevity	20 days	*Salix*: limited longevity	
Recruitment conditions depends on:	water level in the channel, the groundwater table, sediment texture, availability of bare sediment		
Longevity	Up to 400 years	>50 years	5-50 years
Growth rate	High: within their first growing season up to a height of 0.5–1m, rapid root expansion		
Root system	Poplars: downwardly directed 'sinker' roots and horizontal roots and can develop root suckers	Salix species: one main downwardly oriented taproot, which thickens with age	

Autecology	Light	heliophilous		heliophilous		heliophilous	
	Edaphic condition	pH from basic to neutral		pH neutral		pH from basic to neutral	
		coarse alluvial material (sand, gravel, silt), aerated soil		frequently coarse alluvial material (clay, gravel, sand)		alluvial material (clay-silt, sand, gravel or pebble well aerated)	
		Mesohygrophilic, slightly hygrophilic in regularly flooded environment		Mesohygrophilic to mesophililic, on annually flooded soil, occasionally mesoxerophilous when behaving as a pioneer		Mesohygrophilic	
		*	**	*	**	*	**
***Ecological valence** (Julve, 2016) **and** ****Ellenberg indicator values** (Evette et al., 2012)	Light	8	5	8	8	8	5
	Moisture	7	8	8	x	8	8
	Reaction	7	7	7	8	7	8
	Nutrient	7	7	5	x	7	7
	Organic matter	8		1		8	

2014). The species has a good capacity of adaptation to flood-induced constraints such as prolonged submersion, mechanical stress, droughts, or sediment burial, as it has a high phenotypic plasticity. The physiological, morphological (size and shape), and biomechanical (flexibility) properties make *P. nigra* well adapted to this unstable and heterogeneous environment (Corenblit et al., 2014). For a detailed description of the life cycle of *P. nigra*, see Corenblit et al. (2014).

2.3. Field sampling and GIS

A total of 126 vegetation patches were sampled on the 16 alluvial bars. Patches are composed of one of the species *P. nigra*, *S. purpurea*, or *S. alba* or a mixture in varying proportions, with or without the presence of a herbaceous mat. Vegetation height within all sampled patches is <3 m, and all patches are highly connected to hydrogeomorphic processes as they are located on the alluvial bar at a relatively low elevation near the water level. Sampling was undertaken in April 2015 during low water stage when the youngest patches were not submerged. Furthermore, the absence of leaves during this period facilitates the estimation of abiotic and biotic parameters (i.e., biogeomorphic accumulation landforms, stem diameter, density, and vegetation degradation degree). The patch survey includes assessment of the following parameters: geomorphic (main geomorphic process, patch, and alluvium grain size), ecological (species abundance, stem density and diameter, vegetation height and occurrence of a herbaceous mat within the patch), morphometric (ease of delimitation of patches, degree of degradation, and tilting of the vegetation), and biogeomorphic (occurrence of biogeomorphic accumulation landforms and presence of sediment tail on the leeside of the patch). All parameters are visually assessed in the field using categorical groups. The main geomorphic processes are clearly erosion dominated, clearly deposition dominated, or are neither erosion or deposition dominated. The dominant sediment size is assessed as sand, gravel, or coarse gravel. Species abundance is expressed as the percentage of the three species (*P. nigra*, *S. purpurea*, and *S. alba*) within a patch, giving a total of 100%. For stem density, the three categories used are based on the distance between stems, i.e., low (>1 m), medium (0.5-1 m), and high (<0.5 m). Four categories are created for stem diameter: very small (<1 cm), small (1-2 cm), medium (2-4 cm), and large (>4 cm). Vegetation height is determined for each of the three species within each patch, then weighted by the abundance of species to calculate the average weighted height of the patch. The average is divided into four categories: very small (<0.5 m), small (0.5-1 m), medium (1-1.5 m), and tall (>1.5 m). The occurrence of a herbaceous mat within the patch is estimated as

none, very low, high, or very high. The ease of delimitation of patches is also assessed by a visual estimation such as low, medium, or high, as well as the degree of degradation and tilting of the vegetation that are categorized as none, low, or high. The degradation of the vegetation relates to the damage caused by impacts during floods, involving coarse sediment or dead wood, and the resulting broken stems or branches and signs of impact on the stem. The presence or absence of biogeomorphic accumulation landforms is also noted; one of the types of accumulation features is the sediment tail on the leeside of the patch. All patches are localized using a GPS (Trimble GeoXH).

Field data are supplemented with variables calculated in a GIS (e.g., distance from channel, position on the alluvial bar, and minimum age). The fieldwork took place over several days, and the water level was variable during sampling. Therefore, the determination of the distances of the patches from the channel (transverse gradient: close, middle, far) is based on the aerial photographs of 2013 to ensure a constant water line. The aerial photographs were taken between 11 and 14 July 2013 when flow conditions were very similar to those during field sampling. The position of patches along the longitudinal gradient (upstream, central, and downstream) on the alluvial bar is calculated by dividing the alluvial bar into three parts along the water line. The limits of the classes for the transverse gradient are calculated by subtracting or adding the standard deviation from the mean value. The minimum age is considered as an approximate age estimation for the patch based on three aerial photographs (2009 – resolution of 0.30 m, 2011 – resolution of 0.30 m and 2013 – resolution of 0.25 m). This method does not give the exact age because very young or small patches cannot be detected on aerial photographs, and aerial photographs are not available for every year. However, this variable gives an estimation of the duration of existence of the patch with an error of between 1 and 3 years.

2.4. Data analysis

First, we use descriptive statistics and statistical tests to see how longitudinal and transverse gradients control biotic and abiotic variables and which variables are conditioning the occurrence of the biogeomorphic feedback windows of each of the three species on alluvial bars. For qualitative variables, we use contingency tables and a X^2 test of independence along with Fisher's exact probability test. This test determines if the difference with the theoretical value is significant or not; for each cell, the test indicates if the actual value is equal (=), lower (<), or higher (>) than the theoretical value. For quantitative variables, the Kruskal-Wallis nonparametric test is applied with

a Steel-Dwass-Critchlow-Fligner multiple pairwise comparison procedure to identify which samples are responsible for rejecting H_0. Letters are assigned to groups (i.e., A, B) indicating that the groups are significantly different.

In a second step, we use an ordination technique (nonmetric multidimensional scaling, NMDS) with *post hoc* correlation as proposed by Eichel et al. (2015) to assess the relationships between biotic and abiotic variables and geomorphic characteristics. The NMDS is a rank-order-based method that represents as well as possible the ordering relationships among objects (their proximity indicates similarity) along a predetermined small number of axes. Ordinations of objects can be produced from any distance matrix with the ordination axes indicating the main variation (gradient) of the variables. Except for the distance used for NMDS, see Eichel et al. (2015) for a description of the method and for details about the ordination technique. After a comparison of dissimilarity indices for the detection of gradients, the Gower distance appears to be the most appropriate for our dataset. We use nonmetric multidimensional scaling ordination to assess which abiotic factors (position on longitudinal and transverse gradient) influence the species composition, biogeomorphic landforms, and other biotic factors of the patches.

Logistic regression modelling (Logit) is used to predict the probability of occurrence of a given species or biogeomorphic accumulation landform according to the longitudinal and transverse gradients.

The descriptive statistics and statistical tests are carried out within XLSTAT software, while the NMDS is performed with the statistical computing software R (R Core Team, 2015) using metaMDS in the R vegan package (Oksanen et al., 2016). We use Envfit (R vegan) for *post hoc* correlation. Logit models are also computed in R software.

3. Results

3.1. Longitudinal and transverse gradients: sediment and vegetation

Most of the abiotic and biotic parameters on the alluvial bars respond significantly to the longitudinal (upstream–downstream) or transverse (main channel to floodplain) gradients, or both (Table 17). Regarding the longitudinal gradient, significant differences between patches almost exclusively concern up- and downstream locations, i.e., bar

Table 17. Biotic and abiotic parameters along the longitudinal and transverse gradients: the *p*-values of X^2 and pairwise test results (> attraction, < repulsion from the variable) are indicated in grey when significant.

Parameters		Longitudinal gradient			Transverse gradient		
		Upstream	Central	Downstream	Close	Middle	Far
Sediment grain size at the bar surface	Sand	<	<	>	>	>	<
	Gravel	<	>	<	>	<	<
	Coarse gravel	>	>	<	<	>	>
p-value at $\alpha = 0.05$			**<0.0001**			0.26	
Vegetation age	1	>	>	<	>	<	>
	2	<	<	>	>	<	<
	4	<	>	<	<	>	>
	6	>	<	<	<	>	<
p-value at $\alpha = 0.05$			**0.008**			**0.08**	
Vegetation height	Very small	>	>	<	>	<	<
	Small	<	<	>	>	<	<
	Medium	<	<	>	>	<	>
	Tall	<	>	>	<	>	>
p-value at $\alpha = 0.05$			**0.007**			**0.0003**	
Stem diameter	Very small	>	>	<	>	<	<
	Small	<	<	>	>	<	>
	Medium	<	>	>	<	>	>
	Big	>	>	<	<	>	>
p-value at $\alpha = 0.05$			**0.003**			0.19	
Stem density	Low	>	>	<	<	>	<
	Medium	<	<	>	<	<	>
	High	<	<	>	>	>	<
p-value at $\alpha = 0.05$			**0.03**			0.18	
Degree of vegetation degradation through flood damage	None	<	>	>	<	>	>
	Low	>	<	<	>	>	<
	Strong	>	<	<	>	<	<
p-value at $\alpha = 0.05$			**0.008**			**0.0002**	
Occurrence of herbaceous mat	None or very low	>	>	<	>	<	<
	(Very) high	<	<	>	<	>	>
p-value at $\alpha = 0.05$			**0.001**			**0.0005**	

heads and tails. Bar heads display a coarse sediment matrix, whereas the matrix of the central and downstream locations are dominated by sand. Patches older than two-years are positively associated with downstream locations, whereas one-year old patches are mainly found on bar heads where vegetation is of very small height (mean ± SD: 0.82 ± 0.69 m) with very small stem diameter (1.35 ± 1.37 cm). Seventy percent the patches at upstream locations and 79% of the patches close to the main channel are highly damaged, and no herbaceous vegetation cover is present within these patches. In contrast, patches at downstream locations are characterised by the tallest vegetation size classes on the alluvial bars and also the largest diameters (respectively 1.19 ± 0.57 m and 1.68 ± 0.81 cm) and highest stem densities (stem spacing <1 m). These patches are generally (in 77% of the cases) covered by a dense herbaceous mat. Conversely to the longitudinal gradient, the sediment matrix is not structured along the transverse gradient. However, riparian trees are younger and smaller, with smaller stem diameters close to the main channel (0.56 ± 0.33 cm) than close to the floodplain (0.97 ± 0.62 cm). Similarly to upstream locations, the riparian trees are highly damaged and no herbaceous vegetation cover occur within the patches close to the main channel. By contrast, riparian trees in the middle location of the bar or close to the floodplain are older and taller (middle location: 1.04 ± 0.71 m, far: 1.31 ± 0.84 m) with larger stem diameter (middle location: 1.52 ± 1.23 cm, far: 2.02 ± 1.56 cm) than trees close to the main channel. These trees are rarely damaged by flood flow, and a dense herbaceous vegetation cover is present.

3.2. *RSS patches:* P. nigra, S. purpurea *and* S. alba

The three pioneer riparian ligneous species (i.e., *P. nigra*, *S. purpurea*, and *S. alba*) are unequally represented in our study area in terms of abundance. Out of the total number of 126 sampled patches on the 16 alluvial bars, *P. nigra* occurs in 101 patches, *S. purpurea* in 55, and *S. alba* in 26 (Table 18). In terms of average abundance, *P. nigra* again is the dominant species, making up more than 65% of the total abundance for the three species; *S. purpurea* accounts for 25%, and finally, *S. alba* for <10% of the average abundance (Table 18). On monospecific patches, *P. nigra* remains dominant, with a total of 59 monospecific patches among the 126 patches; *S. purpurea* accounts for 20 patches and finally, *S. alba* for only 4 patches. The three species coexist on 43 patches (Table 19).

Table 18. Presence of the three species and comparison of their abundance within vegetation patches according to the longitudinal and transverse gradients (PN=*P. nigra*, SP=*S. purpurea*, SA=*S. alba*; SD=standard deviation; letters are assigned to groups (i.e., A, B) indicating that the groups are significantly different)

Species	Parameters	Longitudinal gradient			Transverse gradient			Abundance of patches	Average abundance (%)
		Upstream	Central	Downstream	Close	Middle	Far		
PN	N	32	37	32	12	66	23	**101**	
	%	*25.40*	*29.37*	*25.40*	*9.52*	*52.38*	*18.25*	***80.16***	
	Mean (%)	58.51	74.93	65.71	31.25	74.73	80.92		
	SD	45.32	41.69	36.81	42.9	37.05	34.11		**66.25**
	Group	**A**	**B**	**AB**	**A**	**B**	**B**		
	***p*-value at $\alpha = 0.05$**		**0.04**			**<0.0001**			
SP	N	25	12	18	23	24	8	**55**	
	%	19.84	*9.52*	*14.29*	*18.25*	*19.05*	*6.35*	***43.65***	
	Mean (%)	34.04	18.75	20.29	65.36	12.84	14.79		
	SD	43.67	37.48	27.41	44.45	25.38	29.94		**24.88**
	Group	**A**	**B**	**AB**	**A**	**B**	**B**		
	***p*-value at $\alpha = 0.05$**		**0.05**			**<0.0001**			
SA	N	6	6	14	3	21	2	**26**	
	%	*4.76*	*4.76*	*11.11*	*2.38*	*16.67*	*1.59*	***20.63***	
	Mean (%)	7.45	6.32	14	3.39	12.43	4.29		
	SD	24.74	22.41	24.34	12.48	27.58	19.99		**8.87**
	Group	**A**	**A**	**B**	A	A	A		
	***p*-value at $\alpha = 0.05$**		**0.01**			0.04			
Total number of patches	N	**47**	**44**	**35**	**38**	**111**	**33**	**126**	
	%	***37.30***	***34.92***	***27.78***	***20.88***	***60.99***	***18.13***	*100*	

Table 19. Presence of monospecific and mixed species patches according to the longitudinal and transverse gradients (PN=*P. nigra*, SP=*S. purpurea*, SA=*S. alba*; the *p*-values of X^2 and pairwise test results (> attraction, < repulsion from the variable) are indicated in grey when significant)

Species		Longitudinal gradient						Transverse gradient						Abundance of monospecific and mixed patches
		Upstream		Central		Downstream		Close		Middle		Far		
PN	N	18	<	29	>	12	<	5	<	40	>	14	>	**59**
	%	*14.29*		*23.02*		*9.52*		*3.97*		*31.75*		*11.11*		***46.8***
SP	N	13	>	6	<	1	<	16	>	3	<	1	<	**20**
	%	*10.32*		*4.76*		*0.79*		*12.70*		*2.38*		*0.79*		***15.9***
SA	N	2	>	1	<	1	<	0	<	4	>	0	<	**4**
	%	*1.59*		*0.79*		*0.79*		*0.00*		*3.17*		*0.00*		***3.2***
MIX	N	14	<	8	<	21	>	7	<	27	>	9	>	**43**
	%	*11.11*		*6.35*		*16.67*		*5.56*		*21.43*		*7.14*		***34.1***
p-value at $\alpha = 0.05$				0.0005						<0.0001				
Sum (PN+SP+SA+MIX)	N	47		44		35		28		74		24		126
	%	*37.30*		*34.92*		*27.78*		*22.22*		*58.73*		*19.05*		*100*

The first NMDS axis is mainly related to the variable that indicates the position on the upstream-downstream profile (Longitudinal; $r^2 = 0.20$); this axis is mostly linked to the longitudinal gradient of energy which classically decreases from bar head to bar tail. However, this variable is also related to the transverse gradient. The second NMDS axis is mainly related to the variable indicating the distance from the main channel (Transverse; $r^2 = 0.26$); and is linked to the transverse gradient of exposure. Four patch types can be identified based on the NMDS results (Figure 38A). Figure 38B shows a schematic representation of the four patch types. Type 1: small *P. nigra* monospecific patches with small diameters and low stem densities found upstream and in central bar locations on the longitudinal gradient and mainly at middle locations away from the main channel in coarse sediment. Type 2: the second group is mainly composed of monospecific patches of *S. purpurea*, which are also small and characterized by small stem diameters. These patches are composed of strongly tilted, flood-damaged riparian vegetation located at upstream or central locations of the alluvial bars, close to the channel in coarse sediment where erosive processes dominate. Type 3: these patches are mainly composed of *P. nigra* and *S. purpurea* at variable locations on the two gradients: the vegetation being taller, older, and damaged by floods and having larger stem diameters and higher stem density. Type 4: older patches composed exclusively of *P. nigra* or a combination of *S. alba* and *P. nigra* of large size and stem diameter, being located mostly downstream or at middle or far locations away from the channel in fine sediment. Dense herbaceous mats and intact patches mostly occur within this type of patch. While *P. nigra* and *S. purpurea* are discriminated by the second axis, they nevertheless occur together mostly at downstream locations or within older patches (influence of the first axis). *Salix alba* is discriminated from the two other species on the first axis.

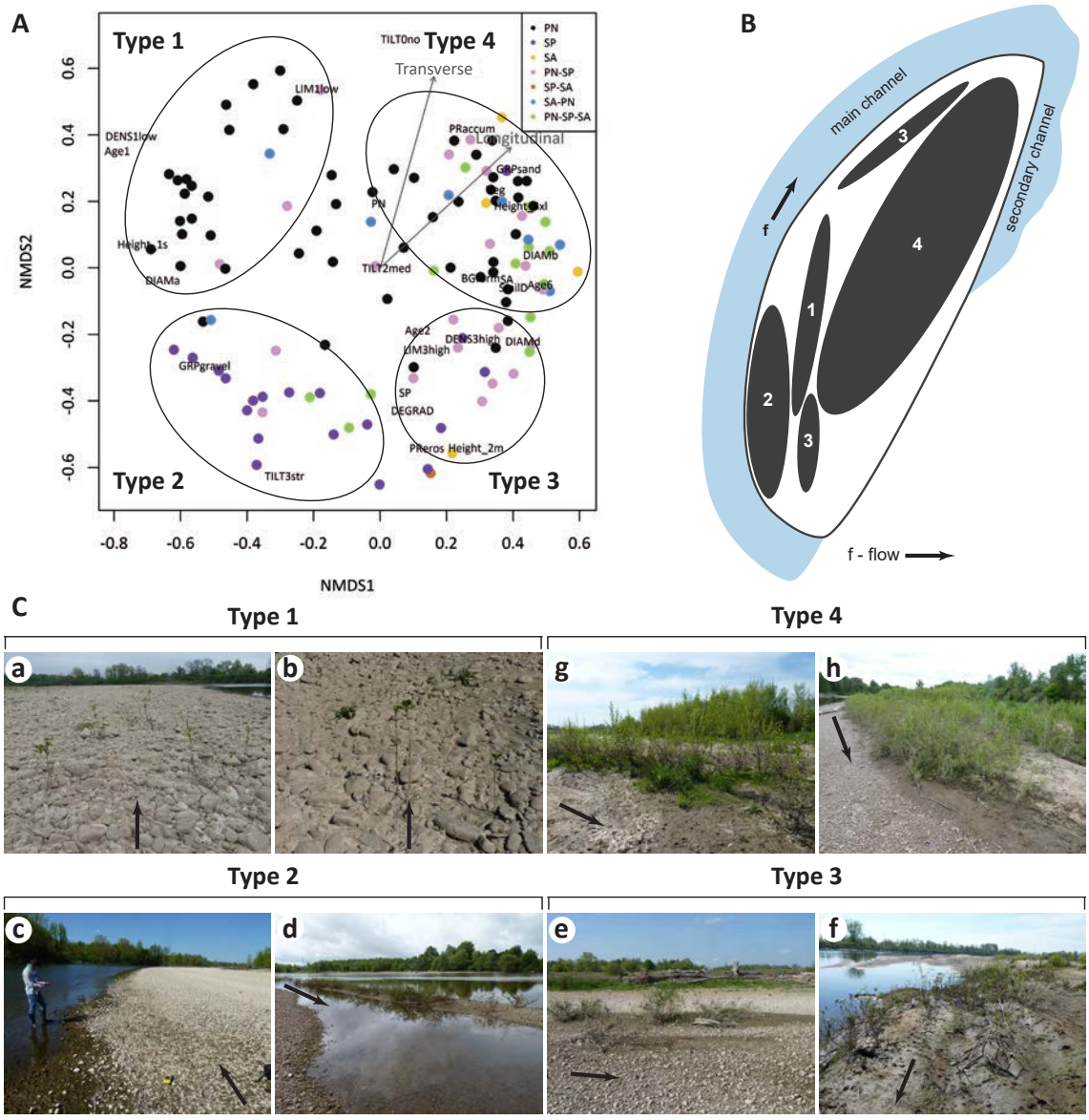

Figure 38. (A) Ordination results and theoretical location of patch types on the alluvial bar. Results of nonmetric multidimensional scaling (NMDS) superimposed on species composition of patches and environmental fit of significant (p<0.01) variables (arrows). Proximity of patches indicates similar biogeomorphic characteristics, arrows indicate the direction of maximum variable change. Arrow length depends on coefficient of determination (r^2). Three dimensions, stress 0.108. (B) Schematic representation of the four patch types on the alluvial bar. (C) Patch types are illustrated with photographs: (a) and (b) small (young) poplars at highly exposed location without vegetation-induced sediment accumulation; (c) highly exposed *S. purpurea* patch with no biogeomorphic accumulation landform; (d) *S. purpurea* patch with biogeomorphic accumulation landform; (e) less exposed patch composed of *S. purpurea* and *P. nigra*, with biogeomorphic accumulation landforms; (f) patch composed of *S. purpurea* and *P. nigra* at a low-exposure location with biogeomorphic accumulation landforms; (g) poplar patch located downstream with biogeomorphic landform creation and dense herbaceous mat; (h) mixed species downstream location patch with well-developed biogeomorphic accumulation landform.

The estimated minimum age is clearly discriminated on the first NMDS axis, with the youngest patches plotting on the left side of the axis, 2- and 4-year-old patches in the central location, and the oldest patches found on the right-hand side (Figure 39). The youngest patches, mainly composed of monospecific *P. nigra*, are located at upstream or central locations on the longitudinal gradient and on all three locations of the transverse gradient. Numerous 2-year-old patches are located downstream, but *S. purpurea* is exclusively present on patches located at upstream or central locations on the longitudinal gradient, or close to the main channel. The 6-year-old riparian tree patches are located at medium location with respect to the distance of the channel.

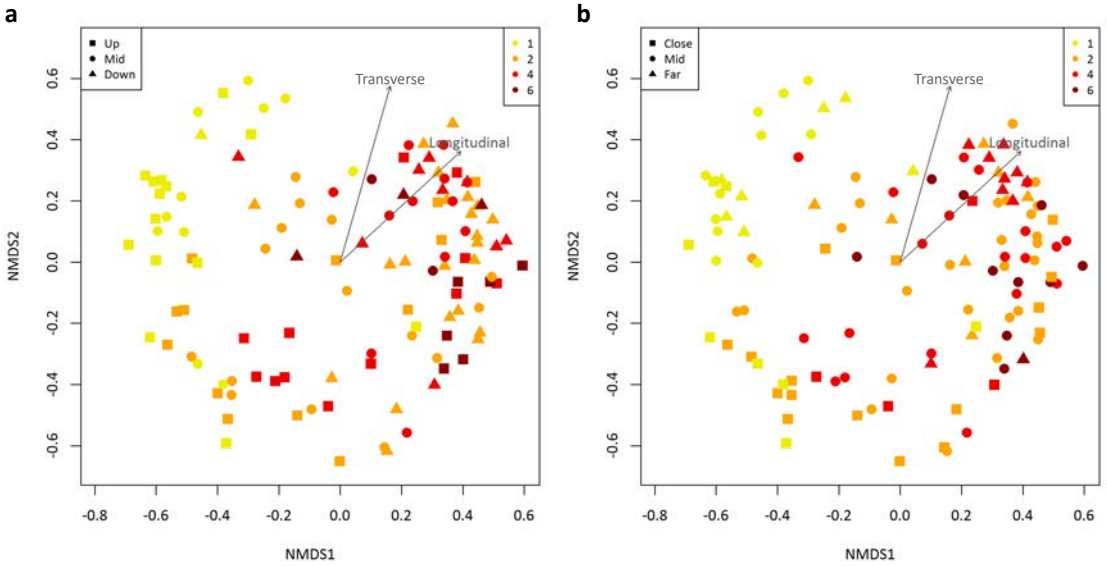

Figure 39. Results of nonmetric multidimensional scaling (NMDS) superimposed on approximate minimum age of patches and positions along (A) the longitudinal gradient and (B) the transverse gradient and environmental fit of significant ($p<0.01$) variables (arrows).

3.3. Establishment area of the three species

The number of patches is unequally distributed along the longitudinal gradients of the alluvial bars. We observe 47 patches upstream, 44 at central locations, and 35 downstream (Table 18). The presence of species within patches also varies along this gradient. Significant difference has been found in the relative abundance of all three species between the three locations (Table 18). *Populus nigra* occurs preferentially in the central location of the alluvial bars and is the less present upstream. *Salix purpurea* occurs mostly upstream and is present less at the central location. The downstream location is not significantly different from upstream and central locations for both species as regards species occurrence. *Salix alba*, on the contrary, is the most abundant species

at the downstream location, and its proportion remains low at the upstream and central locations. Monospecific *P. nigra* patches are more developed at the central location of the alluvial bars, and monospecific *S. purpurea* patches are found upstream. None of the species belonging to the monospecific patches are positively associated with the downstream location (Table 19). Only four *S. alba* monospecific patches are observed out of the total of 126. The presence of mixed species patches is positively associated with the downstream but not with the central location.

The number of patches is unequally distributed also along the transverse gradient: 38 patches are located close to the main channel, 111 at middle distance, and 33 far from the channel (Table 18). The presence of species within patches also varies along the transverse gradient. The abundance of *P. nigra* is higher far from the channel. Conversely, *S. purpurea* shows the highest abundance close to the channel (Table 18). The pairwise comparison procedure does not reveal significant differences in the case of *S. alba* abundance. The presence of monospecific *P. nigra* patches is more apparent farther away from the channel, in contrast to *S. purpurea* (Table 19). The four *S. alba* monospecific patches are observed at the middle location. The presence of mixed species patches is not associated with either of the two gradients.

Logit models show the probability of occurrence of the three species and of monospecific or mixed patches on the longitudinal exposure gradient of alluvial bars (Figure 40). The probability of occurrence of *P. nigra* and *S. alba* increases along the upstream-downstream gradient, whereas the probability of occurrence of *S. purpurea* slightly decreases along this gradient. Monospecific *P. nigra* patches are present at all locations along the longitudinal gradient, whereas the occurrence of monospecific *S. purpurea* patches strongly decreases downstream. The occurrence of mixed patches composed of two different or all three tree species increases along the upstream-downstream gradient.

Logit models show that the probability of occurrence of the *P. nigra* and *S. purpurea* patches across the transverse gradient varies in an opposite way in the case of mixed species patches and monospecific patches (Figure 40). The probability of occurrence of *P. nigra* increases across the transverse gradient of connectivity from the main channel to the floodplain, whereas the probability of occurrence of *S. purpurea* decreases.

We can determine two EAs for each species (Figure 41B,C,D) based on the NMDS results. The exclusive EA corresponds to the successful establishment of monospecific patches. The extensive EA reflects all habitat conditions where a species can be present, even with a low relative abundance. The exclusive EA of *P. nigra* and *S. purpurea* are entirely

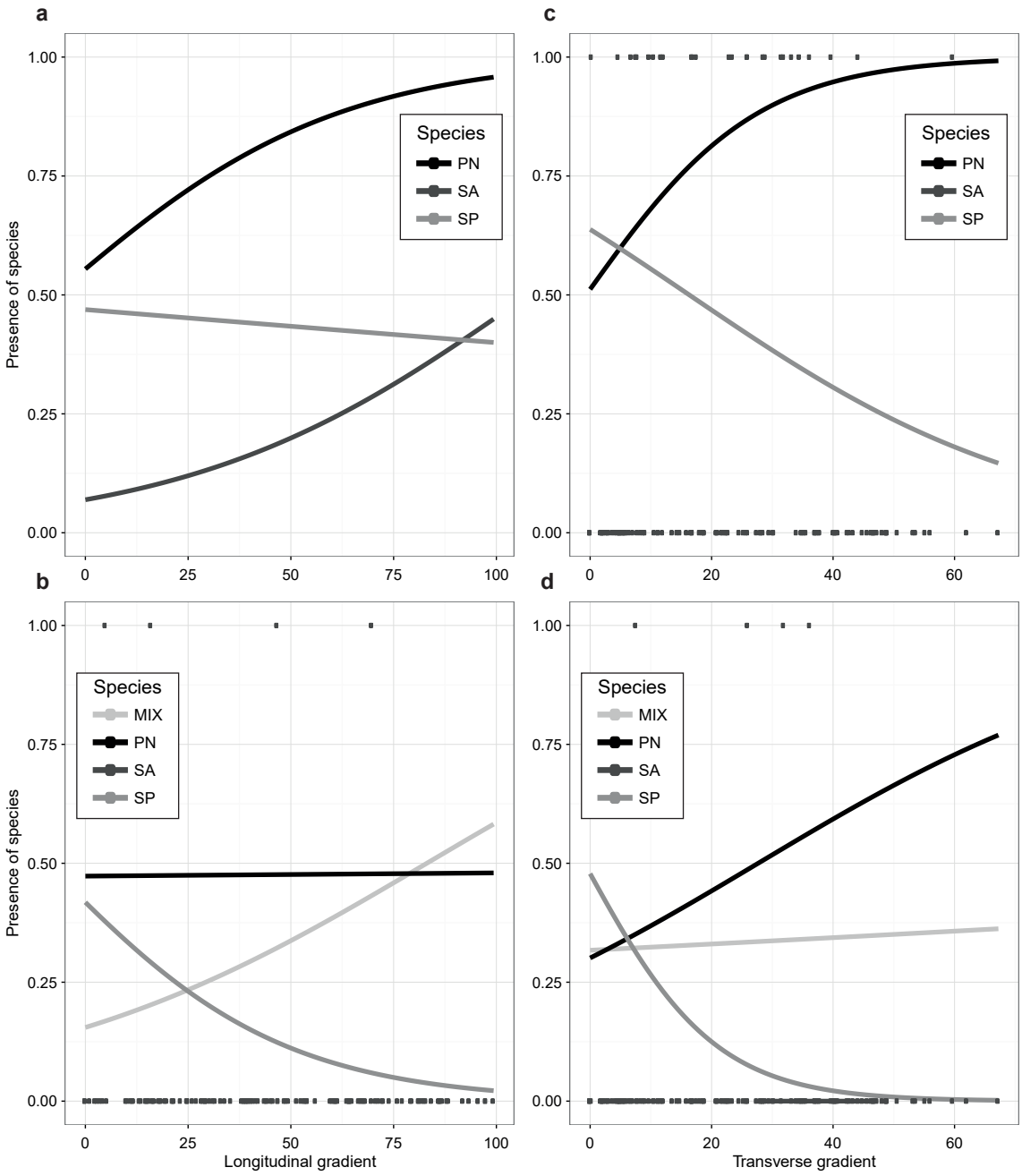

Figure 40. Logit model representing (A) presence of the three studied species along the longitudinal gradient (upstream-downstream) and (B) monospecific and mixed patches along the longitudinal gradient (0=upstream, 100=downstream); (C) presence of the three species and d) monospecific and mixed patches according to the transverse gradient from the main channel to the floodplain (distance in metres).

separated along the second axis, contrary to *S. alba* whose exclusive EA is superposed onto the exclusive EA of *P. nigra* and the extensive EA of *S. purpurea*. The extensive EA of the three species are superposed on the positive side of the first axis. *Populus nigra* displays the largest extensive EA, with an important overlap with the EAs of the other two species.

The results obtained by natural neighbour interpolation (Figure 41E,F,G) correspond to the data points presented in Figure 41B,C,D. However, the interpolation method yields additional information, such as species abundance and a more objective determination of EAs.

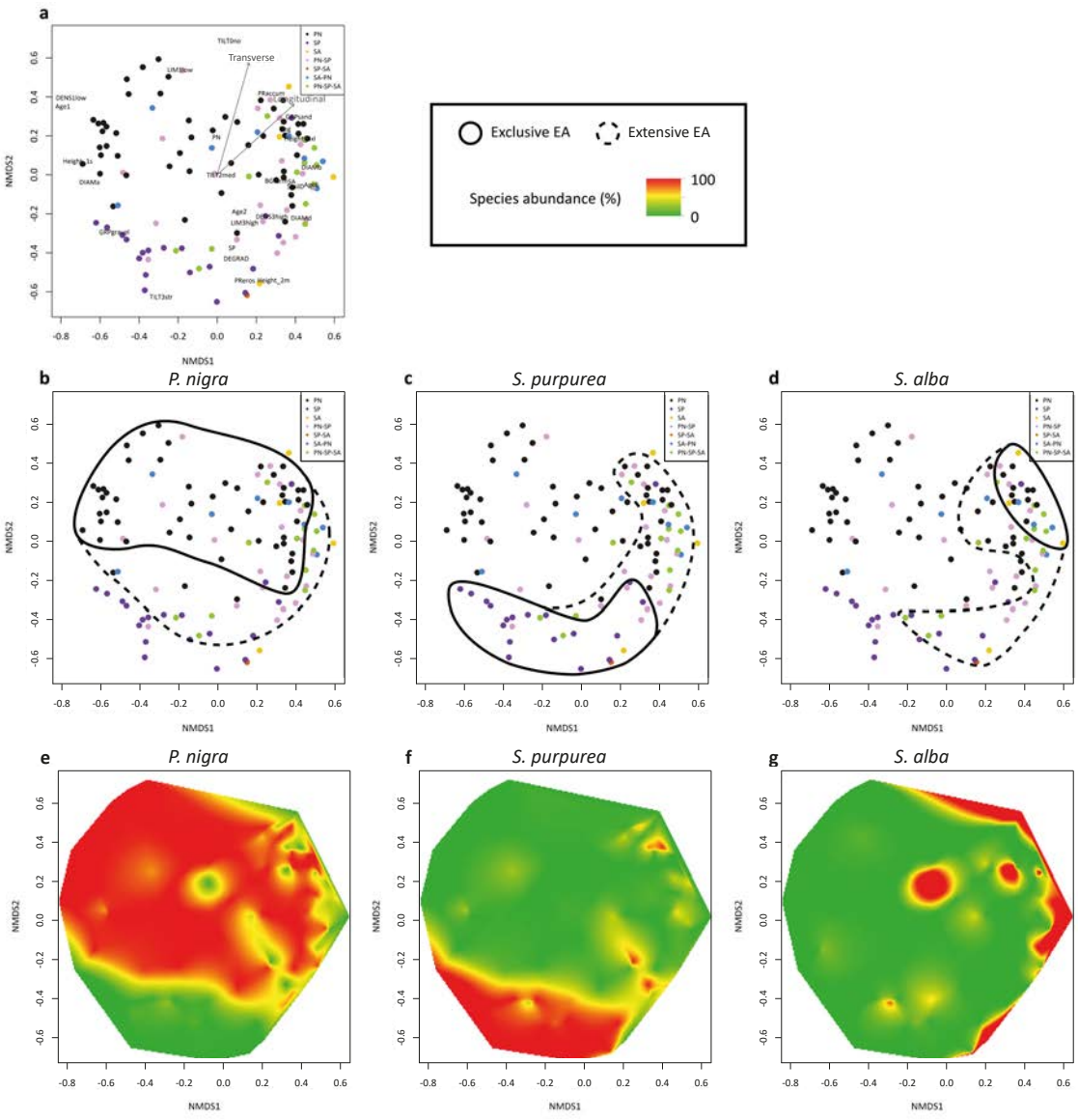

Figure 41. (A) Results of nonmetric multidimensional scaling (NMDS) superimposed on species composition of patches and environmental fit of significant (p<0.01) variables (arrows), showing distribution of exclusive and extensive EAs of (B) *P. nigra*, (C) *S. purpurea*, and (D) *S. alba* and interpolation based on species abundance: (E) *P. nigra*, (F) *S. purpurea*, (G) *S. alba*.

3.4. Biogeomorphic feedback window of the three species

Nearly 70% of the sampled patches show visible effects of vegetation on geomorphology, creating biogeomorphic accumulation landforms. Fifty-six percent of the patches where *P. nigra* is present are characterized by vegetation-induced sediment accumulation, compared with 35% for *S. purpurea* and 20% for *S. alba* (Table 20). In the presence of biogeomorphic accumulation landforms, the abundance of *P. nigra* is lower and the abundance of *S. alba* is higher. Monospecific patches of *P. nigra* marked by biogeomorphic accumulation landforms account for 25% of the total observations, compared with 10% for *S. purpurea*, and 3% for *S. alba*; while mixed patches marked by biogeomorphic accumulation landforms account for 31%. The probability test shows that biosedimentation induced by riparian vegetation is related to mixed patches and to *S. alba* monospecific patches (Table 21).

Table 20. Occurrence of biogeomorphic accumulation landforms according to the presence of each of the three species (PN=*P. nigra*, SP=*S. purpurea*, SA=*S. alba*; SD=standard deviation; letters are assigned to groups (i.e., A, B) indicating that the groups are significantly different)

Species	Parameters	Biogeomorphic accumulation landform	
		Yes	No
PN	N	70	31
	%	*55.56*	*24.6*
	Mean (%)	62.15	75.39
	SD	41.78	41.87
	Group	A	B
p-value at $\alpha = 0.05$		0.01	
SP	N	44	11
	%	*34.92*	*8.73*
	Mean (%)	25.01	24.49
	SD	36.28	41.94
	Group	A	A
p-value at $\alpha = 0.05$		0.15	
SA	N	25	1
	%	*19.84*	*0.79*
	Mean (%)	12.79	0.13
	SD	27.88	0.8
	Group	A	B
p-value at $\alpha = 0.05$		0.001	
Total number of patches	N	87	39
	%	*69.05*	*30.95*

Table 21. Occurrence of biogeomorphic accumulation landforms according to monospecific and mixed species patches (PN=*P. nigra*, SP=*S. purpurea*, SA=*S. alba*; the *p*-values of X^2 and pairwise test results (> attraction, < repulsion from the variable) are indicated in grey when significant)

Species	Parameters	Biogeomorphic accumulation landform			
		Yes		No	
PN	N	32	<	27	>
	%	*25.4*		*21.43*	
SP	N	12	<	8	>
	%	*9.52*		*6.35*	
SA	N	4	>	0	<
	%	*3.17*		*0*	
MIX	N	39	>	4	<
	%	*30.95*		*3.17*	
p-value at $\alpha = 0.05$		0.0004			
Sum (PN+SP+SA+MIX)	N	87		39	
	%	*69.05*		*30.95*	

The test of independence shows that only the longitudinal gradient controls the occurrence of biogeomorphic accumulation landforms. Biogeomorphic accumulation landforms are statistically positively associated with downstream locations but not to upstream locations. The probability test shows that biosedimentation occurs farther away from the main channel (Table 22). The presence or absence of biogeomorphic accumulation landforms is significantly affected by other biotic parameters: minimal estimated age of patches, stem diameters and density (Table 22). Biogeomorphic accumulation landforms mostly occur when vegetation is older than 1 year and also displays the largest diameters and highest stem densities.

Table 22. Occurrence of biogeomorphic accumulation landforms according to the longitudinal and transverse gradients and biotic variables (the *p*-value of X^2 and pairwise test results (> attraction, < repulsion from the variable) are indicated in grey when significant)

Parameters	Class	Biogeomorphic accumulation landform	
		Yes	No
Longitudinal gradient	Upstream	<	>
	Central	<	>
	Downstream	>	<
p-value at $\alpha = 0.05$		**0.009**	
Transverse gradient	Close	<	>
	Middle	>	<
	Far	>	<
p-value at $\alpha = 0.05$		0.10	
Age	1	<	>
	2	>	<
	4	>	<
	6	>	<
p-value at $\alpha = 0.05$		**<0.0001**	
Stem diameter	Very small	<	>
	Small	>	<
	Medium	>	<
	Big	>	<
p-value at $\alpha = 0.05$		**<0.0001**	
Stem density	Low	<	>
	Medium	>	<
	High	>	<
p-value at $\alpha = 0.05$		**<0.0001**	

The probability of occurrence of biogeomorphic accumulation landforms is better controlled by the longitudinal gradient than by the transverse gradient (Figure 42). A biogeomorphic accumulation landform is always developed (except for one patch) when *S. alba* is present in the patch because the species only occur downstream. In

the case of *P. nigra* and *S. purpurea*, the probability of observing a biogeomorphic accumulation landform is higher on the downstream part of alluvial bars (Figure 42A). When *P. nigra* is exclusively present in patches (monospecific stand), a greatly increasing tendency occurrence of biogeomorphic accumulation landforms from the upstream to downstream locations is observed (Figure 42B). The Logit model yields a nonsignificant result for *S. purpurea* monospecific patches as similar numbers of patches at the upstream and central locations either with or without biogeomorphic accumulation landforms occurred. In the case of patches composed of a mixture of species, we observe a high probability of biosedimentation all along the longitudinal gradient. The Logit models representing the probability of occurrence of biogeomorphic accumulation landforms along the transverse gradient are nonsignificant for any of the three species, except for monospecific *P. nigra* patches (Figure 42C). In this case, the probability of observing biogeomorphic accumulation landforms increases with the distance from the main channel (Figure 42D).

The occurrence of biogeomorphic accumulation landforms is remarkably distributed on the first NMDS axis (Figure 43). Although biogeomorphic accumulation landforms may occur at all locations, they are mainly found downstream farther away from the main channel. However, the spatial pattern of biogeomorphic accumulation landforms is not the same for the different species. We note that *S. alba* patches are always characterized by biosedimentation, but this is not the case for the two other species that can establish upstream. Young monospecific *P. nigra* patches (type 1) located at upstream or central locations do not induce the development of biogeomorphic accumulation landforms. On the contrary, *S. purpurea* monospecific patches of 2-4 years can create biogeomorphic accumulation landforms at upstream and central locations and at close or middle locations from the channel (type 2). Biogeomorphic accumulation landforms occur when monospecific *P. nigra* patches are older than 1 year or patches are composed of a mixture of species (types 3 and 4).

We also determine here the exclusive and extensive BFW for each species based on the NMDS results (Figure 43B,C,D). The exclusive BFW allows us to isolate the effect of each species and identify the conditions that favour the capacity to affect geomorphology, while the extensive BFW includes the combined effect of species. As in the case of EA, the exclusive BFW of *P. nigra* and *S. purpurea* are entirely separated along the second axis, contrary to *S. alba* whose exclusive BFWs are superimposed onto the exclusive BFW of *P. nigra* and the extensive BFW of *S. purpurea*. The BFW of *S. alba* is fully superimposed onto its EA as it always affects geomorphology. The BFW of *S. purpurea* is slightly smaller than its EA and excludes some upstream patches. The largest difference between the

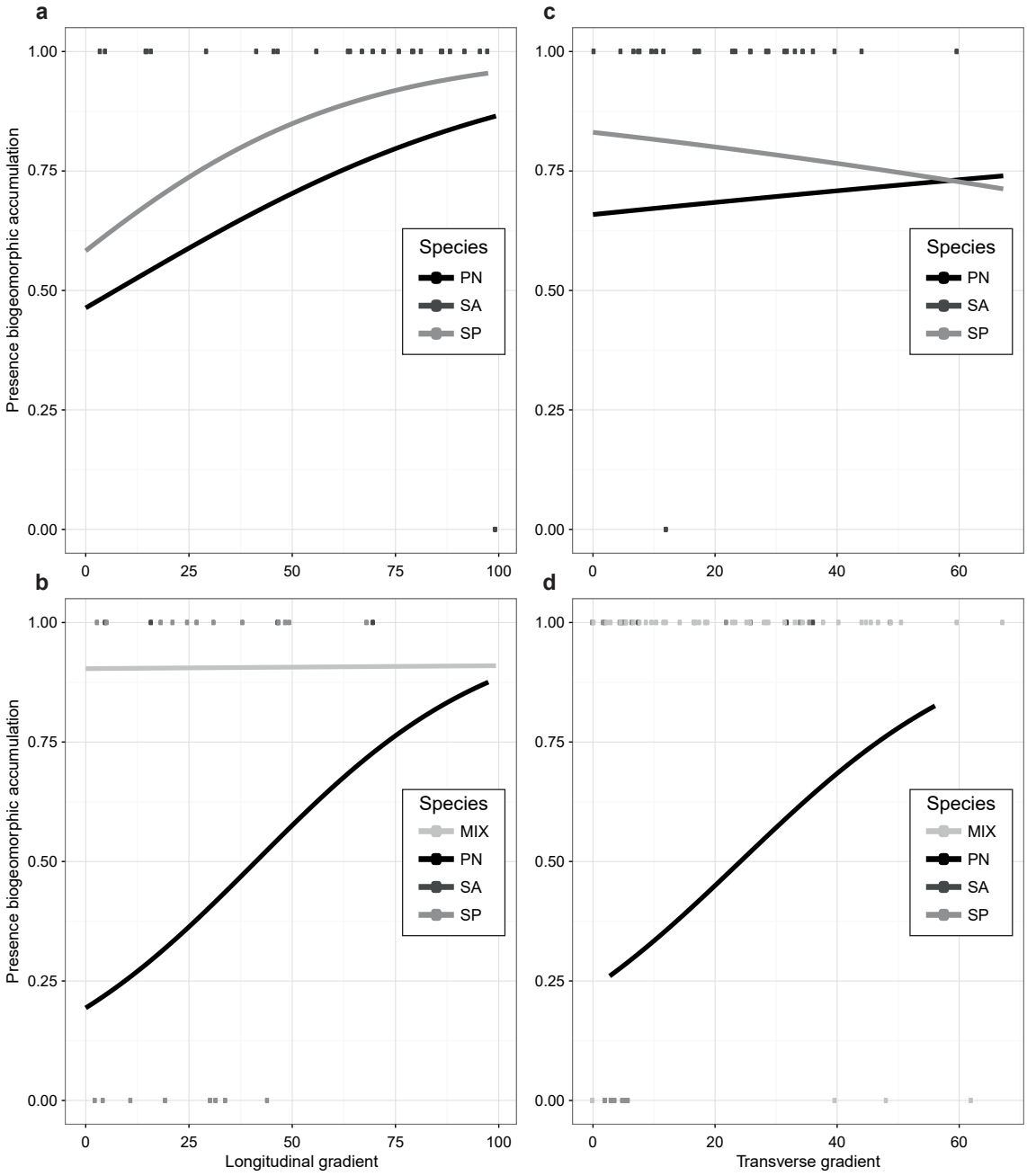

Figure 42. Logit model representing the presence of biogeomorphic accumulation landforms with respect to (A) the simple presence of the three species and (B) monospecific and mixed patches according to the longitudinal gradient (0% upstream, 100% downstream); (C) the simple presence of the three species and (D) monospecific and mixed patches according to the transverse gradient.

exclusive BFW and EA is found for *P. nigra.* Its BFW is notably smaller compared to its EA, excluding the small upstream patches. The extensive BFWs of the three species are superimposed on the positive (right) side of the first axis.

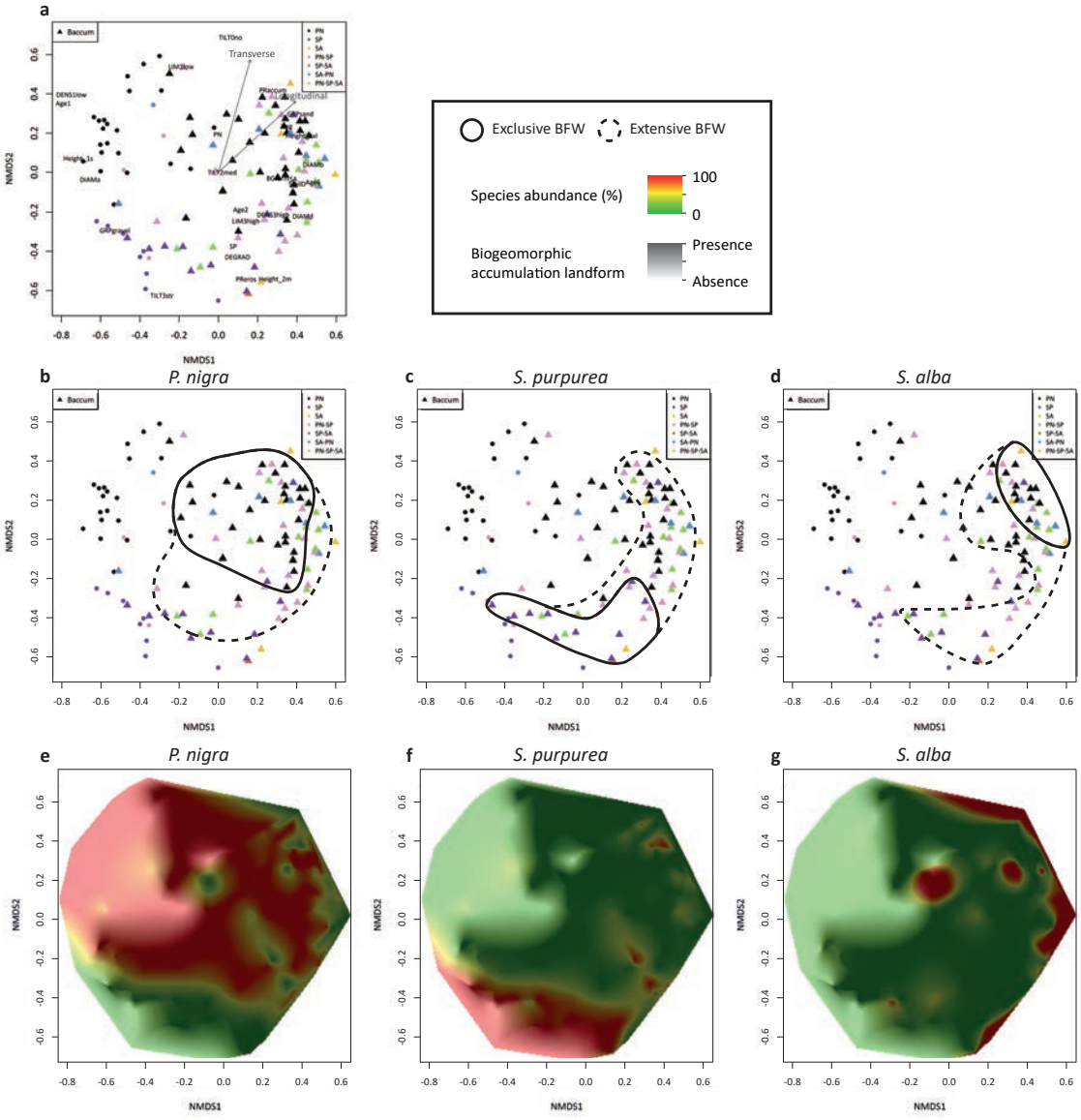

Figure 43. (A) Results of nonmetric multidimensional scaling (NMDS) superimposed on species composition of patches, occurrence of biogeomorphic accumulation landforms, and environmental fit of significant (p<0.01) variables (arrows), with distribution of the exclusive and extensive BFWs of (B) *P. nigra*, (C) *S. purpurea*, and (D) *S. alba* and interpolation based on species abundance superimposed on presence of biogeomorphic accumulation landforms. (E) *P. nigra*, (F) *S. purpurea*, (G) *S. alba*.

4. Discussion

4.1. Establishment areas of the three riparian Salicaceae species

Our results show a significant variation in the location and spatial extent of the establishment areas (EA) on the alluvial bars of the Allier River for the three dominant riparian pioneer species (*P. nigra*, S*. purpurea*, and *S. alba*). *Populus nigra* is currently established at all locations of the longitudinal and transverse gradients, being the most abundant species and displaying the largest EA (Figure 44). The only locations where *P. nigra* establishment remains marginal are in the most exposed upstream areas near the main channel. This observation is in accordance with previous research that demonstrated that *P. nigra* has a high phenotypic plasticity and a strong adaptability to hydrogeomorphic disturbance (submersion, shear stress, erosion, and sediment burial) and stress (e.g., high temperature, drought) (Karrenberg et al., 2003; Chamaillard, 2011; Corenblit et al., 2014). Our observations show that *P. nigra* plants have the capacity to colonize the most exposed locations on the alluvial bars of the Allier River. However, under such conditions, the plants remain small because their aerial biomass is regularly removed or damaged during annual floods (Figure 39). The smaller size and increased flexibility (i.e., resistance and avoidance traits *sensu* Puijalon et al., (2011)) potentially favour the resistance of *P. nigra* individuals under highly exposed situations. This observation is in agreement with Gurnell (2014), who pointed out that hydrogeomorphic disturbances very strongly affect riparian growth within highly exposed active river tracts. Perona et al. (2012) and Garófano-Gómez et al. (2016) noted that *P. nigra* plants increase their root biomass when exposed to drag forces. Hortobágyi et al. (2017a) also showed that *P. nigra* plants adapt their aboveground (e.g., a reduced size) and belowground morphological attributes (e.g., production of structural roots) to increase their resistance on the most exposed locations of the alluvial bars of the Allier River studied here.

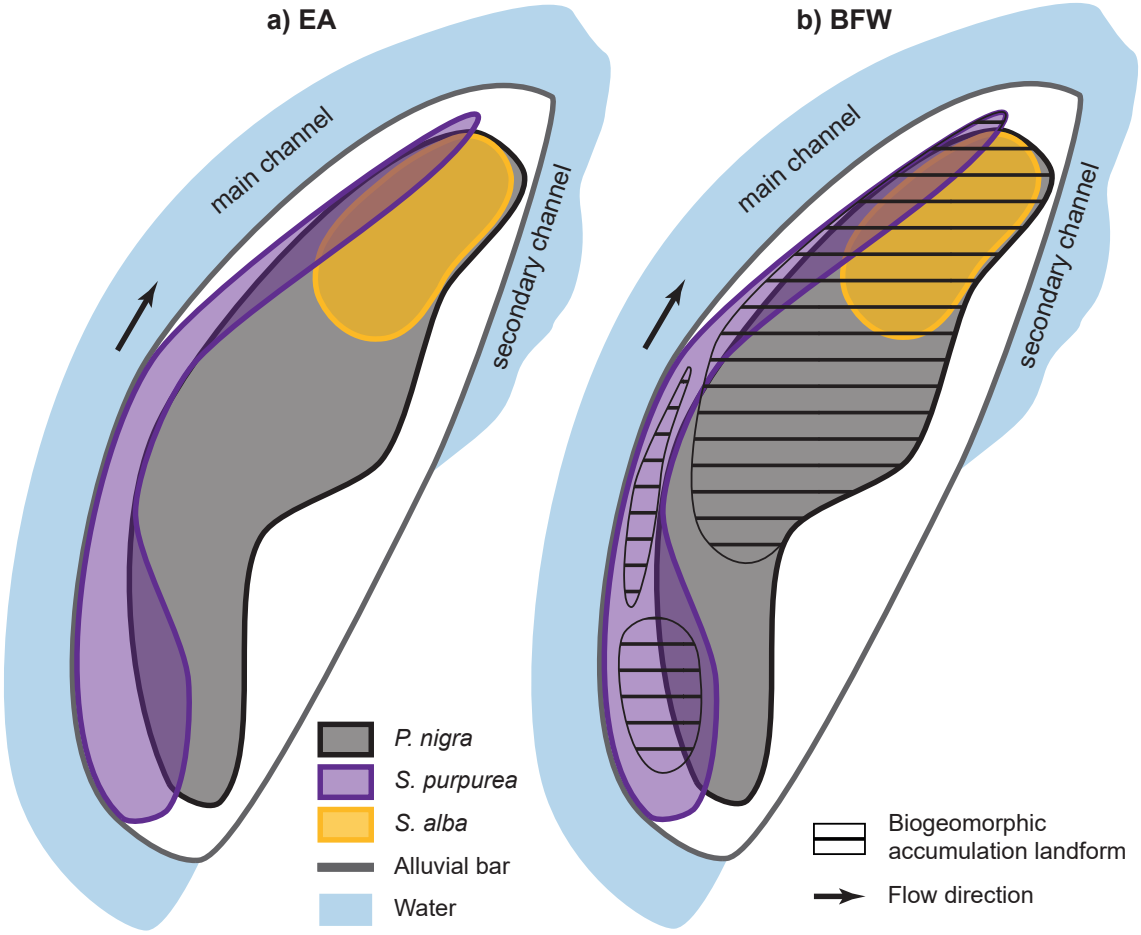

Figure 44. Conceptual model based on statistical analysis of 16 alluvial bars of the Allier River representing (A) the establishment area and (B) the biogeomorphic feedback window of *P. nigra*, *S. purpurea*, and *S. alba*. Only the studied phases (pioneer and biogeomorphic) of the vegetation are represented in this figure.

Salix purpurea shows a smaller exclusive EA than *P. nigra*, occurring mainly in the most exposed upstream to central locations of alluvial bars, close to the main channel where monospecific patches of *P. nigra* and *S. alba* are absent (Figure 44). *S. purpurea* is highly resistant to shear stress and uprooting and, for this reason, it is well adapted for riparian restoration (Lavaine et al., 2015), for example in gully restoration projects (Erktan and Rey, 2013). In particular, *S. purpurea* plants have biomechanical attributes (e.g., a flexible and resistant multistemmed canopy) that provide a high resistance to hydraulic constraints, prolonged submersion, and sediment burial. Close to the floodplain or at downstream locations, *S. purpurea* plants mostly occur in mixed stands with the two other species but with a reduced density.

Overall, *S. alba* has a low abundance and is preferentially located on the downstream or central parts of the alluvial bars, at middle or far locations from the main channel within patches where *P. nigra* is also present, or where all three species coexist (Figure 44).

The downstream location is not only favourable for *S. alba* establishment because of a reduced exposure to hydrogeomorphic constraints but also provides better access to a higher water table connected to secondary channels located at the downstream part (alcoves *sensu* Curtis and Guerrero, (2015)), which function as buffers against water table decline and drought during summer. In addition, fine sediments are preferentially deposited on the downstream parts of gravel bars, thus maintaining better moisture conditions than elsewhere where sediments are coarser and well drained (Pautou et al., 1985). The EA of *S. alba* on the Allier River corroborates the observations of Splunder et al. (1996) on the Rhine River in the Netherlands where *S. alba* is highly sensitive to water-table variations and drought stress occurring on gravel bars during summer. These results are also in concordance with González et al. (2012) who evaluated the mortality rate of four riparian species (*S. alba*, *P. nigra*, *P. alba*, and *Tamarix* spp.) according to variable hydrogeomorphic conditions on the Ebro River, Spain. These authors (*op.cit*.) demonstrated that *S. alba* is the most vulnerable species to drought stress related to deeper water tables, shorter flood durations and lower flood frequencies. In their experiment, González et al. (2012) also showed that *P. nigra* was vulnerable to drought stress but to a much lesser extent than *S. alba*. Using an *ex situ* experiment, Guilloy et al. (2011) demonstrated that *S. alba* plants respond to abrupt water table level drops with a higher mortality rate compared to *P. nigra*. Lavaine (2013) found that *S. alba* is less drought resistant than *S. purpurea*. Our results show that the specific adaptations and ecological requirements of the different species lead to a significant spatial segregation of their EAs that can be statistically mapped (Figure 41 and Figure 44).

The time component of patch dynamics is not explicitly included in our analysis, neither the lateral migration of the main channel nor the subsequent evolution of secondary channels and relative x, y and z positions of the patches. By including these parameters in studies such as performed on the Allier River, we could obtain supplementary information about the spatial extent of the recruitment areas of the three species. Although the Allier River is still a highly dynamic and unstable wandering/meandering river, the patches sampled in 2015 could have been recruited between 2008 and 2014 under different habitat conditions and within different locations on the alluvial bars. We need to consider that *P. nigra*, *S. purpurea*, and *S. alba* seedling recruitment generally occurs near the main and secondary channels (Mahoney and Rood, 1998). However, on the Allier River, lateral channel migration leads to a relative displacement of the established patches toward the inside, i.e., toward the floodplain, bends of the alluvial bars. A dendrochronological study would allow us to determine the exact patch ages and growth rates, leading to more precise description of the conditions of occurrence of the EAs and BFWs. In addition, a three dimensional diachronic multiscale study could

provide additional information about hydrogeomorphic changes (e.g., river channel migration, secondary channel formation and adjustment, topographic changes) as well as vegetation establishment and growth, yielding a better understanding of feedbacks between riparian vegetation and hydrogeomorphic processes (Hortobágyi et al., 2017c). Furthermore, we are aware that additional factors, such as microtopography heterogeneity and the deposition of large woody debris can potentially disturb the statistical model of the EA presented here (Figure 44). For example, the accumulation of large woody debris facilitates the deposition of fine sediment, as well as the recruitment, establishment, and growth of vegetation; uprooted trees may also sprout and develop new root networks enhancing pioneer island formation (Gurnell et al., 2005). On the Allier River, the sexual regeneration strategy of *P. nigra* can sometimes be more important than its vegetative reproduction/propagation (van Oorschot et al., 2016). The sexual regeneration strategy could occasionally be favoured by deposited wood or, on well-established patches, offering a shelter against hydrodynamic forces as observed on the Frome River, UK (Moggridge and Gurnell, 2009). However, the sprouting strategy is also operative in highly exposed locations around older trees (field observations of B. Hortobágyi and P-A. Dejaifve). Beavers (*Castor fiber*) and coypu (*Myocastor coypus*) present on the Allier River may also cause vegetative propagation of the vegetation but also tree damage. Breton et al. (2014) evaluated the response of seven Salicaceae species (including *P. nigra*, *S. purpurea*, and *S. alba*) to high coypu browsing pressure, showing that *P. nigra* and *S. purpurea* are the least affected species. Future studies of vegetation establishment in areas where beavers and coypu occur should take these aspects into consideration.

4.2. Biogeomorphic feedback window

Our results show that resilience, i.e., the ability of fluvial biogeomorphic ecosystems such as the Allier River to retain essential processes when disturbed and maintain their structural and functional integrity before changing to another domain of attraction, is modulated by the functional response and effect traits of engineering plants that can vary between species (interspecific) and within species (intraspecific). Furthermore, the engineering effect of the species is more or less effective depending on the location along the longitudinal and transverse gradients of the alluvial bars. We suggest that interspecific diversity and intraspecific variability of functional traits related to engineer species increase biogeomorphic resilience. Indeed, the three species (or their mixture within dense patches) are developed in EAs and BFWs that are preferentially located along the

longitudinal and transversal gradients. We suggest that taking account of the EA and BFW characteristics of each engineer species and their co-occurrence allows us to consider biogeomorphic resilience in terms of functional traits in contrasted geomorphological situations. In the current hydrogeomorphic context, all three species act as ecosystem engineers *sensu* Jones et al. (1994) because they enhance sediment trapping and landform construction. All three species thus contribute to biogeomorphic resilience on alluvial bars of the Allier River. However, biogeomorphic accumulation landforms are not present in the whole domain encompassing the EA of the three species (Figure 44). The engineer effects of the species and their related impact on biogeomorphic resilience varies in intensity according to the combined effects of exposure to hydrosedimentary disturbances and species physiognomy.

Populus nigra is currently the best adapted species to construct biogeomorphic landforms within the study reach of the Allier River. The BFW of this species occurs mostly in the central to downstream parts of the alluvial bars where individuals are not excessively exposed to annual floods and where they are older than 1 year. The most exposed areas of the alluvial bar, i.e., upstream locations and near the main channel, are excluded from the BFW of *P. nigra*. When present in these locations, *P. nigra* stands are generally composed of individuals with one small stem showing scarification marks related to flow damage. At less exposed locations of the central part of alluvial bars, *P. nigra* plants respond with a flexible multistemmed canopy, a higher biomass, and patch density resulting in very effective sediment trapping, i.e., a strong engineer effect. This physiognomic response of *P. nigra* in less exposed locations leads to a positive feedback between plants and landform dynamics, which results within a few years in the bioconstruction and biostabilization of wooded bars as shown by Corenblit et al. (2016a) on the channelized Garonne River, France (Figure 38).

Within the most exposed parts of the alluvial bars on the Allier River, only *S. purpurea* plants are able to generate a BFW. Within *S. purpurea* monospecific patches, the occurrence of a biogeomorphic accumulation landform is more related to plant physiognomy (stem density, size, and diameter) rather than to the two hydrogeomorphic gradients (i.e., longitudinal and transverse). The BFW of *S. purpurea* occurs mostly all along the gradients where the canopy is well developed with a dense and multistemmed bushy shape, with stems of larger diameter. Such effects of plant morphology on sediment dynamics have been investigated in more detail in fluvial (Euler et al., 2014) and coastal systems (Bouma et al., 2013). Using a field experiment in a context of soil erosion restoration, Erktan and Rey (2013) showed that when *S. purpurea* is exposed to high sediment flow in eroded gullies, stem diameter has the strongest influence on the sediment retention capacity of

the plant. When vegetation is exposed to low sediment flow, other morphological traits, in particular related to the canopy (Burylo et al., 2012) and stem density (Erktan et al., 2012), determine the sediment trapping efficiency.

When *S. alba* is present within a patch, biosedimentation always takes place. This suggests that *S. alba* has the capacity to retain sediment but only at downstream locations near secondary channels that are intrinsically favourable for fine sediment deposition (Barsoum, 2001). Thus, our observations show that the engineer effect of *S. alba* mostly occurs at locations with an intrinsic physical predisposition for fine sediment deposition linked to flow characteristics. Hence, this species acts as a factor favouring sedimentation conjointly with natural hydrodynamic tendencies. Furthermore, *S. alba* plants always act conjointly with *P. nigra* within mixed patches as ecosystem engineer species, which makes it difficult to estimate the relative contribution of *S. alba* to biosedimentation and therefore its role in biogeomorphic landform construction and resilience.

Our observations provide some indications of how riparian engineer species can develop different response traits to hydrogeomorphic constraints, thus allowing their establishment in an unstable and fluctuating geomorphic environment, as suggested by several authors (Karrenberg et al., 2002; Lytle and Poff, 2004; Bornette et al., 2008; Naiman et al., 2008; Corenblit et al., 2015a). A recent study on the same reach of the Allier River showed that young (1-2 years old) *P. nigra* plants develop different response traits depending on their exposure to mechanical stress (Hortobágyi et al., 2017a). *Populus nigra* developed avoidance response traits (i.e., small flexible stems and more strong structural roots) at the most exposed locations of the studied alluvial bars, which improve resistance of the plants to high energy flows. At less exposed locations, plants developed taller, less flexible stems and finer root systems. Consequently, *P. nigra* plants can only affect sediment trapping at locations where they can sufficiently increase their aerial biomass. On the other hand, *S. purpurea* plants develop response traits that result in a higher capacity to trap sediment within the most exposed locations of the alluvial bars. Kui et al. (2014) emphasized the role of plant morphological and biomechanical traits in controlling sediment trapping capacity. These authors (*op. cit.*) showed that species such as *tamarisk* trap more sediment than cottonwood because of their greater frontal area and lower maximum crown density.

In general, the occurrence or absence of a biogeomorphic accumulation landform is significantly controlled by plant physiognomic parameters such as stem diameter, height, and density (Table 22). These results also suggest that patches composed of a combination of two or all three species have a high probability of occurrence of biogeomorphic accumulation landforms because (i) these patches are mostly located

on medium to less-exposed locations of the alluvial bar and (ii) they are generally dense and composed of numerous individuals older than 1 year with different morphologies and biomechanical attributes. Our observations imply that the combination of different morphological and biomechanical traits of the species within mixed patches improves the capacity of the vegetation to trap sediments, as observed within the active tract of the Tech River, France (Corenblit et al., 2009). This is also in line with previous results that suggest that the enhanced sediment trapping capacity of mixed-species patches may be linked to a greater hydraulic roughness originating from a more complex and resistant vegetative aerial structure (e.g., different stem morphologies and flexibilities, complementary crown architectures) (Kui et al., 2014). In addition, Kui et al. (2014) proposed that the sediment trapping capacity of multiple-species patches would increase in a nonlinear way in relation to growth of stem height, diameter, and crown area.

4.3. Interactions between plants

We propose that increasing functional trait diversity on alluvial bars may increase the set of possible interactions between plants. Our results show that positive interactions (facilitation) occurs among the different species in the central and downstream locations of alluvial bars, resulting in an improved capacity to build landforms. In our study, we do not explicitly focus on inter- or intraspecific facilitation effects enhanced by established cohorts. The occurrence of such positive interactions between plants is likely to occur on the alluvial bars of the Allier River. On the same study reach on the Allier River, woody pioneer riparian engineer species not only enhanced fine sediment retention but also controlled seed deposition and the potential of plant diversity resilience (Corenblit et al., 2016b). Seed deposition enhances the resilience of herbaceous mats on exposed areas of alluvial bars where they could not establish without facilitating effects. Herbaceous mats can further enhance an autocatalysed process of plant resilience by stabilizing fine substrates, as well as by trapping additional sediment and seeds. We suggest that biogeomorphic accumulation landforms induced by the three woody engineer species may favour the establishment of herbaceous plants, which also act as additional ecosystem engineers and thus contribute to the biogeomorphic succession (Corenblit et al., 2009).

4.4. Will the EA and BFW of the three species remain stable?

Changes in the frequency and magnitude of river discharge, as induced by climate change, sediment extraction, or dam construction, strongly impact riparian plant community assemblages because of their strong dependence on flow regime and sediment dynamics (Lytle and Poff, 2004). We suggest that the ecological response and related biogeomorphic resilience of the Allier River to changes in the hydrogemorphic regime may result in shifts in the spatial distribution and extent of the EAs and BFWs of the different riparian engineer species. *Populus nigra* has the highest resilience of the three species studied here because it has a strong phenotypic plasticity. Therefore, in the current hydrogeomorphic context of a wandering/meandering style (Petit, 2006), *P. nigra* may increase in dominance as observed in the case of the channelized Garonne River (Corenblit et al., 2016a). The aboveground biomass production of *S. purpurea* is more marked when it is not exposed to severe drought stress (Lavaine et al., 2015). If the occurrence of drought periods decreases and of high flows increases, we might expect that this species could potentially extend its EA and have a greatly intensified effect on biogeomorphic landform construction. However, the hydrogeomorphic disturbance regime will most likely continue to decrease and the river will shift toward a more stable meandering system as suggested by Petit (2006). In such a context, S*. purpurea* may undergo a strong regression in the ecosystem as its EA would become fully superposed with *P. nigra,* the latter species being more competitive in terms of access to water and light. Out of three pioneer species studied here, *S. alba* is the most vulnerable to drought stress and shorter flood duration. The current geomorphic trajectory toward a meandering style, combined with an increased drought stress in summer, could make *S. alba* recruitment and establishment more difficult on alluvial bars.

5. Conclusion and perspectives

Our results lead to a clear identification of the establishment area (EA) and biogeomorphic feedback window (BFW) of three riparian pioneer species on alluvial bars of the lower Allier River. In the current hydrogeomorphic context, the three species studied here are becoming established on the alluvial bars. However, the differences in species abundance and location of the EA suggest that, under the current hydrogeomorphic conditions, *P. nigra* is favoured because it has the strongest plasticity in relation to hydrogeomorphic

disturbances, water stres and scarcity. The EA of *S. purpurea* is mainly developed on the most exposed locations of the alluvial bars, while *S. alba* is found in the less exposed environments. Thus, *P. nigra* and *S. purpurea* not only have their exclusive EAs but also a common EA. Although *S. alba* does not have its own exclusive EA, this species shares its EA with *P. nigra* or with *P. nigra* and *S. purpurea*. We demonstrate that, on the Allier River, *P. nigra*, *S. purpurea*, and *S. alba* can all act as ecosystem engineers. The BFWs of these three species are strongly influenced by the upstream–downstream (longitudinal) gradient of exposure and the main channel-floodplain (transverse) gradient of connectivity. At the bar scale, the biogeomorphic accumulation landform pattern is also controlled by the functional attributes of each of the three species. *Populus nigra* and *S. purpurea* have their own exclusive EA and BFW, but the EAs and BFWs of the different species taken together are also superimposed. Thus, the total EA and BFW of all three species lead to a greater spatial extent than if only one or two of the species were present on the alluvial bars. This highlights the role of biogeomorphic functional diversity in controlling the extent and rate of fluvial landform construction.

In the light of current and future climate change, we stress the importance of considering in more detail the functional characteristics (life history traits) of pioneer riparian species, and thus, at the same time, the functional diversity of traits in riparian ecosystems. The increase of functional trait diversity is supposed to increase the probability of the occurrence of key biogeomorphic engineer species and also the possibility of positive interactions (facilitation) among species (Hooper et al., 2005). In the case of a decreased diversity of functional traits as expressed in terms of response (EA) and effect (BFW), the riparian ecosystem is expected to become less stable and resilient to natural and anthropogenic disturbances. This question of the effect of biogeomorphic functional diversity should be studied in more detail.

We also expect that changes of the hydrogeomorphic regime (e.g., caused by climate change) will be followed by adjustments of intra- and interspecific interactions. A decrease in the frequency of hydrogeomorphic disturbances may give rise to increased competition between plant species, whereas a reinforcement of hydrogeomorphic disturbances may lead, as predicted by the *stress gradient hypothesis* (Bertness and Callaway, 1994), to increased intra- and interspecific positive interactions (i.e., facilitation, or potentially intraspecific cooperation or altruism). Such interactions based on cooperation or altruism correspond to helping strategies within the same species, which could favour plant survival and growth as well as fluvial landform construction (i.e., niche construction) within riparian corridors (see part 2 this issue (Corenblit et al., 2017)).

Chapter V. Above- and belowground responses of *Populus nigra* L. to mechanical stress observed on the Allier River, France

Hortobágyi, B., Corenblit, D., Ding, Z., Lambs, L., Steiger, J., 2017a. Above- and belowground response of *Populus nigra* L. to mechanical stress within the Allier River, France. Géomorphologie Relief Process. Environ. 23, 219–231. doi:0.4000/geomorphologie.11748

Abstract – Pioneer riparian trees such as *Populus nigra* L. which establish on alluvial bars within dynamic riparian corridors strongly influence fluvial geomorphology by trapping sediments and constructing landforms during floods. The engineering effects (changes in the physical state of the habitat by organisms) of *P. nigra* on alluvial bars depend on its biomass and its exposure to mechanical stress. *P. nigra* has a strong phenotypic plasticity that enables individuals to adapt their morphological and biomechanical traits, according to the local hydrogeomorphic conditions. The comprehension and quantification of the variation of morphological and biomechanical response trait attributes of *P. nigra* populations according to their exposure to mechanical stress is fundamental to better understand why riparian plants are capable to impact fluvial geomorphology. In an empirical *in situ* study, we quantified the relation between response trait attributes of *P. nigra* and its exposure to three different levels of mechanical stress. At a highly exposed bar-head, plants clearly developed response traits such as small flexible stems and a strong root system which favour higher mechanical resistance, while at the less exposed bar-tail plants developed taller, less flexible stems and finer root systems. Plants that established in the lower reach of the chute channel developed some common trait attributes in comparison to the bar-tail population and some other trait attributes which were common to the bar-head population. Poplar plants which established on bar-tails favoured bioconstruction, and thus are potentially faster disconnected from hydrogeomorphic disturbances. These results further suggest that fine scale biogeomorphic feedbacks have an influence on larger scale processes within the fluvial corridor requiring hierarchical biogeomorphic bottom-up and top-down cross scale studies for a better understanding of complex biogeomorphic fluvial ecosystems.

Keywords – *Populus nigra* L., above- and belowground response, plant response traits, mechanical stress, Allier River.

1. Introduction

Pioneer riparian trees such as *Populus nigra* L. which establish on gravel bars within dynamic riparian corridors strongly influence fluvial geomorphology by trapping sediments and constructing landforms during floods (Corenblit et al., 2007; Gurnell, 2014; Hortobágyi et al., 2017b). Ecosystem engineers (*sensu* Jones et al., (1994)) are species which can significantly modify geomorphic processes, landforms and habitats, thus control the availability of resources. Hortobágyi et al. (2017b) showed on a laterally dynamic section of the Allier River, France, that after one to two years of growth, *P. nigra* saplings significantly influence sediment dynamics on gravel bars because they reached a sufficient biomass. This stage was defined as the "biogeomorphic feedback window" because the riparian plants and geomorphic processes strongly interact in a reciprocal way (Hortobágyi et al., 2017b). The authors showed that *P. nigra* populations which established on alluvial bars under low to intermediate levels of exposure (e.g. bar-tails) to mechanical stress caused by water flow and sediment transport developed a strong aerial biomass and efficiently trapped fine sediments. At the most exposed locations of alluvial bars (i.e. on bar-heads) *P. nigra* populations were able to resist mechanical stress but they did not develop an important aerial biomass, and thus they did not trap significant quantities of fine sediment. These results suggested that the morphological and biomechanical "traits" and related "attributes" of young *P. nigra* populations which colonize alluvial bars, change according to variations in exposure to mechanical stress (i.e. shear stress imposed by water flow; sediment transport) and that these changes result in varying aptitudes of the plants to trap fine sediments during annual floods. Plant traits are morphological, biomechanical, physiological and phenological characteristics of plants which can be measured at the individual level; the value or the modality taken by a trait is called an "attribute" (*sensu* Violle et al., 2007). When the attribute of a trait varies in response to changes in environmental conditions (e.g. water flow, sediment erosion, transportation, deposition), the trait is called a "response trait". Traits which affect environmental conditions (e.g. flow characteristics, geomorphic landforms), community or ecosystem properties, are considered as "effect traits" (Violle et al., 2007; Corenblit et al., 2015a).

P. nigra has a strong phenotypic plasticity, i.e. individuals can adapt their morphological and biomechanical traits according to the local hydrogeomorphic conditions (Karrenberg et al., 2003; Chamaillard, 2011; Corenblit et al., 2014). Such plasticity improves *P. nigra* individual's probability to establish under harsh environmental conditions (e.g. exposed to flood disturbances) and eventually to reach their biogeomorphic feedback window (*sensu* Eichel et al., (2015); see also Hortobágyi et al., accepted. During establishment

(i.e. first three years following germination; *sensu* Cooper et al., (1999)), the sapling's growth pattern is highly controlled by local hydrogeomorphic conditions, such as sediment texture, topographic level, hydrological regime and exposure to mechanical stress that act as a strong ecological filter. Different authors have suggested that in order to increase their resistance to mechanical stress, saplings develop specific morphological and biomechanical attributes (Karrenberg et al., 2002; Bornette et al., 2008; Puijalon et al., 2011). Variation in trait attributes is supposed to be dependent upon the level of mechanical stress with a trade-off related to the function of anchorage and resource acquisition (Karrenberg et al., 2003; Read and Stokes, 2006; Pasquale et al., 2013).

The quantification of morphological and biomechanical response trait attributes variation in *P. nigra* populations according to their location on alluvial bars is essential to understand why these ligneous riparian plants are capable to impact fluvial morphodynamics and fluvial landforms. To our knowledge, very little is known about the *in situ* aboveground and belowground morphological and biomechanical response of saplings in their early stage of development on alluvial bars with the exception of very recent studies (e.g. Kui and Stella (2016)). We hypothesise that (i) when highly exposed to shear stress, saplings predominantly develop functional morphological and biomechanical traits increasing their resistance to uprooting, such as a reduced size and a strong flexibility which limits drag force, i.e. "avoidance traits", and also other traits such as a strong root system that increases anchorage, i.e. "tolerance traits"; (ii) conversely, under less exposed situations, their morphology will predominantly be the expression of the function of resource acquisition, i.e. water and nutrient uptake, with varying root/shoots ratios but a weaker structural root system (the roots with a smaller diameter) and potentially a taller above-ground size under good growth conditions.

In this empirical *in situ* study, we will focus on the early stage of the widely (on the European continent) distributed *P. nigra* which is also an abundant species on the alluvial bars of the laterally dynamic Allier River, France. The main objective was to explore if contrasted morphological and biomechanical responses exists in-between the *P. nigra* populations in relation with exposure to mechanical stress. Three contrasting locations on alluvial bars were distinguished: (i) on the most exposed upstream location of the alluvial bar, hereafter called bar-head; (ii) on the less exposed downstream location of the alluvial bar, hereafter called bar-tail; and (iii) within the lower reach of a chute channel which is sheltered during low annual floods but more exposed to concentrated water flow during more important floods.

2. Methods

2.1. *Study site and location of* P. nigra *populations*

Populus nigra L. individuals were sampled in spring 2014 within a reach of the lower gravel bed Allier River, France, near Châtel-de-Neuvre (Figure 45) which is evolving from a transitional wandering style to a meandering style. This river reach within the "*Réserve Naturelle Nationale du Val d'Allier*" with a certain protection status and which experienced moderate anthropogenic impacts, is characterized by an active lateral erosion in the outer bends of meanders and point bar formation and migration in the inner bends (Petit, 2006; Dejaifve and Esquirol, 2011). The Allier River has a pluvial hydrological regime with strong seasonal and interannual variability and a mean annual discharge of 117 m^3 s^{-1} (1986-2017; data: Banque Hydro http://www.hydro.eaufrance.fr). *P. nigra* individuals were sampled within three populations located on two alluvial bars juxtaposed in the downstream direction and within one chute channel. The three populations were mainly composed of *P. nigra* individuals chosen from the same local populations, however some *Salix purpurea* L. and *Salix alba* L. individuals were also present within the sampled vegetation patches.

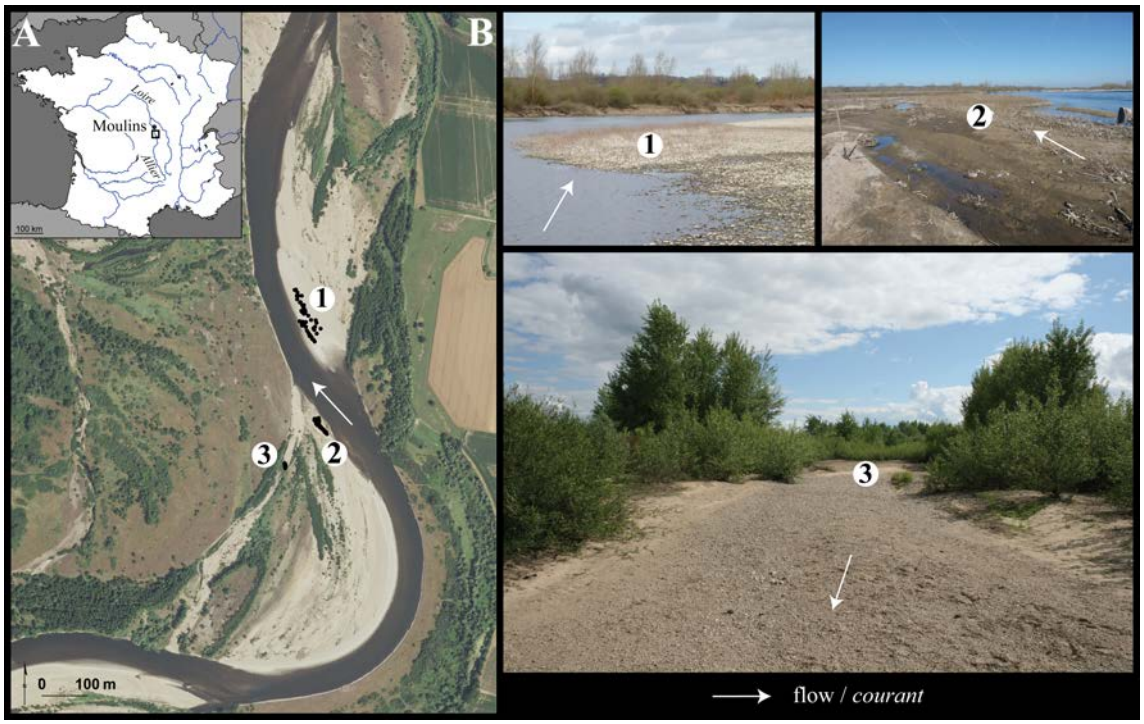

Figure 45. Localisation map. A: France (X: 46.420820, Y: 3.331899); B: sampling sites on the Allier River. 1: bar-head; 2: bar-tail; 3: lower reach of chute channel.

These three populations dating back to 2011 and 2012 were chosen in order to (i) obtain three different levels of exposure to mechanical stress with homogeneous sediment texture at the patch scale, (ii) and to maximise the probability that the populations originated from the same local population, and thus dispose of a close genotype. The first population (Figure 45 n°1) is located on the highly exposed bar-head of the downstream alluvial bar; the second population on a less exposed bar-tail location of the upstream alluvial bar (Figure 45 n°2) and the third population within the lower (downstream) reach of the chute channel of the upstream alluvial bar (Figure 45 n°3).

The flooding threshold of all three populations corresponds to a discharge of about 130 m^3 s^{-1} (Figure 46). Total submersion time, determined from flow hydrographs, of the two year old *P. nigra* saplings was about 342 days. During the first year the saplings were exposed to two quasi-annual floods of 357 and 408 m^3 s^{-1} (return period T: 2 yrs 580 m^3 s^{-1}) and to one flood of 729 m^3 s^{-1} (T: 5 yrs 810 m^3 s^{-1}). During the second year after recruitment, three more floods of 610, 364 and 375 m^3 s^{-1} occurred. The first two floods occurred during autumn and winter when saplings were leafless and the third flood occurred during spring time when leaves had sprouted at the end of the dormancy. The last three floods occurred during spring time, full summer (maximum biomass) and

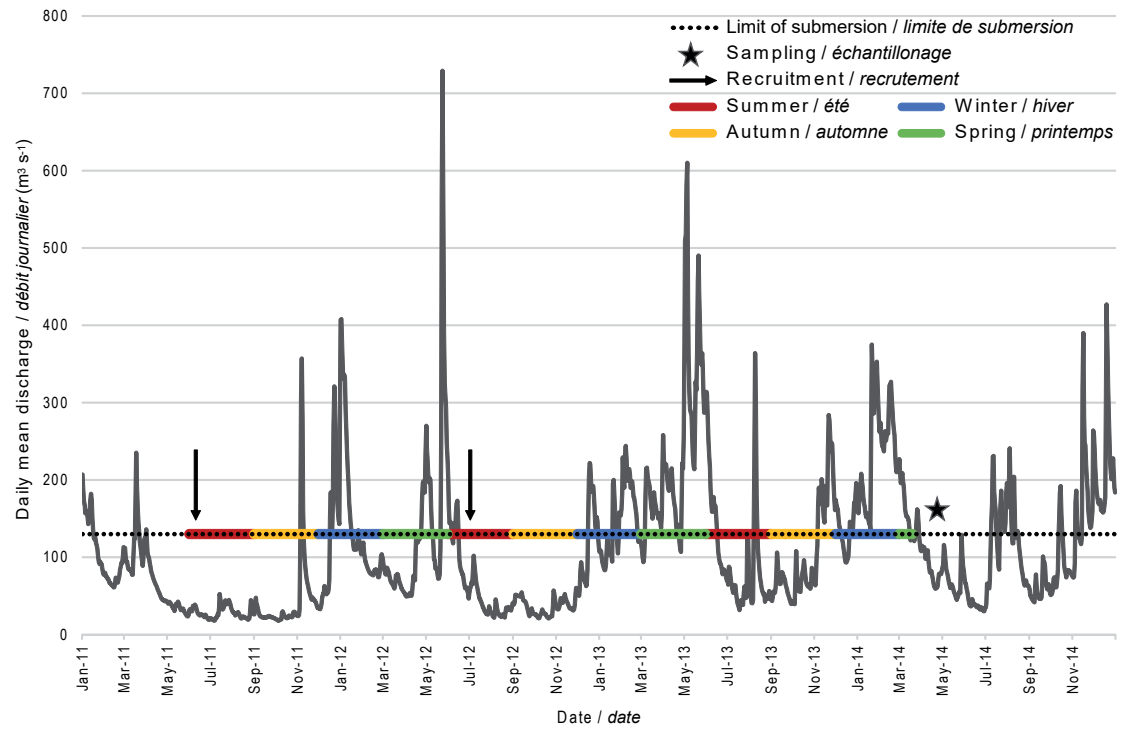

Figure 46. Daily mean discharges (m^3 s^{-1}) at the hydrological station of Châtel-de-Neuvre between 2011 and 2014 and possible recruitment periods of *P. nigra* populations (data: Banque Hydro http://www.hydro.eaufrance.fr; station code: K3400810).

winter (leafless period). Submersion time of one year old *P. nigra* saplings was around 69 days. These saplings were only exposed to the last three floods.

2.2. Field sampling

First, all selected poplar individuals were localised using a DGPS (Magellan PM500). One surface and one sub-surface sediment sample was taken in order characterize overall sediment texture for each of the three populations. The subsurface sample was taken at the level where a clear transition in sediment texture was detected. Sediment texture was determined at the laboratory using standard sieving procedures (Rivière, 1977).

Vegetation parameters were measured *in situ*: the above ground height (cm), diameter (cm) at ground level and at 20 cm, inclination of the stem (degree) and flexibility (Newton). Initial stem inclination was measured along the channel upstream-downstream axis. Higher values than 90° indicate that the stem is bent to the downstream direction. In order to quantify biomechanical properties of the individuals, the stem flexibility was measured with an electronic gauging force (Sauter FH 50; Newton range of 0.01-50): from its initial position, the stem was bent by an additional 10° along the upstream-downstream axis of the flow channel. High values indicated the necessity of applying a strong force to bend the stem, and therefore a low flexibility of the individual. Finally, plants were excavated using conventional shovels in order to measure parameters related to the belowground part of the plants: the length of buried stem (cm), the length (cm) and diameter (cm) of the taproot, diameter of the collar (cm), number of lateral and adventitious roots and the number of roots with a diameter of > 0.3 cm which was chosen because it is suggested that it corresponds to the structural roots (Ding, 2014). Structural roots are more specifically related to the function of anchorage and fine roots to the function of nutrient uptake (Stokes et al., 1995; Read and Stokes, 2006). Between seedling recruitment and field sampling, the river deposited additional sandy sediment on the study sites during high water stages (> 130 $m^3 s^{-1}$). The length of the buried stem was measured between the root collar and the bar or chute channel surface. Roots growing on this part of the stem are *adventitious roots*, while *lateral roots* are growing from the original taproot. Additionally, we calculated the ratio between the aerial and the buried parts of the stem and also the total length of the plant (i.e. the above- plus the belowground part on the plant). In spring 2014, we excavated a total of 96 *P. nigra* individuals within the three populations, (bar-head [pop1]: 46 individuals; bar-tail [pop2]: 40; chute channel [pop3]: 10). From the 96 individuals, 62 individuals

(respectively 23, 32 and 7) were excavated entirely without breakage of the tap root. Stems were cut and sanded at the collar, then they were analysed with a binocular microscope and scanned at a high resolution. Annual growth rings were counted with a high precision. This dendrochronological analysis of each individual confirmed that the three populations had the same age, and that a statistical comparison of their morphological and biomechanical responses to mechanical stress could be carried out.

2.3. Data analysis

We used two datasets for the statistical analyses. The first dataset included all (in total 96), i.e. intact and broken (at tap root level) individuals. This dataset was used to study the aboveground response of *P. nigra* (pop1: 46; pop2: 40; pop3: 10 individuals). The second dataset included only the 62 intact individuals (pop1: 23; pop2: 32; pop3: 7 individuals). This dataset was used to study the belowground and the complex (above- and belowground) response of *P. nigra*.

2.3.1. Descriptive statistics

First, we used descriptive statistics and statistical tests in order to determine if plant response trait attributes varied in relation with the different levels of exposure to mechanical stress (bar-head, bar-tail, chute channel). We used Kruskal-Wallis non-parametric test with Steel-Dwass-Critchlow-Fligner multiple pairwise comparison procedure to identify which sites were responsible for rejecting H_0. Letters are assigned to groups (i.e. A, B) indicating that the groups are significantly different. The analysis was undertaken with XLSTAT software.

2.3.2. Discriminant analysis

P. nigra individuals had known group membership (three distinct locations). After data standardisation, we applied discriminant analysis to explain and predict the membership to several groups. This method allows (i) to check on a two-dimensional chart if the groups are well discriminated; (ii) to describe group properties using explanatory variables; and (iii) to predict to which group an observation belongs. Statistical tests were calculated, such as the Box test (Fisher's F asymptotic approximation) and the Wilks' Lambda test

(Rao's approximation). The Box test is used to verify the assumption of equality for intra-class covariance matrices. The Wilks' Lambda test allows to test if the vector of the means for the various groups are equal or not. In addition, the confusion matrix was calculated showing the correctly and incorrectly assigned observations to groups based on the discriminant analysis. We have also undertaken a cross-validation to compensate for an optimistic apparent error rate. In cross-validation each observation one at a time is removed and the classification function is recalculated using the remaining data, and then the forecast is calculated for the omitted observation. The analysis was undertaken for the complete dataset (aboveground and belowground traits) within the XLSTAT software to better understand the response of the entire plant with a possibly correlated response between the aboveground and belowground traits to different levels of mechanical stress.

In the second part of the analysis, we have undertaken a cartographic analysis to study plant responses within each of the three locations (within-patch analysis). For each observation, its membership class was assigned by the discriminant analysis model, which is deduced by the membership probabilities. We mapped the probability values and the assigned group membership for each observation to determine where incorrectly assigned observations were localised. The cartographic work was undertaken in ArcMap™ using the probabilities and the membership classes of the cross-validation model, which is a more realistic model.

3. Results

3.1. Sediment texture and topography

The three locations differed according to sediment texture. The coarsest sediment texture was found on the bar-head and the finest on the bar-tail (Figure 47). There was a significant difference between the altitudes of the three populations. The population in the secondary channel was located at the highest mean elevation (219.14±0.04 m), then the downstream population (218.63±0.11 m) and finally the upstream one (218.22±0.21 m). The relative altitudes of the three locations are respectively 1.65 m, 1.13 m and 0.81 m above the water level (frequency of 0.45).

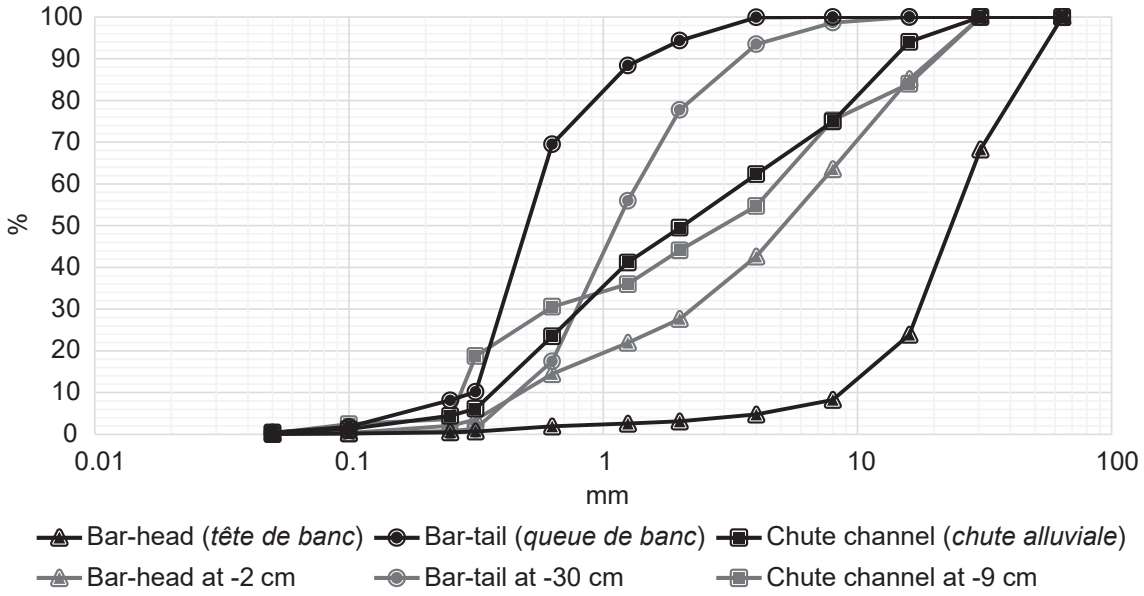

Figure 47. Surface and subsurface cumulated particle size distributions of the three sample sites.

3.2. Age of patches

The dendrochronological analysis showed that the age of *Populus nigra* L. individuals within the three patches was comprised between one and three years. The mean age of the three populations including intact and broken individuals was 1.9 at bar-head, 1.6 at bar-tail and 2.3 years in the chute channel. For the dataset including only intact individuals the mean age was respectively 2, 1.6 and 2.2 years. There was no significant difference (tested with Mann-Whitney) concerning the height, the total length and the root collar diameter within groups between individuals of different age. Thus, age differences within populations did not induce a statistical bias for the in-between population analysis of differences related to response traits. A sign of mechanical impact was recorded between the first and the second ring of seven individuals within the upstream part of the bar-head population.

3.3. Populations' response traits: descriptive statistics

3.3.1. Aboveground response

For all aboveground response traits (height, flexibility, diameter at ground level and at 20 cm and inclination of the stem) the Kruskal-Wallis test rejected the H_0. Thus, *P. nigra*

trait attributes significantly varied between the three populations (Table 23). The height of the plants was significantly different between all three locations (Steel-Dwass-Critchlow-Fligner multiple pairwise comparison) with the tallest individuals located in the chute channel and the smallest within the bar-head population. For all other aboveground traits a significant difference could be detected between the bar-head population and the two others. At the bar-head location, plants had a more flexible stem with smaller diameters and a higher inclination than plants located at the bar-tail location and in the chute channel. However, the sampling size was reduced within the chute channel population and results must therefore be interpreted carefully.

3.3.2. Belowground response

Concerning the belowground response traits, the Kruskal-Wallis test showed significant differences related to the length of the buried stem, the taproot and root collar diameters and the number of structural roots with a diameter of > 0.3 cm. No significant differences were observed regarding the length of taproot and the number of lateral and adventitious root (Table 23). The length of the buried stem was more important at the bar-head and bar-tail locations and was significantly shorter in the chute channel. The ratio of aerial and buried stem was close to the one within the bar-tail population demonstrating that the aerial part of the stem is equal to the buried one. Within the bar-head population the buried stem was longer, while in the chute channel population it was shorter than the aerial part. The total length (sum of the aerial, the buried stem and the taproot) of the plant was the longest on the bar-tail and the shortest at the bar-head population. The taproot and root collar diameters were the smallest at the bar-tail location and the largest on the bar-head and in the chute channel. The number of structural roots with a diameter of > 0.3 cm showed the same pattern as the aboveground traits with a high similarity between the bar-tail and the chute channel populations. At these two locations *P. nigra* individuals exhibited a weaker proportion of structural roots than within the bar-head population.

3.4. *Discriminant analysis: complex (above- and belowground) response of* P. nigra

The Box test confirmed that we need to reject the hypothesis that the covariance matrices are equal between the groups and the Wilks' Lambda test confirmed that the difference between the mean vectors of the groups are statistically significant. The

Table 23. Summary statistics and results of Kruskal-Wallis test (α=0.05) of aboveground and belowground *P. nigra* traits. Letters assigned to groups (i.e. A, B) are indicating that the groups are significantly different.

Trait	Location	Sample nb.	Min.	Max.	Mean	Std. dev.	*p*-value	Groups
Height (cm)	Bar-head	46	18.00	63.00	37.63	11.80		A
	Bar-tail	40	42.00	100.00	67.64	16.88	< 0.0001	B
	Chute ch.	10	61.00	111.00	83.00	17.10		C
Flexibility	Bar-head	46	0.02	2.12	0.33	0.42		A
(newton)	Bar-tail	40	0.04	2.30	0.83	0.53	< 0.0001	B
	Chute ch.	10	0.30	2.40	1.20	0.70		B
Ø (cm; at	Bar-head	46	0.30	1.20	0.59	0.19		A
ground)	Bar-tail	40	0.40	1.10	0.71	0.16	0.0005	B
	Chute ch.	10	0.60	1.10	0.80	0.16		B
Ø (cm;	Bar-head	46	0.10	0.60	0.38	0.13		A
at 20 cm)	Bar-tail	40	0.30	0.80	0.55	0.11	< 0.0001	B
	Chute ch.	10	0.40	0.60	0.53	0.09		B
Inclination	Bar-head	46	95.00	161.00	125.87	14.32		A
(degree)	Bar-tail	40	78.00	128.00	105.94	10.24	< 0.0001	B
	Chute ch.	10	85.00	112.00	101.60	7.29		B
Length of buried	Bar-head	23	55.00	102.00	74.48	13.45		A
stem (cm)	Bar-tail	32	47.00	100.00	71.97	13.75	0.0009	A
	Chute ch.	7	48.00	62.00	53.57	5.00		B
Ratio height/	Bar-head	23	0.19	1.15	0.57	0.20		A
buried stem	Bar-tail	32	0.55	1.79	1.00	0.27	< 0.0001	B
	Chute ch.	7	1.14	1.65	1.40	0.19		C
Total length	Bar-head	23	95.00	167.00	131.22	14.49		A
(cm)	Bar-tail	32	110.00	198.40	160.18	21.79	< 0.0001	B
	Chute ch.	7	125.00	185.00	148.57	18.06		B
Length of	Bar-head	23	11.00	23.00	16.30	3.31		A
taproot (cm)	Bar-tail	32	5.00	46.00	18.34	9.44	0.2269	A
	Chute ch.	7	13.00	25.00	19.86	3.93		A
Ø of taproot	Bar-head	23	0.40	1.10	0.74	0.21		A
(cm)	Bar-tail	32	0.10	1.10	0.55	0.25	0.0130	B
	Chute ch.	7	0.40	1.90	0.94	0.59		A
Ø of collar (cm)	Bar-head	23	0.60	1.70	1.10	0.29		A
	Bar-tail	32	0.40	1.20	0.75	0.22	< 0.0001	B
	Chute ch.	7	0.90	1.70	1.14	0.28		A
Nb. of lateral	Bar-head	23	2.00	13.00	6.35	2.84		A
root	Bar-tail	32	1.00	34.00	10.69	7.94	0.1361	A
	Chute ch.	7	3.00	22.00	10.00	8.04		A
Nb. of	Bar-head	23	14.00	109.00	45.83	21.17		A
adventitious	Bar-tail	32	9.00	101.00	45.59	24.79	0.0617	A
root	Chute ch.	7	7.00	48.00	25.43	15.95		A
Nb. of root Ø >	Bar-head	23	0.00	6.00	2.87	2.14		A
0.3 cm	Bar-tail	32	0.00	5.00	1.09	1.49	0.0007	B
	Chute ch.	7	0.00	1.00	0.14	0.38		B

two-dimensional chart representing the observations on the factor axes confirmed that the tree populations are well discriminated (Figure 48A). Bar-head and bar-tail populations were discriminated along the first axis, while bar-tail and chute channel populations along the second axis. 100% of the variance is represented by the two factors. The correlation between the initial variables and the two factors are represented on the Figure 48B. The factor F1 was the most correlated with the aboveground height, the inclination and the number of structural roots with a diameter of > 0.3 cm; the factor F2 with the diameter of root collar and taproot and the length of the buried stem.

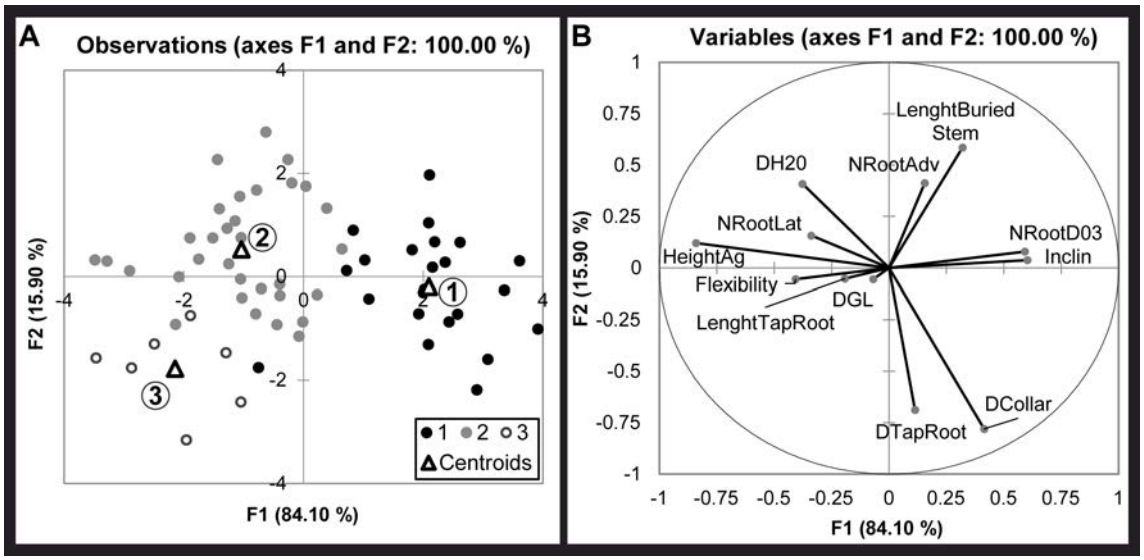

Figure 48. Discriminant analysis based on above- and belowground response traits. A: Two-dimensional chart representing the observations on the factor axes; B: Correlation between the initial variables and the two factors. 1: bar-head; 2: bar-tail; 3: lower reach of chute channel.

The upstream population (bar-head) was characterised by a small height, high inclination, a strong abundance of structural roots with a diameter of > 0.3 cm, large root collar and taproot diameter and a long buried stem. The downstream population (bar-tail) was characterised by an important stem height, low inclination, low abundance of structural roots, small root collar and taproot diameter and a long buried stem. The population in the chute channel was characterised by an important stem height, low inclination, strong number of structural roots, large root collar and taproot diameter and a small buried stem. 100% of the observations were well classified and 80.65% of the observations were well predicted by the cross-validation (Table 24). Only six individuals were classified by the cross-validation as individuals belonging to the downstream population instead of to the bar-head, four as belonging to the bar-head instead of belonging to the downstream

population and two as belonging to the downstream population instead of to the chute channel.

Table 24. Confusion matrix for the estimation sample and for the cross-validation.

Confusion matrix	from \ to	Bar-head	Bar-tail	Chute channel	Total	% correct
Estimation sample	Bar-head	23	0	0	23	100.00%
	Bar-tail	0	32	0	32	100.00%
	Chute channel	0	0	7	7	100.00%
	Total	23	32	7	62	100.00%
Cross-validation	Bar-head	17	6	0	23	73.91%
	Bar-tail	4	28	0	32	87.50%
	Chute channel	0	2	5	7	71.43%
	Total	21	36	5	62	80.65%

The cartographic results suggest that between-patch, as well as within-patch gradients for plant responses were present (Figure 49). Some individuals of the most exposed bar-head location were assigned to lower exposed bar-tail location and conversely. The misclassified individuals within the less exposed chute channel were assigned to the bar-tail group but not to the bar-head one. The misclassified individuals within the bar-head patch are rather located at the downstream part of this patch and the misclassified individuals within the bar-tail patch are rather located at upstream part of this patch.

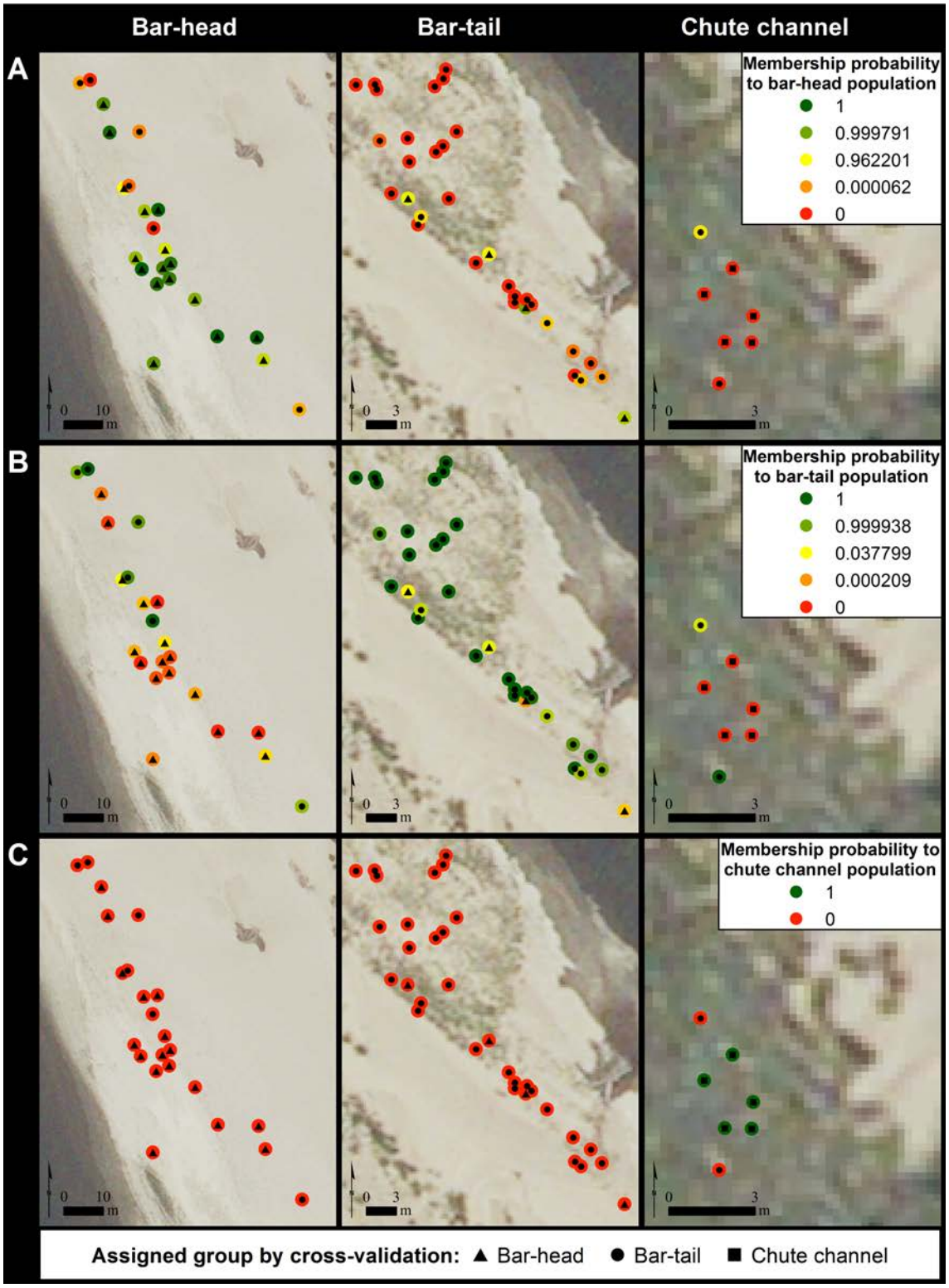

Figure 49. Membership probabilities and membership classes of observations deduced by the probabilities in cross-validation mode. A: Membership probability to be assigned to the bar-head population; B: Membership probability to be assigned to the bar-tail population; C: Membership probability to be assigned to the chute channel population. Note that thresholds between classes are different for A, B and C (see legend).

4. Discussion

In accordance with our first hypothesis that within exposed locations young poplar saplings increase their resistance to uprooting, the *Populus nigra* L. population located on the highly exposed bar-head responded to mechanical stress with a reduced size and a strong flexibility of stems (sections 3.3.1 and 3.4). The stems also showed an inclination in the downstream direction parallel to flow. The development of these two trait attributes related to stem size and flexibility was observed in experimental *in situ* (Puijalon and Bornette, 2004) and *ex situ* (Puijalon et al., 2008) studies, for example on *Mentha aquatica* L. plants in response to mechanical stress related to water flow and for *Ulmus americana* L. plants subjected to flexural treatment in an *ex situ* greenhouse experiment (Telewski and Pruyn, 1998). These observed response trait attributes most likely correspond to avoidance trait attributes as defined by Puijalon et al. (2011): the plants reduce their above-ground size to limit mechanical damage and to prevent uprooting. As corollary of the reduced plant size, the limitation of the drag decreases the potential of the plants to trap large amounts of fine sediment. Hortobágyi et al. (2017b) demonstrated on several alluvial bars of the Allier River within the same study reach (including the present bars) that such a limitation of engineer effects caused by mechanical stress in the most exposed locations on bars seems to reflect an inhibiting effect of niche construction by riparian plants. Sediment texture of the bar-head was constituted of coarse sediments, coarser than the chute channel and the bar-tail (Figure 50), suggesting a limitation of surface plant engineer effects and the occurrence of a dominantly physically-driven sedimentation process. Our results suggest that *P. nigra* plants which establish within exposed bar-head locations are able to resist strong mechanical stress (shear stress and coarse sediment transport and burial) by developing aerial avoidance traits, but they do not significantly contribute to sediment trapping because of their small size and low structural density. A trade-off based on the coast-benefits balance between the function of resisting mechanical constraints and improving resource storage must be found by the plants. Therefore, we argue that in the highly exposed contexts, short term sapling survival is the priority of the individual plant and that engineering effects remain non-significant.

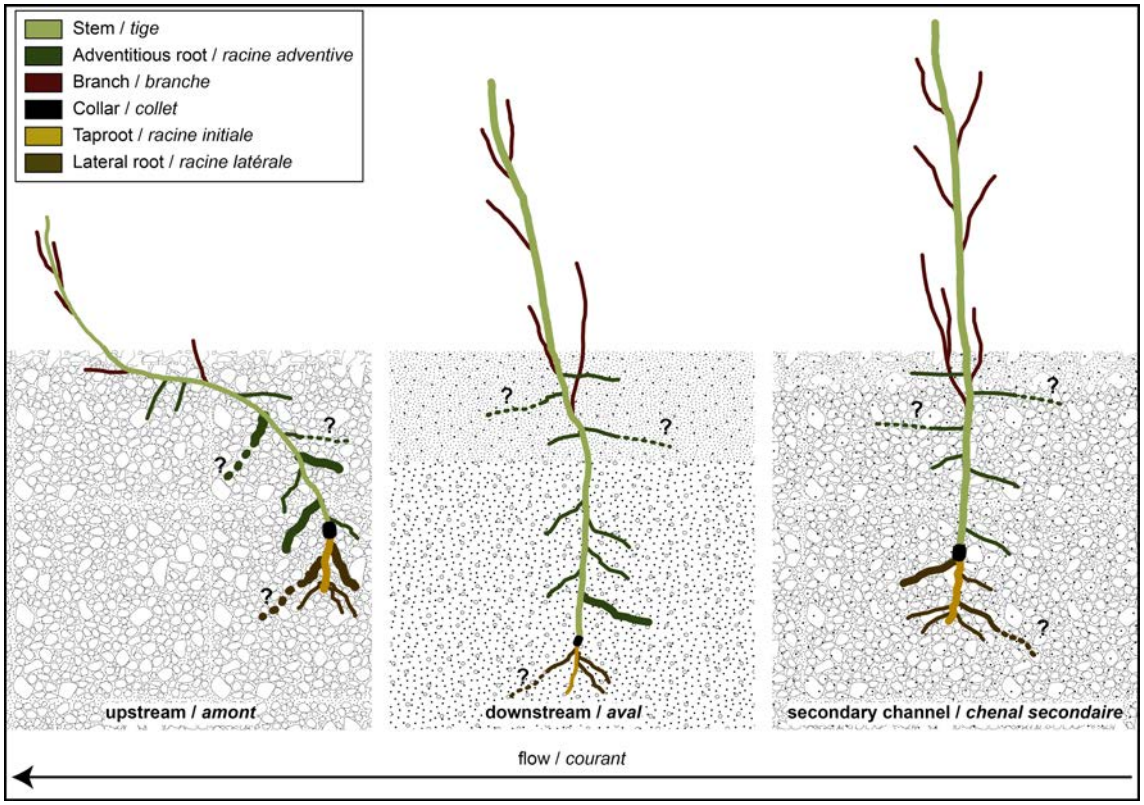

Figure 50. Schematic representation of *Populus nigra* L. exposed to different levels of mechanical stress. The length of adventitious and lateral roots remains unknown since they could not be excavated entirely. Question marks indicate that root lengths are unknown.

Within the bar-head, we also observed that the buried part of the stem of all individuals sampled was proportionally greater than the part of the aerial stems (sections 3.3.2 and 3.4). Furthermore, the buried stems lay close to a horizontal position under a coarse sediment layer (Figure 50). These observations suggest a strong biomechanical impact of floods and especially bedload transport on the exposed saplings resulting in a high stem inclination and coarse sediment burial that could lead to the improvement of anchorage of the plants through specific adaptations. Stokes et al. (1995) showed that for trees exposed to wind stress, windward roots (i.e. roots growing towards the mechanical force, here the wind) are playing an important role in stability. We suggest that the buried stems of the observed *P. nigra* plants and their associated abundant and strong adventitious roots provide an increased anchorage capacity. The high share of buried stems leads to a smaller part of the plant being directly exposed to flow and shear stress and contributes to the further development of adventitious roots and thus to an additional increase of anchorage.

However, within the population of the bar-head, we did not observe any increase in tap root length compared to the two other populations (sections 3.3.2 and 3.4). This

is in line with the results of Tamasi et al. (2005), who studied root response of *Quercus robur* L. plants to wind loading and did not observe significant difference in tap root length between wind loaded plants and the control group. It was suggested that plants are rather investing energy in lateral root growth because they provide the major component of anchorage strength in trees (Stokes et al., 1995). As expected, within the bar-head population, structural roots with a diameter of > 0.3 cm were significantly more abundant, and collar and taproot diameter were more important, than within the population of the bar-tail. This tolerance strategy (*sensu* Puijalon et al., (2011)), which enables plants to reach a higher resistance to uprooting, was also observed in an *ex situ* glasshouse experiment comparing sunflower and maize seedling responses to mechanical stimulation in the form of stem flexing (Goodman and Ennos, 1996). In addition, the development of such tolerance trait attributes (strong root system) certainly impacts geomorphology through the persistence of *P. nigra* individuals under highly exposed locations by increasing sediment cohesion, which is a widely recognized role of riparian vegetation (Abernethy and Rutherfurd, 1998; Polvi et al., 2014).

Adventitious roots that rapidly develop in freshly deposited sediments also improve the capacity of the plants to explore the substrate for water and nutrient uptake. This is especially important on the bar-head within a coarse and rather nutrient poor sediment environment. Therefore, and despite a small aboveground plant size, the adventitious roots contribute through an increase in anchorage and water and nutrient uptake to an improved capacity of the plants to survive under highly disturbed and stressful conditions and to resist mechanical destruction. A further advantage of the development of the adventitious root systems lies in its potential response to changes in geomorphology, e.g. in relation to lateral channel migration or avulsion. Within a less disturbed and stressful environment the earlier developed belowground biomass (long buried stem with adventitious roots) can facilitate rapid aboveground biomass production.

In accordance with our second hypothesis that under less exposed situations plant morphology predominantly expresses the function of resource acquisition, saplings on the bar-tail and within the lower chute channel showed longer, larger, less flexible and less inclined stems (sections 3.3.1 and 3.4). The total plant length was maximal within the bar-tail population (Table 23), suggesting that fine sediment burial under less exposed situations stimulates aboveground biomass production. Some woody plant species of coastal dunes (i.e. *Populus balsamifera* L. and *Salix cordata* Michx.) also respond with increased vertical shoot growth to burial stress (Dech and Maun, 2006). Thus, the positive growth response we observed in the bar-tail population seems clearly to be linked to the combination of the decrease in exposure to mechanical stress and the occurrence of

fine sediment deposition, which provides nutrients and an improved moisture retention capacity during summer (Steiger and Gurnell, 2003; Francis et al., 2009). Furthermore, the correlation between fine sediment trapping and plant morphology attributes was studied in various contexts, such as in a flume experiment on marsh species (Bouma et al., 2013), in a gully erosion project (Erktan and Rey, 2013) and in riparian environment (Euler et al., 2014; Corenblit et al., 2015a; Manners et al., 2015). Within the fluvial environment, higher plants that exhibit a larger biomass are expected to induce greater positive topographic changes (Kui et al., 2014; Diehl et al., 2016). The buried stems covered by fine sediment observed within the bar-tail population suggest such an effect of the *P. nigra* individuals on fine sediment trapping. Hortobágyi et al. (2017b) highlighted on the same alluvial bars of the Allier River, that *P. nigra* engineer effects on sediment trapping are indeed the most efficient when plants are exposed to intermediate and low mechanical stress, and, concurrently, develop a larger aerial biomass. Furthermore, a very high plant density was observed within the bar-tail population leading to a high roughness and thus a very efficient sediment trapping capacity.

Our results combined with the ones obtained by Hortobágyi et al. (2017b) suggest that within the bar-tail population, changes in *P. nigra* morphological and biomechanical trait attributes on alluvial bars are not only a passive response to mechanical stress but that they result from induced fine sediment trapping and positive feedbacks between *P. nigra* plant growth and fluvial landform construction (Corenblit et al., 2007, 2015a; Gurnell, 2014). Landform construction, as observed during *P. nigra* establishment on the Allier River, might be considered as a niche construction strategy leading to a progressive decrease of mechanical stress and modifications of habitat conditions that positively impact *P. nigra* survival and growth (Corenblit et al., 2014). Furthermore, the niche construction process, as observed during the present study, might be reinforced through the sheltering effect of plants growing within the most upstream and exposed areas of the studied vegetation patch. Corenblit et al. (2016a) showed that on the alluvial bars of the channelized Garonne River, France, highly exposed *P. nigra* cohorts offer bioprotection for younger cohorts which establish just downstream. The sheltering effect of upstream established plants was also demonstrated in relation to the survival of seedlings and cuttings of *P. nigra*, *S. alba* and *S. elaeagnos* (Moggridge and Gurnell, 2009). Our within-site results (Figure 49) suggest that a plant sheltering effect exists from the beginning of establishment, i.e. during the first two years following recruitment, within the same patches composed of individuals of the same age or very close age forming dense stands. In such patches, individuals located downstream benefit from the protective effects of the upstream individuals (i.e. intra-specific facilitation). However,

these exploratory results have to be confirmed by repeated sampling within a shorter time period to exclude any differences linked to the development of saplings.

The population located in the chute channel differed from the two others by its aboveground stem which was longest in the chute channel, and its buried stem which was shortest in the chute channel. The total plant length was shorter compared to the bar-tail population. This result emphasizes aerial biomass growth stimulation provided by fine sediment burial that increases the local potential of water and nutrient acquisition. Individual plants that establish in the lower reach of the chute channel developed some common trait attributes in comparison to the bar-tail population and some other trait attributes which were common to the bar-head population. The long, large, less flexible and less inclined stems and the low abundance of structural roots with a diameter > 0.3 cm were similar with the bar-tail population which was less exposed to mechanical stress. However, the larger collar and taproot diameter are common trait attributes in comparison with the bar-head population. This contrast within the same population may be related to the fact that (i) *P. nigra* plants growing within lower chute channels benefit from favourable habitat conditions (i.e. water and nutrients pools combined with a decreased exposure to mechanical stress during annual floods) thus favouring biomass production; (ii) they endure more mechanical stress during higher flows and floods because chute channels function as flood channels where water flow converges. The close resemblance concerning the collar and taproot diameter with the bar-head population might also be explained by the similarity in sediment texture (coarse sediment). An additional explanation which could not be further explored in the present study was given by Ennos (1993) who observed that plants compensate their aboveground growth to develop an optimal anchorage system to its aboveground biomass.

Overall, our observations indicate that *P. nigra* populations can develop a set of variable morphological and biomechanical responses to contrasted hydrogeomorphic constraints, leading to functional diversity and an increased resistance of the plants at the scale of an alluvial bar. At the highly exposed bar-head location, plants rather developed avoidance and tolerance response traits without significantly affecting sediment trapping while at less exposed bar-tail locations effect traits seem to be operant resulting in a positive feedback between plant growth and fluvial landform construction.

5. Conclusion

In this biogeomorphic study we provided a quantitative understanding of the relation between response trait attributes of *Populus nigra* L. plants and their exposure to different levels of mechanical stress caused by flow and sediment transport. At the highly exposed location, plants developed both avoidance and tolerance response traits allowing a higher resistance to mechanical stress, while at the less exposed location plants developed response trait attributes allowing a better resource acquisition and higher growth rate thus favouring bioconstruction. These results support the hypothesis of a positive niche construction by riparian poplar plants within fluvial corridors (Corenblit et al., 2014). Our study, in addition to the one undertaken by Hortobágyi et al. (2017b), suggests that differences in plant response trait attributes and their related effects on fluvial landform construction may lead to different biogeomorphic evolutionary trajectories on alluvial bars from a functional trait perspective. These findings highlight the importance of considering in more detail the role of fine scale biogeomorphic processes occurring at the micro-scale and at short timescale (e.g. development of individual plant response traits to mechanical stress) on those occurring at larger spatio-temporal scales (e.g. construction of wooded pioneer fluvial islands, benches and floodplains; adjustment of the landscape mosaic). We also stress the need to further develop nested hierarchical biogeomorphic bottom-up and top-down cross scale studies within fluvial corridors to better understand complex biogeomorphic fluvial ecosystems.

Chapter VI. General discussion: scale-related biogeomorphic feedbacks and scale linkage on fluvial biogeomorphic ecosystem

According to the initial objective of this thesis, we tested the key components of the biogeomorphic conceptual framework proposed in Chapter I (Figure 1). This schematic conceptual model presented feedbacks between geomorphology and riparian vegetation at three nested spatial scales, i.e. corridor, bar and micro-site. In this chapter, after our observations on the Allier River, we propose a more detailed conceptual model, describing biogeomorphic feedbacks at three hierarchical scales and explain the link between scales. The wandering Allier River will be placed in the context of other fluvial systems along the upstream-downstream gradient of energy.

This thesis investigated the response of riparian woody vegetation to hydrogeomorphic processes, their effect on fluvial landform construction and biogeomorphic feedbacks using a multi-scale hierarchical approach. The three scales of analysis were the followings: (i) the corridor/alluvial bar scale, (ii) the patch scale with the most connected, young vegetation patches on alluvial bars, and finally (iii) the individual trait scale of *Populus nigra* L. In the three hierarchical levels, scale-related biogeomorphic feedbacks were detected. However, the strength of the interactions and feedbacks and their detectability varied between scales. Our results suggest that biogeomorphic processes occurring at broader scale are controlling biogeomorphic processes at finer scales and that finer scales processes are influencing the broader ones. All of the three scales have a cyclical nature (Figure 51). The broadest spatio-temporal scale represents the evolution over several decades of the biogeomorphic mosaic resulting from the balance between constructive (vegetation establishment, growth and succession) and destructive

(floods) forces (Chapter III). The intermediate spatio-temporal scale can be described as the internal biogeomorphic succession of vegetation patches, corresponding to the transition between the geomorphic, pioneer, biogeomorphic and ecological phase of the FBS. Finally, the finest spatio-temporal scale represents the life cycle of engineer plants, during which individual engineer plants respond to hydrogeomorphic processes in order to reach their window of opportunity and afterwards to cross their engineering threshold for reaching sexual maturity.

It is possible to conceptualize each level with four different phases, which can have a different temporality. The evolution of one phase to a later one can be interrupted at any time with a possibility to return to an earlier phase or to be fully reset. The stability and instability of any phase is influenced by broader or finer scale processes (Figure 51).

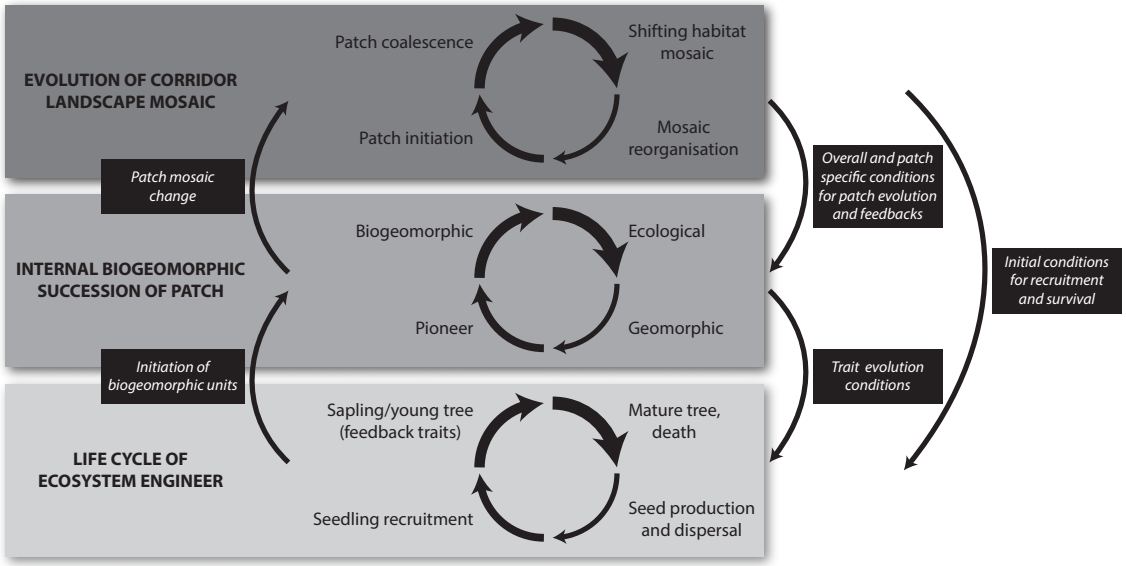

Figure 51. Hierarchical multi-scale organisation of biogeomorphic processes within a fluvial biogeomorphic ecosystem and their interactions.

1. At the corridor scale

At the broadest scale (i.e. corridor), the conditions for biogeomorphic feedbacks to occur and to become detectable are dependant of the quality and intensity of the spatio-temporal sequence of biogeomorphic succession. Biogeomorphic succession is the synergetic inter-related construction of fluvial landforms and vegetation succession, where the importance of geomorphic processes is decreasing, while the biotic ones are increasing with the time (Corenblit et al., 2007). The corridor scale can be described

with its cyclic evolution of the biogeomorphic patch mosaic (e.g. spatio-temporal ratio between the different FBS phases), which depends of the complex and non-linear adjustments between the hydrogeomorphic disturbance regime, the habitat conditions and plant dynamics (Figure 51). Following morphogenic floods, the organisation of biogeomorphic patches is set by the hydrogeomorphic context that varies along the upstream-downstream gradient of energy.

In the biogeomorphic patch initiation phase (i.e. seedling recruitment), the system is highly dominated by hydrogeomorphic processes that control seed dispersal, and the quality of the windows of opportunity. Then, following a successful recruitment, the number of ecosystem engineered patches increases on alluvial bars, meanwhile the facilitation and protection effect induced by established patches also increase. Later on, in the absence of large destructive floods, the proportion of patches in early successional phase decreases, and the ones in later or ecological successional phase increases. Biogeomorphic patches become more and more coalescent, mosaic patchiness decreases with the formation of a post-pioneer riparian forest (Corenblit et al., 2010, 2016a). During the shifting habitat mosaic phase, the biogeomorphic patch mosaic organisation and structure can eventually reach a dynamic equilibrium that is characterised by a relatively stable relative proportion of each of the four FBS phases (Garófano-Gómez et al., 2017). In such ideal/theoretical situation, the resistance of the system (i.e. the magnitude of disturbance what the system can absorb) is increasing and its resilience (speed to return after a disruptive event to the pre-event state) is decreasing in time. The aptitudes of a biogeomorphic system to reach the mature phase at the corridor scale and the biogeomorphic turnover also depend of the balance between the role of hydrogeomorphic processes in landform dynamics and the vegetation-mediated landform construction. This balance greatly varies along the upstream-downstream gradient of energy from torrential head-water reaches to low land plain river reaches. Along the gradient of energy, the stream power is decreasing from upstream to downstream.

Our results suggest that the wandering style represent a very particular case because it is a transition between the high and low energy domains. Within a high energy wandering river reach, such as the one of the Allier River, the biogeomorphic patch mosaic organisation is complex. The biogeomorphic succession and its characteristic signature in topography at the corridor scale are disrupted and partly occulted by the important and rapid channel shifts and avulsions, leading to increasing patchiness and decreasing connectedness between biogeomorphic patches. On the Allier River, the riparian vegetation established on alluvial bars locally increases its cohesion and diverts flow towards the opposite bank (see also Tal and Paola, (2010); Corenblit et al. (2016a)).

The rejuvenation of patches by high frequency, low magnitude floods, remains also very significant because of the spatial extensiveness of high vegetated sandy banks that are easily eroded. Following a high magnitude, low frequency flood event, the system enters at an extensive spatial scale into the mosaic reorganisation phase. This phase is characterised by a rejuvenated system in which the initial habitat conditions that control the window of opportunities is reset. After such rare event, the new habitat conditions potentially can drive new patch-internal successional trajectories depending on the species that successfully reach their window of opportunity and their feedback window.

At the scale of the corridor, the engineering effect of vegetation can be expressed within the fluvial corridor with variable types of biogeomorphic units (e.g. sediment tails, wooded fluvial islands, point bars, floodplain levees). These biogeomorphic units are characterised by specific spatio-temporal scales of occurrence and turnover. For example a sediment tail induced by an individual tree may persist only for few days or weeks between two high water level stages or flow pulses. Such biogeomorphic features are not detectable at the spatio-temporal scale of the corridor (it becomes noise). Meanwhile the construction of floodplains levees take longer time (from several hundred to several thousands of years (Trimble, 2007)) and are much persistent biogeomorphic units that should be detectable at the corridor scale.

The difficulties we had to detect the topographic signature of vegetation at the corridor scale on the River Allier leads to the following questions: Which are the dominant detectable biogeomorphic units within a fluvial corridor? What is their turnover? Which is the most appropriate spatio-temporal scale to detect the topographic signature of the vegetation? It seems to vary along the upstream-downstream gradient of energy and to be context-dependant. At corridor scale, the island braided system is characterised by a patchy landscape of many pioneer to some mature vegetated islands. Those fluvial islands are frequently initiated by dead driftwood and have a high turnover (Gurnell et al., 2005; Francis et al., 2009) (Figure 52). For example, the Tagliamento, island braided river is characterised as a shifting habitat mosaic, with a high turnover in the habitat mosaic. During high frequency floods, vegetation patches are eroding, aggrading and can become coalescent and evolve into larger vegetated islands and ultimately mature fluvial islands (Gurnell et al., 2001). The system is reinitiated by low frequency, high magnitude floods, resulting into the reset of the bar surfaces within the entire active tract and the reorganisation of drift deadwood deposition (Bertoldi et al., 2009). However, the island-braided system is characterised by (i) a high turnover of biogeomorphic patch dynamics, (ii) a smaller vegetation age range and (iii) a faster and very well spatially delineated biogeomorphic feedback mechanism (i.e. pioneer fluvial island construction) (Francis

et al., 2009). Therefore, topographic signature can be detected easier on the River Tagliamento at the meso-scale of fluvial islands but also at the scale of the corridor (see Bertoldi et al. (2011)). If we examine a river reach characterised by an even higher level of energy (i.e. torrential and braided systems), the topographic signature of vegetation can only be captured on a very fine spatio-temporal scales. The detectable biogeomorphic unit is the sediment tail which develops at the downstream part of an individual during a flood event which has a high, nearly annual turnover. The biogeomorphic unit exists until the individual (probably resulted from a clonal fragment) is destroyed by the following flood. Meanwhile, a meandering system, is characterised by larger biogeomorphic units of low turnover, i.e. more or less mature woody point bars, floodplain levees, which are developing along the transverse gradient of connectivity; which can facilitate the visual and quantitative detection of the topographic signature of vegetation (Figure 52) (Corenblit et al., 2016a). If we move even more downstream on the gradient of energy (anastomosing and linear sections), the topographic signature of the vegetation can probably be captured at the scale of the entire floodplain which are characterised by a very low (hundreds to millennial of years) turnover. The Allier River remains between these two categories of very high to very low energy systems. It has a high landscape mosaic variability characterized by the coexistence of several types of biogeomorphic units which have different spatio-temporal scales and turnover. We can find fine-scale young biogeomorphic units of high turnover in the close neighbour of older and biggest disconnected units which have a lower turnover. The hydrogeomorphic dynamics of the Allier River is still high enough to prevent the kinds of biogeomorphic closing and full biogeomorphic resilience that were observed at the scale of the corridor on the River Garonne (Corenblit et al., 2016a) and Tech (Corenblit et al., 2010). Because of its particular structure (occurrence of high sandy banks colonized by tall riparian trees within a dynamic hydrogeomorphic context), it can maintain a partially open, complex landscape mosaic without the occurrence of catastrophic flood events. The youngest areas characterised with the highest turnover are the alluvial bars. The young age of woody vegetation in the Châtel-de-Neuvre study area (mainly under 15 years) (Figure 53) indicates a high biogeomorphic turnover. This high turnover of biogeomorphic unit is mainly related to the strong progressive lateral dynamic of the channel occurring during intermediate floods combined to abrupt channel avulsions occurring during large floods. Our results and all the difficulty to capture the topographic signature of vegetation at the corridor scale have demonstrated that hydrogeomorphic processes (i.e. the physical one) and the specific structure (presence of extensive dry high alluvial bare surfaces) still have on the Allier River a dominant role in fluvial dynamics at the corridor scale over decadal time scale. The vegetation-mediated landform construction is activated during high frequency, low magnitude floods, on alluvial bars at patch scale, but it remains

poorly detectable at the corridor scale (spatial dilution effect). Our results suggest that under the current conditions, biogeomorphic patches in progress in the FBS have no possibility to coalesce at the corridor scale and to form large homogeneous wooded areas. Therefore, the vegetation's topographic signature remains well detectable only at the patch scale, which we describe in the following section as the patch internal biogeomorphic succession. The high patchiness of landscape mosaic, might thus be the practical reason why it is difficult to capture the topographic signature of vegetation at the overall corridor scale.

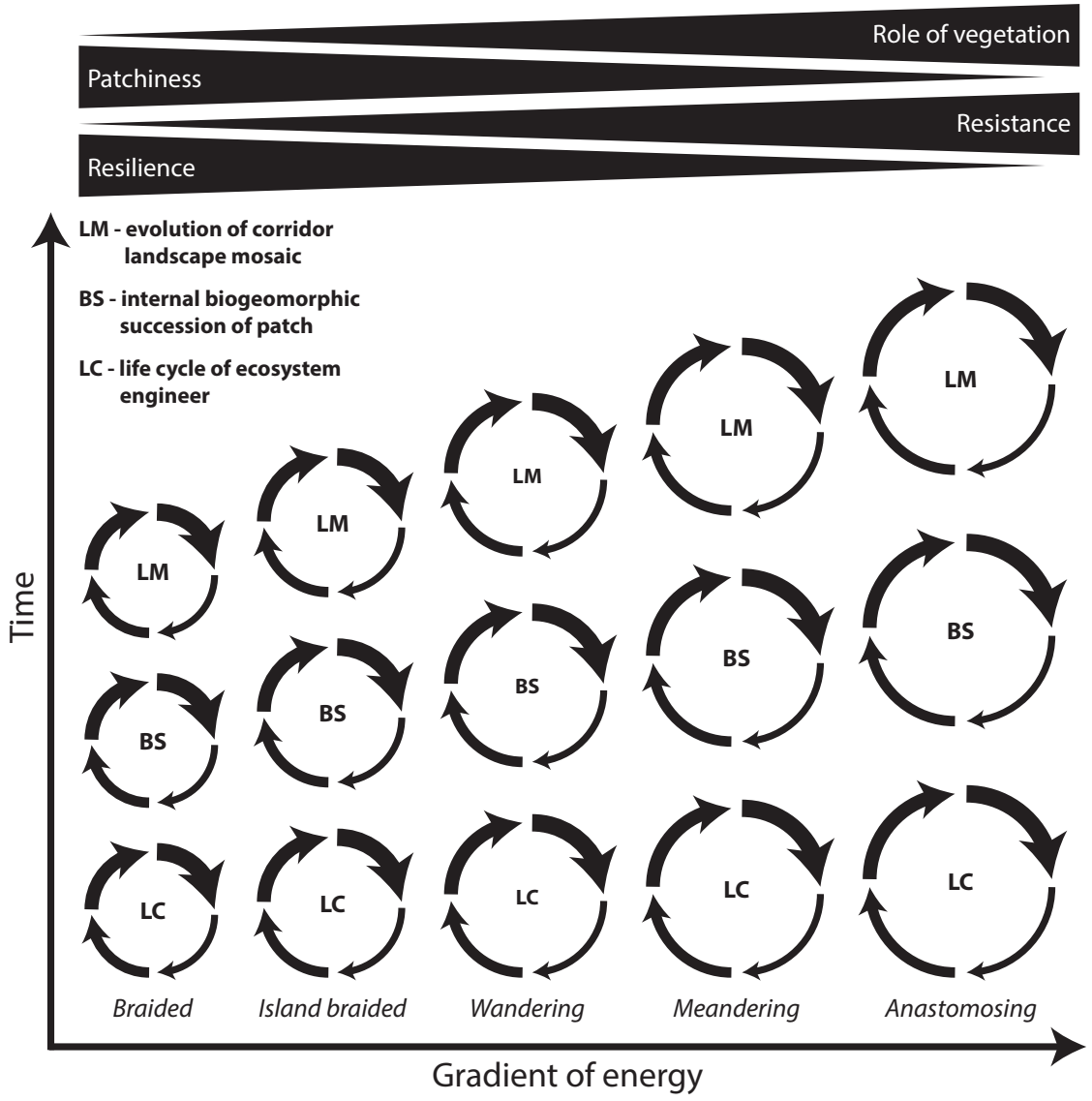

Figure 52. Hierarchical multi-scale organisation of biogeomorphic processes along the gradient of energy within three fluvial biogeomorphic ecosystem.

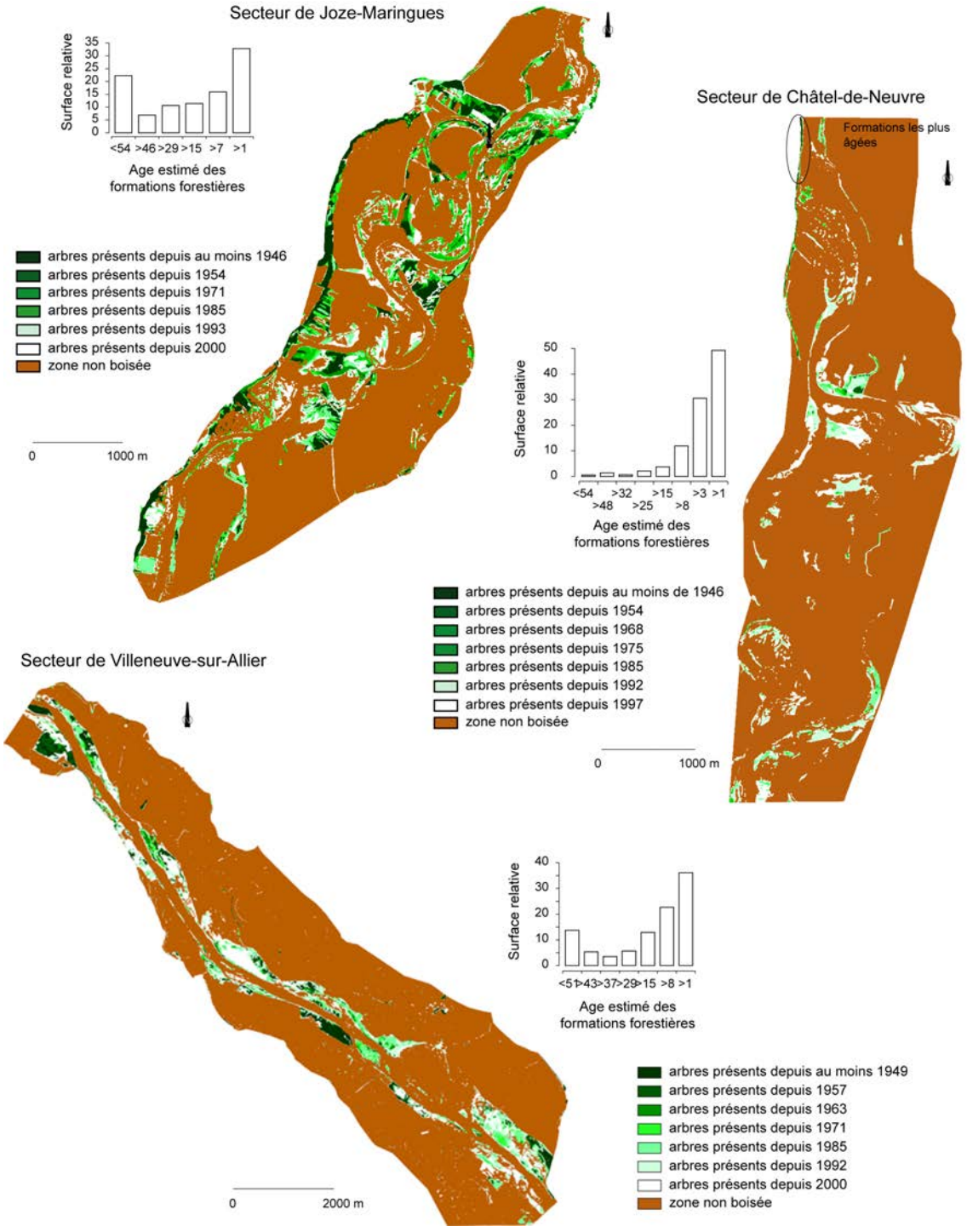

Figure 53. Minimum age of woody vegetation based on a series of aerial photographs in three sectors of the Allier River. The Châtel-de Neuvre sector corresponds to the broadest scale study area of this thesis of Chapter III (S. Petit, non published data).

2. At the patch scale

At the intermediate/patch scale, the conditions of biogeomorphic feedbacks are well described by the concept of biogeomorphic feedback window (BFW) (Eichel et al., 2015). The occurrence of the BFW will depend on the (i) geomorphic disturbance regime, (ii) species plant traits which determine their resistance and resilience, and (iii) recruitment conditions which determine vegetation patch properties (e.g. stem density and growth rate) (Chapter IV). Feedbacks between engineering plants (e.g. *P. nigra*, *S. purpurea*, *S. alba*) and hydrogeomorphic processes in the biogeomorphic feedback window can create accreting biogeomorphic units. Within these biogeomorphic units, positive feedbacks occur, resulting in landform construction, substrate stabilisation, and vegetation growth. Biogeomorphic units can also be considered functional from an ecological perspective because they (i) promote further fine sediment depositions, (ii) favour seed deposition and thus the potential of plant diversity resilience, and (iii) offer a shelter for the next cohort generation. Therefore, biogeomorphic units have good resistance and resilience abilities through feedback mechanisms between plant response and effect traits and landform structure (Corenblit et al., 2016a, 2016b).

Within the hierarchical conceptual model, the intermediate spatio-temporal scale can be described as the cycle of the internal biogeomorphic succession of vegetation patches, which is characterised by the changing intensity of biogeomorphic feedbacks. The fluvial biogeomorphic succession (FBS) model (Corenblit et al., 2007) comprises four phases of biogeomorphic ecosystem development: (i) geomorphologic (ii) pioneer (iii) biogeomorphic and (iv) ecological phase. A critical engineering threshold must be exceeded to allow biogeomorphic feedbacks to occur during the biogeomorphic phase (Corenblit et al., 2007). The biogeomorphic feedback window (BFW) (Eichel et al., 2015) is a specific spatio-temporal envelope of interactions taking place between hydrogeomorphic and ecosystem engineers dynamics (e.g., *Populus nigra* L., *Salix purpurea* L., and *Salix alba* L.) that trigger strong biogeomorphic feedbacks. On the most connected part of the alluvial bars of the Allier River, the BFWs of the three species are strongly influenced by the upstream-downstream (longitudinal) gradient of exposure and the main channel-floodplain (transverse) gradient of connectivity. At the bar scale, the biogeomorphic accumulation landform pattern is also controlled by the functional attributes of each of the three species. The BFWs of all three species taken together lead to a greater spatial extent than if only one or two of the species were present on the alluvial bars. This highlights the role of biogeomorphic functional diversity in controlling the extent and rate of fluvial landform construction.

3. At the individual scale

At the finest scale, the biogeomorphic feedbacks are explained by *P. nigra* acting as ecosystem engineer within dense patches (i.e. induces changes in the physical state of the habitat). On the lower Allier River we showed, that three woody species can act as ecosystem engineer (*P. nigra*, *Salix purpurea*, *Salix alba*), however *P. nigra* is currently strongly dominating the fluvial corridor's landscape. Our results show that *P. nigra* exhibits functional morphological and biomechanical responses to hydrogeomorphic constraints in order to establish on alluvial bars and potentially to reach their feedback window. *P. nigra* plant develop different response and related effect traits depending on local hydrogeomorphic conditions, which influence the capacity of plants to enhance fluvial landform construction. Within our hierarchical conceptual model (Figure 51), the life cycle of an engineer plant goes through the steps of diaspore dispersal, recruitment during a disturbance free period (occurrence of a Window of Opportunity), establishment and growth (development of response and effect traits), ecosystem engineering effect (development of feedback traits), sexual reproduction during the mature phase and death. The concept of biogeomorphic life cycle establishes the linkages between *P. nigra* life stages from the diaspore dispersal to the sexual maturity and the co-occurring hydrogeomorphic processes and landforms (Corenblit et al., 2014). The length and related number of reachable life cycle steps of engineer plants varies along the upstream-downstream gradient of energy, and some properties of the phases might also be different because they are context-dependant. For example, within higher energy systems (e.g. braided and island braided), the role of asexual reproduction have a greater importance compared to lower energy systems (e.g. meandering), where sexual reproduction is dominant. The facilitative effect provided by deadwood or established pioneer patches can be necessary within higher energy systems for the successful establishment of new cohorts of engineer riparian trees. Once the engineer plants cross the establishment threshold, it prioritises survival with a reduced canopy or resource acquisition and reproduction with a higher aboveground biomass depending on site-specific environmental conditions and hydrogeomorphic processes (Chapter V). Our results show, that on the alluvial bars of the Allier in the highly exposed location, plants developed both avoidance and tolerance response traits allowing a higher resistance to mechanical stress, while at the less exposed location plants developed response trait attributes allowing a better resource acquisition and higher growth rate thus favouring the evolution towards the ecosystem engineering phase and thus, potentially, sexual maturity. Our results suggest that a riparian pioneer tree, which established in a highly disturbed and stressful location of alluvial bar, can also rapidly adjust its morphology

and biomechanics if changes in geomorphic conditions occur, e.g. in relation to lateral channel migration or an avulsion. In new, more adequate conditions (e.g. less exposed), plants potentially develop trait attributes which allow a better resource acquisition and higher growth rate; thus favouring engineering effect. Results of this thesis (Chapter IV and V) also suggest that within the bar-tail population, changes in *P. nigra* morphological and biomechanical trait attributes on alluvial bars are not only a passive response to mechanical stress but that they result from induced fine sediment trapping and positive feedbacks between *P. nigra* plant growth and fluvial landform construction (Corenblit et al., 2007, 2015a; Gurnell, 2014). Landform construction, as observed during *P. nigra* establishment on the Allier River, might be possibly considered as a niche construction strategy leading to a progressive decrease of mechanical stress and improvement of habitat conditions that positively impact *P. nigra* survival and growth (Corenblit et al., 2014). Moreover, the engineering effect of plants varies between species. Different species affect geomorphology differently because they are not distributed over the same range of exposure to hydrogeomorphic constraints and they display different morphologies and biomechanical attributes at the interspecific level, but also at the intraspecific level in relation with environmental conditions (Chapter IV). The death of an ecosystem engineer has different reasons, such as (i) competition with other species, (ii) age, (iii) environmental constraints, and (iv) destruction by hydrogeomorphic processes (burial, removal, bank erosion). After the death of the engineer species, the cycle restarts.

4. Link between scales

As suggested earlier, higher level processes and structures control lower level processes and structures, and *vice versa*. First the top-down, then the bottom-up interactions will be described (Figure 51).

The broadest scale cycle of patch mosaic dynamic has a key control role on the lowest level cycle, because the balance between the destructive and constructive forces is determined at the broadest level. At the broadest level, the arrival of ecosystem engineer plants into the system will be set by the initial conditions for their recruitment, i.e. the Window of Opportunity, which are the followings: (i) hydrogeomorphology (i.e. sediment and topographic conditions; hydrological variability), (ii) availability of open space and (iii) availability of diaspore. The mosaic structure at the corridor scale will control the

formation of the recruitment sites because it controls the spatio-temporal distribution of water and sediment fluxes. The patch mosaic cycle will also set conditions for patch internal biogeomorphic succession by influencing its location within the patch mosaic. It will modulate, for example, positive (facilitation) or negative (competition) interactions, the exposure to flow and sediment characteristics, and in general, conditions for feedbacks (Corenblit et al., 2017).

The intermediate level of biogeomorphic succession of patches will determine the development of engineer plants at lower level, by influencing survival and trait evolution. These conditions concern disturbance intensity, since advancing in the phases of patch's biogeomorphic succession, the exposure to hydrogeomorphic constraint is decreasing. During the beginning of the patch internal biogeomorphic succession cycle, at the finest level, the engineer plant is exposed to high hydrogeomorphic constraints. Therefore, young individuals can be easily destroyed and the cycle restarts. Conversely, during the later phases of the patch internal biogeomorphic succession cycle, engineers can better resist, they can be eventually partly destroyed, but the cycle continues.

At the lowest level, the life cycle of engineer plant influences the patch internal biogeomorphic succession by the development of adequate traits allowing the occurrence of biogeomorphic feedbacks, and therefore the shift in the internal patch biogeomorphic succession to the biogeomorphic phase. At the beginning of the life cycle, plants develop in priority response traits favouring their survival, but not enhancing engineering effect. During the second part of the ecosystem engineer life cycle, engineer plants can develop traits which allow a better resource acquisition and higher growth rate, thus favouring engineering effect. As soon as the engineering threshold is crossed, the internal biogeomorphic succession can proceed to the biogeomorphic and after to the ecological phase.

Patch internal biogeomorphic succession will influence the overall patch mosaic dynamics at the broadest spatio-temporal scale. When patches reach the transition into the feedback window where strong biogeomorphic feedbacks initiate the biogeomorphic succession, this can lead to a shift in the patch mosaic characterised by increasing patch coalescence and decreasing role of geomorphic processes. In contrary, if the internal biogeomorphic succession is slow, the patch mosaic remains in a state where geomorphic process dominate and that is regularly reorganised.

5. Concluding remarks

This chapter presented the multi-scale organisation of biogeomorphic processes within a fluvial biogeomorphic ecosystem. We showed (i) how broad scale biogeomorphic processes occurring at corridor scale set conditions for processes occurring at fine spatio-temporal scale and (ii) how fine scale biogeomorphic processes occurring at plant trait scale are influencing those occurring at larger spatio-temporal scales. Moreover, we described the interactions between scales. Beside fluvial and coastal systems (Corenblit et al., 2015a), Eichel (2017a) demonstrated, that lateral moraines are also biogeomorphic ecosystems. In this recent work, the author applied the panarchy theory (Gunderson and Holling, 2002) to link hierarchically organised scales of lateral moraine which inspired elements of the hierarchical cyclical model of this thesis. Each level of the system was considered as an adaptive cycle which interact. The link between scales is described by *Remember* (influence of broader scale adaptive cycles on finer ones) and *Revolt* interactions (influence of finer scale adaptive cycles on broader ones). It would be an interesting perspective to apply the panarchy theory on fluvial biogeomorphic ecosystems.

Chapter VII. General conclusion and perspectives

The main objective of this thesis was to gain better understanding of biogeomorphic feedbacks of the wandering Allier River. We investigated the interactions between riparian vegetation and hydrogeomorphic processes using a nested multi-scalar approach combining field as well as spatial data obtained by the method of photogrammetry and LiDAR. Our results allowed us to demonstrate the scale-related characteristics of this fluvial biogeomorphic ecosystem. The objective of this thesis had a double component: (i) a methodological component aiming to test the applicability of recent remote sensing methods in biogeomorphic studies and (ii) a fundamental research component focusing on the response of riparian plants to hydrogeomorphic constraints and their effect on fluvial geomorphology.

In Chapter I, we presented the objectives of the thesis, the state of art, and proposed a multi-scale biogeomorphic conceptual framework which we tested in this thesis.

In Chapter II, we tested the applicability of the method of photogrammetry to quantify the response and the effect of riparian vegetation and biogeomorphic feedbacks at different spatio-temporal scales (i.e. corridor, alluvial bar and individual). We identified some difficulties or failures to properly apply photogrammetry in biogeomorphic feedback studies. However, photogrammetry appeared as a useful tool to quantify a set of relevant parameters to respond to fundamental research questions concerning biogeomorphic feedbacks at the three nested spatial scales. The biggest advantages of this method are (i) its low cost, especially compared to LiDAR; (ii) it opens the possibility to exploite archival images to study past and long-term evolution of fluvial biogeomorphic processes; (iii) it can be applied to different spatio-temporal scales.

In Chapter III, we searched for the topographic signature of riparian vegetation in the landscape at the corridor scale, using photogrammetric and LiDAR data. At this broadest scale, the topographic signature of vegetation was not easy to capture because of the complex shifting mosaic of landforms of the Allier River. However, by focusing on more connected, restricted areas (i.e. alluvial bars), the signature of vegetation could be

captured. The topographic signature seems to increase with increasing vegetation height corresponding to the evolutionary phases of the biogeomorphic succession model.

In Chapter IV, we investigated the aptitude of three dominant pioneer riparian Salicaceae species (*Populus nigra* L., *Salix purpurea* L. and *Salix alba* L.) to establish and to act as ecosystem engineers by trapping fine sediment on alluvial bars. At this intermediate scale, biogeomorphic feedbacks could be well identified. The capacity of riparian plants to establish and act as ecosystem engineers depended both on species and their physiognomy, their age and their location on alluvial bars. From a functional trait perspective our results suggest, that intra-specific and inter-sepcific functional trait diversity of riparian engineer species plays an important role in plant resilience and in controlling the extent of fluvial landform construction.

In Chapter V, we quantified the relation between response trait attributes of young *P. nigra* plants and their exposure to three different levels of mechanical stress. For this finest scale study, we selected three sites: (i) a highly exposed bar-head, (ii) a less exposed bar-tail, and (iii) in the lower reach of a chute channel. We captured the contrasting morphological and biomechanical response of *P. nigra* to variable mechanical stress exposure from a trait perspective. Beside that, our results suggested that the development of different response trait attributes influences the capacity of plants to enhance fluvial landform construction.

Based on our results, in Chapter VI we proposed a synthetic hierarchical conceptual model which describe scale-related biogeomorphic feedbacks and the linkage between scales. The three scales were considered as cycles composed of four different phases, which can have a variable temporality. The broadest spatio-temporal scale represents the evolution over several decades of the landscape mosaic resulting from the balance between constructive (vegetation establishment, growth and succession) and destructive (floods) forces. The intermediate spatio-temporal scale is the internal biogeomorphic succession of vegetation patches, here corresponding to the transition into the feedback window where strong biogeomorphic feedbacks initiate the biogeomorphic succession. Finally, the finest spatio-temporal scale represents the life cycle of engineer plants, during which engineer plants are adapting to hydrogeomorphic processes that lead them to reach their window of opportunity and afterwards to cross their engineering threshold. Scales are linked by top-down and bottom-up interactions. Higher-level processes are controlling lower-level processes, and *vice versa*.

This thesis demonstrated that fine scale (individual) plant response trait attributes and their related effects on fluvial landform construction at meso-scale (patch) may

influence evolutionary trajectories of the fluvial landscape (corridor). Our findings highlight the importance of considering in more detail the role of biogeomorphic processes occurring at fine spatial and at short timescale (e.g. development of individual plant response traits to mechanical stress) on those occurring at broad spatial and at long timescale (e.g. construction of wooded pioneer fluvial islands, benches and floodplains; adjustment of the landscape mosaic) and *vice versa*. Therefore, further hierarchical biogeomorphic bottom-up and top-down cross-scale studies are needed to fully understand biogeomorphic fluvial ecosystems functioning and thus, to better understand and predict river responses to anthropogenic impacts and environmental change. As suggested earlier, future climate change might affect engineer species' life cycle and functional trait characteristics. These fine scale modifications could result in biogeomorphic resistance and resilience modifications and therefore eventually induce irreversible changes at the corridor scale (fluvial metamorphosis).

A major perspective would be to integrate time component in this multi-scale study. At corridor scale, a 3D diachronic analysis, including information about topographic evolution under vegetation cover and its vegetation's height, should be crucial to insure, that accreting landforms are created by riparian vegetation or result from physical processes on the Allier River. This diachronic analysis could also allow a better quantification of riparian vegetation's role on geomorphic processes and an understanding of spatial organization and the trajectories of the biogeomorphc patch mosaic.

At intermediate scale, a two-year monitoring work was undertaken during this thesis within vegetation patches located on alluvial bars. The monitoring of the set of hydrological, topographic, sedimentological and vegetation parameters (i.e. species relative abundance; stem density, height, diameter and flexibilty) could lead us to the quantification of vegetation's effect on geomorphology, and its response to hydrogeomorphic dynamics and to the biotically controled geomorphic changes. Monitoring at patch scale would be complementary to the diachronic study at corridor scale, since at the bradest scale data acquisition with fine accuracy is not accessible. Patch scale monitoring could also allow a better understanding of intra-patch protecting and facilitation effects (e.g. protection of downstream part of the patch from high exposure to mechanical stress). The existance and the role of positive interactions (e.g. cooperation, altruisme; see Corenblit et al. (2017)) could also be interesting to study at finer scale, for example between *Populus nigra* individuals. It has been suggested, that between poplar individuals root grafting can occur resulting an advantage for nutrient acquisiton and exchange, as well as for anchorage.

And last but not least, the already existing knowledge and new quantitative data on fluvial biogeomorphic feedbacks should be intergrated into numerical models (e.g. van Oorschot et al. (2016)) and help their calibration for a greater contribution to an effective environmental management.

References

Abernethy, B., Rutherfurd, I.D., 1998. Where along a river's length will vegetation most effectively stabilise stream banks? Geomorphology 23, 55–75. doi:10.1016/S0169-555X(97)00089-5

Alber, A., Piégay, H., 2011. Spatial disaggregation and aggregation procedures for characterizing fluvial features at the network-scale: Application to the Rhône basin (France). Geomorphology 125, 343–360. doi:10.1016/j.geomorph.2010.09.009

Allen, T.F.H., Starr, T.B., 1982. Hierarchy Perspectives for Ecological Complexity. University of Chicago Press, 1982.

Amoros, C., Roux, A.L., Reygrobellet, J.L., Bravard, J.P., Pautou, G., 1987. A method for applied ecological studies of fluvial hydrosystems. Regul. Rivers Res. Manag. 1, 17–36. doi:10.1002/rrr.3450010104

Anderson, K., Gaston, K.J., 2013. Lightweight unmanned aerial vehicles will revolutionize spatial ecology. Front. Ecol. Environ. 11, 138–146. doi:10.1890/120150

Antonarakis, A.S., Richards, K.S., Brasington, J., 2008. Object-based land cover classification using airborne LiDAR. Remote Sens. Environ. 112, 2988–2998. doi:10.1016/j.rse.2008.02.004

Arroyo, L.A., Johansen, K., Armston, J., Phinn, S., 2010. Integration of LiDAR and QuickBird imagery for mapping riparian biophysical parameters and land cover types in Australian tropical savannas. For. Ecol. Manag. 259, 598–606. doi:10.1016/j.foreco.2009.11.018

Aucelli, P.P., Fortini, P., Rosskopf, C.M., Scorpio, V., Viscosi, V., 2011. Recent channel adjustments and riparian vegetation response: some examples from Molise (Italy). Geogr. Fis. E Din. Quat. 34, 161–173. doi:10.4461/GFDQ.2011.34.15

Balenović, I., Seletković, A., Pernar, R., Jazbec, A., 2015. Estimation of the mean tree height of forest stands by photogrammetric measurement using digital aerial images of high spatial resolution. Ann. For. Res. 58, 125–143. doi:10.15287/afr.2015.300

Balke, T., Bouma, T., Horstman, E., Webb, E., Erftemeijer, P., Herman, P., 2011. Windows of opportunity: thresholds to mangrove seedling establishment on tidal flats. Mar. Ecol. Prog. Ser. 440, 1–9. doi:10.3354/meps09364

Balke, T., Herman, P.M.J., Bouma, T.J., 2014. Critical transitions in disturbance-driven ecosystems: identifying Windows of Opportunity for recovery. J. Ecol. 102, 700–708. doi:10.1111/1365-2745.12241

Barsoum, N., 2001. Relative contributions of sexual and asexual regeneration strategies in *Populus nigra* and *Salix alba* during the first years of establishment on a braided gravel bed river. Evol. Ecol. 15, 255–279. doi:10.1023/A:1016028730129

Barsoum, N., Muller, E., Skot, L., 2004. Variations in levels of clonality among *Populus nigra* L. stands of different ages. Evol. Ecol. 18, 601–624. doi:10.1007/s10682-004-5146-4

Bätz, N., Verrecchia, E.P., Lane, S.N., 2015. The role of soil in vegetated gravelly river braid plains: more than just a passive response? Earth Surf. Process. Landf. 40, 143–156. doi:10.1002/esp.3631

Bemis, S.P., Micklethwaite, S., Turner, D., James, M.R., Akciz, S., Thiele, S.T., Bangash, H.A., 2014. Ground-based and UAV-based photogrammetry: A multi-scale, high-resolution mapping tool for structural geology and paleoseismology. J. Struct. Geol. 69, 163–178. doi:10.1016/j.jsg.2014.10.007

Benda, L., Poff, N.L., Miller, D., Dunne, T., Reeves, G., Pess, G., Pollock, M., 2004. The Network Dynamics Hypothesis: How Channel Networks Structure Riverine Habitats. BioScience 54, 413–427. doi:10.1641/0006-3568(2004)054[0413:TNDHHC]2.0.CO;2

Bendix, J., 1999. Stream power influence on southern Californian riparian vegetation. J. Veg. Sci. 10, 243–252. doi:10.2307/3237145

Bendix, J., 1994. Scale, direction, and pattern in riparian vegetation-environment relationships. Ann. Assoc. Am. Geogr. 84, 652–665. doi:10.1111/j.1467-8306.1994.tb01881.x

Bendix, J., Hupp, C.R., 2000. Hydrological and geomorphological impacts on riparian plant communities. Hydrol. Process. 14, 2977–2990. doi:10.1002/1099-1085(200011/12)14:16/17<2977::AID-HYP130>3.0.CO;2-4

Bennett, S.J., Wu, W., Alonso, C.V., Wang, S.S.Y., 2008. Modeling fluvial response to in-stream woody vegetation: implications for stream corridor restoration. Earth Surf. Process. Landf. 33, 890–909. doi:10.1002/esp.1581

Bertness, M.D., Callaway, R., 1994. Positive interactions in communities. Trends Ecol. Evol. 9, 191–193. doi:10.1016/0169-5347(94)90088-4

Bertoldi, W., Gurnell, A., Surian, N., Tockner, K., Zanoni, L., Ziliani, L., Zolezzi, G., 2009. Understanding reference processes: linkages between river flows, sediment dynamics and vegetated landforms along the Tagliamento River, Italy. River Res. Appl. 25, 501–516. doi:10.1002/rra.1233

Bertoldi, W., Gurnell, A.M., Drake, N.A., 2011. The topographic signature of vegetation development along a braided river: Results of a combined analysis of airborne lidar, color air photographs, and ground measurements. Water Resour. Res. 47. doi:10.1029/2010WR010319

Birdseye, C.H., 1940. Stereoscopic Phototopographic Mapping. Ann. Assoc. Am. Geogr. 30, 1–24. doi:10.2307/2561128

Birken, A.S., Cooper, D.J., 2006. Processes Of Tamarix Invasion And Floodplain Development Along The Lower Green River, Utah. Ecol. Appl. 16, 1103–1120. doi:10.1890/1051-0761(2006)016[1103:POTIAF]2.0.CO;2

Bizzi, S., Demarchi, L., Grabowski, R.C., Weissteiner, C.J., Van de Bund, W., 2016. The use of remote sensing to characterise hydromorphological properties of European rivers. Aquat. Sci. 78, 57–70. doi:10.1007/s00027-015-0430-7

Bornette, G., Tabacchi, E., Hupp, C., Puijalon, S., Rostan, J.C., 2008. A model of plant strategies in fluvial hydrosystems. Freshw. Biol. 53, 1692–1705. doi:10.1111/j.1365-2427.2008.01994.x

Bouma, T.J., Temmerman, S., van Duren, L.A., Martini, E., Vandenbruwaene, W., Callaghan, D.P., Balke, T., Biermans, G., Klaassen, P.C., van Steeg, P., Dekker, F., van de Koppel, J., de Vries, M.B., Herman, P.M.J., 2013. Organism traits determine the strength of scale-dependent bio-geomorphic feedbacks: A flume study on three intertidal plant species. Geomorphology 180–181, 57–65. doi:10.1016/j.geomorph.2012.09.005

Boureau, J.G., 2008. Manuel d'interprétation des photographies aériennes infrarouges. Application aux milieux forestiers et naturels. Inventaire Forestier National, Nogent-sur-Vernisson.

Breton, V., Forestier, O., Guindon, O., Evette, A., 2014. Ecological restoration under pressure from invasive animal species: Use of salicaceae cuttings in a river bank overrun by coypu. River Res. Appl. 30, 1002–1012. doi:10.1002/rra.2688

Brookes, C., Hooke, J., Mant, J., 2000. Modelling vegetation interactions with channel flow in river valleys of the Mediterranean region. CATENA 40, 93–118. doi:10.1016/S0341-8162(99)00065-X

Brown, D.G., Arbogast, A.F., 1999. Digital photogrammetric change analysis as applied to active coastal dunes in Michigan. Photogramm. Eng. Remote Sens. 65, 467–474.

Burckhardt, J.C., Todd, B.L., 1998. Riparian forest effect on lateral stream channel migration in the glacial till plains. J. Am. Water Resour. Assoc. 34, 179–184. doi:10.1111/j.1752-1688.1998.tb05970.x

Burylo, M., Rey, F., Bochet, E., Dutoit, T., 2012. Plant functional traits and species ability for sediment retention during concentrated flow erosion. Plant Soil 353, 135–144. doi:10.1007/s11104-011-1017-2

Butler, D.R., 1995. Zoogeomorphology: Animals as Geomorphic Agents. Cambridge University Press, Cambridge, UK.

Bywater-Reyes, S., Wilcox, A.C., Diehl, R.M., 2017. Multiscale influence of woody riparian vegetation on fluvial topography quantified with ground-based and airborne lidar. J. Geophys. Res. Earth Surf. 122, 1218–1235. doi:10.1002/2016JF004058

Bywater-Reyes, S., Wilcox, A.C., Stella, J.C., Lightbody, A.F., 2015. Flow and scour constraints on uprooting of pioneer woody seedlings. Water Resour. Res. 51, 9190–9206. doi:10.1002/2014WR016641

Cammeraat, L.H., 2002. A review of two strongly contrasting geomorphological systems within the context of scale. Earth Surf. Process. Landf. 27, 1201–1222. doi:10.1002/esp.421

Camporeale, C., Perucca, E., Ridolfi, L., Gurnell, A.M., 2013. Modeling the interactions between river morphodynamics and riparian vegetation. Rev. Geophys. 51, 379–414. doi:10.1002/rog.20014

Carbonneau, P., Piégay, H., 2012. Fluvial remote sensing for science and management. John Wiley & Sons Ltd., Chichester.

Carbonneau, P.E., Lane, S.N., Bergeron, N.E., 2003. Cost-effective non-metric close-range digital photogrammetry and its application to a study of coarse gravel river beds. Int. J. Remote Sens. 24, 2837–2854. doi:10.1080/01431160110108364

Carpenter, S., Walker, B., Anderies, J.M., Abel, N., 2001. From Metaphor to Measurement: Resilience of What to What? Ecosystems 4, 765–781. doi:10.1007/s10021-001-0045-9

Chamaillard, S., 2011. Efficience d'utilisation de l'eau chez le peuplier noir (*Populus nigra* L.): variabilité et plasticité en réponse aux variations de l'environnement (PhD thesis). Université d'Orléans, Orléans.

Chandler, J., Ashmore, P., Paola, C., Gooch, M., Varkaris, F., 2002. Monitoring river-channel change using terrestrial oblique digital imagery and automated digital photogrammetry. Ann. Assoc. Am. Geogr. 92, 631–644. doi:10.1111/1467-8306.00308

Church, M., 1996. Space, time and the mountain–how do we order what we see, in: Rhoads, B.L., Thorn, C.E. (Eds.), The Scientific Nature of Geomorphology. Wiley, New York, pp. 147–170.

Cooper, D.J., Merritt, D.M., Andersen, D.C., Chimner, R.A., 1999. Factors controlling the establishment of Fremont cottonwood seedlings on the Upper Green River, USA. Regul. Rivers Res. Manag. 15, 419–440. doi:10.1002/(SICI)1099-1646(199909/10)15:5<419::AID-RRR555>3.0.CO;2-Y

Corenblit, D., 2006. Structure et dynamique du paysage fluvial : études des rétroactions entre processus hydro-géomorphologiques et dynamique de la végétation du Tech (Pyrénées orientales). Université Toulouse 3 - Paul Sabatier, Toulouse, France.

Corenblit, D., Baas, A., Balke, T., Bouma, T., Fromard, F., Garófano-Gómez, V., González, E., Gurnell, A.M., Hortobágyi, B., Julien, F., Kim, D., Lambs, L., Stallins, J.A., Steiger, J., Tabacchi, E., Walcker, R., 2015a. Engineer pioneer plants respond to and affect geomorphic constraints similarly along water-terrestrial interfaces world-wide: Biogeomorphic feedbacks along water-terrestrial interfaces. Glob. Ecol. Biogeogr. 24, 1363–1376. doi:10.1111/geb.12373

Corenblit, D., Baas, A.C.W., Bornette, G., Darrozes, J., Delmotte, S., Francis, R.A., Gurnell, A.M., Julien, F., Naiman, R.J., Steiger, J., 2011. Feedbacks between geomorphology and biota controlling Earth surface processes and landforms: A review of foundation concepts and current understandings. Earth-Sci. Rev. 106, 307–331. doi:10.1016/j.earscirev.2011.03.002

Corenblit, D., Davies, N.S., Steiger, J., Gibling, M.R., Bornette, G., 2015b. Considering river structure and stability in the light of evolution: feedbacks between riparian vegetation and hydrogeomorphology. Earth Surf. Process. Landf. 40, 189–207. doi:10.1002/esp.3643

Corenblit, D., Garófano-Gómez, V., González, E., Hortobágyi, B., Julien, F., Lambs, L., Otto, T., Roussel, E., Steiger, J., Tabacchi, E., Till-Bottraud, I., 2017. Niche construction within riparian corridors. Part II: The unexplored role of intra-specific positive interactions in Salicaceae species. Geomorphology. doi:https://doi.org/10.1016/j.geomorph.2017.09.016

Corenblit, D., Steiger, J., 2009. Vegetation as a major conductor of geomorphic changes on the Earth surface: toward evolutionary geomorphology. Earth Surf. Process. Landf. 34, 891–896. doi:10.1002/esp.1788

Corenblit, D., Steiger, J., Charrier, G., Darrozes, J., Garófano-Gómez, V., Garreau, A., González, E., Gurnell, A.M., Hortobágyi, B., Julien, F., Lambs, L., Larrue, S., Otto, T., Roussel, E., Vautier, F., Voldoire, O., 2016a. *Populus nigra* L. establishment and fluvial landform construction: biogeomorphic dynamics within a channelized river: Biogeomorphic dynamics within a channelized river. Earth Surf. Process. Landf. 41, 1276–1292. doi:10.1002/esp.3954

Corenblit, D., Steiger, J., González, E., Gurnell, A.M., Charrier, G., Darrozes, J., Dousseau, J., Julien, F., Lambs, L., Larrue, S., Roussel, E., Vautier, F., Voldoire, O., 2014. The biogeomorphological life cycle of poplars during the fluvial biogeomorphological succession: a special focus on *Populus nigra* L. Earth Surf. Process. Landf. 39, 546–563. doi:10.1002/esp.3515

Corenblit, D., Steiger, J., Gurnell, A.M., Tabacchi, E., Roques, L., 2009. Control of sediment dynamics by vegetation as a key function driving biogeomorphic succession within fluvial corridors. Earth Surf. Process. Landf. 34, 1790–1810. doi:10.1002/esp.1876

Corenblit, D., Steiger, J., Tabacchi, E., 2010. Biogeomorphologic succession dynamics in a Mediterranean river system. Ecography 33, 1136–1148. doi:10.1111/j.1600-0587.2010.05894.x

Corenblit, D., Steiger, J., Tabacchi, E., Gurnell, A.M., 2008. A conceptual and methodological framework for the study of vegetated fluvial landscape evolutionary trajectories., in: Russo, R.E. (Ed.), Wetlands : Ecology, Conservation and Restoration. Nova Science Publishers, Hauppauge, NY, pp. 271–293.

Corenblit, D., Tabacchi, E., Steiger, J., Gurnell, A.M., 2007. Reciprocal interactions and adjustments between fluvial landforms and vegetation dynamics in river corridors: A review of complementary approaches. Earth-Sci. Rev. 84, 56–86. doi:10.1016/j.earscirev.2007.05.004

Corenblit, D., Vidal, V., Cabanis, M., Steiger, J., Garófano-Gómez, V., Garreau, A., Hortobágyi, B., Otto, T., Roussel, E., Voldoire, O., 2016b. Seed retention by pioneer trees enhances plant diversity resilience on gravel bars: Observations from the river Allier, France. Adv. Water Resour. in press. doi:10.1016/j.advwatres.2016.02.015

Côté, J.-F., Widlowski, J.-L., Fournier, R.A., Verstraete, M.M., 2009. The structural and radiative consistency of three-dimensional tree reconstructions from terrestrial lidar. Remote Sens. Environ. 113, 1067–1081. doi:10.1016/j.rse.2009.01.017

Crespel, L., Sigogne, M., Donès, N., Relion, D., Morel, P., 2013. Identification of relevant morphological, topological and geometrical variables to characterize the architecture of rose bushes in relation to plant shape. Euphytica 191, 129–140. doi:10.1007/s10681-013-0902-6

Curtis, J.A., Guerrero, T.M., 2015. Geomorphic mapping to support river restoration on the Trinity River downstream from Lewiston Dam, California, 1980–2011 (Open-File Report No. 2015–1047). U.S. Geological Survey, Reston, Virginia.

Dandois, J.P., Ellis, E.C., 2013. High spatial resolution three-dimensional mapping of vegetation spectral dynamics using computer vision. Remote Sens. Environ. 136, 259–276. doi:10.1016/j.rse.2013.04.005

de Boer, D.H., 1992. Hierarchies and spatial scale in process geomorphology: a review. Geomorphology 4, 303–318. doi:10.1016/0169-555X(92)90026-K

Dech, J.P., Maun, M.A., 2006. Adventitious root production and plastic resource allocation to biomass determine burial tolerance in woody plants from central Canadian coastal dunes. Ann. Bot. 98, 1095–1105. doi:10.1093/aob/mcl196

Dejaifve, P.-A., Esquirol, N., 2011. Quantification et répartition du bois mort échoué dans la Réserve Naturelle Nationale du Val d'Allier. Réserve Naturelle Nationale du Val d'Allier - DIREN-Auvergne, Moulins.

Diehl, R.M., Merritt, D.M., Wilcox, A.C., Scott, M.L., 2017a. Applying Functional Traits to Ecogeomorphic Processes in Riparian Ecosystems. BioScience 67, 729–743. doi:10.1093/biosci/bix080

Diehl, R.M., Wilcox, A.C., Stella, J.C., Kui, L., Sklar, L.S., Lightbody, A., 2017b. Fluvial sediment supply and pioneer woody seedlings as a control on bar-surface topography. Earth Surf. Process. Landf. 42, 724–734. doi:10.1002/esp.4017

Diehl, R.M., Wilcox, A.C., Stella, J.C., Kui, L., Sklar, L.S., Lightbody, A., 2016. Fluvial sediment supply and pioneer woody seedlings as a control on bar-surface topography. Earth Surf. Process. Landf. doi:10.1002/esp.4017

Dietrich, J.T., 2016. Riverscape mapping with helicopter-based Structure-from-Motion photogrammetry. Geomorphology 252, 144–157. doi:10.1016/j.geomorph.2015.05.008

Dietrich, W.E., Perron, J.T., 2006. The search for a topographic signature of life. Nature 439, 411–418. doi:10.1038/nature04452

Ding, Z., 2014. Réponse du système racinaire de *Populus nigra* L. aux contraintes hydrogéomorphologiques sur les bancs alluviaux de l'Allier (Master thesis). Université Blaise Pascal - Clermont-Ferrand II, Clermon-Ferrand, France.

Dollar, E.S.J., James, C.S., Rogers, K.H., Thoms, M.C., 2007. A framework for interdisciplinary understanding of rivers as ecosystems. Geomorphology 89, 147–162. doi:10.1016/j.geomorph.2006.07.022

Dufour, S., Bernez, I., Betbeder, J., Corgne, S., Hubert-Moy, L., Nabucet, J., Rapinel, S., Sawtschuk, J., Trollé, C., 2013. Monitoring restored riparian vegetation: how can recent developments in remote sensing sciences help? Knowl. Manag. Aquat. Ecosyst. 410, 1–15. doi:10.1051/kmae/2013068

Dufour, S., Muller, E., Straatsma, M., Corgne, S., 2012. Image utilisation for the study and management of riparian vegetation: overview and applications, in: Carbonneau, P.E., Piégay, H. (Eds.), Fluvial Remote Sensing for Science and Management. Chichester, UK, pp. 215–239.

Dunford, R., Michel, K., Gagnage, M., Piégay, H., Trémelo, M.-L., 2009. Potential and constraints of Unmanned Aerial Vehicle technology for the characterization of Mediterranean riparian forest. Int. J. Remote Sens. 30, 4915–4935. doi:10.1080/01431160903023025

Eardley, A.J., 1942. Aerial photographs: their use and interpretation. Harper & Brothers, New York, United States.

Edwards, P.J., Kollmann, J., Gurnell, A.M., Petts, G.E., Tockner, K., Ward, J.V., 1999. A conceptual model of vegetation dynamics on gravel bars of a large Alpine river. Wetl. Ecol. Manag. 7, 141–153. doi:10.1023/A:1008411311774

Eichel, J., 2017a. Biogeomorphic dynamics in the Turtmann glacier forefield, Switzerland. University of Bonn, Bonn, Germany.

Eichel, J., 2017b. Linking biogeomorphic feedbacks from ecosystem engineer to landscape scale: a panarchy approach. Presented at the EGU General Assembly Conference Abstracts, Vienna, Austria, p. 8412.

Eichel, J., Corenblit, D., Dikau, R., 2015. Conditions for feedbacks between geomorphic and vegetation dynamics on lateral moraine slopes: a biogeomorphic feedback window. Earth Surf. Process. Landf. 41, 406–419. doi:10.1002/esp.3859

Ennos, A.R., 1993. The Scaling of Root Anchorage. J. Theor. Biol. 161, 61–75. doi:10.1006/jtbi.1993.1040

Erktan, A., Pianu, B., Lucisine, P., Rey, F., 2012. Role of the morphology of *Salix* tillers barriers in marly sediment trapping efficiency in gully floor under ecological restoration: a flume experiment, in: EGU General Assembly Conference Abstracts. p. 1864.

Erktan, A., Rey, F., 2013. Linking sediment trapping efficiency with morphological traits of *Salix* tiller barriers on marly gully floors under ecological rehabilitation. Ecol. Eng. 51, 212–220. doi:10.1016/j.ecoleng.2012.12.003

Erskine, W., Chalmers, A., Keene, A., Cheetham, M., Bush, R., 2009. Role of a rheophyte in bench development on a sand-bed river in southeast Australia. Earth Surf. Process. Landf. 34, 941–953. doi:10.1002/esp.1778

Euler, T., Zemke, J., Rodrigues, S., Herget, J., 2014. Influence of inclination and permeability of solitary woody riparian plants on local hydraulic and sedimentary processes. Hydrol. Process. 28, 1358–1371. doi:10.1002/hyp.9655

Farid, A., Goodrich, D.C., Sorooshian, S., 2006. Using airborne lidar to discern age classes of cottonwood trees in a riparian area. West. J. Appl. For. 21, 149–158.

Fonstad, M.A., Dietrich, J.T., Courville, B.C., Jensen, J.L., Carbonneau, P.E., 2013. Topographic structure from motion: a new development in photogrammetric measurement. Earth Surf. Process. Landf. 38, 421–430. doi:10.1002/esp.3366

Forsman, M., Börlin, N., Holmgren, J., 2016. Estimation of tree stem attributes using terrestrial photogrammetry with a camera rig. Forests 7, 1–20. doi:10.3390/f7030061

Fox, A.J., Cziferszky, A., 2008. Unlocking the time capsule of historic aerial photography to measure changes in antarctic peninsula glaciers. Photogramm. Rec. 23, 51–68. doi:10.1111/j.1477-9730.2008.00463.x

Francis, R.A., 2006. Allogenic and autogenic influences upon riparian vegetation dynamics. Area 38, 453–464. doi:10.1111/j.1475-4762.2006.00706.x

Francis, R.A., Corenblit, D., Edwards, P.J., 2009. Perspectives on biogeomorphology, ecosystem engineering and self-organisation in island-braided fluvial ecosystems. Aquat. Sci. 71, 290–304. doi:10.1007/s00027-009-9182-6

Francis, R.A., Gurnell, A.M., Petts, G.E., Edwards, P.J., 2005. Survival and growth responses of *Populus nigra*, *Salix elaeagnos* and A*lnus incana* cuttings to varying levels of hydric stress. For. Ecol. Manag. 210, 291–301. doi:10.1016/j.foreco.2005.02.045

Friedman, J.M., Osterkamp, W.R., Lewis, W.M., 1996. The role of vegetation and bed-level fluctuations in the process of channel narrowing. Fluv. Geomorphol. Veg. 14, 341–351. doi:10.1016/0169-555X(95)00047-9

Frissell, C.A., Liss, W.J., Warren, C.E., Hurley, M.D., 1986. A hierarchical framework for stream habitat classification: Viewing streams in a watershed context. Environ. Manage. 10, 199–214. doi:10.1007/BF01867358

Fritz, A., Kattenborn, T., Koch, B., 2013. UAV-based photogrammetric point clouds—Tree stem mapping in open stands in comparison to terrestrial laser scanner point clouds. Int Arch Photogramm Remote Sens Spat Inf Sci 40, 141–146. doi:10.5194/isprsarchives-XL-1-W2-141-2013

Garófano-Gómez, V., Corenblit, D., Moulin, B., Steiger, J., Abadi, M., Chaleil, P., Evette, A., Forestier, O., Garreau, A., González, E., Hortobágyi, B., Julien, F., Lambs, L., Masip, J., Ploquin, S., Voldoire, O., 2016. Black poplar (*Populus nigra* L.) root response to hydrogeomorphological constraints: An experimental approach. Presented at the Eco Summit, Montpellier, France.

Garófano-Gómez, V., Metz, M., Egger, G., Díaz-Redondo, M., Hortobágyi, B., Geerling, G., Corenblit, D., Steiger, J., 2017. Vegetation succession processes and fluvial dynamics of a mobile temperate riparian ecosystem: the lower Allier River (France). Géomorphologie Relief Process. Environ. 23, 187–202. doi:10.4000/geomorphologie.11805

Geerling, G., Ragas, A., Leuven, R., Berg, J., Breedveld, M., Liefhebber, D., Smits, A., 2006. Succession and rejuvenation in floodplains along the River Allier (France). Hydrobiologia 565, 71–86. doi:10.1007/s10750-005-1906-6

Geerling, G.W., Vreeken-Buijs, M.J., Jesse, P., Ragas, A.M.J., Smits, A.J.M., 2009. Mapping river floodplain ecotopes by segmentation of spectral (CASI) and structural (LiDAR) remote sensing data. River Res. Appl. 25, 795–813. doi:10.1002/rra.1181

Gillan, J.K., Karl, J.W., Duniway, M., Elaksher, A., 2014. Modeling vegetation heights from high resolution stereo aerial photography: An application for broad-scale rangeland monitoring. J. Environ. Manage. 144, 226–235. doi:10.1016/j.jenvman.2014.05.028

Glasby, T.M., Underwood, A.J., 1996. Sampling to differentiate between pulse and press perturbations. Environ. Monit. Assess. 42, 241–252. doi:10.1007/BF00414371

Gomez, C., Hayakawa, Y., Obanawa, H., 2015. A study of Japanese landscapes using structure from motion derived DSMs and DEMs based on historical aerial photographs: New opportunities for vegetation monitoring and diachronic geomorphology. Geomorphology 242, 11–20. doi:10.1016/j.geomorph.2015.02.021

Gong, P., Biging, G.S., Standiford, R., 2000. Technical Note: Use of Digital Surface Model for Hardwood Rangeland Monitoring. J. Range Manag. 53, 622–626. doi:10.2307/4003157

González, E., González-Sanchis, M., Comín, F.A., Muller, E., 2012. Hydrologic thresholds for riparian forest conservation in a regulated large Mediterranean river. River Res. Appl. 28, 71–80. doi:10.1002/rra.1436

Goodman, A.M., Ennos, A.R., 1996. A comparative study of the response of the roots and shoots of sunflower and maize to mechanical stimulation. J. Exp. Bot. 47, 1499–1507. doi:10.1093/jxb/47.10.1499

Gregory, S.V., Swanson, F.J., McKee, W.A., Cummins, K.W., 1991. An Ecosystem Perspective of Riparian Zones: Focus on links between land and water. BioScience 41, 540–551. doi:10.2307/1311607

Guilloy, H., González, E., Muller, E., Hughes, F.M.R., Barsoum, N., 2011. Abrupt drops in water table level influence the development of *Populus nigra* and *Salix alba* seedlings of different ages. Wetlands 31, 1249–1261. doi:10.1007/s13157-011-0238-8

Guilloy-Froget, H., Muller, E., Barsoum, N., Hughes, F.M.M., 2002. Dispersal, germination, and survival of *Populus nigra* L. (Salicaceae) in changing hydrologic conditions. Wetlands 22, 478–488. doi:10.1672/0277-5212(2002)022[0478:DGASOP]2.0.CO;2

Gunderson, L.H., Allen, C.R., Holling, C.S. (Eds.), 2010. Foundations of ecological resilience. Island Press, New York.

Gunderson, L.H., Holling, C.S. (Eds.), 2002. Panarchy: understanding transformations in human and natural systems. Island Press, Washington, DC.

Gurnell, A., 2014. Plants as river system engineers. Earth Surf. Process. Landf. 39, 4–25. doi:10.1002/esp.3397

Gurnell, A., Petts, G., 2006. Trees as riparian engineers: the Tagliamento river, Italy. Earth Surf. Process. Landf. 31, 1558–1574. doi:10.1002/esp.1342

Gurnell, A., Tockner, K., Edwards, P., Petts, G., 2005. Effects of deposited wood on biocomplexity of river corridors. Front. Ecol. Environ. 3, 377–382. doi:10.1890/1540-9295(2005)003[0377:EODWOB]2.0.CO;2

Gurnell, A.M., Bertoldi, W., Corenblit, D., 2012. Changing river channels: The roles of hydrological processes, plants and pioneer fluvial landforms in humid temperate, mixed load, gravel bed rivers. Earth-Sci. Rev. 111, 129–141. doi:10.1016/j.earscirev.2011.11.005

Gurnell, A.M., Petts, G.E., 2002. Island-dominated landscapes of large floodplain rivers, a European perspective. Freshw. Biol. 47, 581–600. doi:10.1046/j.1365-2427.2002.00923.x

Gurnell, A.M., Petts, G.E., Hannah, D.M., Smith, B.P., Edwards, P.J., Kollmann, J., Ward, J.V., Tockner, K., 2001. Riparian vegetation and island formation along the gravel-bed Fiume Tagliamento, Italy. Earth Surf. Process. Landf. 26, 31–62. doi:10.1002/1096-9837(200101)26:1<31::AID-ESP155>3.0.CO;2-Y

Gurnell, A.M., Rinaldi, M., Belletti, B., Bizzi, S., Blamauer, B., Braca, G., Buijse, A.D., Bussettini, M., Camenen, B., Comiti, F., Demarchi, L., García de Jalón, D., González del Tánago, M., Grabowski, R.C., Gunn, I.D.M., Habersack, H., Hendriks, D., Henshaw, A.J., Klösch, M., Lastoria, B., Latapie, A., Marcinkowski, P., Martínez-Fernández, V., Mosselman, E., Mountford, J.O., Nardi, L., Okruszko, T., O'Hare, M.T., Palma, M., Percopo, C., Surian, N., van de Bund, W., Weissteiner, C., Ziliani, L., 2016. A multi-scale hierarchical framework for developing understanding of river behaviour to support river management. Aquat. Sci. 78, 1–16. doi:10.1007/s00027-015-0424-5

Habersack, H.M., 2000. The river-scaling concept (RSC): a basis for ecological assessments. Hydrobiologia 422, 49–60. doi:10.1023/A:1017068821781

Harrison, S., 2001. On reductionism and emergence in geomorphology. Trans. Inst. Br. Geogr. 26, 327–339. doi:10.1111/1475-5661.00025

Hervouet, A., Dunford, R., Piégay, H., Belletti, B., Trémélo, M.-L., 2011. Analysis of post-flood recruitment patterns in braided-channel rivers at multiple scales based on an image series collected by unmanned aerial vehicles, ultra-light aerial vehicles, and satellites. GIScience Remote Sens. 48, 50–73. doi:10.2747/1548-1603.48.1.50

Hickin, E.J., 1984. Vegetation and River Channel Dynamics. Can. Geogr. Géographe Can. 28, 111–126. doi:10.1111/j.1541-0064.1984.tb00779.x

Holling, C.S., 2001. Understanding the Complexity of Economic, Ecological, and Social Systems. Ecosystems 4, 390–405. doi:10.1007/s10021-001-0101-5

Holling, C.S., 1973. Resilience and stability of ecological systems. Annu. Rev. Ecol. Syst. 4, 1–23. doi:10.1146/annurev.es.04.110173.000245

Hooper, D.U., Chapin, F.S., Ewel, J.J., Hector, A., Inchausti, P., Lavorel, S., Lawton, J.H., Lodge, D.M., Loreau, M., Naeem, S., Schmid, B., Setälä, H., Symstad, A.J., Vandermeer, J., Wardle, D.A., 2005. Effects of biodiversity on ecosystem functioning: a consensus of current knowledge. Ecol. Monogr. 75, 3–35. doi:10.1890/04-0922

Hortobágyi, B., 2012. Interactions entre processus hydrogéomorphologiques et dynamique de la végétation riveraine : l'exemple des crues de 2003, 2005 et 2008 sur le bas Allier (Master thesis). Université Blaise Pascal - Clermont-Ferrand II, Clermon-Ferrand, France.

Hortobágyi, B., Corenblit, D., Ding, Z., Lambs, L., Steiger, J., 2017a. Above- and belowground response of *Populus nigra* L. to mechanical stress within the Allier River, France. Géomorphologie Relief Process. Environ. 23, 219–231. doi:0.4000/geomorphologie.11748

Hortobágyi, B., Corenblit, D., Steiger, J., Peiry, J.-L., 2017b. Niche construction within riparian corridors. Part I: Exploring biogeomorphic feedback windows of three pioneer riparian species, Allier River, France. Geomorphology. doi:http://dx.doi.org/10.1016/j.geomorph.2017.08.048

Hortobágyi, B., Corenblit, D., Vautier, F., Steiger, J., Roussel, E., Burkart, A., Peiry, J.-L., 2017c. A multi-scale approach of fluvial biogeomorphic dynamics using photogrammetry. J. Environ. Manage. 202, 348–362. doi:10.1016/j.jenvman.2016.08.069

Hough-Snee, N., Roper, B.B., Wheaton, J.M., Lokteff, R.L., 2015. Riparian Vegetation Communities of the American Pacific Northwest are Tied to Multi-Scale Environmental Filters. River Res. Appl. 31, 1151–1165. doi:10.1002/rra.2815

Houston Durrant, T., de Rigo, D., Caudullo, G., 2016. *Salix alba* in Europe: distribution, habitat, usage and threats, in: San-Miguel-Ayanz, J., de Rigo, D., Caudullo, G., Houston Durrant, T., Mauri, A. (Eds.), European Atlas of Forest Tree Species. Luxembourg.

Hugenholtz, C.H., Whitehead, K., Brown, O.W., Barchyn, T.E., Moorman, B.J., LeClair, A., Riddell, K., Hamilton, T., 2013. Geomorphological mapping with a small unmanned aircraft system (sUAS): Feature detection and accuracy assessment of a photogrammetrically-derived digital terrain model. Geomorphology 194, 16–24. doi:10.1016/j.geomorph.2013.03.023

Hughes, F.M.R., 1997. Floodplain biogeomorphology. Prog. Phys. Geogr. 21, 501–529. doi:10.1177/030913339702100402

Hupp, C.R., Osterkamp, W.R., 1996. Riparian vegetation and fluvial geomorphic processes. Geomorphology 14, 277–295. doi:10.1016/0169-555X(95)00042-4

Isebrands, J.G., Richardson, J. (Eds.), 2014. Poplars and willows: trees for society and the environment, MA: CABI. ed. Boston.

James, M.R., Robson, S., 2014. Mitigating systematic error in topographic models derived from UAV and ground-based image networks. Earth Surf. Process. Landf. 39, 1413–1420. doi:10.1002/esp.3609

James, M.R., Robson, S., 2012. Straightforward reconstruction of 3D surfaces and topography with a camera: Accuracy and geoscience application. J. Geophys. Res. Earth Surf. 117, F03017. doi:10.1029/2011JF002289

Javernick, L., Brasington, J., Caruso, B., 2014. Modeling the topography of shallow braided rivers using Structure-from-Motion photogrammetry. Geomorphology 213, 166–182. doi:10.1016/j.geomorph.2014.01.006

Jensen, J., Mathews, A., 2016. Assessment of image-based point cloud products to generate a bare earth surface and estimate canopy heights in a woodland ecosystem. Remote Sens. 8, 1–13. doi:10.3390/rs8010050

Jensen, J.R., 1986. Introductory digital image processing: A remote sensing perspective. Univ. of South Carolina, Columbus.

Johnson, C.W., 2000. Tree recruitment and survival in rivers: influence of hydrological processes. Hydrol. Process. 14, 3051–3074. doi:10.1002/1099-1085(200011/12)14:16/17<3051::AID-HYP134>3.0.CO;2-1

Jones, C.G., Lawton, J.H., Shachak, M., 1994. Organisms as ecosystem engineers. Oikos 69, 373–386. doi:10.2307/3545850

Karrenberg, S., Blaser, S., Kollmann, J., Speck, T., Edwards, P.J., 2003. Root anchorage of saplings and cuttings of woody pioneer species in a riparian environment. Funct. Ecol. 17, 170–177. doi:10.1046/j.1365-2435.2003.00709.x

Karrenberg, S., Edwards, P.J., Kollmann, J., 2002. The life history of Salicaceae living in the active zone of floodplains. Freshw. Biol. 47, 733–748. doi:10.1046/j.1365-2427.2002.00894.x

Kondolf, G.M., Curry, R.R., 1986. Channel erosion along the Carmel river, Monterey county, California. Earth Surf. Process. Landf. 11, 307–319. doi:10.1002/esp.3290110308

Korpela, I., 2007. 3D treetop positioning by multiple image matching of aerial images in a 3D search volume bounded by lidar surface models. Photogramm. Fernerkund. Geoinformation 1/2007, 35–44.

Korpela, I., 2004. Individual tree measurements by means of digital aerial photogrammetry, Silva Fennica Monographs. Finnish Soc. of Forest Science, Helsinki.

Kui, L., Stella, J.C., 2016. Fluvial sediment burial increases mortality of young riparian trees but induces compensatory growth response in survivors. For. Ecol. Manag. 366, 32–40. doi:10.1016/j.foreco.2016.02.001

Kui, L., Stella, J.C., Lightbody, A., Wilcox, A.C., 2014. Ecogeomorphic feedbacks and flood loss of riparian tree seedlings in meandering channel experiments. Water Resour. Res. 50, 9366–9384. doi:10.1002/2014WR015719

Lake, P.S., 2008. Flow-Generated Disturbances and Ecological Responses: Floods and Droughts, in: Hydroecology and Ecohydrology. John Wiley & Sons, Ltd, pp. 75–92. doi:10.1002/9780470010198.ch5

Lane, S.N., 2000. The measurement of river channel morphology using digital photogrammetry. Photogramm. Rec. 16, 937–961. doi:10.1111/0031-868X.00159

Lane, S.N., Richards, K.S., 1997. Linking river channel form and process: time, space and causality revisited. Earth Surf. Process. Landf. 22, 249–260.

Lane, S.N., Richards, K.S., Chandler, J.H., 1993. Developments in photogrammetry; the geomorphological potential. Prog. Phys. Geogr. 17, 306–328. doi:10.1177/030913339301700302

Latterell, J.J., Scott Bechtold, J., O'Keefe, T.C., Pelt, R., Naiman, R.J., 2006. Dynamic patch mosaics and channel movement in an unconfined river valley of the Olympic Mountains. Freshw. Biol. 51, 523–544. doi:10.1111/j.1365-2427.2006.01513.x

Lavaine, C., 2013. Evaluation des capacités biotechniques de boutures de Salicaceae et Tamaricaceae sur un gradient de sécheresse. École normale supérieure, Lyon, France.

Lavaine, C., Evette, A., Piégay, H., 2015. European Tamaricaceae in bioengineering on dry soils. Environ. Manage. 56, 221–232. doi:10.1007/s00267-015-0499-8

Lavorel, S., Garnier, E., 2002. Predicting changes in community composition and ecosystem functioning from plant traits: revisiting the Holy Grail. Funct. Ecol. 16, 545–556. doi:10.1046/j.1365-2435.2002.00664.x

Leviandier, T., Alber, A., Le Ber, F., Piégay, H., 2012. Comparison of statistical algorithms for detecting homogeneous river reaches along a longitudinal continuum. Geomorphology 138, 130–144. doi:10.1016/j.geomorph.2011.08.031

Levin, S.A., 1992. The Problem of Pattern and Scale in Ecology: The Robert H. MacArthur Award Lecture. Ecology 73, 1943–1967. doi:10.2307/1941447

Liang, X., Hyyppä, J., Kaartinen, H., Holopainen, M., Melkas, T., 2012. Detecting changes in forest structure over time with bi-temporal terrestrial laser scanning data. ISPRS Int. J. Geo-Inf. 1, 242–255. doi:10.3390/ijgi1030242

Liang, X., Jaakkola, A., Wang, Y., Hyyppä, J., Honkavaara, E., Liu, J., Kaartinen, H., 2014a. The use of a hand-held camera for individual tree 3D mapping in forest sample plots. Remote Sens. 6, 6587–6603. doi:10.3390/rs6076587

Liang, X., Kankare, V., Yu, X., Hyyppä, J., Holopainen, M., 2014b. Automated stem curve measurement using terrestrial laser scanning. IEEE Trans. Geosci. Remote Sens. 52, 1739–1748. doi:10.1109/TGRS.2013.2253783

Livny, Y., Yan, F., Olson, M., Chen, B., Zhang, H., El-Sana, J., 2010. Automatic reconstruction of tree skeletal structures from point clouds. ACM Trans. Graph. TOG 29, 151. doi:10.1145/1882261.1866177

Lytle, D.A., Poff, N.L., 2004. Adaptation to natural flow regimes. Trends Ecol. Evol. 19, 94–100. doi:10.1016/j.tree.2003.10.002

Magnusson, M., Fransson, J.E.S., Olsson, H., 2007. Aerial photo-interpretation using Z/I DMC images for estimation of forest variables. Scand. J. For. Res. 22, 254–266. doi:10.1080/02827580701262964

Mahoney, J.M., Rood, S.B., 1998. Streamflow requirements for cottonwood seedling recruitment—An integrative model. Wetlands 18, 634–645. doi:10.1007/bf03161678

Malavoi, J.-R., Bravard, J.-P., 2010. Éléments d'hydromorphologie fluviale. Onema.

Manners, R.B., Wilcox, A.C., Kui, L., Lightbody, A.F., Stella, J.C., Sklar, L.S., 2015. When do plants modify fluvial processes? Plant-hydraulic interactions under variable flow and sediment supply rates. J. Geophys. Res. Earth Surf. 120, 325–345. doi:10.1002/2014JF003265

Marston, R.A., Girel, J., Pautou, G., Piégay, H., Bravard, J.-P., Arneson, C., 1995. Channel metamorphosis, floodplain disturbance, and vegetation development: Ain River, France. Geomorphology 13, 121–131. doi:10.1016/0169-555X(95)00066-E

Mason, D.C., Cobby, D.M., Horritt, M.S., Bates, P.D., 2003. Floodplain friction parameterization in two-dimensional river flood models using vegetation heights derived from airborne scanning laser altimetry. Hydrol. Process. 17, 1711–1732. doi:10.1002/hyp.1270

Merritt, D.M., 2013. Reciprocal Relations between Riparian Vegetation, Fluvial Landforms, and Channel Processes, in: Shroder, J.F. (Ed.), Treatise on Geomorphology. Academic Press, San Diego, pp. 219–243. doi:10.1016/B978-0-12-374739-6.00239-6

Micheletti, N., Chandler, J.H., Lane, S.N., 2015. Structure from motion (SFM) photogrammetry, in: Clarke, L., Nield, J. (Eds.), Geomorphological Techniques (Online Edition). London, pp. 247–275.

Michez, A., Piégay, H., Toromanoff, F., Brogna, D., Bonnet, S., Lejeune, P., Claessens, H., 2013. LiDAR derived ecological integrity indicators for riparian zones: Application to the Houille river in Southern Belgium/Northern France. Ecol. Indic. 34, 627–640. doi:10.1016/j.ecolind.2013.06.024

Millar, R.G., 2000. Influence of bank vegetation on alluvial channel patterns. Water Resour. Res. 36, 1109–1118. doi:10.1029/1999WR900346

Miller, D.R., Quine, C.P., Hadley, W., 2000. An investigation of the potential of digital photogrammetry to provide measurements of forest characteristics and abiotic damage. For. Ecol. Manag. 135, 279–288.

Miller, J.R., Schulz, T.T., Hobbs, N.T., Wilson, K.R., Schrupp, D.L., Baker, W.L., 1995. Changes in the landscape structure of a southeastern Wyoming riparian zone following shifts in stream dynamics. Biol. Conserv. 72, 371–379. doi:10.1016/0006-3207(94)00049-V

Mitchell, A.L., Lucas, R.M., Donnelly, B.E., Pfitzner, K., Milne, A.K., Finlayson, M., 2007. A new map of mangroves for Kakadu National Park, Northern Australia, based on stereo aerial photography. Aquat. Conserv. Mar. Freshw. Ecosyst. 17, 446–467. doi:10.1002/aqc.818

Moggridge, H.L., Gurnell, A.M., 2009. Controls on the sexual and asexual regeneration of Salicaceae along a highly dynamic, braided river system. Aquat. Sci. 71, 305–317. doi:10.1007/s00027-009-9193-3

Montgomery, D.R., Buffington, J.M., 1998. Channel processes, classification, and response, in: Naiman, R.J., Bilby, R. (Eds.), River Ecology and Management: Lessons from the Pacific Coastal Ecoregion. New York, pp. 13–42.

Moreels, P., Perona, P., 2007. Evaluation of Features Detectors and Descriptors based on 3D Objects. Int. J. Comput. Vis. 73, 263–284. doi:10.1007/s11263-006-9967-1

Murray, A.B., Knaapen, M.A.F., Tal, M., Kirwan, M.L., 2008. Biomorphodynamics: Physical-biological feedbacks that shape landscapes. Water Resour. Res. 44. doi:10.1029/2007WR006410

Murray, A.B., Paola, C., 2003. Modelling the effect of vegetation on channel pattern in bedload rivers. Earth Surf. Process. Landf. 28, 131–143. doi:10.1002/esp.428

Naiman, R.J., Decamps, H., 1997. The Ecology of Interfaces: Riparian Zones. Annu. Rev. Ecol. Syst. 28, 621–658.

Naiman, R.J., Latterell, J.J., Pettit, N.E., Olden, J.D., 2008. Flow variability and the biophysical vitality of river systems. Comptes Rendus Geosci. 340, 629–643. doi:10.1016/j.crte.2008.01.002

Nanson, G., Beach, H., 1977. Forest Succession and Sedimentation on a Meandering-River Floodplain, Northeast British Columbia, Canada. J. Biogeogr. 4, 229–251. doi:10.2307/3038059

Naylor, L., Viles, H., Carter, N., 2002. Biogeomorphology revisited: looking towards the future. Geomorphology 47, 3–14. doi:10.1016/S0169-555X(02)00137-X

Nepf, H., Rominger, J., Zong, L., 2013. Coherent Flow Structures in Vegetated Channels, in: Coherent Flow Structures at Earth's Surface. John Wiley & Sons, Ltd, pp. 135–147. doi:10.1002/9781118527221.ch9

Newson, M.D., Newson, C.L., 2000. Geomorphology, ecology and river channel habitat: mesoscale approaches to basin-scale challenges. Prog. Phys. Geogr. 24, 195–217.

Notebaert, B., Piégay, H., 2013. Multi-scale factors controlling the pattern of floodplain width at a network scale: The case of the Rhône basin, France. Geomorphology, The Field Tradition in Geomorphology 43rd Annual Binghamton Geomorphology Symposium, held 21-23 September 2012 in Jackson, Wyoming USA 200, 155–171. doi:10.1016/j.geomorph.2013.03.014

Nouwakpo, S.K., Weltz, M.A., McGwire, K., 2016. Assessing the performance of structure-from-motion photogrammetry and terrestrial LiDAR for reconstructing soil surface microtopography of naturally vegetated plots. Earth Surf. Process. Landf. 41, 308–322. doi:10.1002/esp.3787

Odling-Smee, F.J., Laland, K.N., Feldman, M.W., 2003. Niche construction: the neglected process in evolution. Princeton University Press, Princeton.

O'Hare, J.M., O'Hare, M.T., Gurnell, A.M., Scarlett, P.M., Liffen, T., McDonald, C., 2012. Influence of an ecosystem engineer, the emergent macrophyte Sparganium erectum, on seed trapping in lowland rivers and consequences for landform colonisation: Influence of an ecosystem engineer on seed trapping in lowland rivers. Freshw. Biol. 57, 104–115. doi:10.1111/j.1365-2427.2011.02701.x

O'Hare, M.T., Mountford, J.O., Maroto, J., Gunn, I.D.M., 2016. Plant Traits Relevant To Fluvial Geomorphology and Hydrological Interactions: Plant Traits in Physical Processes. River Res. Appl. 32, 179–189. doi:10.1002/rra.2940

Oksanen, J., Blanchet, F.G., Kindt, R., Legendre, P., Minchin, P.R., O'Hara, R.B., Simpson, G.L., Solymos, P., H. Stevens, M.H., Wagner, H., 2016. vegan: Community Ecology Package.

Olofsson, K., Holmgren, J., Olsson, H., 2014. Tree stem and height measurements using terrestrial laser scanning and the RANSAC algorithm. Remote Sens. 6, 4323–4344. doi:10.3390/rs6054323

O'Neill, R.V., 1986. A Hierarchical Concept of Ecosystems. Princeton University Press, Princeton.

O'Neill, R.V., Johnson, A.R., King, A.W., 1989. A hierarchical framework for the analysis of scale. Landsc. Ecol. 3, 193–205. doi:10.1007/BF00131538

O'Neill, R.V., Turner, S.J., Cullinan, V.I., Coffin, D.P., Cook, T., Conley, W., Brunt, J., Thomas, J.M., Conley, M.R., Gosz, J., 1991. Multiple landscape scales: An intersite comparison. Landsc. Ecol. 5, 137–144. doi:10.1007/BF00158061

Osterkamp, W.R., Hupp, C.R., 2010. Fluvial processes and vegetation — Glimpses of the past, the present, and perhaps the future. Geomorphology, Geomorphology and Vegetation: Interactions, Dependencies, and Feedback Loops 116, 274–285. doi:10.1016/j.geomorph.2009.11.018

Parsons, M., Thoms, M.C., 2007. Hierarchical patterns of physical–biological associations in river ecosystems. Geomorphology 89, 127–146. doi:10.1016/j.geomorph.2006.07.016

Parsons, M., Thoms, M.C., Norris, R.H., 2003. Scales of Macroinvertebrate Distribution in Relation to the Hierarchical Organization of River Systems. J. North Am. Benthol. Soc. 22, 105–122. doi:10.2307/1467981

Pasquale, N., Perona, P., Francis, R., Burlando, P., 2013. Above-ground and below-ground *Salix* dynamics in response to river processes. Hydrol. Process. 28, 5189–5203. doi:10.1002/hyp.9993

Pasternack, G.B., Wyrick, J.R., 2017. Flood-driven topographic changes in a gravel-cobble river over segment, reach, and morphological unit scales: Fluvial response to large flood. Earth Surf. Process. Landf. 42, 487–502. doi:10.1002/esp.4064

Pautou, G., Decamps, H., Amoros, C., Bravard, J.P., 1985. Successions végétales dans les couloirs fluviaux : l'exemple de la plaine alluviale du Haut Rhône français. Bull. Décologie 16, 203–212.

Pautou, G., Peiry, J.-L., Girel, J., Blanchard, E., Hughes, F., Richards, K., Harris, T., El-Hames, A., 1997. Space-Time Units in Floodplains: The Example of the Drac River Upstream of Grenoble (French Alps). Glob. Ecol. Biogeogr. Lett. 6, 311–319. doi:10.2307/2997745

Perona, P., Molnar, P., Crouzy, B., Perucca, E., Jiang, Z., McLelland, S., Wüthrich, D., Edmaier, K., Francis, R., Camporeale, C., Gurnell, A., 2012. Biomass selection by floods and related timescales: Part 1. Experimental observations. Adv. Water Resour. 39, 85–96. doi:10.1016/j.advwatres.2011.09.016

Petit, S., 2006. Reconstitution de la dynamique du paysage alluvial de trois secteurs fonctionnels de la rivière Allier (1946-2000), Massif Central, France. Géographie Phys. Quat. 60, 271–287. doi:10.7202/018000ar

Petts, G., 1990. The role of ecotones in aquatic landscape management., in: Naiman, R.J., Décamps, H. (Eds.), The Ecology and Management of Aquatic-Terrestrial Ecotones. The Parthenon Publishing Group, Carnforth, UK, pp. 227–261.

Phillips, J.D., 1995. Biogeomorphology and landscape evolution: The problem of scale. Geomorphology 13, 337–347. doi:10.1016/0169-555X(95)00023-X

Phillips, J.D., van Dyke, C., 2016. Principles of geomorphic disturbance and recovery in response to storms: Geomorphic Disturbance and Recovery. Earth Surf. Process. Landf. 41, 971–979. doi:10.1002/esp.3912

Pickett, S.T.A., White, P.S., 1985. The Ecology of Natural Disturbance and Patch Dynamics. Academic Press, New York.

Piégay, H., 1996. La rivière, un corridor naturel à gérer / Rivers : concepts for managing natural corridors. Rev. Géographie Lyon 71, 275–276.

Piégay, H., Pautou, G., Ruffinoni, C., 2003. Les forêts riveraines des cours d'eau: écologie, fonctions et gestion, Institut pour le DéveloppementForestier. ed. Forêt privée française, Paris.

Pimm, S.L., 1984. The complexity and stability of ecosystems. Nature 307, 321–326. doi:10.1038/307321a0

Poff, N.L., Allan, J.D., Bain, M.B., Karr, J.R., Prestegaard, K.L., Richter, B.D., Sparks, R.E., Stromberg, J.C., 1997. The Natural Flow Regime. BioScience 47, 769–784. doi:10.2307/1313099

Polvi, L.E., Wohl, E., Merritt, D.M., 2014. Modeling the functional influence of vegetation type on streambank cohesion. Earth Surf. Process. Landf. 39, 1245–1258. doi:10.1002/esp.3577

Puijalon, S., Bornette, G., 2004. Morphological variation of two taxonomically distant plant species along a natural flow velocity gradient. New Phytol. 163, 651–660. doi:10.1111/j.1469-8137.2004.01135.x

Puijalon, S., Bouma, T.J., Douady, C.J., van Groenendael, J., Anten, N.P.R., Martel, E., Bornette, G., 2011. Plant resistance to mechanical stress: evidence of an avoidance-tolerance trade-off. New Phytol. 191, 1141–1149. doi:10.1111/j.1469-8137.2011.03763.x

Puijalon, S., Léna, J.-P., Rivière, N., Champagne, J.-Y., Rostan, J.-C., Bornette, G., 2008. Phenotypic plasticity in response to mechanical stress: hydrodynamic performance and fitness of four aquatic plant species. New Phytol. 177, 907–917. doi:10.1111/j.1469-8137.2007.02314.x

R Core Team, 2015. R: a language and environment for statistical computing. R Foundation for Statistical Computing, Vienna, Austria.

Rameau, J.C., Mansion, D., Dumé, G., 2008. Flore forestière française: Plaines et collines. Institut pour le développement forestier, Paris, France.

Rango, A., Laliberte, A., Herrick, J.E., Winters, C., Havstad, K., Steele, C., Browning, D., 2009. Unmanned aerial vehicle-based remote sensing for rangeland assessment, monitoring, and management. J. Appl. Remote Sens. 3, 033542. doi:10.1117/1.3216822

Räpple, B., Piégay, H., Stella, J.C., Mercier, D., 2017. What drives riparian vegetation encroachment in braided river channels at patch to reach scales? Insights from annual airborne surveys (Drôme River, SE France, 2005–2011). Ecohydrology 10. doi:10.1002/eco.1886

Read, J., Stokes, A., 2006. Plant biomechanics in an ecological context. Am. J. Bot. 93, 1546–1565. doi:10.3732/ajb.93.10.1546

Rhemtulla, J.M., Hall, R.J., Higgs, E.S., Macdonald, S.E., 2002. Eighty years of change: vegetation in the montane ecoregion of Jasper National Park, Alberta, Canada. Can. J. For. Res. 32, 2010–2021. doi:10.1139/x02-112

Richter, B.D., Richter, H.E., 2000. Prescribing flood regimes to sustain riparian ecosystems along meandering rivers. Conserv. Biol. 14, 1467–1478. doi:10.1046/j.1523-1739.2000.98488.x

Rivière, A., 1977. Méthodes granulométriques, techniques et interprétation. Masson, Paris.

Rodrigues, S., Bréhéret, J.-G., Macaire, J.-J., Greulich, S., Villar, M., 2007. In-channel woody vegetation controls on sedimentary processes and the sedimentary record within alluvial environments: a modern example of an anabranch of the River Loire, France. Sedimentology 54, 223–242. doi:10.1111/j.1365-3091.2006.00832.x

Rosnell, T., Honkavaara, E., 2012. Point cloud generation from aerial image data acquired by a quadrocopter type micro unmanned aerial vehicle and a digital still camera. Sensors 12, 453–480. doi:10.3390/s120100453

Rupnik, E., Nex, F., Toschi, I., Remondino, F., 2015. Aerial multi-camera systems: cccuracy and block triangulation issues. ISPRS J. Photogramm. Remote Sens. 101, 233–246. doi:10.1016/j.isprsjprs.2014.12.020

Salo, J., 1990. External processes influencing origin and maintenance of inland water-land ecotones, in: The Ecology and Management of Aquatic–terrestrial Ecotones. Naiman, R.J. and Decamps, H., New Jersey: Parthenon, pp. 37–64.

Samani, J.M.V., Kouwen, N., 2002. Stability and Erosion in Grassed Channels. J. Hydraul. Eng. 128, 40–45. doi:10.1061/(ASCE)0733-9429(2002)128:1(40)

Schumm, S.A., Lichty, R.W., 1965. Time, space, and causality in geomorphology. Am. J. Sci. 263, 110–119. doi:10.2475/ajs.263.2.110

Scott, M.L., Auble, G.T., Friedman, J.M., 1997. Flood dependency of cottonwood establishment along the Missouri River, Montana, USA. Ecol. Appl. 7, 677–690. doi:10.1890/1051-0761(1997)007[0677:FDOCEA]2.0.CO;2

Shafroth, P.B., Stromberg, J.C., Patten, D.T., 2000. Woody riparian vegetation response to different alluvial water table regimes. West. North Am. Nat. 60, 66–76.

Simon, A., Collison, A.J.C., 2002. Quantifying the mechanical and hydrologic effects of riparian vegetation on streambank stability. Earth Surf. Process. Landf. 27, 527–546. doi:10.1002/esp.325

Slaymaker, O., 2006. Towards the identification of scaling relations in drainage basin sediment budgets. Geomorphology 80, 8–19. doi:10.1016/j.geomorph.2005.09.004

Smith, D.G., 1976. Effect of vegetation on lateral migration of anastomosed channels of a glacier meltwater river. Geol. Soc. Am. Bull. 87, 857–860. doi:10.1130/0016-7606(1976)87<857:EOVOLM>2.0.CO;2

Splunder, I.V., Voesenek, L., Vries, X.D., Blom, C., Coops, H., 1996. Morphological responses of seedlings of four species of Salicaceae to drought. Can. J. Bot. 74, 1988–1995. doi:10.1139/b96-238

Stallins, A., Corenblit, D., 2017. Interdependence of geomorphic and ecologic resilience properties in a geographic context. Geomorphology. doi:10.1016/j.geomorph.2017.09.012

Stallins, J.A., 2006. Geomorphology and ecology: Unifying themes for complex systems in biogeomorphology. Geomorphology 77, 207–216. doi:10.1016/j.geomorph.2006.01.005

Stanford, J., Lorang, M., Hauer, F., 2005. The shifting habitat mosaic of river ecosystems. Int. Ver. Theor. Angew. Limnol. Verhandlungen 29, 123–136.

Stanley, E.H., Powers, S.M., Lottig, N.R., 2010. The evolving legacy of disturbance in stream ecology: concepts, contributions, and coming challenges. J. North Am. Benthol. Soc. 29, 67–83. doi:10.1899/08-027.1

Steiger, J., Gurnell, A.M., 2003. Spatial hydrogeomorphological influences on sediment and nutrient deposition in riparian zones: observations from the Garonne River, France. Geomorphology 49, 1–23. doi:10.1016/S0169-555X(02)00144-7

Steiger, J., Gurnell, A.M., Ergenzinger, P., Snelder, D., 2001a. Sedimentation in the riparian zone of an incising river. Earth Surf. Process. Landf. 26, 91–108. doi:10.1002/1096-9837(200101)26:1<91::AID-ESP164>3.0.CO;2-U

Steiger, J., Gurnell, A.M., Petts, G.E., 2001b. Sediment deposition along the channel margins of a reach of the middle River Severn, UK. Regul. Rivers Res. Manag. 17, 443–460. doi:10.1002/rrr.644

Steiger, J., Tabacchi, E., Dufour, S., Corenblit, D., Peiry, J.-L., 2005. Hydrogeomorphic processes affecting riparian habitat within alluvial channel-floodplain river systems: a review for the temperate zone. River Res. Appl. 21, 719–737. doi:10.1002/rra.879

Stella, J.C., Battles, J.J., 2010. How do riparian woody seedlings survive seasonal drought? Oecologia 164, 579–590. doi:10.1007/s00442-010-1657-6

Stella, J.C., Hayden, M.K., Battles, J.J., Piégay, H., Dufour, S., Fremier, A.K., 2011. The role of abandoned channels as refugia for sustaining pioneer riparian forest ecosystems. Ecosystems 14, 776–790. doi:10.1007/s10021-011-9446-6

Stella, J.C., Vick, J.C., Orr, B.K., 2004. Riparian vegetation dynamics on the Merced River, in: The Wilderness Society Riparian Floodplains Conference Proceedings. Sacramento, CA, pp. 302–314.

Stepper, C., Straub, C., Pretzsch, H., 2015. Assessing height changes in a highly structured forest using regularly acquired aerial image data. Forestry 88, 304–316. doi:10.1093/forestry/cpu050

Stokes, A., Fitter, A.H., Courts, M.P., 1995. Responses of young trees to wind and shading: effects on root architecture. J. Exp. Bot. 46, 1139–1146. doi:10.1093/jxb/46.9.1139

St-Onge, B., Jumelet, J., Cobello, M., Véga, C., 2004. Measuring individual tree height using a combination of stereophotogrammetry and lidar. Can. J. For. Res. 34, 2122–2130. doi:10.1139/x04-093

St-Onge, B., Vega, C., Fournier, R.A., Hu, Y., 2008. Mapping canopy height using a combination of digital stereo-photogrammetry and lidar. Int. J. Remote Sens. 29, 3343–3364. doi:10.1080/01431160701469040

Straatsma, M., Middelkoop, H., 2007. Extracting structural characteristics of herbaceous floodplain vegetation under leaf-off conditions using airborne laser scanner data. Int. J. Remote Sens. 28, 2447–2467. doi:10.1080/01431160600928633

Tabacchi, E., Correll, D.L., Hauer, R., Pinay, G., Planty-Tabacchi, A.-M., Wissmar, R.C., 1998. Development, maintenance and role of riparian vegetation in the river landscape. Freshw. Biol. 40, 497–516. doi:10.1046/j.1365-2427.1998.00381.x

Tabacchi, E., Lambs, L., Guilloy, H., Planty-Tabacchi, A.-M., Muller, E., Decamps, H., 2000. Impacts of riparian vegetation on hydrological processes. Hydrol. Process. 14, 2959–2976.

Tal, M., Gran, K., Murray, A.B., Paola, C., Hicks, D.M., 2004. Riparian Vegetation as a Primary Control on Channel Characteristics in Multi-Thread Rivers, in: Bennett, S.J., Simon, A. (Eds.), Riparian Vegetation and Fluvial Geomorphology. American Geophysical Union, pp. 43–58. doi:10.1029/008WSA04

Tal, M., Paola, C., 2010. Effects of vegetation on channel morphodynamics: results and insights from laboratory experiments. Earth Surf. Process. Landf. 35, 1014–1028. doi:10.1002/esp.1908

Tamasi, E., Stokes, A., Lasserre, B., Danjon, F., Berthier, S., Fourcaud, T., Chiatante, D., 2005. Influence of wind loading on root system development and architecture in oak (*Quercus robur* L.) seedlings. Trees 19, 374–384. doi:10.1007/s00468-004-0396-x

Tan, P., Zeng, G., Wang, J., Kang, S.B., Quan, L., 2007. Image-based tree modeling. ACM Trans. Graph. 26, 87. doi:10.1145/1239451.1239538

Telewski, F.W., Pruyn, M.L., 1998. Thigmomorphogenesis: a dose response to flexing in *Ulmus americana* seedlings. Tree Physiol. 18, 65–68. doi:10.1093/treephys/18.1.65

Thoms, M.C., Hill, S.M., Spry, M., Mount, T.J., Chen, X.J., Sheldon, F., 2004. The geomorphology of the Darling Basin, in: Breckwodt, R., Boden, R., Andrew, J. (Eds.), The Darling. Canberra, pp. 68–105.

Thoms, M.C., Parsons, M., 2002. Eco-geomorphology: an interdisciplinary approach to river science. Int. Assoc. Hydrol. Sci. Publ. 276, 113–119p.

Thorne, C., 1990. Effects of vegetation on river bank erosion and stability, in: Thornes, J.B. (Ed.), Vegetation and Erosion: Processes and Environments. Chichester, UK, pp. 125–144.

Thorp, J.H., Thoms, M.C., Delong, M.D., 2006. The riverine ecosystem synthesis: biocomplexity in river networks across space and time. River Res. Appl. 22, 123–147. doi:10.1002/rra.901

Tormos, T., Kosuth, P., Durrieu, S., Villeneuve, B., Wasson, J.G., 2011. Improving the quantification of land cover pressure on stream ecological status at the riparian scale using High Spatial Resolution Imagery. Phys. Chem. Earth 36, 549–559. doi:10.1016/j.pce.2010.07.012

Trimble, S., 2007. Encyclopedia of Water Science, Second Edition. ed. CRC Press, Boca Raton. doi:10.1201/NOE0849396274

Turner, M.G., Dale, V.H., Gardner, R.H., 1989. Predicting across scales: theory development and testing. Landsc. Ecol. 3, 245–252. doi:10.1007/BF00131542

Urban, D.L., O'Neill, R.V., Shugart, H.H., 1987. Landscape ecology: a hierarchical perspective can help scientists undertand spatial patterns. BioScience 37, 119–127. doi:10.2307/1310366

van Oorschot, M., Kleinhans, M., Geerling, G., Middelkoop, H., 2016. Distinct patterns of interaction between vegetation and morphodynamics. Earth Surf. Process. Landf. 41, 791–808. doi:10.1002/esp.3864

Vannote, R.L., Minshall, G.W., Cummins, K.W., Sedell, J.R., Cushing, C.E., 1980. The River Continuum Concept. Can. J. Fish. Aquat. Sci. 37, 130–137. doi:10.1139/f80-017

Vautier, F., Corenblit, D., Hortobágyi, B., Fafournoux, L., Steiger, J., 2016. Monitoring and reconstructing past biogeomorphic succession within fluvial corridors using stereophotogrammetry. Earth Surf. Process. Landf. 41, 1448–1463. doi:10.1002/esp.3962

Véga, C., 2006. Cartographie des changements de hauteur du couvert forestier, de l'âge et de l'indice de qualité de station par altimétrie laser et photogrammétrie (Thesis). Université de Québec à Montréal.

Véga, C., St-Onge, B., 2008. Height growth reconstruction of a boreal forest canopy over a period of 58 years using a combination of photogrammetric and lidar models. Remote Sens. Environ. 112, 1784–1794. doi:10.1016/j.rse.2007.09.002

Violle, C., Navas, M.-L., Vile, D., Kazakou, E., Fortunel, C., Hummel, I., Garnier, E., 2007. Let the concept of trait be functional! Oikos 116, 882–892. doi:10.1111/j.0030-1299.2007.15559.x

Wackrow, R., Chandler, J.H., 2011. Minimising systematic error surfaces in digital elevation models using oblique convergent imagery. Photogramm. Rec. 26, 16–31. doi:10.1111/j.1477-9730.2011.00623.x

Wackrow, R., Chandler, J.H., 2008. A convergent image configuration for DEM extraction that minimises the systematic effects caused by an inaccurate lens model. Photogramm. Rec. 23, 6–18.

Ward, J.V., 1998. Riverine landscapes: Biodiversity patterns, disturbance regimes, and aquatic conservation. Biol. Conserv. 83, 269–278. doi:10.1016/S0006-3207(97)00083-9

Ward, J.V., 1989. The Four Dimensional Nature of Lotic Ecosystems. J. North Am. Benthol. Soc. 8. doi:10.2307/1467397

Ward, J.V., Tockner, K., Arscott, D.B., Claret, C., 2002. Riverine landscape diversity. Freshw. Biol. 47, 517–539. doi:10.1046/j.1365-2427.2002.00893.x

Watanabe, T., Hanan, J.S., Room, P.M., Hasegawa, T., Nakagawa, H., Takahashi, W., 2005. Rice morphogenesis and plant architecture: measurement, specification and the reconstruction of structural development by 3D architectural modelling. Ann. Bot. 95, 1131–1143. doi:10.1093/aob/mci136

Watt, A.S., 1947. Pattern and Process in the Plant Community. J. Ecol. 35, 1–22. doi:10.2307/2256497

Westaway, R.M., Lane, S.N., Hicks, D.M., 2003. Remote survey of large-scale braided, gravel-bed rivers using digital photogrammetry and image analysis. Int. J. Remote Sens. 24, 795–815. doi:10.1080/01431160110113070

Westoby, M.J., Brasington, J., Glasser, N.F., Hambrey, M.J., Reynolds, J.M., 2012. 'Structure-from-Motion' photogrammetry: A low-cost, effective tool for geoscience applications. Geomorphology 179, 300–314. doi:10.1016/j.geomorph.2012.08.021

Wharton, C.H., Kitchens, W.M., Pendleton, E.C., Sipe, T.W., 1982. The ecology of bottomland hardwood swamps of the southeast: a community profile. U. S. Fish and Wildlife Service, Biological Services Program, Washington, D.C.

White, J., Wulder, M., Vastaranta, M., Coops, N., Pitt, D., Woods, M., 2013. The utility of image-based point clouds for forest inventory: a comparison with airborne laser scanning. Forests 4, 518–536. doi:10.3390/f4030518

Winemiller, K.O., Flecker, A.S., Hoeinghaus, D.J., 2010. Patch dynamics and environmental heterogeneity in lotic ecosystems. J. North Am. Benthol. Soc. 29, 84–99. doi:10.1899/08-048.1

Wolman, M.G., Miller, J.P., 1960. Magnitude and Frequency of Forces in Geomorphic Processes. J. Geol. 68, 54–74. doi:10.1086/626637

Woodget, A.S., Carbonneau, P.E., Visser, F., Maddock, I.P., 2015. Quantifying submerged fluvial topography using hyperspatial resolution UAS imagery and structure from motion photogrammetry: submerged fluvial topography from UAS imagery and SfM. Earth Surf. Process. Landf. 40, 47–64. doi:10.1002/esp.3613

Wu, B., Zheng, S., Thorne, C.R., 2012. A general framework for using the rate law to simulate morphological response to disturbance in the fluvial system. Prog. Phys. Geogr. 36, 575–597. doi:10.1177/0309133312436569

Wu, J., 1999. Hierarchy and scaling: extrapolating information along a scaling ladder. Can. J. Remote Sens. 25, 367–380. doi:10.1080/07038992.1999.10874736

Wu, J., Levin, S.A., 1997. A patch-based spatial modeling approach: conceptual framework and simulation scheme. Ecol. Model. 101, 325–346. doi:10.1016/S0304-3800(97)00056-2

Wu, J., Loucks, O.L., 1995. From balance of nature to hierarchical patch dynamics: a paradigm shift in ecology. Q. Rev. Biol. 70, 439–466. doi:10.1086/419172

Yu, X., Liang, X., Hyyppä, J., Kankare, V., Vastaranta, M., Holopainen, M., 2013. Stem biomass estimation based on stem reconstruction from terrestrial laser scanning point clouds. Remote Sens. Lett. 4, 344–353. doi:10.1080/2150704X.2012.734931

Université Clermont Auvergne, Clermont-Ferrand
UFR Lettres Culture et Sciences Humaines
GEOLAB (UMR 6042 CNRS/UCA/UL)

Interactions multi-échelles entre la végétation riveraine et les processus hydrogéomorphologiques (bas-Allier)

(version française abrégée)

Borbála HORTOBÁGYI

Thèse pour l'obtention du Doctorat de géographie

présentée et soutenue publiquement le 16 mars 2018

Membres du jury

Walter BERTOLDI, Docteur, Université de Trento
Dov CORENBLIT, Maître de conférences, Université Clermont Auvergne
Simon DUFOUR, Maître de conférences, Université Rennes 2
Emmanuèle GAUTIER, Professeur, Université Paris 1
Jean-Luc PEIRY, Professeur, Université Clermont Auvergne
Hervé PIÉGAY, Directeur de recherche CNRS, École Normale Supérieure de Lyon
Michal TAL, Maître de conférences, Aix-Marseille Université

Dans les écosystèmes, tels que les rivières, les marais salés, les mangroves, les dunes côtières, qui sont exposés à des flux hydrogéomorphologiques fréquents et réguliers (c'est-à-dire à des perturbations physiques), des rétroactions se mettent en place entre la géomorphologie (eau, sédiments et formes fluviales) et les plantes (par exemple *Populus nigra* L., *Salix alba* L., *Salix purpurea* L. dans les rivières). L'établissement de la végétation est contrôlé par des processus hydrogéomorphologiques qui, en retour, sont modulés par la végétation. De telles rétroactions contrôlent la dynamique des écosystèmes riverains. L'objectif principal de cette thèse est de mieux comprendre les rétroactions biogéomorphologiques de la rivière Allier (France) en utilisant des données de terrain ainsi que des données topographiques géoréférencées obtenues par photogrammétrie et imagerie LiDAR. Cette thèse a deux principaux objectifs : (i) sa composante méthodologique vise à tester l'applicabilité des méthodes de télédétection récentes dans les études biogéomorphologiques et (ii) sa composante de recherche fondamentale est centrée sur la réponse des plantes riveraines aux contraintes hydrogéomorphologiques et leurs effets sur la géomorphologie fluviale. Nous avons abordé deux questions principales afin de mieux comprendre les rétroactions entre la végétation riveraine et les processus hydrogéomorphologiques : (i) comment la végétation riveraine répond-elle aux contraintes hydrogéomorphologiques ? (ii) comment et dans quelle mesure les plantes ingénieures, une fois établies, affectent-elles la géomorphologie fluviale ? Nous avons étudié ces questions sur la rivière Allier à travers une approche emboîtée multi-échelles allant de l'échelle du patron paysager au trait de plante. Nous avons testé l'applicabilité de la méthode de photogrammétrie pour quantifier la réponse et l'effet de la végétation riveraine et des rétroactions biogéomorphologiques à différentes échelles spatio-temporelles (corridor, banc alluvial et individu).

Dans le chapitre I sont présentés les objectifs de la thèse, l'état de l'art, et est proposé un cadre conceptuel biogéomorphologique multi-échelles que nous avons testé dans cette thèse. Ce modèle conceptuel (Figure 1) décrit les interactions entre les processus

géomorphologiques et la végétation riveraine à trois échelles spatiales (corridor, banc, micro-site). Ces trois échelles spatiales sont considérées comme pertinentes car à chacune d'elles la congruence entre les processus géomorphologiques et biologiques conduit à une rétroaction biogéomorphologique caractéristique qui concerne (i) l'effet hydrogéomorphologique initial sur la végétation ; (ii) l'effet de la végétation sur la géomorphologie ; (iii) la rétroaction (la réponse de la végétation à la modification qu'elle a induit sur la géomorphologie).

La réponse et l'effet de la végétation sur l'hydrogéomorphologie et les rétroactions peuvent être appréhendés à partir de multiples échelles spatio-temporelles. De nombreux paramètres biologiques s'ajustent à l'environnement géomorphologique : à l'échelle d'un individu de plante (par exemple les traits morphologiques et biomécaniques), à l'échelle du patch de végétation (par exemple sa composition taxonomique, la valeur de trait moyen et la physionomie de la population ou de la communauté) ; à l'échelle de la mosaïque végétale riveraine (par exemple l'assemblage floristique et la valeur moyenne de trait et la physionomie des communautés correspondantes). Les changements géomorphologiques causés par les effets de la végétation sur les processus hydrogéomorphiques se produisent également à différentes échelles spatio-temporelles, par exemple par la formation des traînées sédimentaires (c'est-à-dire des marques d'obstacles) à l'aval des arbres isolés lors des événements de crue unique ; par la formation d'îles fluviales pionnières à l'échelle de la cohorte et de la communauté sur plusieurs années ; et par la formation d'une mosaïque dynamique (*steady state*) du paysage fluvial sur plusieurs décennies. Pour une meilleure compréhension et quantification des rétroactions entre la géomorphologie fluviale et la végétation riveraine, la quantification des paramètres pertinents géomorphologiques et biologiques est nécessaire à différentes échelles spatio-temporelles emboîtées.

Dans le chapitre II, nous avons testé l'applicabilité de la méthode photogrammétrique pour quantifier la réponse et l'effet de la végétation riveraine et des rétroactions biogéomorphologiques à différentes échelles spatio-temporelles (corridor, banc alluvial et individu). Nous avons testé deux méthodes photogrammétriques : (i) la photogrammétrie stéréoscopique et (ii) la photogrammétrie multi-images ou SfM (*Structure from Motion*). Nous avons identifié les difficultés et les erreurs à ne pas commettre pour appliquer correctement la photogrammétrie dans les études des rétroactions biogéomorphologiques. En tout état de cause, la photogrammétrie s'est avérée être un outil performant pour quantifier un ensemble de paramètres pertinents pour répondre à des questions de recherche fondamentale aux trois

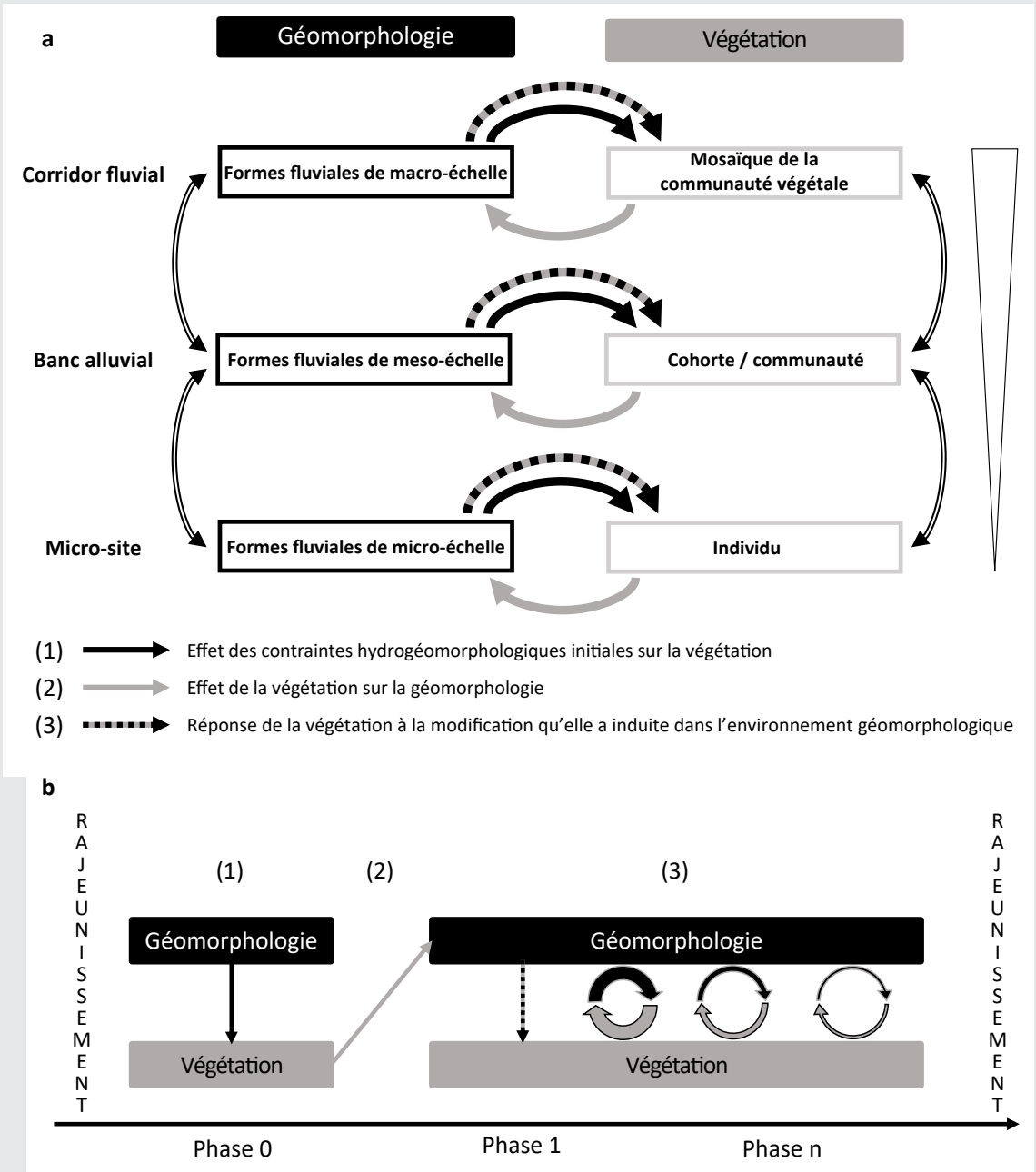

Figure 1. a) Cadre conceptuel biogéomorphologique avec trois échelles spatiales emboîtées : des rétroactions entre la géomorphologie et la végétation se produisent entre les composantes liés aux échelles de corridor, de banc et de micro-site. b) Au stade initial (phase 0), les sédiments nus après rajeunissement ou fraîchement déposés permettent le recrutement de la végétation (1). Une fois établie, la végétation modifie la géomorphologie, par exemple en augmentant le piégeage des sédiments (2). Enfin, la végétation répond à la modification qu'elle a induite dans l'environnement géomorphologique et des boucles de rétroaction entre la géomorphologie et la végétation se produisent (3). À l'origine, les rétroactions sont fortes mais diminuent lentement au cours de la progression de la succession biogéomorphologique jusqu'à ce que le rajeunissement suivant réinitialise le système à sa supposée phase initiale.

échelles spatiales considérées. Le RMSE a varié entre 0,01 et 2 m enfonction de l'échelle spatiale et des méthodes photogrammétriques mises en oeuvre. Les principaux avantages de cette méthode sont (i) son faible coût, surtout comparé à celui de l'imagerie LiDAR ; (ii) la possibilité d'exploiter des images d'archives pour étudier l'évolution passée et à long terme des processus biogéomorphologiques fluviaux ; (iii) la possibilité de l'appliquer à différentes échelles spatio-temporelles.

Dans le chapitre III, à l'échelle du corridor fluvial, nous avons recherché la signature topographique de la végétation riveraine dans le paysage en utilisant des données photogrammétriques et LiDAR. Pour capturer la signature topographique, nous avons utilisé le modèle de relief local comme indicateur de la construction des formes fluviales induite par la végétation. Notre analyse a montré que la signature topographique de la végétation dépend fortement de l'échelle à laquelle on l'observe. À l'échelle la plus large, la signature topographique de la végétation est particulièrement difficile à identifier en raison de la dynamique complexe des formes fluviales de la rivière Allier. Cependant, en concentrant les observations sur des zones de taille réduite et fortement connectées (bancs alluviaux bordant le chenal), la signature de la végétation a pu être identifiée par cette méthode.

À l'échelle du corridor, nous avons quantifié la différence d'altitude que présentent les surfaces végétalisées par rapport aux surfaces nues (bancs de gravier). Le rôle des gradients de connectivité est moins marqué à cette échelle qu'à l'échelle plus fine, ce qui suggère une mosaïque de paysage très hétérogène. En revanche, à l'échelle plus fine des bancs alluviaux, les gradients de connectivité jouent un fort rôle sur l'organisation spatiale de la végétation riveraine. La confrontation de nos résultats au modèle des successions biogéomorphologiques fluviales montre un accord partiel : i) sur la rivière Allier, la signature topographique semble augmenter avec la croissance de la hauteur végétale (progression temporelle de la succession biogéomorphologique), ce qui est en accord avec le modèle de succession biogéomorphologique fluviale ; ii) cependant, sur la partie la plus connectée des bancs alluviaux, le long du gradient longitudinal, la distribution de la hauteur végétale est l'opposée de celle décrite dans le modèle des successions biogéomorphologiques fluviales. Nos résultats suggèrent que cet écart au modèle est lié à la forte mobilité latérale du chenal, à la position relative des taches de végétation et leur forte variabilité de leur localisation sur les bancs alluviaux (liées à la migration du chenal) étant ainsi des paramètres complémentaires intéressants du modèle de succession biogéomorphologique fluviale. Cependant, nos résultats ne

permettent pas d'estimer le rôle de la végétation ligneuse riveraine sur la trajectoire évolutive de la rivière Allier à l'échelle du corridor fluvial.

Nous avons pu voir qu'à l'échelle du banc la végétation ligneuse favorise la construction de la forme fluviale le plus efficacement pour la classe de taille de 5 à 10 m. Ensuite ces taches pourraient (i) être déconnectées des inondations fréquentes, ce qui stimulerait l'accumulation de sédiments en leur sein, ou (ii) en raison de la migration latérale du chenal, être exposées à des processus hydrogéomorphologiques érosifs. Nos résultats suggèrent également que la végétation établie sur les bancs alluviaux fortement connectés aux processus hydrogéomorphologiques présente une signature topographique, mais que ces unités biogéomorphologiques ont un taux de renouvellement élevé avec une faible résistance et une forte résilience. Par conséquent, la présence des plus vieilles taches de végétation dans le corridor fluvial pourrait résulter (i) d'un changement soudain de la position du chenal, (ii) d'une régénération asexuée de *P. nigra*, ou (iii) du développement d'une succession secondaire proche des chenaux abandonnés. Sur la rivière Allier, très mobile et très dynamique du point de vue géomorphologique, les processus physiques jouent un rôle plus important dans la dynamique des formes fluviales que celui de la végétation. Une étude diachronique permettrait de vérifier si cela a évolué dans le temps. Elle serait également utile pour identifier les successions primaires et secondaires, les zones de destruction et d'établissement de la végétation et de lier la hauteur de la végétation à son âge. Une étude diachronique en 3D permettrait aussi de quantifier l'effet de la végétation sur les changements topographiques dans l'espace et dans le temps, y compris le paramètre du taux de croissance de la végétation.

Dans le chapitre IV, à l'échelle intermédiaire du banc alluvial, nous avons étudié l'aptitude des trois espèces pionnières dominantes riveraines de Salicaceae (*Populus nigra* L., *Salix purpurea* L. et *Salix alba* L.) à s'établir et à agir comme ingénieurs d'écosystème en piégeant les sédiments fins. Nous avons identifié la zone d'établissement (EA) et la fenêtre de rétroaction biogéomorphologique (BFW) de trois espèces pionnières riveraines sur les bancs alluviaux de la rivière Allier. Basé sur nos résultats statistiques, un modèle conceptuel a été conçu représentant la probabilité d'occurrence des espèces et leur effet ingénieur sur les bancs alluviaux (Figure 2).

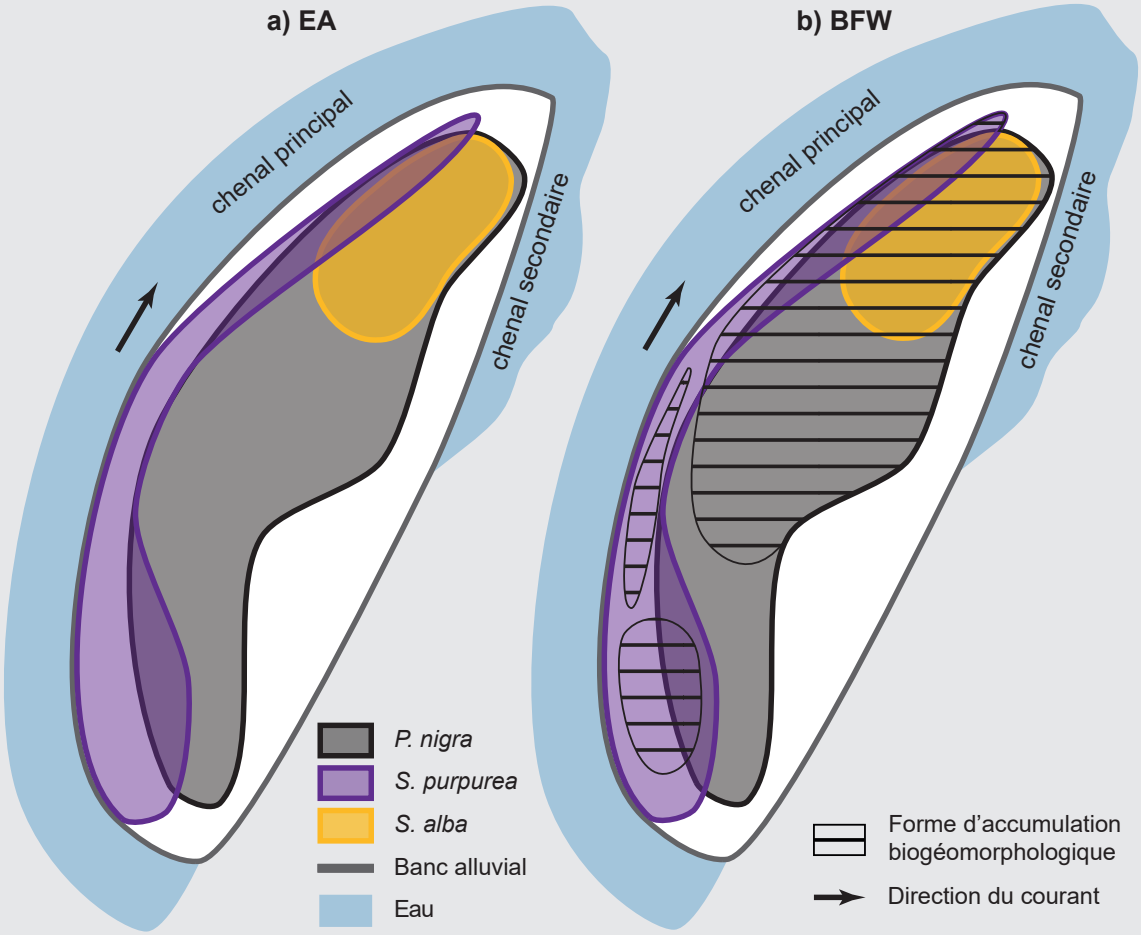

Figure 2. Modèle conceptuel basé sur l'analyse statistique de 16 bancs alluviaux de l'Allier représentant a) la zone d'établissement (EA) et b) la fenêtre de rétroaction biogéomorphologique (BFW) de *P. nigra*, *S. purpurea* et *S. alba*. Seules les phases étudiées (pionnière et biogéomorphologique) de la végétation sont représentées sur cette figure.

Dans le contexte hydrogéomorphologique actuel, les trois espèces étudiées s'établissent sur les bancs alluviaux. Cependant, les différences dans l'abondance des espèces et leur localisation suggèrent que, dans les conditions hydrogéomorphologiques actuelles, *P. nigra* est favorisé car il présente la plasticité la plus forte par rapport aux perturbations hydrogéomorphologiques et aux stress. La zone d'établissement de *S. purpurea* est principalement localisée sur les points les plus exposés des bancs alluviaux, tandis que *S. alba* se trouve dans les environnements les moins exposés. Ainsi, *P. nigra* et *S. purpurea* ont non seulement des zones d'établissement exclusif mais aussi une zone d'établissement commune. Bien que *S. alba* n'ait pas de zone d'établissement exclusif, cette espèce partage sa zone d'établissement avec *P. nigra* ou avec *P. nigra* et *S. purpurea*. Nous avons ainsi démontré que, sur la rivière Allier, *P. nigra*, *S. purpurea* et *S. alba* peuvent tous les trois agir comme des ingénieurs d'écosystème. Les fenêtres de rétroactions biogéomorphologiques de ces trois espèces sont fortement influencées par

le gradient d'exposition amont-aval (longitudinal) et le gradient de connectivité chenal-plaine d'inondation (transversal). À l'échelle du banc, le patron des formes d'accumulation biogéomorphologiques est également contrôlé par les attributs fonctionnels de chacune des trois espèces. *Populus nigra* et *S. purpurea* ont leurs propres zones d'établissement et fenêtre de rétroaction biogéomorphologique exclusive, mais les zones d'établissement et les fenêtres de rétroaction biogéomorphologique des différentes espèces prises ensemble sont également superposées. Ainsi, la zone d'établissement et la fenêtre de rétroaction biogéomorphologique combinée des trois espèces conduisent à une plus grande étendue spatiale que si seulement une ou deux des espèces étaient présentes sur les bancs alluviaux. D'un point de vue fonctionnel, nos résultats suggèrent que la diversité des traits fonctionnels intra-spécifiques et inter-spécifiques des espèces d'ingénieurs riverains joue un rôle important dans la résilience des plantes et dans le contrôle de l'étendue de la construction des formes fluviales. La capacité des plantes riveraines à s'établir et à agir comme ingénieurs d'écosystème dépend à la fois des espèces et de leur physionomie, de leur âge et de leur position respective sur les bancs alluviaux.

Dans le chapitre V, à l'échelle la plus fine du trait de plante, nous avons quantifié la relation existant entre les attributs de trait de réponse des jeunes plants de *Populus nigra* L. et leur exposition à trois niveaux différents de stress mécanique (tête de banc fortement exposée, queue de banc moins exposée, chute alluviale). Les arbres riverains pionniers, tels que *Populus nigra* L., établis sur des bancs alluviaux au sein de corridors fluviaux dynamiques, influencent fortement la géomorphologie fluviale en piégeant des sédiments et en construisant des formes fluviales pendant les crues. L'effet ingénieur (changements de l'état physique de l'habitat par les organismes) de *P. nigra* sur les bancs alluviaux dépend de sa biomasse et de son degré d'exposition à la contrainte mécanique. *P. nigra* a une plasticité phénotypique élevée qui sous-tend une grande variation de ses traits morphologiques et biomécaniques selon les conditions hydrogéomorphologiques locales. La compréhension et la quantification de la variation des traits de réponses morphologiques et biomécaniques au sein des populations de *P. nigra* en fonction de leur exposition à la contrainte mécanique est fondamentale pour mieux comprendre pourquoi et comment les plantes sont capables d'influer sur la géomorphologie. Dans une étude empirique *in situ*, nous avons quantifié la variation des traits de réponses morphologiques et biomécaniques de populations de *P. nigra* selon trois niveaux différents de contrainte mécanique. En contexte très exposé (tête de banc alluvial), les plantes ont développé des traits de réponses permettant une plus grande résistance, notamment une taille réduite, une tige flexible et inclinée et un système racinaire plus robuste (Tableau 1, Figure 3).

Tableau 1. Statistiques sommaires et résultats du test de Kruskal-Wallis (α=0.05) des traits aériens et souterrains du *P. nigra*. Les lettres associées aux groupes (i.e. A, B) indiquent que les groupes sont significativement différents.

Trait	Location	Sample nb.	Min.	Max.	Mean	Std. dev.	*p*-value	Groups
Height (cm)	Bar-head	46	18.00	63.00	37.63	11.80		A
	Bar-tail	40	42.00	100.00	67.64	16.88	< 0.0001	B
	Chute ch.	10	61.00	111.00	83.00	17.10		C
Flexibility (newton)	Bar-head	46	0.02	2.12	0.33	0.42		A
	Bar-tail	40	0.04	2.30	0.83	0.53	< 0.0001	B
	Chute ch.	10	0.30	2.40	1.20	0.70		B
Ø (cm; at ground)	Bar-head	46	0.30	1.20	0.59	0.19		A
	Bar-tail	40	0.40	1.10	0.71	0.16	0.0005	B
	Chute ch.	10	0.60	1.10	0.80	0.16		B
Ø (cm; at 20 cm)	Bar-head	46	0.10	0.60	0.38	0.13		A
	Bar-tail	40	0.30	0.80	0.55	0.11	< 0.0001	B
	Chute ch.	10	0.40	0.60	0.53	0.09		B
Inclination (degree)	Bar-head	46	95.00	161.00	125.87	14.32		A
	Bar-tail	40	78.00	128.00	105.94	10.24	< 0.0001	B
	Chute ch.	10	85.00	112.00	101.60	7.29		B
Length of buried stem (cm)	Bar-head	23	55.00	102.00	74.48	13.45		A
	Bar-tail	32	47.00	100.00	71.97	13.75	0.0009	A
	Chute ch.	7	48.00	62.00	53.57	5.00		B
Ratio height/ buried stem	Bar-head	23	0.19	1.15	0.57	0.20		A
	Bar-tail	32	0.55	1.79	1.00	0.27	< 0.0001	B
	Chute ch.	7	1.14	1.65	1.40	0.19		C
Total length (cm)	Bar-head	23	95.00	167.00	131.22	14.49		A
	Bar-tail	32	110.00	198.40	160.18	21.79	< 0.0001	B
	Chute ch.	7	125.00	185.00	148.57	18.06		B
Length of taproot (cm)	Bar-head	23	11.00	23.00	16.30	3.31		A
	Bar-tail	32	5.00	46.00	18.34	9.44	0.2269	A
	Chute ch.	7	13.00	25.00	19.86	3.93		A
Ø of taproot (cm)	Bar-head	23	0.40	1.10	0.74	0.21		A
	Bar-tail	32	0.10	1.10	0.55	0.25	0.0130	B
	Chute ch.	7	0.40	1.90	0.94	0.59		A
Ø of collar (cm)	Bar-head	23	0.60	1.70	1.10	0.29		A
	Bar-tail	32	0.40	1.20	0.75	0.22	< 0.0001	B
	Chute ch.	7	0.90	1.70	1.14	0.28		A
Nb. of lateral root	Bar-head	23	2.00	13.00	6.35	2.84		A
	Bar-tail	32	1.00	34.00	10.69	7.94	0.1361	A
	Chute ch.	7	3.00	22.00	10.00	8.04		A
Nb. of adventitious root	Bar-head	23	14.00	109.00	45.83	21.17		A
	Bar-tail	32	9.00	101.00	45.59	24.79	0.0617	A
	Chute ch.	7	7.00	48.00	25.43	15.95		A
Nb. of root Ø > 0.3 cm	Bar-head	23	0.00	6.00	2.87	2.14		A
	Bar-tail	32	0.00	5.00	1.09	1.49	0.0007	B
	Chute ch.	7	0.00	1.00	0.14	0.38		B

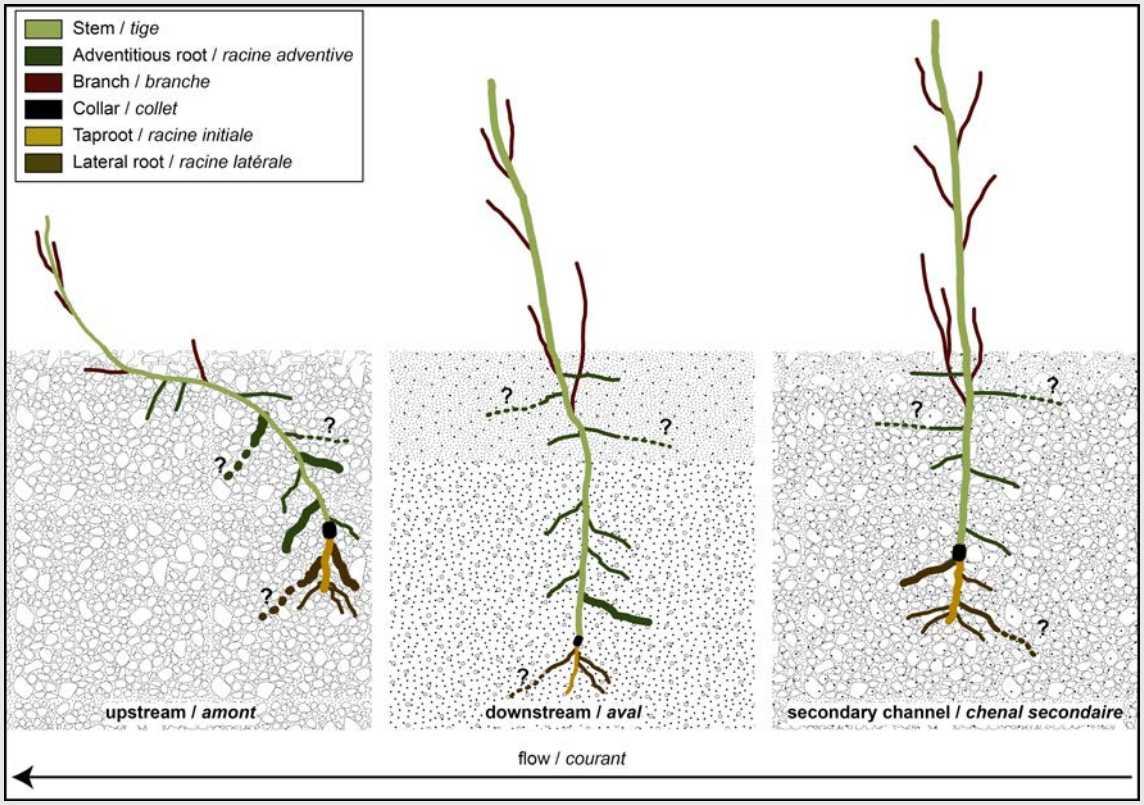

Figure 3. Représentation schématique d'un plant de *Populus nigra* L. exposé à différents niveaux de stress mécanique. La longueur des racines adventives et latérales est inconnue, celles-ci n'ayant pas été excavées dans leur intégralité. Les points d'interrogation indiquent le manque d'information sur la longueur des racines.

Néanmoins, ces réponses morphologiques et biomécaniques réduisent le potentiel « ingénieur » des plantes, c'est-à-dire leur aptitude au piégeage des sédiments fins. Nous avons démontré sur la rivière Allier l'effet ingénieur limité du peuplier noir dans les zones les plus exposées (chapitre IV), ce qui traduit un effet inhibiteur de la construction de niche par les contraintes mécaniques liées à l'écoulement. En contextes moins exposés (en queue de banc et dans le chenal secondaire), les peupliers ont développé une tige plus large, plus longue, moins flexible et moins inclinée. Cette réponse exprime une fonction préférentiellement dédiée à l'acquisition des ressources et à la bioconstruction. Le fait que la longueur totale des plantes soit maximale en queue de banc suggère que l'enfouissement par des sédiments fins stimule la production de la biomasse aérienne, celle-ci renforçant le potentiel photosynthétique. La construction des formes fluviales par le peuplier noir peut être considérée dans notre cas d'étude et de manière plus générale comme une stratégie de construction de niche conduisant à la diminution progressive des contraintes mécaniques et à l'accumulation des sédiments fins, de la matière organique et des nutriments qui influencent de manière positive la survie et la croissance des peupliers (Corenblit et al., 2014). Nos résultats suggèrent que les

processus biogéomorphologiques se produisant à une échelle fine influencent également les processus à un niveau hiérarchique supérieur (échelle plus large).

Dans tous les niveaux hiérarchiques, des rétroactions biogéomorphologiques liées aux échelles ont été détectées et synthétisées dans un modèle conceptuel (Figure 4). Aux trois échelles, nous avons considéré qu'elles prennent la forme de cycles composés de quatre phases distinctes et qui peuvent avoir une temporalité variable. L'échelle spatio-temporelle la plus large représente l'évolution de la mosaïque paysagère sur plusieurs décennies résultant de l'équilibre entre les forces constructives (établissement de la végétation, croissance et succession) et destructrices (crues morphogènes). L'échelle spatio-temporelle intermédiaire est la succession biogéomorphologique des taches de végétation, qui correspond à la transition entre les phases géomorphologique, pionnière, biogéomorphologique et écologique de la succession biogéomorphologique fluviale. Enfin, l'échelle spatio-temporelle la plus fine représente le cycle de vie des plantes ingénieures, au cours duquel les plantes ingénieures s'adaptent aux processus hydrogéomorphologiques qui les conduisent à saisir leur fenêtre d'opportunité et à franchir ensuite leur seuil d'ingénierie. Les échelles sont liées par des interactions *top-down* et *bottom-up*.

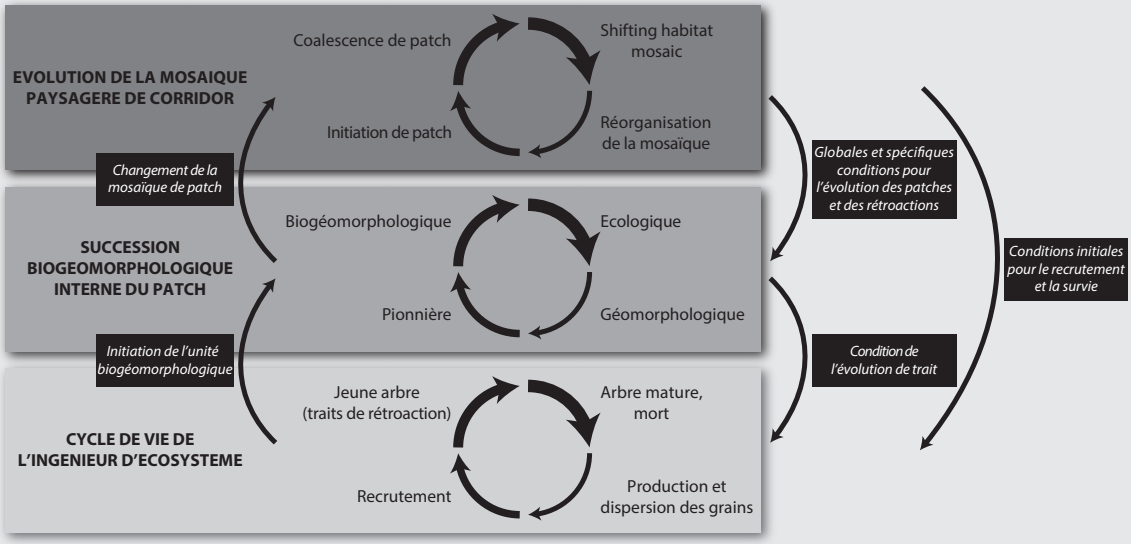

Figure 4. Organisation hiérarchique multi-échelles des processus biogéomorphologiques et leurs interactions au sein d'un écosystème biogéomorphologique fluvial.

Cette thèse a démontré que les traits d'attributs de réponse végétale à échelle fine (individuelle) et leurs effets liés sur la construction des formes fluviales à l'échelle intermédiaire (tache) peuvent influencer les trajectoires d'évolution du paysage fluvial (corridor). Nos résultats soulignent l'importance de considérer plus en détail le rôle des processus biogéomorphologiques se produisant à des échelles spatiales fines et courtes (développement de traits de réponse individuels à des contraintes mécaniques) sur ceux se produisant à des échelles spatiales larges et longues (par exemple le développement des bancs fluviaux, des îles fluviales pionnières, et des plaines alluviales, et les ajustements de la mosaïque paysagère) et *vice versa*. Cela pointe la nécessité de développer des études biogéomorphologiques hiérarchiques selon des approches ascendantes (*bottom-up*) et descendantes (*top-down*) pour renforcer notre compréhension du fonctionnement des écosystèmes biogéomorphologiques fluviaux. Les changements climatiques futurs pourraient affecter le cycle de vie des espèces et les caractéristiques des traits fonctionnels. Ces modifications à l'échelle fine pourraient entraîner des modifications de la résistance biogéomorphologique et de la résilience et, par conséquent, provoquer des changements irréversibles à l'échelle du corridor (métamorphose fluviale).

Enfin et surtout, les connaissances déjà existantes et les nouvelles données quantitatives sur les rétroactions biogéomorphologiques fluviales devraient être intégrées dans des modèles numériques et aider à leur étalonnage pour une contribution plus importante à une gestion environnementale efficace.

List of figures / Liste des figures

List of tables / Liste des tableaux

Contents